NASA TM X- 66175

PROCEEDINGS OF THE CONFERENCE ON PARALLEL IMAGE PROCESSING FOR EARTH OBSERVATION SYSTEMS

MARCH 1972
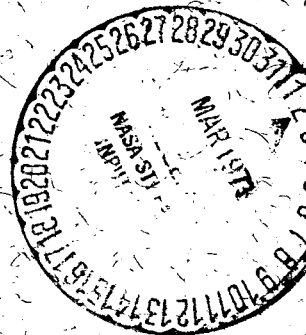
GSFC ——— GODDARD SPACE FLIGHT CENTER ———
GREENBELT, MARYLAND

Proceedings

of the

CONFERENCE ON PARALLEL IMAGE PROCESSING

FOR EARTH OBSERVATION SYSTEMS

held at Goddard Space Flight Center

on March 2 and 3, 1972

Conference Organizer:

Dr. Akram S. Husain-Abidi

GODDARD SPACE FLIGHT CENTER
Greenbelt, Maryland

Parallel Image Processing

(A Definition)

" 'Parallel Image Processing' is image process-
ing where all points of an image are operated upon
simultaneously."

INTRODUCTION

In anticipation of the future need for high speed image processing both on the ground and aboard spacecraft, a conference on PARALLEL IMAGE PROCESSING FOR EARTH OBSERVATION SYSTEMS, sponsored by the Goddard Space Flight Center, The Office of Aeronautics and Space Technology of NASA Headquarters and The Office of Applications of NASA Headquarters was held on March 2 and 3, 1972 at the Goddard Space Flight Center. The aim of the conference was to bring together those involved in optical and digital image data processing technology, and those in the earth resources field.

The conference was attended by 297 people. This large number of attendees required the transfer of the conference from the Bldg. 3 auditorium to the large Bldg. 8 auditorium.

Eighty-two Goddard employees attended. Fifteen non-Goddard NASA employees were present including 6 from NASA Headquarters. Ames, Marshall, JPL, Manned, Langley, and Wallops were represented. Sixty-eight Government employees attended representing the Army, Air Force, Navy, USGS, NOAA, DOT, NSA, USDA, NBS, CIA, the Smithsonian Astrophysical Observatory and, surprisingly, the Bureau of Outdoor Recreation.

Twenty universities and 30 different companies were represented. Eight foreign nationals were present.

Dr. Clark greeted the attendees for Goddard, and R. D. Ginter, Head of the Technology Applications Office of OAST at NASA Headquarters, gave greetings on behalf of OAST. Unfortunately, Dr. De Noyer, of the Office of Applications at Headquarters, was unable to give the keynote address. His place was ably taken by Pitt Thome, the Deputy Director for Flight Programs, Earth Observations Programs, of OA.

Technical Session I consisted of review papers of optical and digital image processing techniques. The aim of the session was to acquaint Earth Resources specialists with advanced methods of image processing. Session II in the afternoon turned the tables and acquainted the data processing experts with the problems of earth observation, including Goddard's ERTS ground processing requirements.

Session III on Friday morning presented new developments in the image processing field. Real time devices to convert from the non-coherent to coherent realm were described. Real time methods of performing cross

correlation were described. One of the most interesting aspects of this session was the interleaving of Dr. Lee's, Dr. Strong's and Dr. Preston's papers. These three papers together appeared to point the way that optical techniques may enter the traditional computer field (as opposed to the strictly image processing field). The session ended with excellent reviews of Marshall and JPL image processing work by John Williams of Marshall and Fred Billingsley of JPL.

Friday afternoon four workshops were convened. All the workshops were well attended, and all created considerable excitement among the participants. Two of the workshops felt that permanent committees should be formed to address specific questions.

The conference was a success due to the efforts of persons throughout NASA.

Special mention is directed to Mike Michalak who was in charge of all the detailed arrangements. Most importantly there would have been no conference without Dr. Husain-Abidi's unstinting efforts as the conference organizer.

Due to the efforts of people in all parts of NASA and Goddard, we were able to have a conference that brought together many parts of the Government, industry, and the academic area. It is our hope that this conference and these conference proceedings will not only benefit NASA but will also benefit a much larger image handling community throughout the Nation.

David H. Schaefer
Conference Chairman

CONTENTS

v

CONTENTS (Cont'd)

CONTENTS (Cont'd)

WORKSHOP REPORTS

WELCOMING REMARKS

Dr. John F. Clark
Director, Goddard Space Flight Center

I don't know how we managed to have such beautiful weather today, but I am grateful for it. My meteorologist friends tell me that we can expect some thunderstorms this afternoon. It is not exactly conventional for March 2nd.

It was both a surprise and a delight to us to have such a large turnout for this conference. As a matter of fact in the last couple of days we have shifted the site to this larger auditorium.

I think it is fair to say, for other than the important series of Nimbus research and development spacecraft, that NASA spacecraft have historically been numbers collectors, as opposed to pictures. That is to say, they have measured quantities such as particle counts and magnetic field intensities. In a word, we have been dealing in the field of one-dimensional measurements.

In contrast to this, the NASA Earth Observations Program of the future will be dealing predominantly with a collection of two-dimensional images, or one might say, measuring corn fields rather than magnetic fields.

Our number collector spacecraft routinely condition these numbers with a large collection of well-developed devices; differentiators, counters, integrators, logarithmic amplifiers, and we have actually started recently to fly reprogrammable computers aboard our spacecraft.

Image collectors presently have no such stable of devices which are especially designed for and suited to image inputs, much less computer systems uniquely suited to process image data.

Goddard is pursuing the development of image data processing systems, and in this we feel that an exchange of views is needed as the types of subsystems that should be developed. This is a prime reason why this conference has been convened.

Earth resource experts must know the potential of advanced image data systems, and conversely, the data processing community must become aware of the needs of the earth resource community. It is our hope that this conference will provide a large degree of cross-fertilization between these two

very important groups represented by you who are attending this conference. I hope that we can maximize the important signal-to-noise ratio in this process.

I wish you success today and tomorrow. I sincerely wish I could spend most of it with you.

WELCOMING REMARKS

R. D. Ginter, Director, Technology Applications Office
Office of Aeronautics and Space Technology, NASA Headquarters

My boss, Mr. Roy Jackson, the associate administrator of OAST, has asked me to express his personal interest and his very definite enthusiasm in your conference and in your efforts here. He had wanted to be here to make his own remarks, however, there's a thing called authorization hearings for a subcommittee on the Hill this morning and that seemed to take precedence on his schedule.

As some of you know, we in OART—and you will notice that I have been there a long time and I can't say OAST all the time—have been rather directly involved in much of your work, and because of this involvement are most interested, but not only in parallel image processing and what it can do for earth observations from spacecraft, but how this work and these techniques might be applied to the processing of information in many areas.

As easily can be imagined from our title, our organization is very concerned about aeronautics, and there is a critical need for processing images quickly and accurately. These might allow planning systems to accommodate more airplanes per unit time, provide practical collision avoidance techniques, and maybe even to improve air traffic control procedures.

The advent of the space shuttle, which has in fact brought about a sort of marriage between aeronautical and space technology, also brings with it similar problems.

This spacecraft, really airplane, must obviously perform and operate as a high-performance airplane if it is to be successful, and it probably will not be allowed the luxury of waiting for ground control to decide whether it can accept another landing regardless of weather or other conditions.

As most good bureaucrats do, you put in a bit of a plug for your own organization, mine is called the Office of Technology Applications, and we are responsible in OAST for two primary activities.

First, and probably most important, is the technology support to the Office of Applications, and to do this in a manner which is similar to what we have provided to the Office of Manned Space Flight on the shuttle and some of their other mission considerations.

We are now in the process of developing the programmatic and personal interface which should lead to a better understanding of their technology requirements and eventually implementation of the necessary work through our appropriate discipline divisions and in conjunction with the program divisions of the Office of Applications.

The other major responsibility of my office is to manage an effort which uses the NASA capability to develop solutions in public sector problems. And that is a fairly broad charter and I will not attempt to explain all the wonderful little things we have going on in there.

Maybe the most important thing though, is that both of these activities have some rather similar characteristics. One, is the need for understanding of what the actual problem is, development of technical managerial planning, and eventual demonstration of a solution.

I have to admit, as an image processing, data gathering, data handling, layman, that 10^{13} bits seems somewhat awesome, and having worked on space station and others, have learned to parrot that number with great ease as though I knew what I was talking about.

Certainly one of our OAST problems, and I suspect one of yours, is to develop the techniques which may most effectively or efficiently process the data and worry about how they are to be used. And this leads to a determination of what data are actually needed, and I know of no easy or pat answer to that.

So to me, the critical problem is to obtain and deliver, and I suspect with supreme confidence in the quality, those particles of intelligence which are in fact needed by the user. This problem is recurrent throughout most of the OAST activities as viewed from that standpoint. Whether we are concerned with technical support to the Office of Applications, helping the law enforcement organizations, or whether we are attempting to foster the development of a Goddard technique for quick automated detection of bacteria, the fundamental problem remains. We have to learn how to sense, process and finally deliver intelligence.

OAST and myself wish you all good luck in your meeting and hope you can move significantly along this path.

KEYNOTE ADDRESS

Pitt Thome, Deputy Director for Flight Programs,
Earth Observations Programs, Office of Applications, NASA Headquarters

Ladies and gentlemen, Dr. DeNoyer sends his regrets he cannot be with you here today and give this address, but he asked me to stand in for him. I think you can understand that the hearings going on in defense of our budget next year is rather basic in excusing him for being absent this morning.

I would like to start off by outlining some results of a study that I recently had the opportunity to review. The study is about at the half-way mark, but I think some of the preliminary results of that study are very important and germane to this conference.

The study dealt with the data management problems of the space station, in particular the plans for the data dissemination system for our space station: how to handle the space station experiment data; how to get the data to the users in a timely manner, and how to provide the proper amount of interactive control that these users may require with the experiments being conducted on the space station.

The time period of the space station that was postulated for the study is the late 1970s, early 1980s, and like all the space station studies they address all the relevant space science and applications disciplines.

This latest study reaffirmed what has been pointed out by several earlier studies, that the prime driver in the whole data management area deals with the disciplines inherent in the earth observations programs, and particularly the earth resources survey disciplines.

The study assumed that in the earth observations area there were basically six types of experiment areas that would be covered by the space station. These included weather and atmospheric studies, world-land use mapping, study of air and water pollution, the resource recognition and identification, natural disaster assessment, and ocean resource surveys.

From these experiment areas the study identified the type of data that is required to do research in these areas, as to the characteristics of the data, that is the requirements for the quantity, the accuracy and the timeliness of the data.

The study then went on and identified the sensors that will be required to collect this data. As an example, they came up with a candidate payload which included just for the earth observations areas, six different imagers, metric cameras, multispectral scanners, multispectral cameras, three radiometers, two spectrometers and a host of other miscellaneous types of sensors required to collect the required R&D data. These assumptions, as far as sensors and associated data requirements in this time frame, were arrived at by extrapolating from the requirements placed in the past on the aircraft program, the ERTS program and the Skylab program.

These postulated future requirements maintain the trend that we have been seeing for several years, towards the need for more data, the need for data with higher resolution, both spectral and spatial, and the need for increased accuracy.

The results of the study I found extremely interesting. I don't remember exactly the quantity of data returned, but my recollection was just for the earth resources area, that this type of space station that was postulated as needed in the late '70s, early '80s, would return up to 10^{13} bits per day and 50,000 images a day.

If allowance is made for some reduction in these requirements, reducing some of the requirements on data collection and other rather simple techniques, the study concluded that in addition to the earth resources processing capability that we now have at the Manned Spacecraft Center to support the aircraft program, to support the Skylab program, in addition to the data processing facilities we have here at Goddard to support the ERTS program, and in addition to the capability we have at the Marshall Space Flight Center and Slidell Computer Facility, that 7 to 8 new centers would be required to process this data. Seven or 8 new centers in terms of data handling capacity comparable to what we have today here at Goddard would be required to process this data.

If one were to also consider the resources required to analyze this data, the problem could be even more staggering.

The reason I summarize these study results, is to illustrate the potential situation that we could get into, what has commonly been called and very aptly so, data pollution. If we are not careful, and if we do not do our homework well we may, indeed, be faced with a serious data pollution problem.

We have the increased pressure, as I indicated before, to increase coverage, to provide more data, to provide higher resolution both spectral and spatial, and to provide increased accuracy. If we yield to these pressures

indiscriminately, we will be collecting more and more data that must be sent back down to the earth, quantities that cannot be effectively used.

This then puts strain on our bandwidth capacity in spacecraft, it puts strain on our computer capacity to process all this data, it puts strain on the analysis effort to effectively utilize this data and turn it into information. Hence, because of the strain in these various areas, it will be very difficult to even keep up with the data. Therefore, I think we must take the necessary steps to minimize data pollution as much as possible.

Well, what are some of the possible solutions? I wanted to mention several areas that should be pursued, areas that are not new to anybody here, but ones that a conference of this nature on looking at imaging processing systems should keep in mind. We must not just arbitrarily embark on improving the techniques for processing larger and larger amounts of data indiscriminately, but explore ways of reducing the quantity of collected data.

I think, first of all, we have to be selective on where the data needs to be collected. It should start right at the source of the problem, that is, the whole data collection phase. We should be selective on how often the data is collected. If the data is not needed but once every quarter, no sense in collecting it every week and archiving it or choking the processing facilities. We should be selective as to the spatial and spectral resolution required. It doesn't make sense to keep pushing for higher and higher resolution in those areas where it is not required, and to confine data collected that we do obtain for higher resolution, to those areas for which it is directly required.

We have learned a lot about this in the last few years, with the data from the aircraft program, and we are going to learn a lot more in the next few years with the experiments that will be conducted on the ERTS program and the Skylab program. However, I think there are other things we need to give consideration to at this point in time.

There ought to be more consideration given to the use of real time inter-action with the data collection phase to eliminate the collection of data that is not useful, rather than collecting the data for periods of weeks and months before it is given to the ultimate user and analyzed and determined whether it is useful. There must be a quick response time back into the data collection phase. We need to look more at onboard processing to reduce the amount of data that is transmitted back to the earth; give greater consideration to the use of both unsupervised and supervised programs in our spacecraft. We also need to look at the total system concepts to provide efficient data dissemination. Is the best approach one where the data from satellites is transmitted directly to a central receiving and processing station and then data disseminated at

the users? Should then a data relay satellite be used to relay this processed data out of the central receiving and processing center to the ultimate users? Would that indeed improve the effectiveness in the dissemination process? Or with more onboard processing, is it possible and desirable to transmit the data directly to regional centers by means of a data relay satellite? How can we provide for more real time interaction by the users to reduce the data collected?

Another area that needs studying, is how to make the most effective use of the unique capabilities of the space shuttle. This capability will present additional problems dealing with the timelier readout of data, the timelier ulitization of data and the interaction with the collection process. This needs to be studied.

This conference cannot find solutions to all these problems. I think that we should first of all assess what technology we have now that could be used to solve these problems. We should also identify what new technology is needed to assist in minimizing the data pollution problem. I think to do this properly it has to be put in a framework that requires a systems look. Maybe all this cannot be accomplished here in this conference, but I think a start should be made on it. A system look at the data collection phase, minimizing the data collected, going more to onboard processing of the spacecraft – considering also new techniques in ground processing, and new techniques for the dissemination of data the to the ultimate user in a more effective manner. All system concepts of this nature and others should be considered.

In conclusion, I would like to say that this conference is extremely timely. With the ERTS and Skylab capability that we will have shortly, the amount of data being generated by these satellites, the data pollution problem is, indeed, a very real problem. Solutions are urgently needed to build into the next generation of spacecraft and ground systems, if we are to effectively realize the great potential inherent in our remote sensing technology.

REVIEW OF COHERENT OPTICAL DATA PROCESSING

A. Vander Lugt, Research Manager
Radiation, Inc., Ann Arbor, Michigan

N73-18685

INTRODUCTION

When we consider the vast amount of data collected for the study of Earth Resource imagery, we find that we have many users wanting to extract specific information from large data bases. As the keynote speaker indicated, the total problem is one of data collection, data storage, data processing, data dissemination, and data utilization. The principal topic of this conference is to discuss parallel processing of images collected by earth observation systems. Parallel processing is clearly a requirement when one considers that a single image formed by a sensor in just one part of the spectral region may contain from 10^6 to 10^8 pixels. Furthermore, if we consider that many sensors may be acquiring data simultaneously, we find that the total amount of data collected per unit time is staggering.

The key question to ask is how we can process this data to extract the information of interest to a particular user. The solution to this problem presupposes that the user knows what information he is trying to extract and that he has some knowledge of the sensor characteristics. Our efforts here ought to focus on determining what kinds of parallel processing systems are available for potential application to image processing. I shall review the fundamental features of coherent optical data processing systems and give some representative illustrations of how they can be used.

Optical processing systems are inherently parallel processors. They are capable of performing operations on images containing millions of pixels in extremely short time intervals. The throughput is, in fact, generally limited by peripheral devices and not by the processing speed of the optical system itself. If, in addition, the optical system is coherently illuminated, we have the advantage of being able to operate on the two-dimensional Fourier transform of the image and can therefore perform two-dimensional spatial filtering operations in parallel.

The basic theory of optical spatial filtering is well developed (Fig. 1). The data to be processed modulate a coherent beam of light. The light diffracted by the data is collected by a lens that displays the two-dimensional Fourier transform of the data at the image plane (frequency plane) of the

primary light source. A transparency or mask placed in the frequency plane is the spatial filter that modified the Fourier transform of the data. The filtered data, displayed at the image plane, can then be detected for further processing.

Since the desired filtering operations frequently require the use of filters that have complex values (both phase and amplitude information), means for recording such filters are required. Spatial carrier frequency filters, in which a complex-valued function is encoded as a non-negative function, can be constructed by using a technique closely related to one used in holography for recording holograms. The filter construction system, therefore, consists of a signal beam in which the Fourier transform of the desired impulse response is displayed, and an off-axis reference beam. If the sum of the reference beam and the Fourier transform is detected by a square-law detector, the recorded function can be used directly as the desired filter. Alternatively, the filter may be generated by a computer and recorded by one of several means.

One application of coherent optical systems is immediately suggested if we note that the Fourier transform exists as a physical, measurable light distribution. Figure 2 shows an aerial image of the surface of an area of water. Within the small inserts we note the Fourier transform (which is an estimate of the power spectrum) of several subregions of the image. From the Fourier transform we can learn something about the structure or texture of the surface of the water. This same technique could be used to classify terrain in various parts of the spectrum according to their distinctive spatial frequency content. This could be the first step in many data reduction
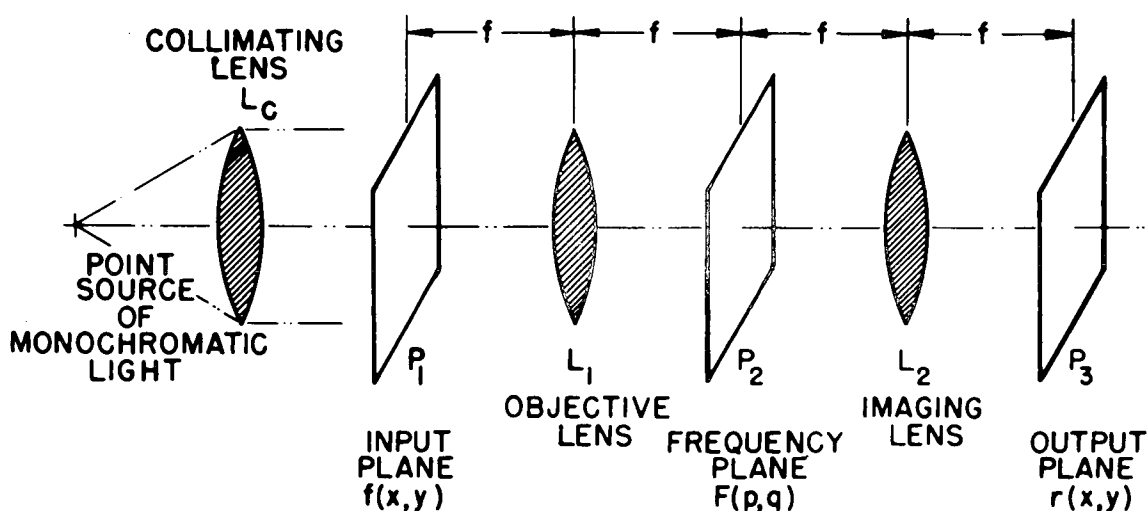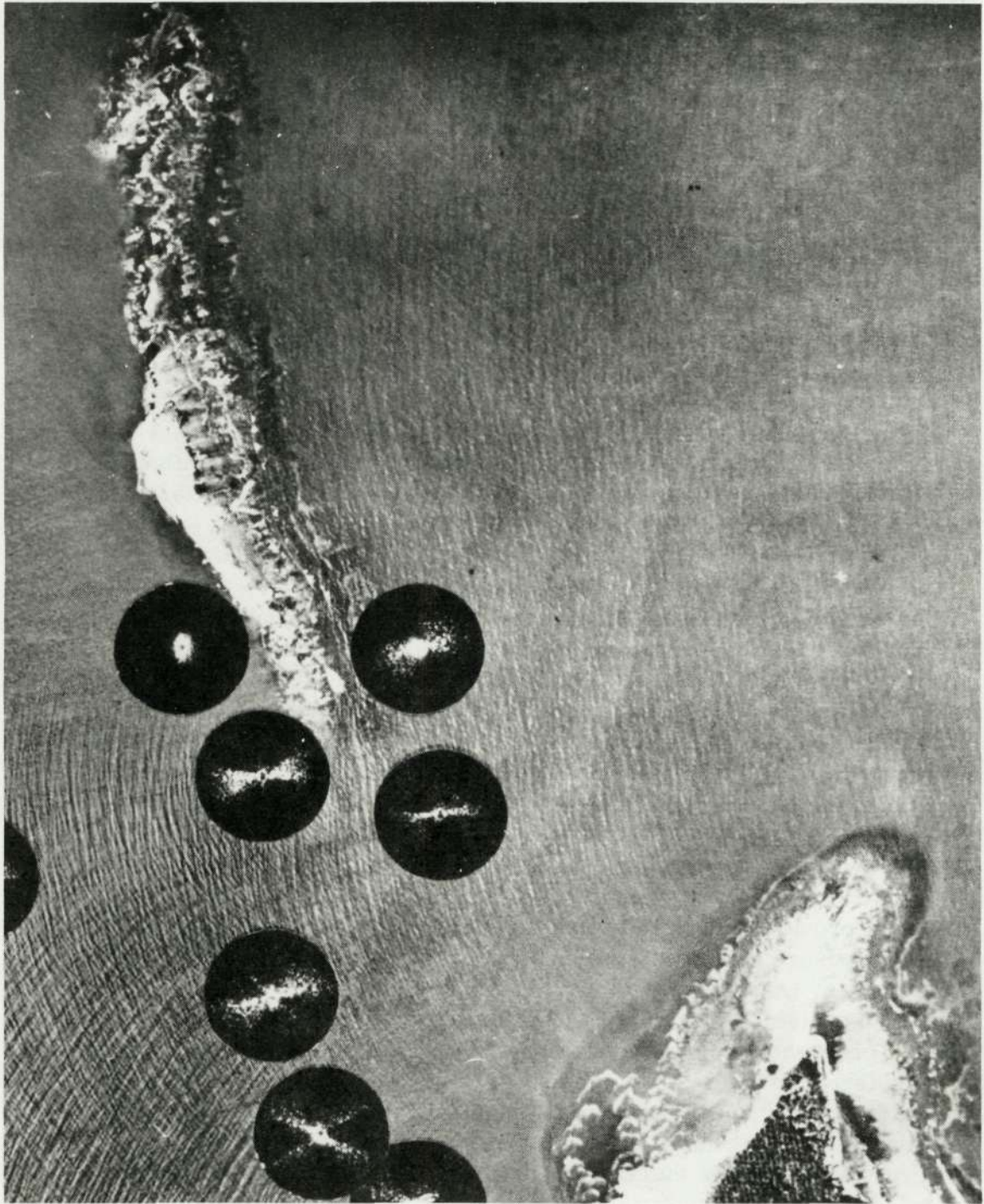

Figure 1. Coherent Optical System

Figure 2. Aerial Image of a Surface of Water

11

processes. The technique shown here is only one of several that may be applied, depending on the specific information to be extracted.

More powerful data processing operations can be implemented, however, if we use spatial filters in the frequency plane to modify the Fourier transform of the image. In this paper we review two related applications which illustrate some features of parallel processing. Both are concerned with image correlation, that is, to solve the problem of locating one image (or a part of an image) relative to another. The two images do not necessarily have to be produced by the same sensor nor do they have to be taken at the same time or from the same vantage point.

The first application could be termed image mapping. Suppose that we have a reference library of images obtained from a given sensor and that we construct spatial filters for these images. It may be noted that if we consider the optical processor as a computer, then the filters are equivalent to the memory of the computer. Each filter contains as much information as an entire image, e.g., 10^6 to 10^8 data points. Several hundred filters can be recorded on one role of film to give a mass storage capability. Once the filter library has been recorded, we are in a position to process data.

Figure 3 illustrates the steps required for image mapping. Figure 3a can be considered a frame of imagery which was recorded and stored as a spatial carrier frequency filter to form a part of a reference library. Figure 3d shows the autocorrelation of Figure 3a; its position serves to associate the output plane coordinates with the reference data. Figure 3e shows the cross-correlation of Figure 3a with the new image, Figure 3b. Note that the cross-correlation peak has moved upwards and to the right, indicating the position of the frame of imagery relative to the stored reference function. In this example we show that we do not need to use all of the imagery to locate its position; rather, only the portion shown in Figure 3c was used. The reduced area still provides a cross-correlation peak with sufficient signal-to-noise ratio to measure accurately the location of the entire frame. It is not, in this example, important which part of the imagery is used; every part of Figure 3b contained in Figure 3a correlates equally well, and each part produces a cross-correlation peak having the same location so that the position of the mission imagery is unambiguous. The intensity of the cross-correlation peak did not vary as a function of which subportion was illuminated because the terrain has very small changes in elevation and in illumination; different camera viewing angles therefore caused only small changes in the geometry.

Since it may be an expensive proposition to obtain reference imagery covering large areas of the earth, we have investigated an alternative means
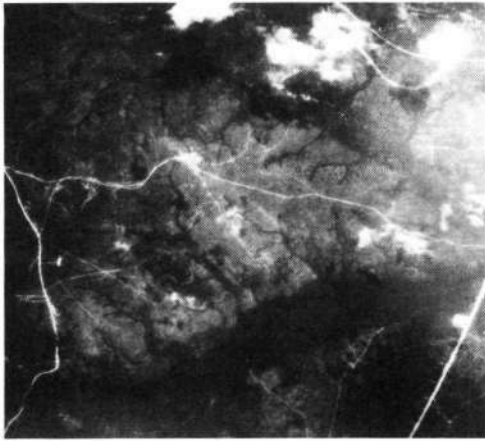
(a)
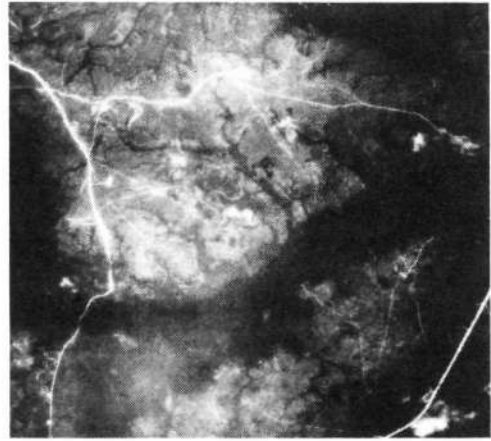
(b)

(c)

(d)

(e)

Figure 3. Steps in Imaging Mapping

13

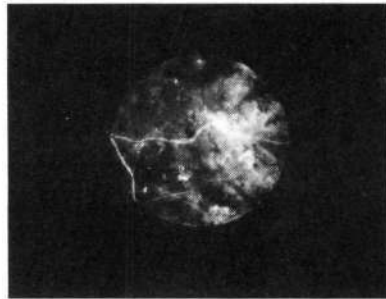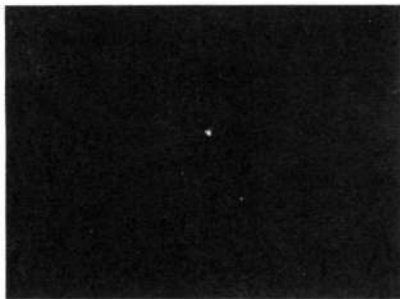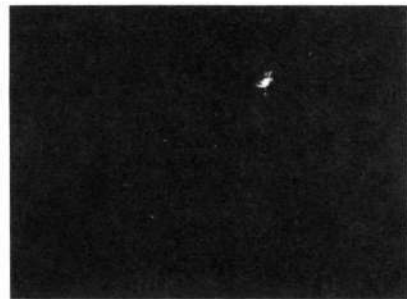for mapping. If we can find the center coordinates and orientation for at least one frame of imagery, and if there is some overlap of the frames, we can carry out the mapping by finding the position of each frame relative to the previous frame. The key to this technique is the use of an erasible recording material in the frequency plane which will be described later.

A related application is that of cloud motion analysis. Again, we have a sequence of frames of imagery and want to determine, in this case, the motion of the cloud patterns. From these movements we can make a first order estimate of the wind velocities. The procedure is similar to that described before except that now the correlation plane contains many subcorrelation peaks, one for each cloud pattern, that must be sorted.

The motion of individual patterns can be determined by allowing only the pattern of interest to appear in an aperture placed in the input plane of the system. By moving the aperture in the input plane and recording the position of the cross-correlation peak in the output for each position of the aperture, a synoptic picture of the cloud motion over the entire field of view can be developed. Cloud rotation can be measured simply by rotating one frame until the cross-correlation in the output plane is maximized.

The circled areas shown in Figure 4 show the approximate locations of the various cloud regions that were sampled. By means of a movable aperture, which may be under operator control, we sort the subcorrelation peaks. Each division (1 inch) on the scales in Figure 5 represents approximately 25 mph. The variable geometry of the scene has not been considered in determining velocities.

The magnitude of the cross-correlation is a measure of the similarity of the patterns in each frame. If the shape of the patterns changes significantly between frames, the correlation peak will be correspondingly reduced. Thus, this technique also offers an objective measure of the similarity between patterns which is useful in determining the rate at which clouds change shape. The same comments apply to measuring changes in, for example, the seasonal texture of terrain.

At the Electro-Optics Center we have used photoplastic devices to construct spatial carrier-frequency filters in situ in real time. Spatial filters for use in applications such as pattern recognition, target detection, character recognition and signature detection have usually been recorded on a nonreusable material such as photographic film. The required filters were, therefore, recorded before the data was processed to form a reference library.
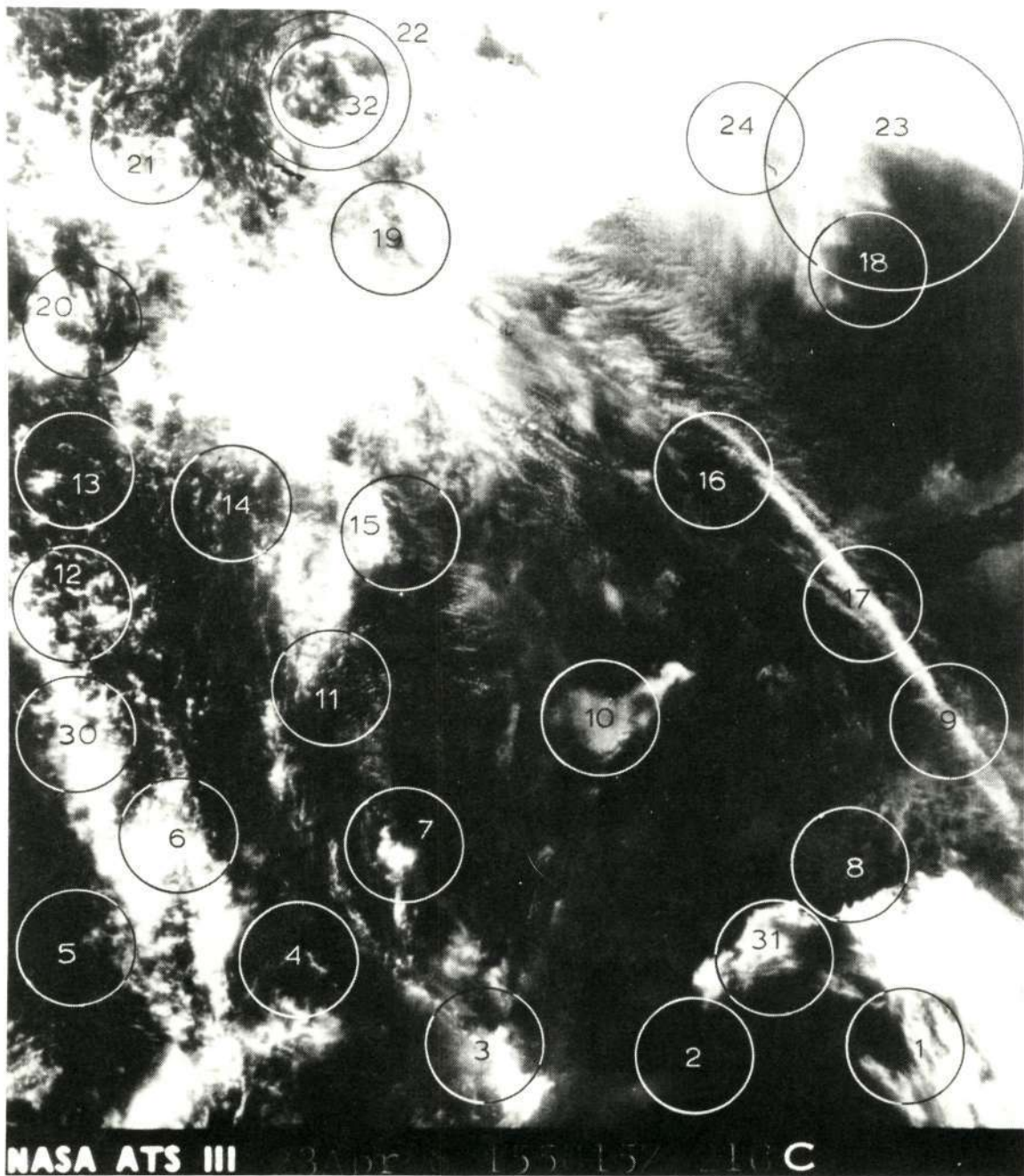
Figure 4. Cloud Coverage

SQUARES are Half-Hour Intervals

DIAMONDS are One-Hour Intervals
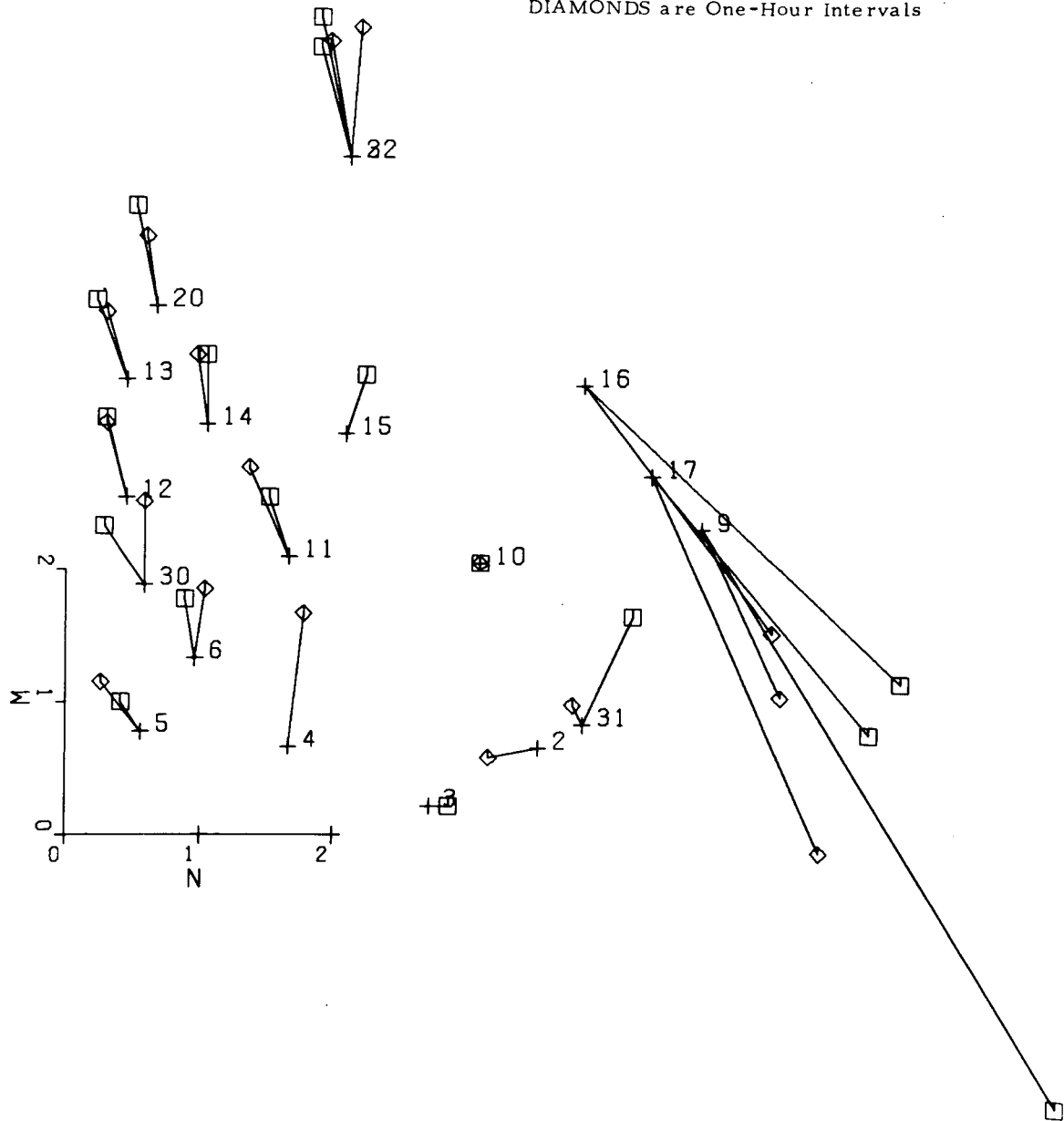
Figure 5. Synoptic Picture of Motion of Clouds in Figure 4

In some applications it is desirable to construct a filter in situ for a pattern not contained in the library. Although this can be done by using self-developing materials such as photopolymers, these materials are not reusable. Reusable materials such as photochromics are either insensitive and are not practical for use in spatial filters. The photoplastic realtime device developed at the Electro-Optics Center is reusable. It can be recycled many times; moreover, its sensitivity is comparable to that of 649F photographic emulsion on which filters are typically recorded. This device considerably extends the flexibility and usefulness of coherent data processing systems because it gives us the opportunity to update the memory of the computer.

We have also made efforts to improve the flexibility of optical processing by developing a hybrid system in which the optical system performs the high-speed, fixed routine operations while a digital computer performs low-speed flexible routine operations. Furthermore, such a system has considerable potential for use in a human interactive system. Figure 6 shows a hybrid optical system which is a dual-purpose system, i.e., it can both generate
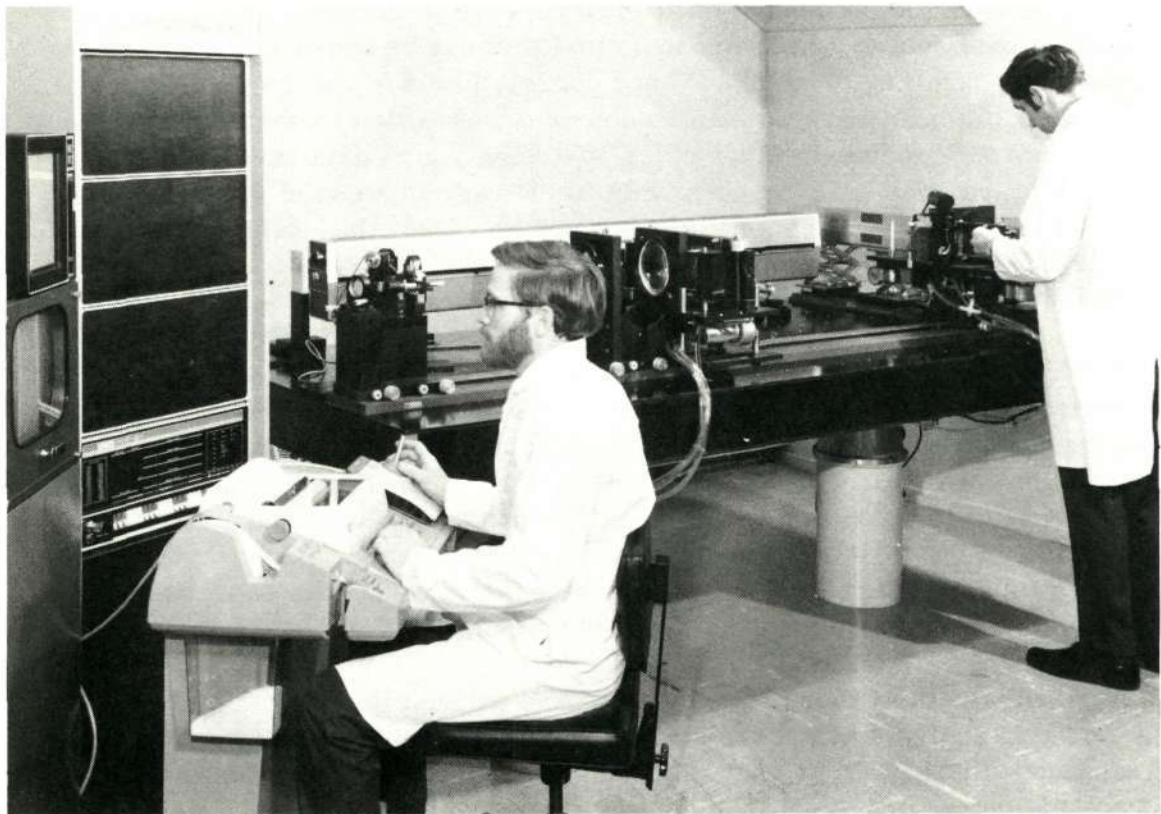
Figure 6. Hybrid Optical System

filters and process data. Of particular interest is the readout system which consists of the image orthicon, a threshold device, a cell generator, a PDP-8/I computer, a graphics display unit, and a TV monitor.

The TV camera detects the light distribution at the output plane of the optical system, the resulting video signal is thresholded and fed into a cell generator which is a high-speed, double-buffered memory composed of shift registers and various other logic circuits. The cell generator organizes the thresholded video signal into a number of cells; each cell represents a small rectangular area at the output plane of the optical system. A cell is active if there is at least one video peak exceeding threshold in the area represented by the cell. The state of a cell is indicated by the state (0 or 1) of the corresponding flip-flop in the shift registers. The cell generator can be operated in an almost arbitrary format, but it normally creates a 32 x 32 array of cells.

The function of the electronic readout system is to collect, collate, and display the processed data. In a typical processing application the output of the optical system contains correlation peaks which must be detected and processed further. A basic concept in cross-correlation operations is that the output data rate can be reduced significantly relative to the input data rate. This concept is particularly important in optical processing because a frame of input data may contain 10^8 pixels. Since correlation is a linear operation, the output detector must have the same number of resolution elements as the input and, unless data reduction takes place, extremely high data rates may be required to transfer the processed data to the user in a useful form. For example, if a frame of imagery is processed in 1 sec, data rates in excess of 100 Mb/s are required at the output. Clearly, such data rates cannot be handled by conventional data display systems.

A third area in which further progress is needed is that of input interface devices. Although photographic film is an ideal input media, we often would like to process electrical analog or digital data. Data composing devices such as the light valve, ferroelectric materials, thermoplastic materials, and the like are useful for inputting two-dimensional data whereas acousto-optic cells have potential for inputting one-dimensional time signals. As further improvements are made in input and output interface devices, we can expect to see even wider use made of coherent processing systems.

The illustrations given here by no means exhaust the list of applications. But spectral analysis and correlation offer two powerful operations that are of great general utility. For example, another important application is image deconvolution (or image enhancement or image deblurring). This method belongs, however, to the correlation class of operations. Other applications are

differentiation, subtraction processes for change detection, and cross spectral estimation. Furthermore, the optical processor can perform nonlinear as well as linear operations.

In the future, then, we can expect to see optical processors used in conjunction with digital computers to carry out the required processing operation. Each system will be used to perform those operations for which it is best suited; the digital computer for numerical calculations and for operations not easily implemented optically, and the optical computer for performing integral operations and other parallel operations on the entire image simultaneously.

OPTICAL PROCESSING IN INCOHERENT LIGHT

W. T. Maloney

Sperry Rand Research Center, Sudbury, Massachusetts 01776

ABSTRACT   **N73-18686**

Not every kind of optical input signal can be processed
in a coherent optical processor. Light from self-luminous
or incoherently illuminated objects has a randomly corru-
gated light phase front. Consequently, the Fourier trans-
form of the input signal does not appear in the transform
plane. Therefore, before they can be used in coherent proc-
essors, these objects must be converted into usable formats,
such as non-diffusing transparencies. Unfortunately, no
good, convenient, real-time method of preparing instant
transparencies exists at this time.

As an alternative to the coherent processor, one may
choose to utilize the filtering properties of an incoherent
imaging system. In such an imaging system, the input
object is convolved with the image of a point-object. This
point-object image, more often called the intensity impulse
response or the point spread function of the system, can be
controlled by proper design of the imaging system. In
particular, holography provides an extremely convenient
means for designing the impulse response. Although no
Fourier plane exists in an incoherent system, proper
tailoring of the impulse response allows implementation of
many linear filtering operations including matched filtering
and low-pass filtering. Two applications of this approach
are optical filtering of oscilloscope traces and optical
recognition of characters printed on ordinary paper. Un-
fortunately, the requirement that the image be everywhere
positive rules out high-pass filtering and hence precludes
contrast enhancement.

The basic principles of incoherent image processing
are presented and the advantages and disadvantages of this
approach are discussed.

INTRODUCTION

As man's ability to collect ever greater masses of data in ever shorter time intervals outstrips his ability to process these data, he is led to consider optical processors, drawn by the extremely large information handling capacity of such systems. Although interest commonly centers on the coherent optical processor because of its great versatility and elegance, there are times when such a system is seriously slowed down because the data are not present in a usable format. To be specific, it is essential that the input to a coherent processor be in the form of an equivalent transparency which modulates the amplitude and phase of the light front with information but does not diffuse or destroy the coherence of the illumination. In particular, patterns imprinted on paper or real scenes viewed directly do not satisfy this non-diffusing criterion.

An older class of processors known as incoherent is able to work directly from diffuse or incoherently illuminated inputs. The possibility of processing CRT patterns or objects viewed in filtered sunlight then arises. In this paper we discuss briefly the possibilities and shortcomings of these incoherent processors. We shall confine our discussion to systems capable of operation in real time and to systems based on physical optics. We shall thus not deal with photographic processing or the well-established geometrical optics approach called optical correlography.

COHERENT PROCESSORS

Let us begin our discussion of incoherent processing techniques by looking at the more familiar coherent processor represented in Fig. 1. We note that, reduced to simplest terms, it is an imaging system.[1-11] An object $o(x_0)$ is located in the front focal plane of lens L_1; the spatial Fourier transform $O(\omega)$ of this object is formed in the back focal plane. $O(\omega)$ is then retransformed by lens L_2 into the image $i(x)$ in the output plane. The Fourier plane exists because of the coherence of the illumination. One can modify the image by manipulating the amplitude transmittance in this Fourier plane, for example by inserting a transparency $H(\omega)$. Because one can thus operate directly on the spectrum of $o(x_0)$, the implementation of filtering operations is straightforward and low-pass, hi-pass, band-pass, and matched filtering are all possible. With skill and imagination, differentiation, addition and subtraction can also be achieved. The image is the transform of the product $O(\omega)H(\omega)$ and is therefore given by the convolution of the transforms of o and h, i.e.,

$$i(x) = \int d\omega O(\omega)H(\omega)e^{-i\omega x} \tag{1}$$

$$= \int dx_o o(x_o)h(x-x_o) \tag{2}$$

$$= o(x) * h(x) \tag{3}$$

where the asterisk is a shorthand notation for convolution. In all that follows, we shall usually represent spatial functions by lower case and the corresponding transforms by upper case letters with the notation

$$f(x) <=> F(\omega) \tag{4}$$

When $H(\omega)$ is different from unity, the images may no longer look at all like the object. In the case of matched [10] filtering ($H(\omega) = O*(\omega)$), the "image" will in fact be the autocorrelation function of the object:

$$i(x) = \int d\omega O(\omega)O*(\omega)e^{-i\omega x} \tag{5}$$

$$= \int dx_o o(x+x_o)o*(x_o) \tag{6}$$

$$\equiv o(x) \circledast o*(x) \tag{7}$$

where we introduce the notation $\circledast$ for the correlation operation.

For all its flexibility and high data handling capacity, the coherent optical processor suffers from one severe defect. The object must be present in the form of a non-diffusing transparency. Thus, either a photographic transparency must be prepared (thereby precluding real-time operation) or a coherent light gate must be employed. Although a wide range of candidates exists, there is as yet no satisfactory solution for high data rates. While work goes forward to develop such real-time transparencies, we shall turn our attention to another class of processors which are capable of operating directly from incoherent or diffusely illuminated sources. They do not have quite the flexibility of the coherent systems but do nevertheless have useful applications.

INCOHERENT PROCESSORS

General

The incoherent optical processor is also based on the properties of an imaging system such as that shown in Fig. 2. Note that the limitation to unit

magnification is for simplicity only.[8,9] Although there is no plane in which the Fourier transform is displayed, one can nevertheless still modify the spatial frequency response of the imaging system to implement a number of useful filter functions. Note from Fig. 2 that we are now dealing with intensity objects $|o(x_o)|^2$ and intensity images $|i(x)|^2$. We shall deal with spatial frequencies of these intensity distributions.

If the system of Fig. 2 were ideal, the image would resemble the object in every detail. As we know, this perfection can never be attained. The image always exhibits less contrast and less definition than the object. In other words, the system is operating as a low-pass filter due to the presence of a finite aperture or pupil. Let us consider the simplest object, the point object shown in Fig. 3. The image of such an object is not a point but an Airy diffraction pattern,[12] characterizing the pupil. As the diameters of the imaging lens and pupil increase, the image approaches more and more closely the ideal point response.

$$i(x) = \int o(x_o)\, h(x - x_o)\, dx_o$$
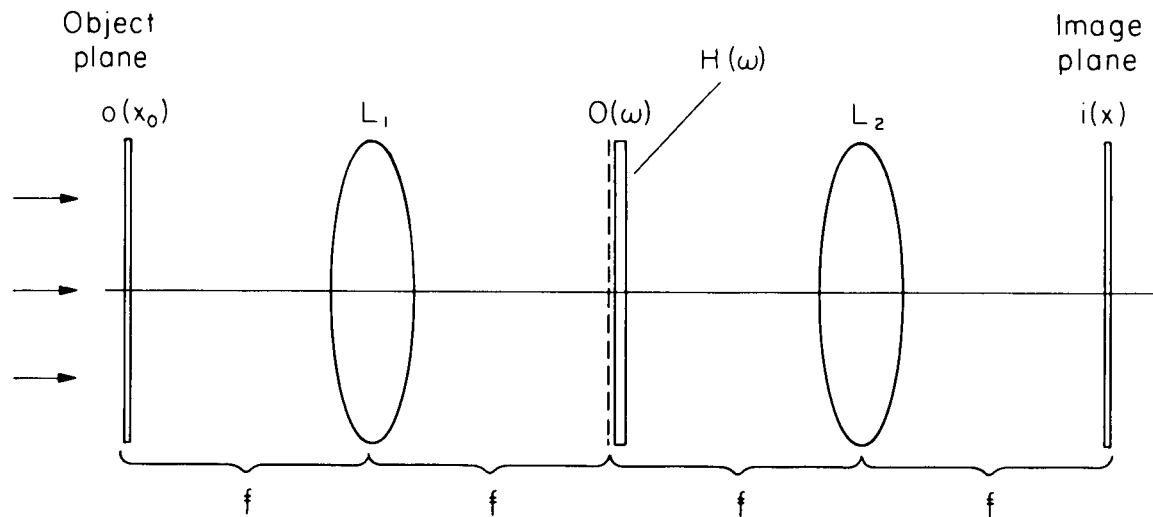
$$h(x) <=> H(\omega)$$

Figure 1. Coherent Optical Processor. The Image i(x) of the Object o(x_o) is Processed by Modifying the Transmittance in the Spatial Frequency Plane

Object plane

$\left|o(x_0)\right|^2$

Pupil plane

Image plane

$\left|i(x)\right|^2$

2f

2f
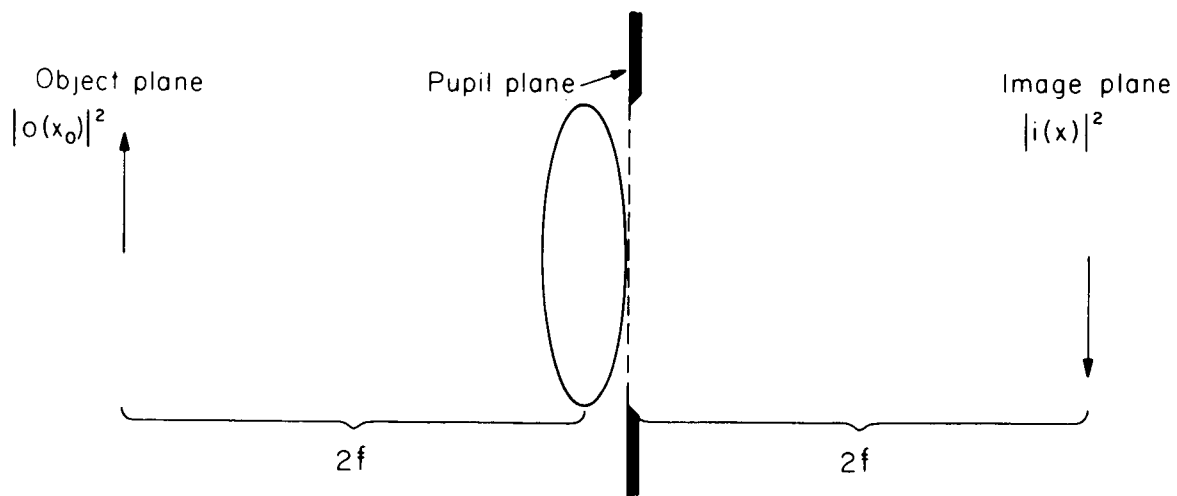
Figure 2. Incoherent Optical Processor. Processing is Accomplished by
Modifying The Transmission in the Pupil Plane

$\left|o(x_0)\right|^2 = \delta(x_0)$

$\left|i(x)\right|^2 = \left|h(x)\right|^2$

x_0

2a

x

$$\left|h(x)\right|^2 = \frac{\left[2J_1\left(\frac{\pi a x}{\lambda f}\right)\right]^2}{\left[\frac{\pi a x}{\lambda f}\right]^2}$$

Figure 3. Incoherent Optical Processor With Point Source of Light as an Input
Object. For any Real Imaging System with A Circular Pupil, the
Image is an Airy Diffraction Pattern

25

The image of a point source in an imaging system is called the impulse response or the intensity point spread function and is denoted here by $|h(x)|^2$. It is directly analogous to the impulse response of an electrical filter[10] and completely characterizes the properties of the imaging system. The philosophy of incoherent processing is as follows. Since a circular aperture can modify the impulse response from a point to an Airy pattern, perhaps other pupil functions exist which could provide other useful impulse responses. If one can tailor the impulse response of the filtering system, one can hope to implement various kinds of filters.

Shaping the pupil function to modify the impulse response has been studied for years by astronomers who wish to separate two nearby stars of widely differing magnitudes. If the secondary maxima could be removed, then the weak star would be distinguishable. In astronomy this technique is known as apodization[13,14] (removing the feet). The analogous radar problem is called side-lobe reduction.

We are concerned, of course, with objects more complicated than simple points. Let us see how the image of such an object can be built up from the impulse response.[1,15] In a well-corrected (isoplanatic) system,[15] the only result of a lateral shift of the object point is a corresponding lateral shift of the image pattern. Thus, the response to $\delta(x_o - \bar{x})$ is $|h(x-\bar{x})|^2$. Under this condition, the image of an extended object is the sum of impulse responses due to each point of the object:

$$|i(x)|^2 = \int dx_o \, |o(x_o)|^2 \, |h(x-x_o)|^2 \qquad (8)$$

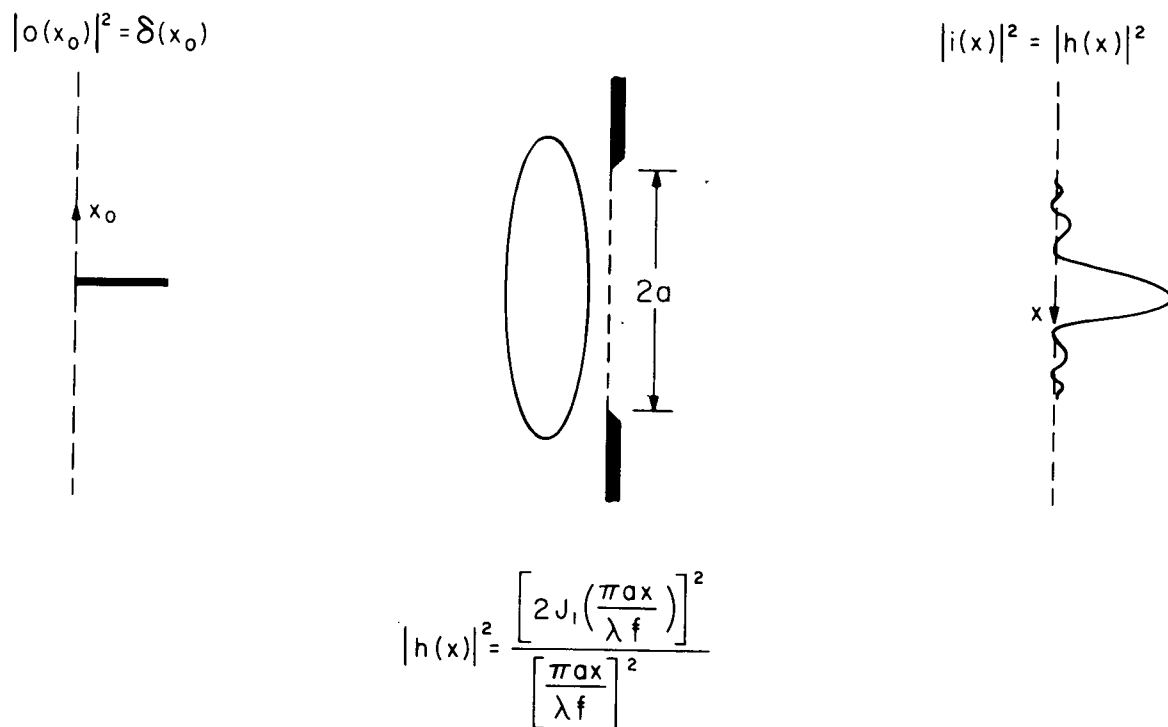This result is formally similar to the response of the coherent system with intensities replacing amplitudes. Thus, even in the absence of an explicit Fourier plane, linear filtering can be accomplished.

Although the Fourier plane does not exist, we may nevertheless take the transforms formally. If we define

$$|i(x)|^2 \, <=> \, \mathscr{I}(\omega)$$

$$|o(x)|^2 \, <=> \, \mathcal{O}(\omega) \qquad (9)$$

$$|h(x)|^2 \, <=> \, \mathcal{L}(\omega)$$

then Eq. (8) becomes

$$\mathscr{I}(\omega) = \mathcal{O}(\omega)\mathcal{L}(\omega) \qquad (10)$$

where $\mathcal{L}(\omega)$ is the Frequency Transfer Function for the intensity spectrum. It prescribes the transmission of spatial frequencies of intensity through the system. In the special case where $\mathcal{L}(\omega) = \mathcal{O}^*(\omega)$ the filter is matched to the object and the autocorrelation output is obtained.

$$|i(x)|^2 = \int d\omega O(\omega) O^*(\omega) e^{-i\omega x} \tag{11}$$

$$= \int dx_o |O(x+x_o)|^2 |O(x_o)|^2 \tag{12}$$

$$= |o(x)|^2 \circledast |o(x)|^2 \tag{13}$$

In spite of the formal similarity of Eq. (8) to Eq. (2), the frequency transfer function $\mathcal{L}(\omega)$ is very different from $H(\omega)$. Figure 4 compares these two functions[14] for the simple case of a circular pupil. Note that, whereas $H(\omega)$ is constant out to the cutoff frequency, $\mathcal{L}(\omega)$, for the same pupil, is maximum at $\omega = 0$ and extends out to a cutoff frequency which is twice that for the coherent case. This central peaking of $\mathcal{L}(\omega)$ is an essential feature of incoherent processors, as we shall now demonstrate.

$\mathcal{L}(\omega)$ is the Fourier transform of the intensity impulse response $|h(x)|^2$ which response is non-negative. It may be expressed as the transform of a product. Thus, $\mathcal{L}(\omega)$ is the convolution of the transforms of $h(x)$ abd $h^*(x)$ Since $H(\omega)$ is the transform of $h(x)$ and $H^*(-\omega)$ is the transform of $h^*(x)$, it is easily shown that $\mathcal{L}(\omega)$ may be expressed as

$$\mathcal{L}(\omega) = \int dx h(x) h^*(x) e^{-i\omega x} \tag{14}$$

$$= \int d\omega_o H(\omega+\omega_o) H^*(\omega_o) \tag{15}$$

$$= H(\omega) \circledast H^*(\omega) \tag{16}$$

In other words, $\mathcal{L}(\omega)$ is restricted to be a member of the class of autocorrelation functions,[16] and this restriction arises solely from the requirement that the impulse response $|h(x)|^2$ be everywhere non-negative. Since the maximum value of an autocorrelation function must occur at $\omega = 0$, the incoherent processing system must have its maximum frequency transmission at $\omega = o$, High-pass filtering is thereby precluded. Contrast enhancement is not possible.

Direct Pupil-Plane Masking

In spite of this limitation, many filtering operations can be implemented if the proper pupil function can be realized to produce the $|h(x)|^2$ desired. The simplest way of implementing a pupil function is by means of phase and/or amplitude transparencies located in the pupil function.[17,21] Sayanagi[17,18] has covered the pupil plane with randomly distributed discs of half-wave thickness. Figure 5 shows the very narrow frequency transfer function obtained by this
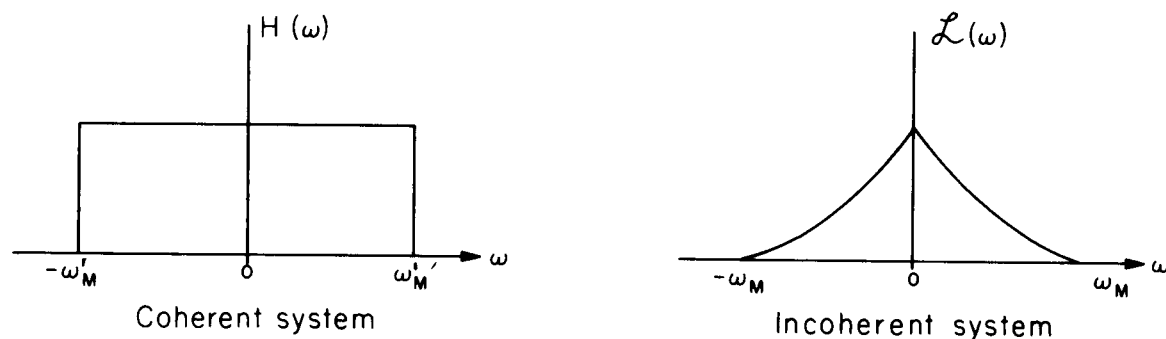
Figure 4. Comparison of Spatial Frequency Transfer Functions for Processors with Circular Apertures. Left, Coherent System; Right, Incoherent System.
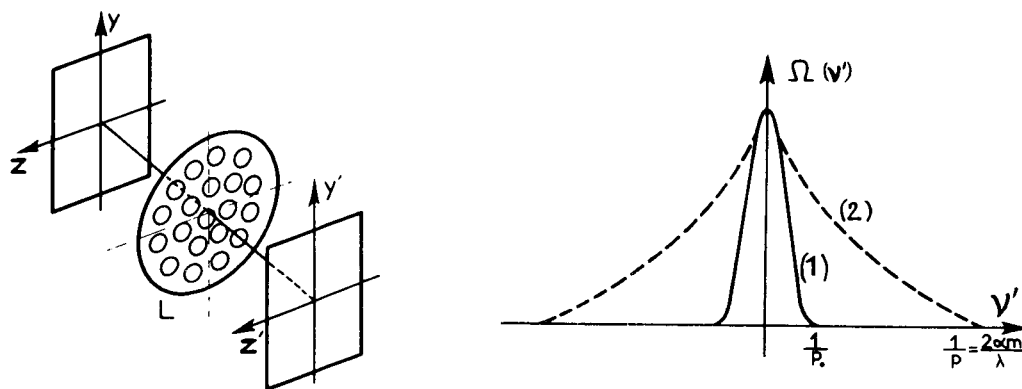
Figure 5. Left. Incoherent Imaging System with Pupil Plane Covered with Randomly Positioned Discs of Half-wave Thickness. Right. Modified Frequency Transfer Function Due to this Modified Pupil Function. Dotted Line Shows Transfer Function for Unmodified Circular Pupil. Note: Ω Replaces $\mathcal{L}$ and v' Replaces ω. After Sayanagi.[18]
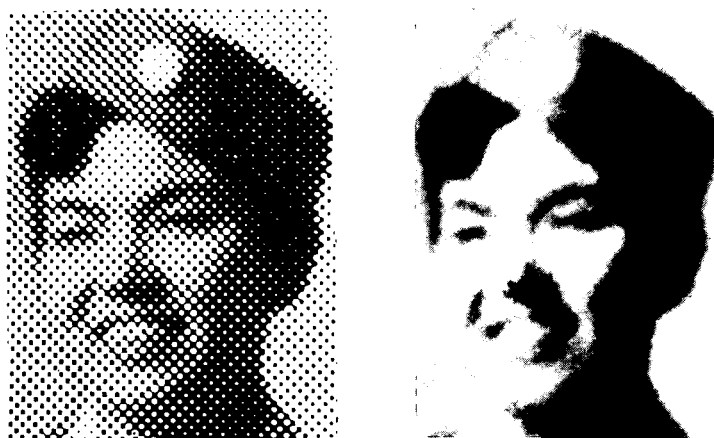
Figure 6. Left. Image of Screened Object in Unmodi-
fied Incoherent Imaging System. Right.
Image of Screened Object in Modified Sys-
tem of Fig. 5. After Sayanagi.

approach. When the halftone object (left) of Fig. 6. was located in the input
plane, the processed image (right) of Fig. 6 was obtained because the spatial
frequency of the dot pattern fell beyond the cutoff frequency of the modified
imaging system.

It is theoretically possible to prescribe a function $|h(x)|^2$ and proceed from
there to implement a pupil function which will produce it. Born and Wolf[15]
show that the pupil function required to implement an amplitude function $h(x)$
is the Fourier transform of the function $h(x)$. To implement an intensity
impulse response $|h(x)|^2$ the pupil-plane transmittance must be the transform
of $|h(x)|e^{i\phi(x)}$, where $\phi(x)$ is any phase function. One is still left with the non-
trivial problem of choosing a $\phi(x)$ which leads to a conveniently implementable
pupil function.

A much more convenient way to implement a complex transmission func-
tion in the pupil function is the holographic approach.[22,23]

Holographic Filters

The system of Fig. 7 is due to Lowenthal and Werts in France.[22] A thin
hologram is made as shown in Fig. 7b. A point source and a beam conveying
information on $h(x)$ impinge on a photographic plate. After development, it is
clear that reillumination of the plate by the point source will reconstruct a
virtual image of $h(x)$ in its original location. If a lens is inserted at the plate
such that $h(x)$ is 2f in front, a real image of $h(x)$ will appear 2f behind the

lens. Thus, an imaging system has been created between the input and output planes and this imaging system has the desired impulse response $|h(x)|^2$. When an incoherently illuminated object (of essentially the same optical wavelength) is placed in the input plane as shown in Fig. 7a, the desired filtering will be accomplished in the output plane. An example of such a system acting as a matched filter for the character N is given in Fig. 8. The bright spots in the lower part of Fig. 8 are the autocorrelation functions which indicate recognition.
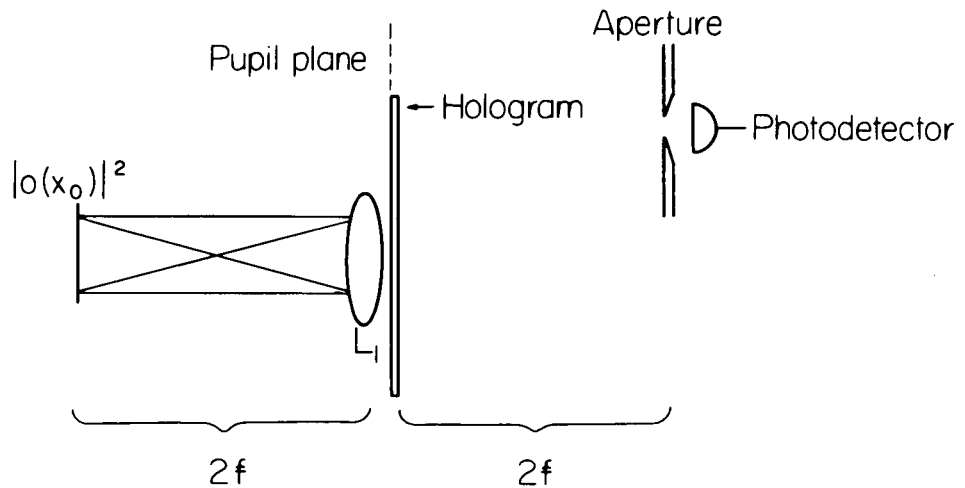
(a)   Incoherent holographic processor
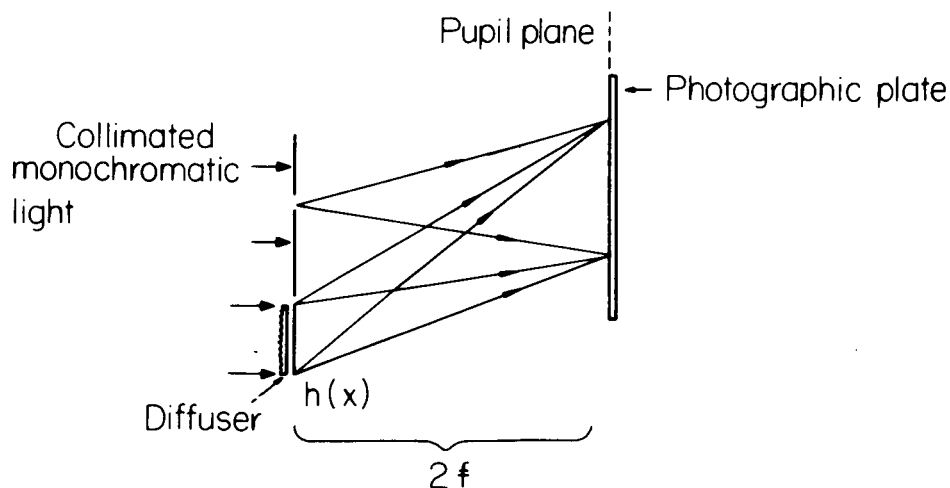
(b)   Hologram recording

Figure 7. Incoherent Holographic Optical Filtering System. Lower Figure Shows the Technique for Recording the Holographic Filter. Upper Figure Shows the Holographic Filter as Installed in the Processing System.

As in any imaging system, their locations are dictated by the locations of the objects (here the N's) in the input plane. In the recognition phase, narrow band illumination at 6438 Å was obtained from a cadmium lamp.

High efficiency in holograms requires a large angle between the two recording beams. Simultaneous implementation of a large number of filter functions (parallel optical systems) also requires filters to be located considerably off axis. To incorporate these features in the above system requires an extremely well corrected lens in each processor. A modified system which avoids this limitation is shown in Fig. 9.[24-27] The function h(x) is here recorded with a converging rather than diverging reference beam. When the developed

LE FILTRAGE DES FREQUENCES SPATIALES

EST UNE METHODE OPTIQUE DE

TRAITEMENT DE L'INFORMATION
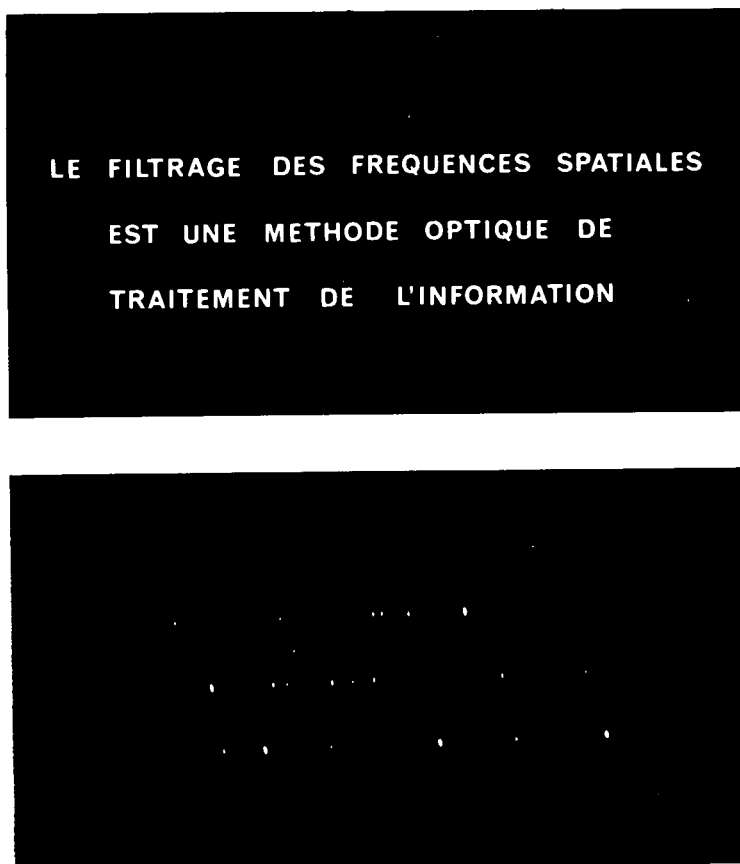
Figure 8. Input (Above) and Output (Below) from an Incoherent Holographic Optical Processor Designed to Recognize the Character N. Bright Dots Indicate Location of the Recognized Character. After Lowenthal and Werts.[22]

31
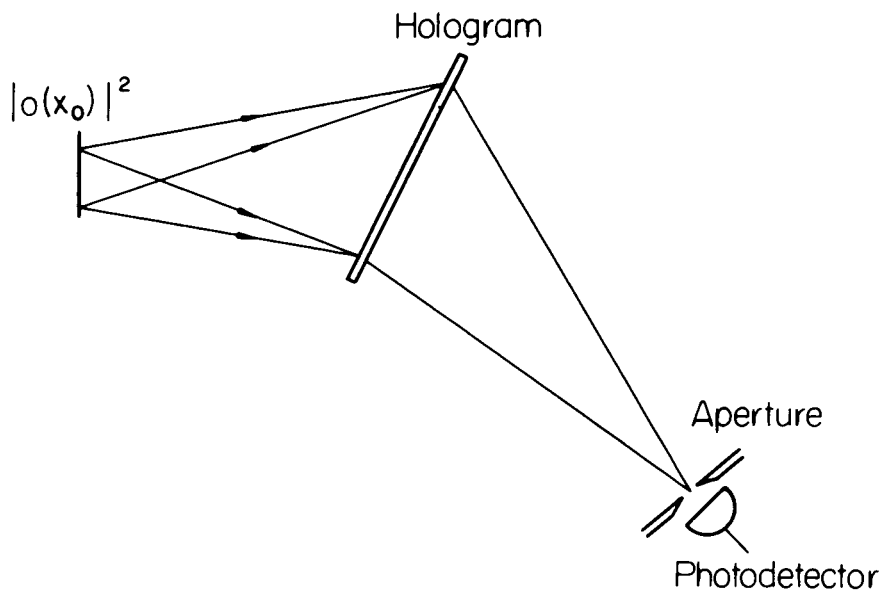
(a)   Incoherent lensless holographic processor
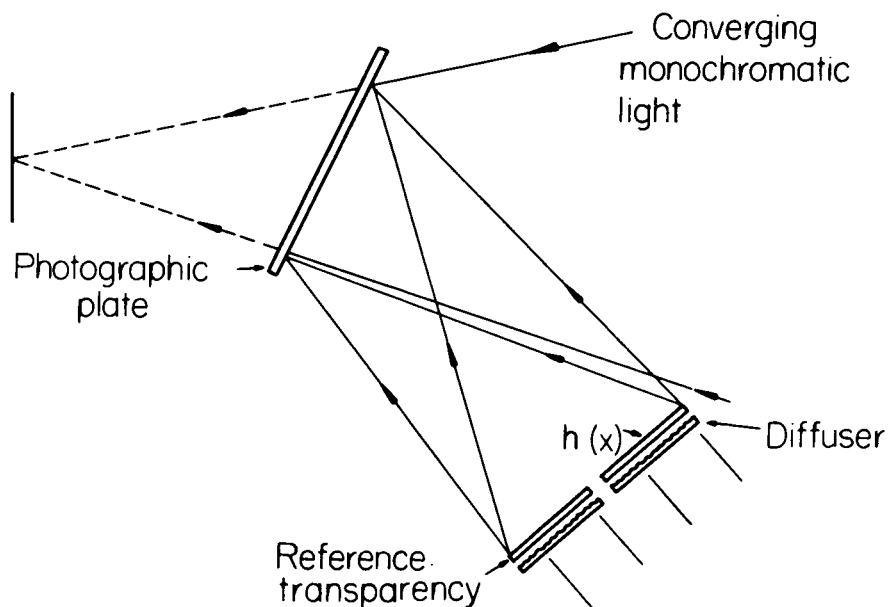
(b) Hologram recording

Figure 9. Lensless Incoherent Holographic Optical Processor. Both the
Imaging Lens and the Filter Function are Recorded on the
Holographic Plate. Lower Figure Shows Method of Construc-
tion of the Hologram.

hologram is reilluminated by a point source located as shown in Fig. 10b, the impulse response $|h(x)|^2$ is reconstructed to the right of the hologram in its original position. Thus, the holographic plate is now both lens and filter and the imaging system has the desired properties. No real lens is required in the processing system at all. Moreover, the lens used in the recording step need be corrected only for spherical aberration since it is used on axis.

If a number of impulse responses are recorded on the same photographic plate, the resulting processor constitutes a bank of parallel optical filtering channels. Operation is in effect as if one replaced the lens of Fig. 7 by a fly's eye lens, each lenslet of which had its pupil function modified to provide a desired filtering. As an example, we shall now consider a system designed to recognize alphabetic characters printed by a typewriter on ordinary paper.[27] We shall point out in passing a way of solving the problem of distinguishability that is common to all optical processors when they are used in pattern recognition applications.

Figure 10. Lensless, Incoherent, Holographic Character Recognition System. Filters are Matched to Features of Characters. Presence or Absence of Features is Determined by Optical Fibers and Detectors which Sense the Central Values of the Correlation Functions and by Thresholding Devices. Simple Logic Circuits Infer Identity of Characters from the Feature Information Obtained.

Figure 10 shows the character recognition system. The input document containing character $|o(x)|^2$ printed or typed on ordinary paper is lighted by a laser beam (a convenient source of nearly monochromatic light). The reflected light falls on the holographic multifilter made as described above. The output correlations are located in the plane of the detection apertures where the peaks of these correlation functions are sensed by an array of optical fibers and detectors. The system is designed to recognize the subalphabet of Fig. 11.

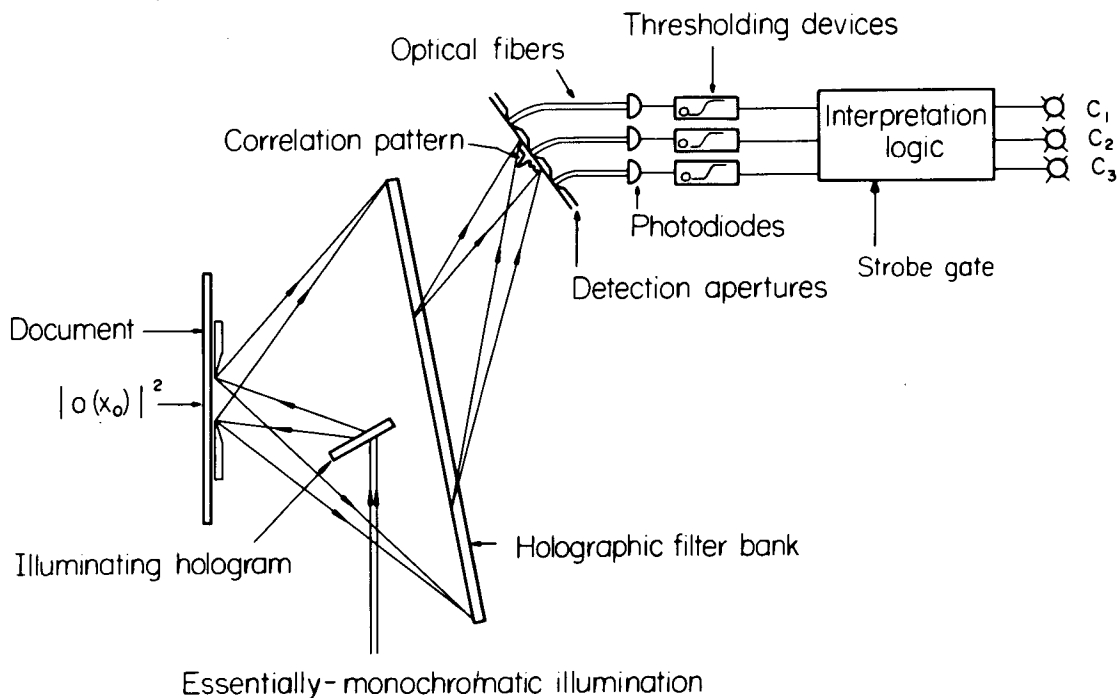In the usual character recognition system, the filters are made to be matched to each of the characters of the alphabet. As a result, it is very difficult to distinguish very similar characters such as O and Q. The optical filters of the system of Fig. 10 are matched, however, not to the characters of Fig. 11, but to features of these characters. These features are chosen to be independent so that the recognition system need only decide the presence or absence of each and not the relative amplitudes of two very similar correlation peaks. Simple combinatorial logic then decides, on the basis of the features present, the identity of the unknown character. Although feature extraction is not strictly a part of optical processing per se, it is an essential ingredient of any system that is to work with an alphabet of similar patterns! The set of features employed is shown in Fig. 12a superimposed on the character E. Figure 12b is an actual photograph of the impulse response of the multifilter. The photographic film was located in the aperture plane while a point source of light was placed in the input window. The five bars (the center bar of the top row is not a real feature but a positioning index) are shown as they appear when a point source of light is located in the document plane. With this system, the 10 characters are still distinguishable even at document contrast ratios down to 1.7:1. Further discussion of this system will be found in ref. 27.

Although the laser is a convenient source of approximately monochromatic light, it is by no means essential. CRT input is possible[28] if a phosphor such as one of those shown in Fig. 13 is employed. The ten characters above were recognized when present as transparencies backlighted by a CRT raster. The phosphor employed has the emission spectrum shown in Fig. 13a. The configuration is shown more clearly in Fig. 14 where the laser illumination of Fig. 10 has been replaced by the CRT face. Although limited by phoshor brilliance,

BEFHKLPRUV

Figure 11. Subalphabet of Characters Used in Demonstrating the
Recognition System of Fig. 10.
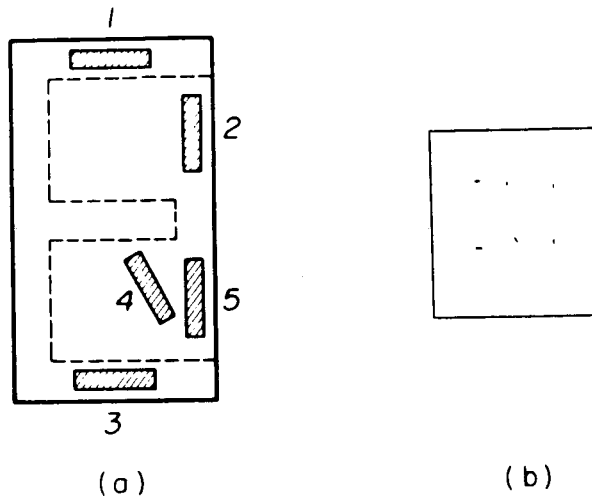
Figure 12. Features Employed in System of Fig. 10. a)
Five Features Shown Superimposed on the
Character E. b) Actual Photograph of the
Impulse Response of the Recognition System.
The Five Features are Shown Together with
One Positioning Mark.
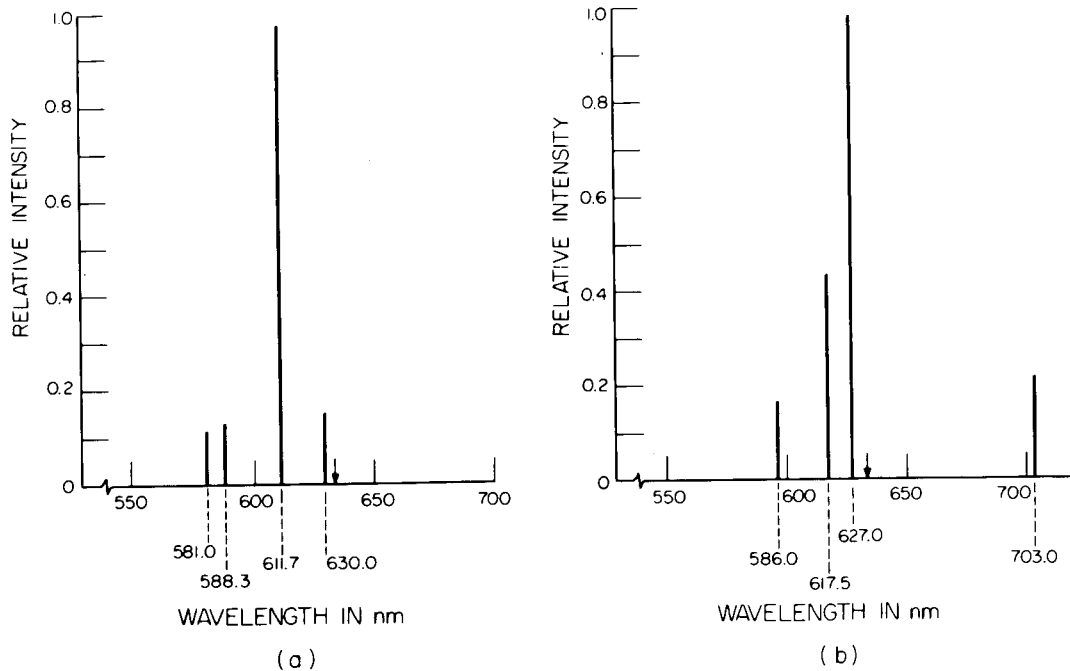
Figure 13. Emission Lines of Two Rare-Earth Red Phosphors Commonly Utilized in
Color Television. A CRT was Constructed Using the Phosphor of
Fig. 13a.
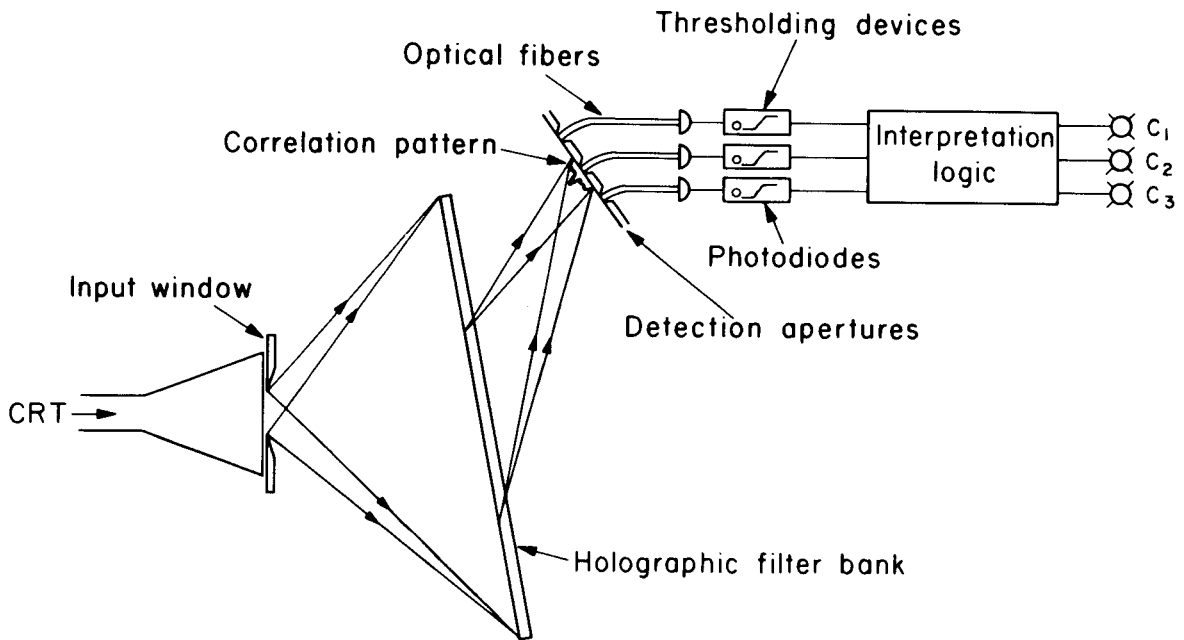
Figure 14. Lensless, Incoherent, Holographic Character Recognition System Using CRT Illumination.

hysteresis, aging and persistence, the CRT does allow the possibility of processing any signal present as an electric current. Moreover, contrast enhancement may be achievable electronically. Unless operated in a raster mode, a serious drawback does arise from the tendency of the CRT to draw patterns of constant total light power rather than constant intensity.

CONCLUSION

The incoherent optical processor is capable of performing many of the desirable filtering operations normally associated with the coherent processor. Although it cannot achieve high-pass filtering, it can nevertheless process inputs present as diffusing or incoherently illuminated patterns which the coherent processor cannot handle. Thus, the possibility of processing CRT display images or real-time objects illuminated by sunlight may be considered. When the filters are implemented holographically, the optical system can consist simply of an input plane, a hologram plate and an output plane with no lenses needed at all. These properties make such a system an interesting candidate for on-board processing of earth satellite data.

REFERENCES

1. A. Papoulis, "Systems and transforms with applications in optics," McGraw-Hill Book Co., New York, 1968.

2. L. J. Cutrona, E. N. Leith, C. J. Palermo, and L. J. Porcello, "Optical data processing and filtering systems," IRE Trans. Information Theory, vol. IT-6, June 1960.

3. K. Preston, Jr., "Use of the Fourier transformable properties of lenses for signal spectrum analysis," Optical and Electro-optical Information Processing," Ed. by J. T. Tippett et al., M.I.T. Press, Cambridge, 1965. pp. 59-68.

4. A. Vander Lugt, F. B. Rotz, and A. Klooster, Jr., "Character reading by optical spatial filtering," Optical and Electro-optical Information Processing, Ed. by J. T. Tippett et al., M.I.T. Press, Cambridge, 1965, pp. 125-141.

5. A. Vander Lugt, "Signal detection by complex spatial filtering," IEEE Trans. Information Theory, vol. IT-10, pp. 139-145, 1964.

6. E. N. Leith and J. Upatnieks, "Reconstructed wavefronts and communication theory," J. Opt. Soc. Am., vol. 52, pp. 1123-1130, Oct. 1962.

7. D. Gabor, "Character recognition by holography," Nature, vol. 208, pp. 422-423, Oct. 1965.

8. A. Vander Lugt, "Practical considerations for the use of spatial carrier-frequency filters," Appl. Optics, vol. 5, pp. 1760-1765, Nov. 1966.

9. A. Vander Lugt, "Operational notation for the analysis and synthesis of optical data-processing systems," Proc. IEEE, vol. 54, pp. 1055-1063, Aug. 1966.

10. G. L. Turin, "An introduction to matched filters," IRE Trans. Information Theory, vol. IT-6, pp. 311-329, June 1960.

11. A. Vander Lugt, "A review of optical data-processing techniques," Optica Acta, vol. 15, pp. 1-33, Jan. 1968.

12. M. Born and E. Wolf, Principles of Optics, Pergamon Press, New York, 1959, pp. 423-427.

13. P. Jacquinot and B. Roizen-Dossier, "Apodisation," Progress in Optics, vol. 3, Ed. by E. Wolf, New Holland Pub. Co., Amsterdam, 1964.

14. A. Maréchal, "Optique géométrique générale," Handbuch der Physik, vol. 24, Springer-Verlag, Berlin, pp. 44-170, 1956.

15. M. Born and E. Wolf, Principles of Optics, Pergamon Press, New York, 1959, pp. 481-483.

16. W. Lukosz, "Übertragung nich-negativen signale durch lineare filter," Optica Acta, vol. 9, pp. 335-363, Oct. 1962.

17. K. Sayanagi, "Optical noise filter," J. App. Phys. Japan, vol. 27, pp. 623-632, Oct. 1958.

18. M. Francon, "Modern applications of physical optics," Interscience Publishers, London, 1963.

19. J. D. Armitage and A. W. Lohmann, "Character recognition by incoherent spatial filtering," Appl. Optics, vol. 4, pp. 461-467, Apr. 1965.

20. T. J. Harley, Jr., "Comments on a paper by J. D. Armitage and A. W. Lohmann," Appl. Optics, vol. 4, 1966, Dec. 1965.

21. J. D. Armitage and A. W. Lohmann, "Author's Reply," Appl. Optics, vol. 4, pp. 1666, Dec. 1965.

22. S. Lowenthal and A. Werts, "Filtrage des fréquences spatiales en lumière incoherente à l'aide d'hologrammes," C. R. Acad. Sc., Paris, vol. 226, Feb. 1968.

23. A. W. Lohmann, "Matched filtering with self-luminous objects," Appl. Optics, vol. 7, pp. 561-563, Mar. 1968.

24. G. Groh, "Optical multiplex system for pattern recognition utilizing point holograms," Optics Communications, vol. 1, pp. 454-456, Apr. 1970, and references therein.

25. G. Groh, "Multiple imaging by means of point holograms," Appl. Optics, col. 7, pp. 1643-1644, Aug. 1968.

26. S. Lowenthal, S. A. Werts, and M. Rembault, "Formation de réseaux d'images à l'aide d'un hologramme multiplicateur éclairé en lumière spatialement incohérente," C. R. Acad. Sc., Paris, vol. 267B, pp 120-123, July 1968.

27. W. T. Maloney, "Lensless holographic recognition of spatially incoherent patterns in real time," Appl. Opt., vol. 10, pp. 2127-2131, Sept. 1971.

28. W. T. Maloney, "Real-time holographic filtering of oscilloscope traces," Appl. Opt., vol. 10, pp. 2554-2555, Nov. 1971.

DIGITAL IMAGE PROCESSING
FOR PHOTO-RECONNAISSANCE APPLICATIONS*

Fred C. Billingsley
Jet Propulsion Laboratory, Pasadena, California

INTRODUCTION

Images (usually, but not necessarily, photographs) may be considered to be the record of events or conditions, and are generally used in one of two ways: Inspection and analysis by eye, where the preciseness of the brightness reproduction is secondary; and/or numerical analysis and data extraction, where the preciseness of geometry and/or brightness may be of paramount importance. It is quite likely that a given picture, although taken for a particular reason, may not be in the optimum condition to fulfill its objectives. In addition, if a given picture is used for other than its intended original purposes, a completely new approach to the presentation of its data may be indicated. Therefore, it may be expected that image processing will be of benefit in optimizing the image use.

Available in a practical sense are four different techniques for image processing: Incoherent optical processing has been utilized for years in the photographic industry, as exemplified by the darkroom manipulation for contrast manipulation, density, slicing, dodging, photogrammetric rectification and the like. Photographic manipulation of black and white separations of color images allows wide variations in the color produced. Multi-film sandwiching operations produce such effects as unsharp masking, difference comparisons and superpositions.

With the advent of the laser, coherent optical processing has become popular in the last few years. Its main impact has been to give access to the Fourier transform plane for such operations as spatial frequency filtering and correlation. In addition, the production and reproduction of holographic images fall in this category.

Analog electronic techniques have been widely used to vary the condition of electronic signals which when reproduced as images result in image alteration.

Preceding page blank

The most popular exemplification of this technique is the set of video adjustments (contrast, brightness, hue) found on every television set. In addition, horizontal and vertical image sharpening is accomplished during the transmission of television programs.

The modern <u>digital</u> computer has made practical processing techniques for handling non-linear operations in both the geometrical and intensity domains, various types of noise cleanup processes which are non-uniform over the extent of the picture and has made possible numerical analyses of pictures. The entire gamut of processing operations is available: affine or non-affine geometrical transformation, application of camera calibration data, intensity shading and contrast manipulations, one or two dimensional spatial filtering, coherent or non-coherent noise removal, numerical data extraction, multi-picture comparison, etc.

Our primary concern here will be with the digital processing, using as illustrations pictures processed by the Image Processing Laboratory of the Jet Propulsion Laboratory. The techniques for image processing have been developed primarily for processing pictures as returned from the NASA space vehicles (for example, Ranger, Surveyor, and Mariner) to the Jet Propulsion Laboratory. However, these same techniques, and to a very large extent even the same specific programs, have been utilized to process pictures from electron and light microscopes, industrial and medical radiographs, Apollo pictures of the earth and moon, and various aerial photographs. Some of these will be illustrated later.

It is useful to consider the image processing techniques to be grouped into three general areas depending upon the use to which the processed image is to be put:

●   Enhancement - The modification of subjective features of a picture to alter the impact of that picture on the viewer. In general, the enhancement processing will not produce a picture with numerically accurate data.

●   Quantitative Restoration - The application of camera calibration or other numerical data to the picture content so that the resulting picture has point-for-point numerical meaning. The primary effort here has been the application of camera calibration data to remove camera artificats, although the removal of other contaminants such as atmospheric effects belongs in this category.

● Information Extraction - The conversion of the picture data into the information or decision required by the analyst, perhaps with a reduction in the quantity of information required.

Images taken on photographic film will show appreciable film grain noise if analysis of very fine detail is required. This effect is particularly noticeable in the high-speed film used to photograph very faint images. An example of this type of noise is shown in Figure 1, in which the upper left hand framelet shows considerable contamination of the picture content by the noise. In this processing sequence, a series of eight exposures of the same object was made. These were digitized independently and registered in the computer, following which 2, 4, and all 8 of the images were averaged in the computer. The result of the noise cleanup from this averaging process is shown in the other three framelets of Figure 1.

One of the early applications for digital processing was the analysis of the roughness of the lunar surface. For this analysis, altitude contours of the lunar surface were derived from the (monoscopic) pictures taken by the Ranger spacecraft by utilizing the known photometric function (reflected brightness vs. viewing angle) (1). One of the Ranger pictures, its photogrammetrically rectified equivalent, and the altitude contours are shown in Figure 2.

Since this analysis used the reflected brightness to determine surface slope, it is important that the brightness be accurate. Since television camera systems are not sufficiently uniform in their intensity response over the face of the picture, corrections must be applied. For this purpose a brightness response function is derived for every pixel in the picture from a sequence of flat field pictures taken at different brightnesses. The results of this process is illustrated by one of the Surveyor pictures, Figure 3. A demonstration of the variation in camera response across the test field is shown in Figure 4, in which are shown the flat fields as seen by a Mariner '69 camera at two different brightnesses.

The true ground coverage plot of the contours shown in Figure 2 was produced by geometrically rectifying the incoming picture. This, and other geometric manipulations to be described below, is done digitally by defining to the computer the new desired locations of known points. Locations of all the intermediate points are generated by interpolation and the output picture generated.

A major use for digital filtering at JPL has been for the enhancement of the high spatial frequency content (fine details) of the pictures. An example of this process is given in Figure 5, which shows the appreciable sharpening of a
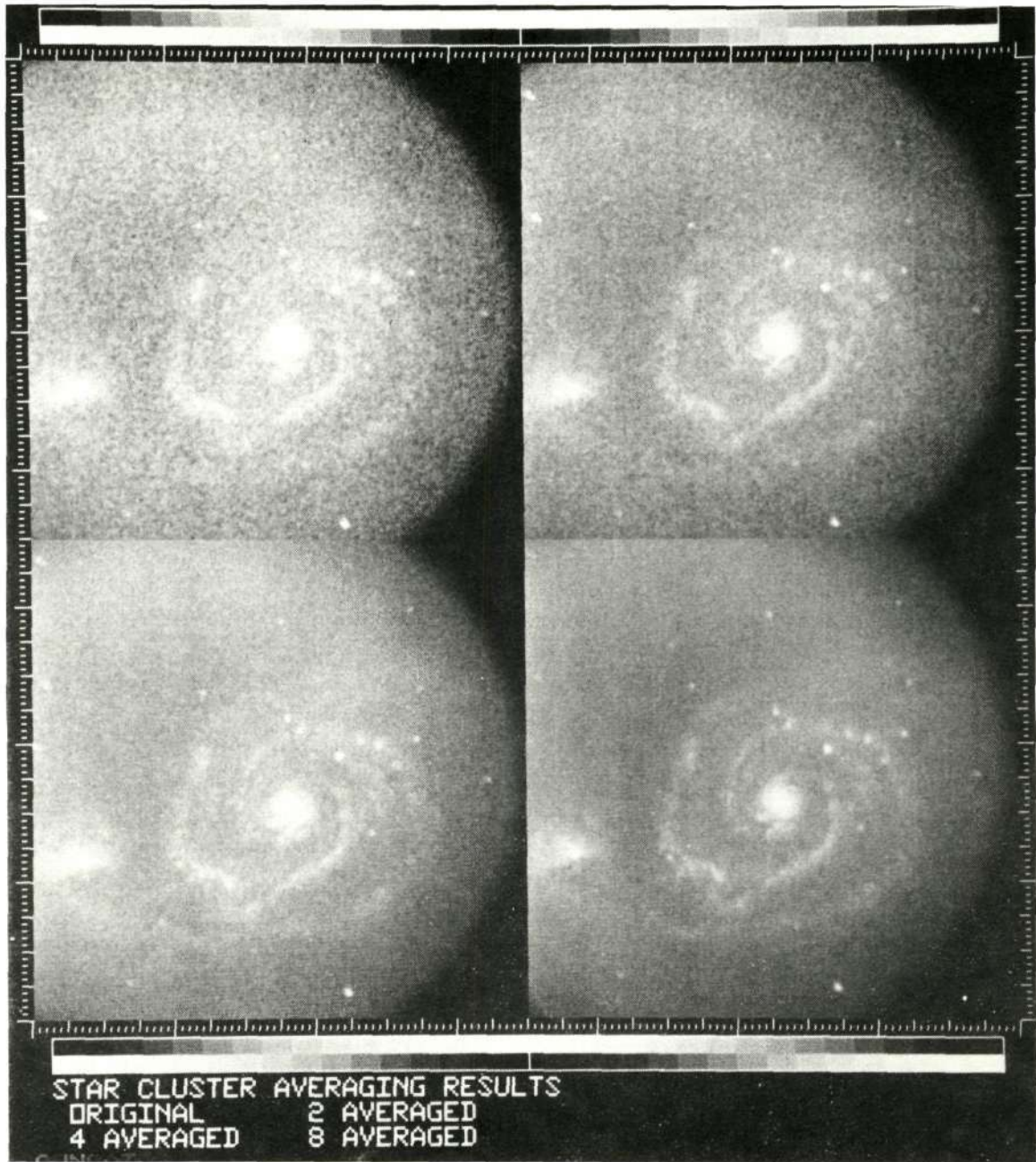
Figure 1. A Single Image (Upper Left) Shows Appreciable Film Noise – Original Nebula Diameter Was Approximately 4mm. The Result of Computer Averaging of 2, 4, and 8 Independent Original Images is Shown in the Upper Right, Lower Left, and Lower Right.
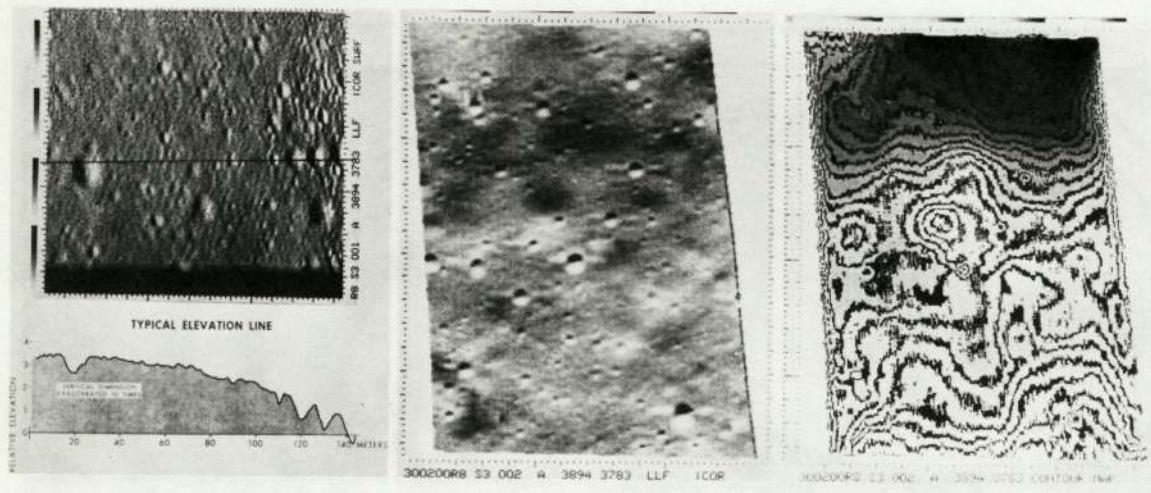
a. Original Ranger   b. Photogrammetrically   c. Altitude Contours
   Picture   Rectified Picture   Derived from b

Figure 2. Derivation of Altitude Contours from Photometry
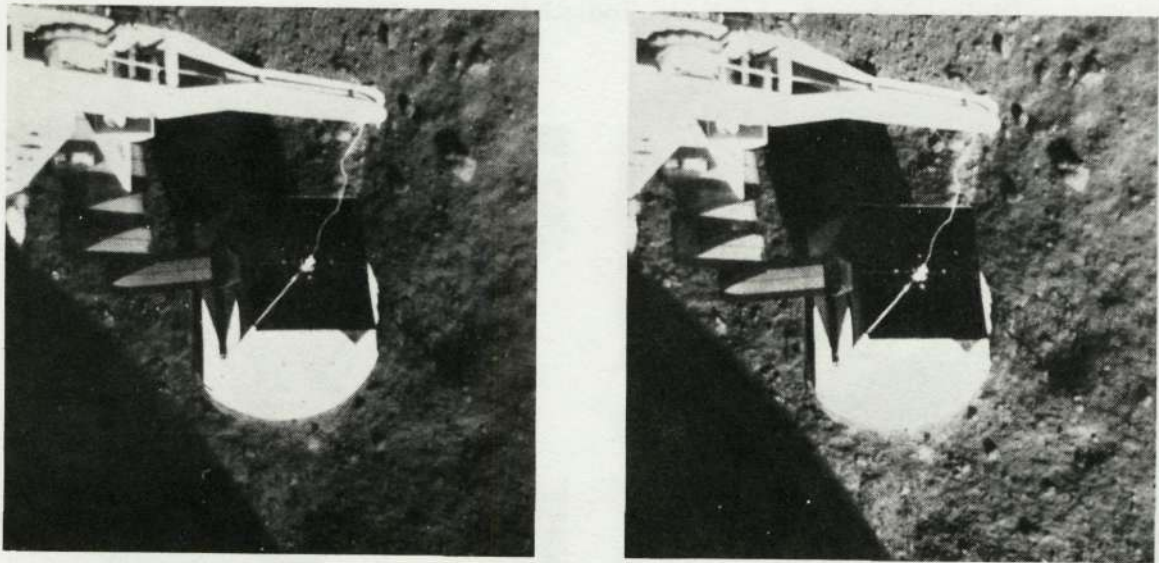
a. Before Correction   b. After Correction

Figure 3. Correction of Intensity of a Surveyor Picture
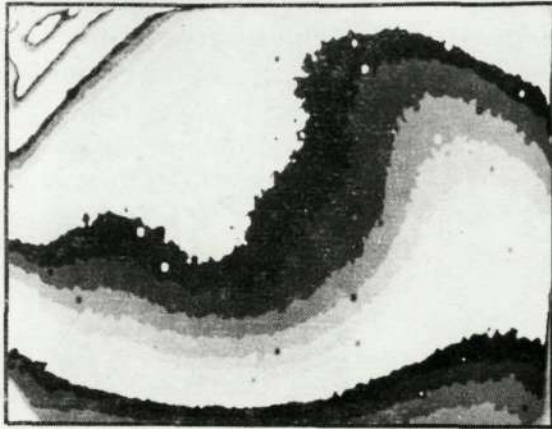
100 FOOT-LAMBERTS   1600 FOOT-LAMBERTS

Figure 4. Intensity of the Mariner '69 Camera to Flat Fields of Different Bright-
nesses. The Contouring has been Produced by Removing the Three Most
Significant Bits and Stretching the Remainder to Cover the Entire Bright-
ness Range. Thus Each Contour Sequence Represents a Range of 8
Digital Numbers of the Original Data.
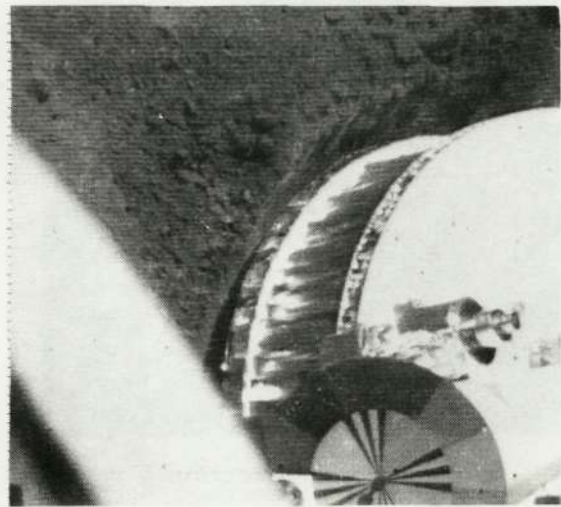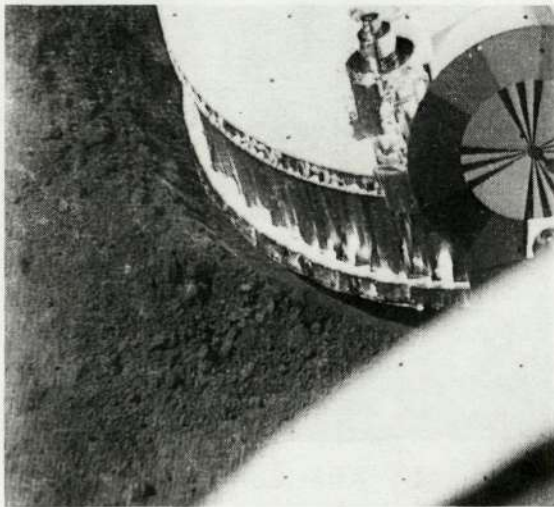
Figure 5. Enhancement of High Spatial Frequencies on a Surveyor Picture

picture due to this type of filtering. Our approach to this process is discussed by Nathan (2) and illustrated in Figure 6. Consider the image of a star. Due to the geometry involved, this image should be essentially a delta function, having zero dimension. In practice, however, this image will have a finite diameter, due to light which should have impinged at the delta function point arriving instead in the nearby area. The job of the high frequency enhancement filter is to gather this nearby light and re-insert it at the delta function point. A ring of negative values around the central pixel will remove the unwanted light and a very high value at the center will re-insert it there. This effect and the numerical values of a practical filter are given in Figure 6, together with the equivalent effect in the spatial frequency domain.

The most recent JPL space missions, the Mars flybys in 1969 and 1971, required, in addition to the above types of processing, a more complete noise removal (3). Because of the complexity of the coherent noise pattern (Figure 7a) filtering was done using two-dimensional Fourier transform techniques. The

MTF ROLLOFF CORRECTION

δ Function Object   Point-Spread Image   Correction Function   Truncated Correction

SPACE DOMAIN

FREQUENCY DOMAIN

-.0016	-.0002	-.0019	.0022	.0003	-.0016	-.0027	-.0030	← Center Column
-.0008	.0017	.0020	-.0010	-.0040	-.0041	-.0026	-.0017	
.0007	.0024	-.0008	-.0051	-.0037	.0026	.0079	.0096	
.0020	.0010	-.0048	-.0051	.0048	.0146	.0156	.0137	
.0026	-.0014	-.0070	.0002	.0156	.0149	-.0067	-.0206	
.0023	-.0039	-.0068	.0075	.0199	-.0080	-.0696	-.1029	
.0019	-.0054	-.0056	.0129	.0169	-.0417	- 1432	-.1953	
.0016	-.0059	-.0049	.0147	.0143	-.0579	-.1763	2.7637	← Center Row

UPPER LEFT QUADRANT - MTF CORRECTION MATRIX

Figure 6. Action of a High Frequency Filter in the Real and Fourier Domains

Fourier transform process produces a "picture" displaying as brightness the spatial frequency content of the picture in two dimensions. A coherent noise will display itself as a geometrically arrayed series of bright areas as shown in Figure 8a. The first step in the filtering is to locate each of these areas. The inverse transform of the array of areas is the noise pattern itself (Figure 7b), which may be subtracted from the picture directly. An alternate method of filtering is to suppress the areas containing the noise spikes in the Fourier domain and then to re-transform the picture-sans-noise spikes back to the real domain. The result is shown in Figure 8b.

a. Original Picture
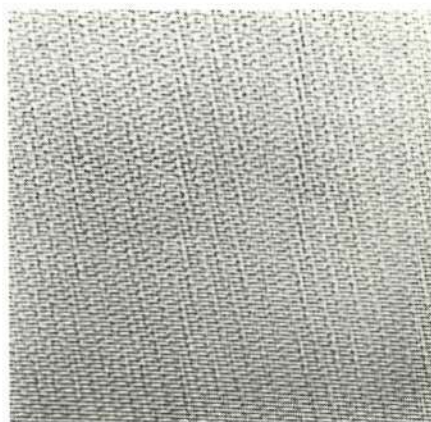
b. Isolated Noise

Figure 7. Mariner '69 Picture with Coherent Noise
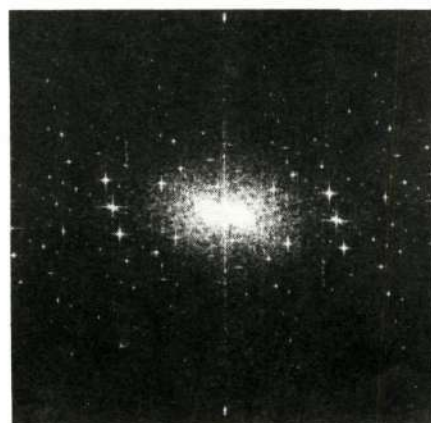
a. Fourier Transform
of Picture of 7a

b. Picture After Removal
of Noise

Figure 8. Removal of Coherent Noise by Fourier Techniques .

The difference in processing required for different uses of a picture is shown in Figures 9 and 10. Figure 9 is one of the Mariner '69 pictures which has been correctly photometrically rectified (i.e., photometric calibration has been applied). The large difference in brightness between the south polar cap and the surrounding areas fairly thoroughly obliterates detail in these areas, although the numbers in the digital form of the picture are correct and useful for photometric analyses. To render more of the detail visible, the low spatial frequency photometry was deliberately destroyed by using a filter which greatly reduces the low spatial frequency content. This reduces the large black-to-white excursions and superimposes all of the fine detail on a more or less medium gray background. This "maximum discriminability" picture has proven quite useful in the analysis of surface features where photometry was of secondary consideration.

COLOR CONSIDERATIONS

Operations in the color or multispectral domain have proven useful for both enhancement for human viewing and for numerical data extraction. Because the eye is more sensitive to changes in hue than it is to changes in brightness, a conversion of brightness to hue will render subleties of detail more readily visible.

A step-wise conversion of this type is shown in Figure 11. In Figure 11 is a picture taken by the S-158 Lunar Multispectral Photography Experiment on Apollo 12, together with seven slice pictures. These slice pictures were
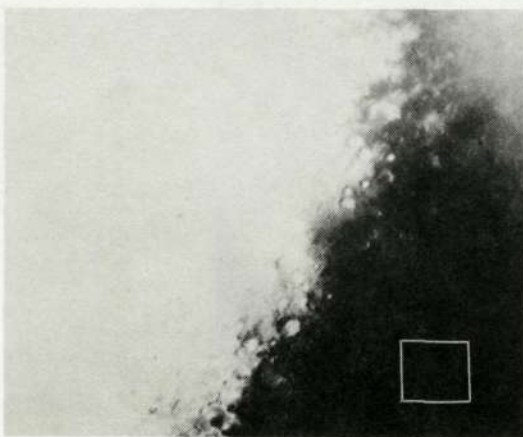
Figure 9. Mariner '69 Picture Processed for Photometric Restoration
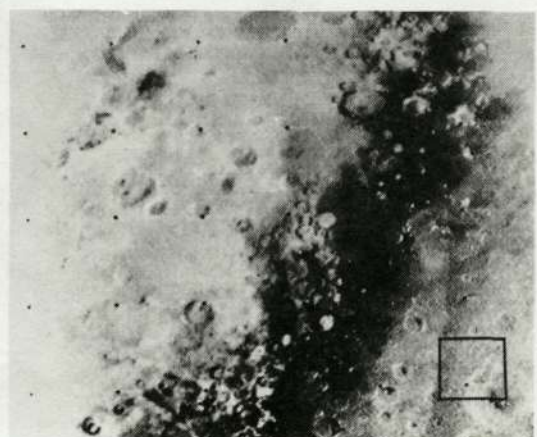
Figure 10. Mariner '69 Picture Processed for Maximum Discriminability
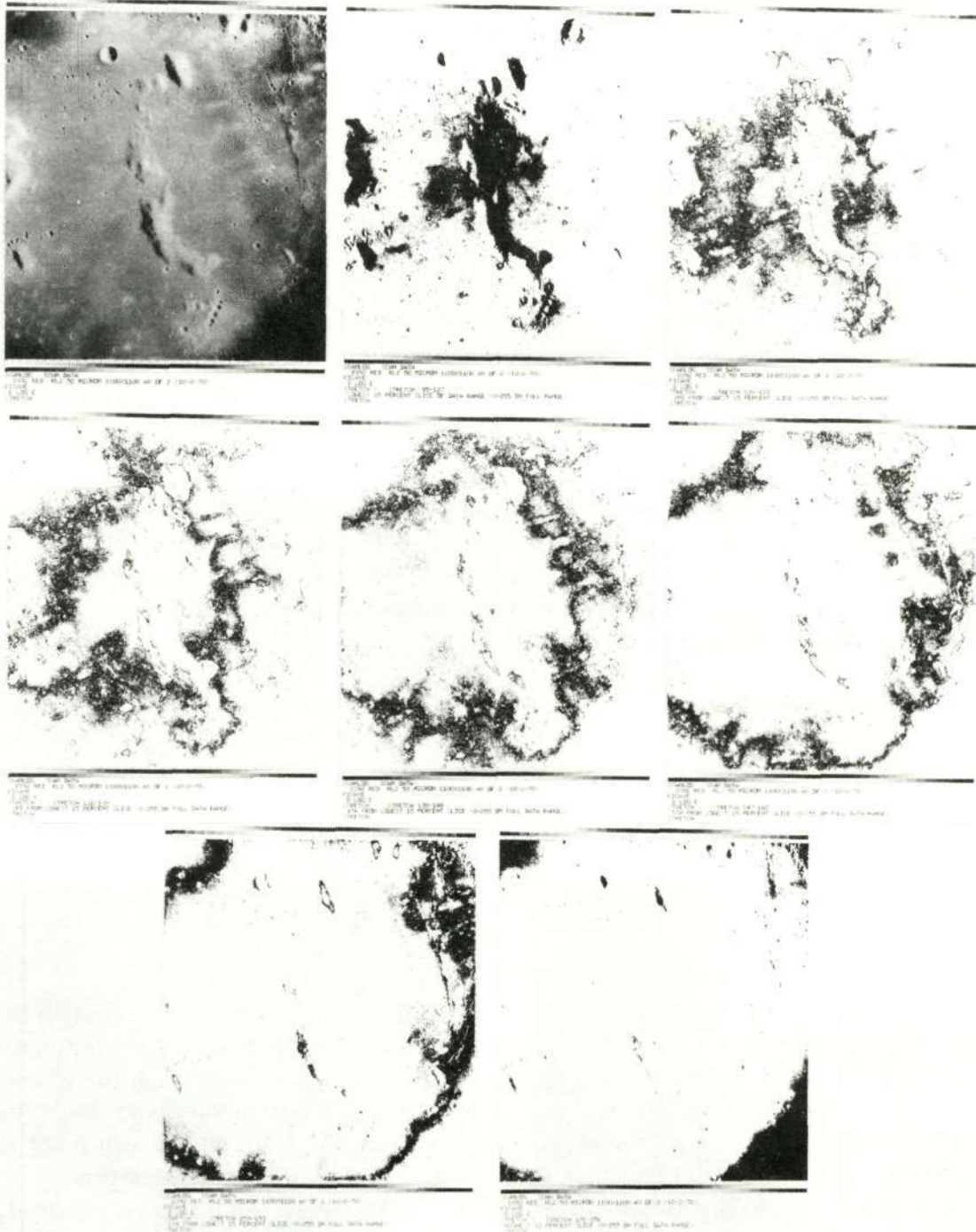
Figure 11. Apollo S-158 Image. Original, and Seven Platform Slices of Equal Data Quantity

E

formed by dividing the original brightness range into seven sub-ranges such that each sub-range contains the same number of data points. Each slice picture is then formed by printing its data points in black on a white background. Each slice range may be reproduced in a different color and the ranges superimposed to give a rendition in which color represents brightness. A similar type of platforming is currently available in hardware which operates in real time on pictures obtained by television camera pickup.

Manipulations of multispectral data can be used to isolate areas of various spectral properties. Various combinations of visible and infrared multispectral imagery have been used for a wide variety of investigations in the areas of geology, meteorology, oceanography, agriculture, and forestry. The more successful of these investigations are those using computer-based multivariate analysis, although some success has been achieved using visually interpreted multicolor photography (4).

Multispectral work will be illustrated here with two examples from the S-158 experiment. In the first example, two spectral bands are used to determine the relative redness-blueness of various areas of the lunar surface (5).

Lunar color and its variation across the surface has interested planetary astronomers for many years. This interest has heightened with the growing weight of evidence, obtained from accurate earth-based photoelectric photometry, which points toward a positive correlation between color and compositional differences (6).

Of course, the variations in composition are of paramount interest in lunar exploration. Once we have obtained ground observational data at several sites of differing color, it should be possible to extrapolate compositional color information to large areas of the moon which will not be sampled in situ.

For this purpose, pictures of the same area were taken on black-white film through two color filters (Figure 12). After registration in the computer, the data was intensity corrected to log exposure, after which the pictures were subtracted, one from the other. The conversion to log exposure and the subsequent subtraction produces a picture whose numerical value at a given point is a measure of the red/blue ratio at that point. The resultant picture thus represents the red/blue ratio rather than the brightness for the area covered, for the digital processing has eliminated the brightness component. Figure 13 shows the red, gray, and blue areas each brought to saturation to indicate the respective locations. Color versions of these pictures are given in reference 5.

For the flight pictures from S-158, the extraction and presentation of color data was carried one step further to the simultaneous presentation of two color ratios (red/green and blue/green) derived from three input pictures. To do this, the hue ratios were assigned as the two axes of a Cartesian coordinate plane in which a unique color is assigned to each point. During the processing, at each picture element (pixel) location the red/green and blue/green ratios are determined and used as entry points into the color plane. The required color for that particular red/green, blue/green intersection is then generated by computer and inserted at the corresponding pixel location in the output picture. The actual output of the computer process is a set of four color separation negatives which are to be combined in a color printing process to produce the output color picture covering the originally photographed area. Color versions of these are given in reference 8.

An example drawn from a traffic motion study is shown in Figure 14. The left-most two framelets were taken a short interval apart so that moving

Figure 12. Mare Imbrium Area of the Moon

vehicles occur at different places. The third framelet results from the registration and subtraction of one original framelet from the other. In this, the freeway structure and stationary vehicles cancel and all moving vehicles are represented by an image pair. Thus, knowing the timing between the pictures and the spacing of the image pair, the vehicle speeds may be calculated. The right framelet results from displacing one of the originals from the other by an amount corresponding to, say, the speed limit. In this case, all vehicles going at that speed cancel and vehicles going above or below this limit show as differential pairs.

An example of geometric stretching of pictures for registration with other images (in this case a map) is taken from coherent sidelooking radar. The left framelet of Figure 15 is an original radar image after reconstruction to the real domain, with a computer grid superimposed. By knowing the aircraft
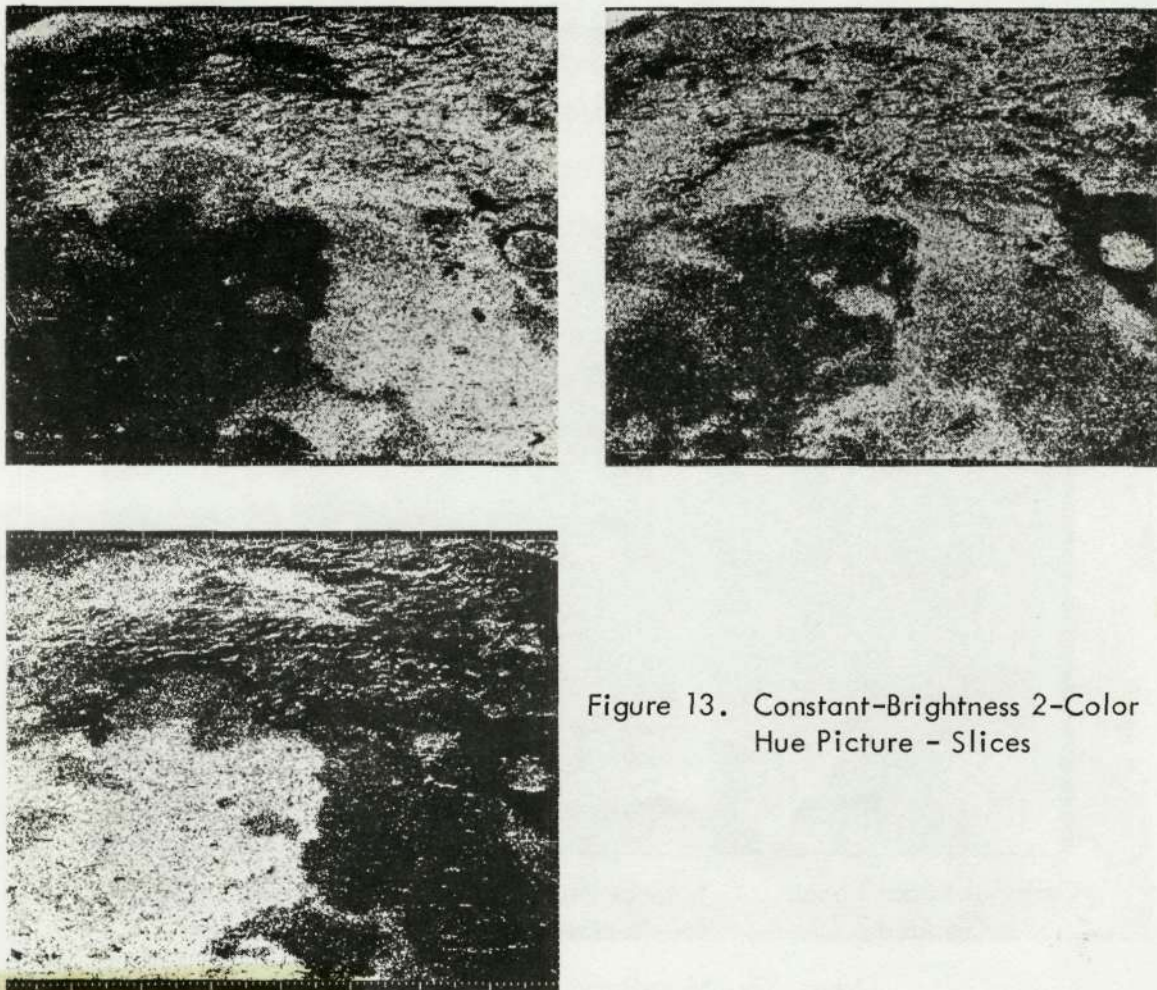
Figure 13. Constant-Brightness 2-Color
Hue Picture - Slices
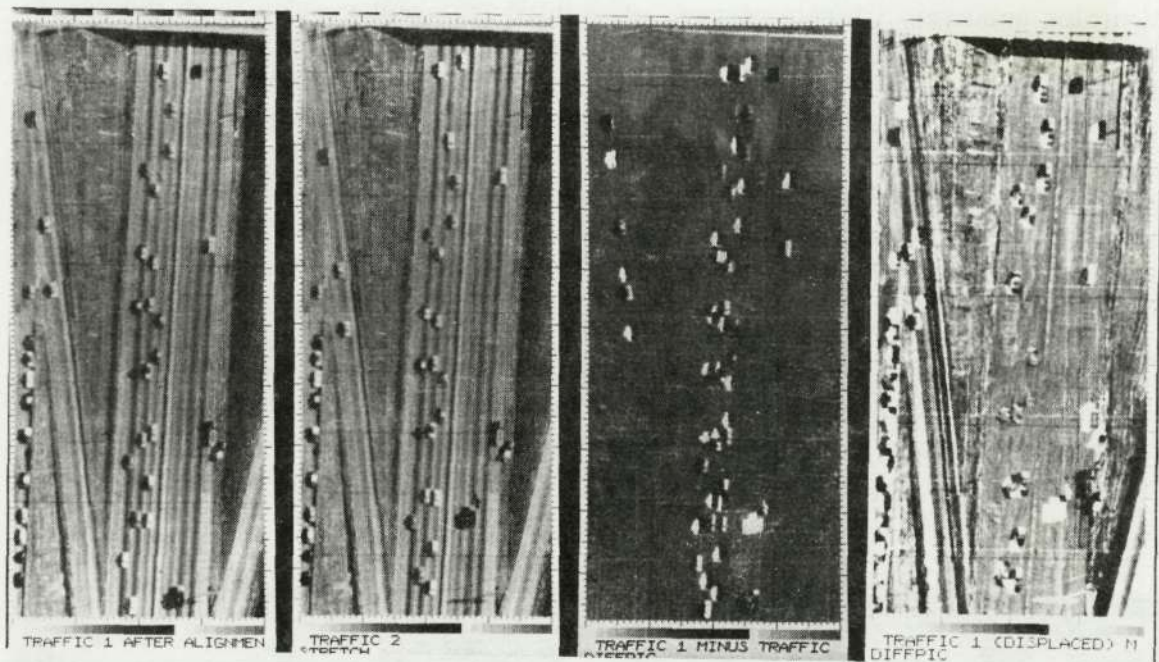
Figure 14. Traffic Motion
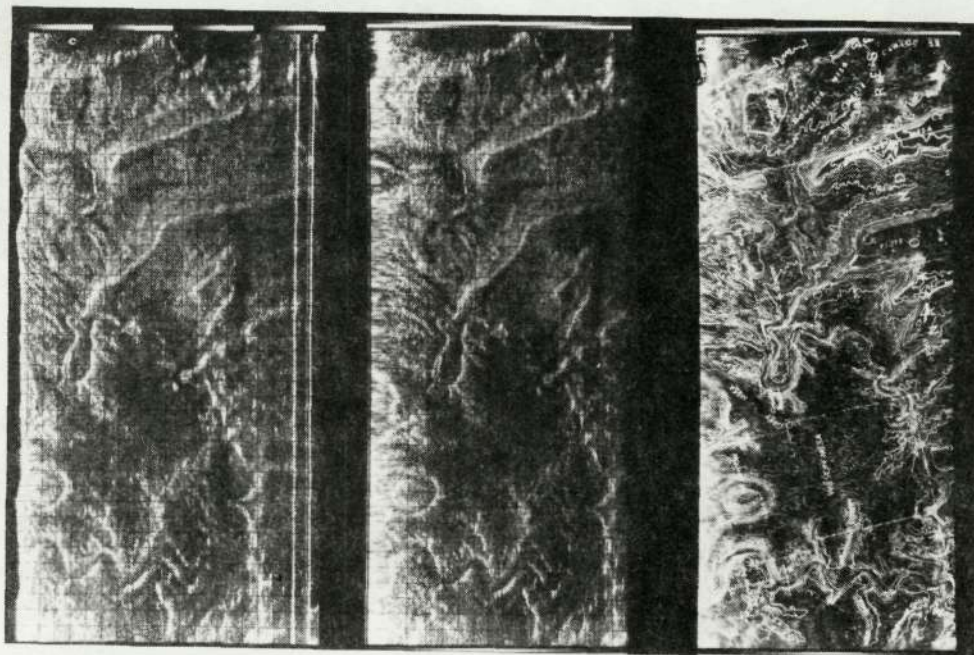
Original Radar Image
Gridded

Lateral Distortion
Removed

All Map Contours
Added

Figure 15. Radar Images

altitude and the geometry of the radar, the geometrical distortion caused by the sideways sweep may be calculated. The corresponding correction function may then be used to geometrically stretch the picture to produce true ground coverage of the image as shown in the center framelet. The right framelet is the same image softened by computer filtering and with computer superposition of contours from a topographic map to show the correlation between the radar and the mapped coverage.

The final example illustrates the use of geometric stretching of pictures to produce an orthographic photomap from a sequence of computer mosaicked picutres (Figure 16). In this sequence, five images from the Mariner 7 mission have each been geometrically distorted to display the picture in an orthographic projection. Following this, the individual frames were mosaicked by computer to produce the finished photomap. Details of the process are given in Reference 7.

CONCLUSION

The imaging processing techniques developed for enhancement and calibration of the JPL imaging experiments has proven useful, not only for the original application, but has successfully been applied to images from a wide variety of sources. As computer processing becomes more available and the processing costs decrease, and as the techniques are improved to produce more and more useful results, the use of computer processing for enhancement of imagery will increase.

As the techniques of parallel image processing improve, it is expected that some of the processes illustrated here will be so implemented. It is hoped that this discussion will prove useful in suggesting a group of processes which have been utilized, and which could benefit by some form of parallel processing.

ACKNOWLEDGMENTS

All of the above work was performed by personnel of the Imaging Processing Laboratory of the Jet Propulsion Laboratory. In particular, I would like to acknowledge the work of Dr. Robert Nathan, who fathered the original image processing development, Tom Rindfleisch, who developed the Ranger photoclinometry and guided the Mariner '69 processing effort, and Jack Lindsley for the radar processing.
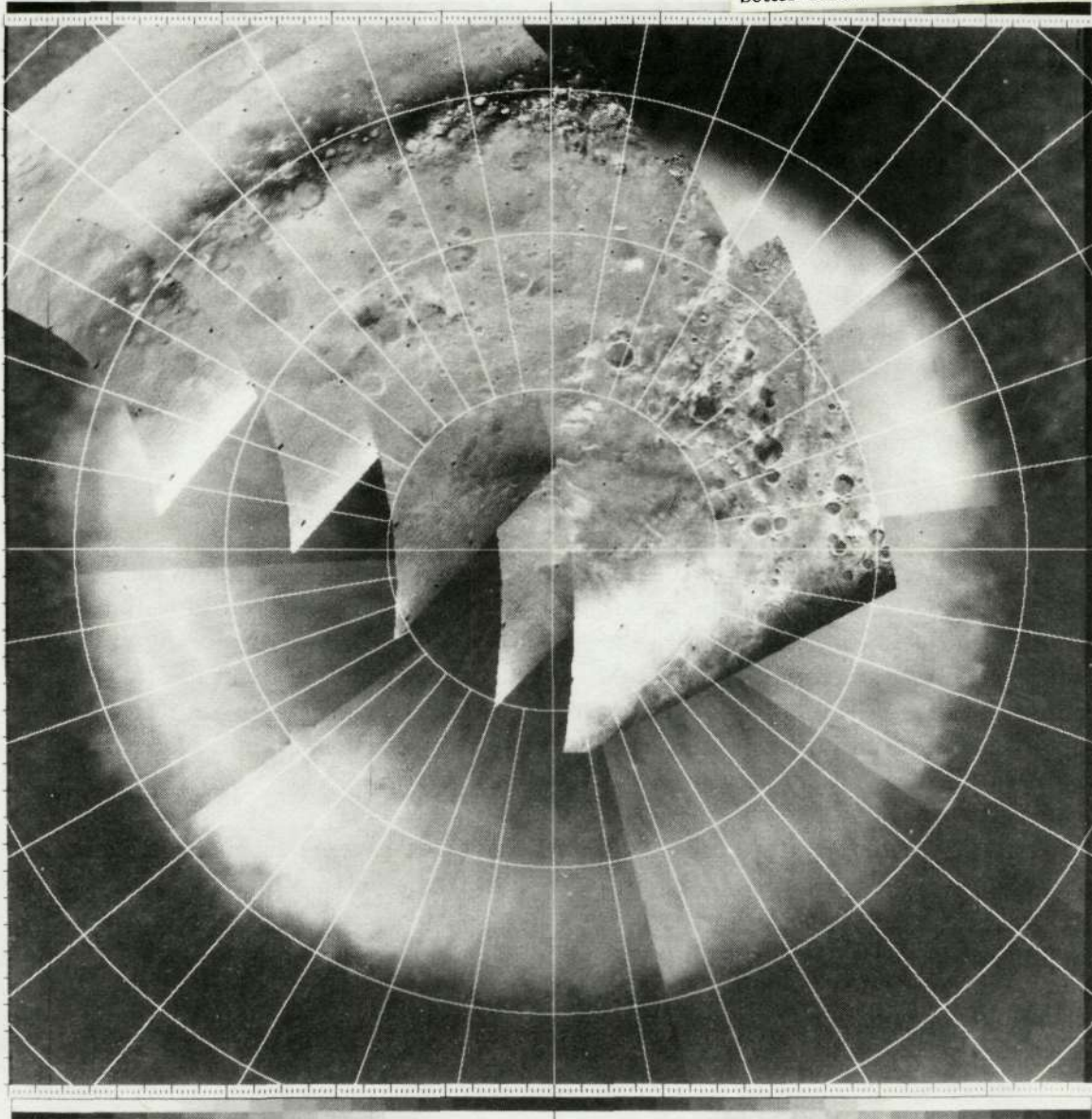
ORTHOGRAPHIC PHOTOMOSAIC OF THE SOUTH POLE OF MARS, MAX-D

08-30-71 215615 JPL/IPL

Figure 16. Five Frames (7N11, 7N13, 7N15, 7N17, and 7N19) from the Mariner 7 Mission have been Processed for Maximum Discrimibility, Computer-stretched for Proper Geometry, and Computer-mosaicked to Produce this Orthophotograph of the Martian South Polar Cap

REFERENCES

1. Rindfleisch, T. C., Photogrammetric Eng. 32, 1966, p. 262.

2. Nathan, R., Digital Video Data Handling, Techn. Rept. 32-887, Jet Propulsion Laboratory, Pasadena, Calif., 1966.

3. Rindfleisch, T. C., Dunne, J. A., Frieden, H. J., Stromberg, W. D., and Ruiz, R. M., Digital Processing of the Mariner 6 and 7 Pictures, Jour. Geo. Res., Vol. 76, No. 2, Jan. 10, 1971, p. 394-417.

4. Yost, E. and Wenderoth, S., Agricultural and Oceanographic Applications of Multi-Spectral Color Photography, 6th Symposium of Remote Sensing of Environment, Ann Arbor, Michigan, p. 145-173.

5. Billingsley, F. C., Goetz, A. F. H., and Lindsley, J. N., Color Differentiation by Computer Image Processing, Photographic Science & Engineering, Vol. 14, No. 1, Jan.-Feb. 1970, p. 28-35.

6. McCord, T. B., Color Differences on the Lunar Surface, Jour. Geo. Res., Vol. 74, 1969, p. 3131.

7. Gillespie, A. R. and Soha, J. M., An Orthographic Photomap of the South Pole of Mars from Mariner 7, Icarus, Vol. 16, No. 3, June 1972, p. 522-527.

8. Billingsley, F. C., Computer-Generated Color Image Display of Lunar Spectral Reflectance Ratios, Phot. Sci. & Engrg. 16:1, Jan-Feb. 1972, p. 51-57.

REVIEW OF OPTICAL MEMORY TECHNOLOGIES

D. Chen

Honeywell Corporate Research Center, Hopkins, Minnesota 55343

N73-18688

ABSTRACT

The demand for large capacity fast access time memory
has increased to an extent beyond the reach of conventional
magnetic memory technology. New approaches involving
optical technology have been introduced to meet this chal-
lenge. Using optic beam for addressing, the information bit
size can be as small as optical wavelength, resulting in a
packing density of 10^7-10^8 bits/cm^2. The ability to focus a
beam at a distance eliminates the problem of crash and wear
between the read-write transducer and the medium. With the
introduction of inertialess beam deflectors, and the use of
page oriented technique such as the holographic storage, the
access time of such a large memory may be reduced to
microseconds.

The basis for these promises is founded in the research
progress made in recent years in the areas of materials,
optical phenomena and laser applications. Of the various
optical memory techniques advanced to date, magneto-optic
and electro-optic approaches appear to be most promising
and therefore will be reviewed in particular. In the for-
mer case, the thermomagnetic effects induced by localized
heating on a suitable magnetic medium from a focused laser
beam is utilized for writing and magneto-optic effect is
utilized for reading. The electro-optic writing techniques
include the laser damage, the ferroelectric and ferroelectric-
photoconductive effects. The read-out signal is derived from
the electric discharge or the electro-optic effect. Besides
these, other optical techniques such as the photochromic,
thermoplastic, and amorphous semiconductor will also be
reviewed.

To make a mass memory system from these technologies,
there are a number of essential considerations and trade-offs
that require careful examination. Considerations such as
the laser heating requirements, the depth of field for the

Preceding page blank

focusing optical system, the practical packing density and the problems associated with the signal-to-noise ratio in the readout have to be studied together. Trade-offs between the packing density, access time, data rate, and other important parameters are of prime concern to the memory system design. These topics will be discussed with particular reference to a system using MnBi films.

Beyond the bit-by-bit type memory, holographic memory system offers unique advantages and warrants further discussion. It is believed that the advantages offered by optical memory technique can be extremely useful for the onboard bulk memory and data processing needs in future earth observation systems.

DATA PROCESSING REQUIREMENTS FOR THE EARTH RESOURCES TECHNOLOGY SATELLITE (ERTS)

John Y. Sos
NASA Goddard Space Flight Center

INTRODUCTION

N73-18689

The concept for an ERTS, the first in a series of earth observation satellites, was published in 1967. Between that time and the approval of the ERTS project in January 1969, the subsequent studies in 1969-70, and the implementation phase which started in July of 1970, the data handling requirements for the system were being formulated. There were many problems in trying to assess these requirements as is the case in any interdisciplinary program of that magnitude. In particular it was difficult to clearly identify the users, determine their requirements for product types and to estimate the data volume.

In this paper some of the data handling considerations that led to the formulation of the data processing requirements for the ERTS system will be discussed. The significant parameters that influenced these requirements are: (1) payload characteristics, (2) spacecraft characteristics such as orbit, attitude and attitude rates, (3) payload coverage, and (4) product types and quantities. Items 3 and 4 have had the most significant influence on the generation of the requirements.

PAYLOADS

The ERTS imaging sensors consist of a return beam vidicon (RBV) camera and a multispectral scanner (MSS). The scanning geometry of the sensors is shown in Figure 1.

The MSS images the surface of the earth in four spectral bands through the same optical system. The scanner covers spectral range of 0.5-1.1 micrometers. It uses an oscillating mirror which scans normal to the spacecraft velocity factor. The spacecraft motion provides along the track progression of the scan lines. The MSS detector outputs are sampled, coded to six bits, and formated into a continuous data stream of 15 megabits per second.

Since the MSS is a line-by-line continuous scanning device, the geometry of MSS images recorded on film is influenced by spacecraft attitude rates in all three axes (pitch, roll, yaw).
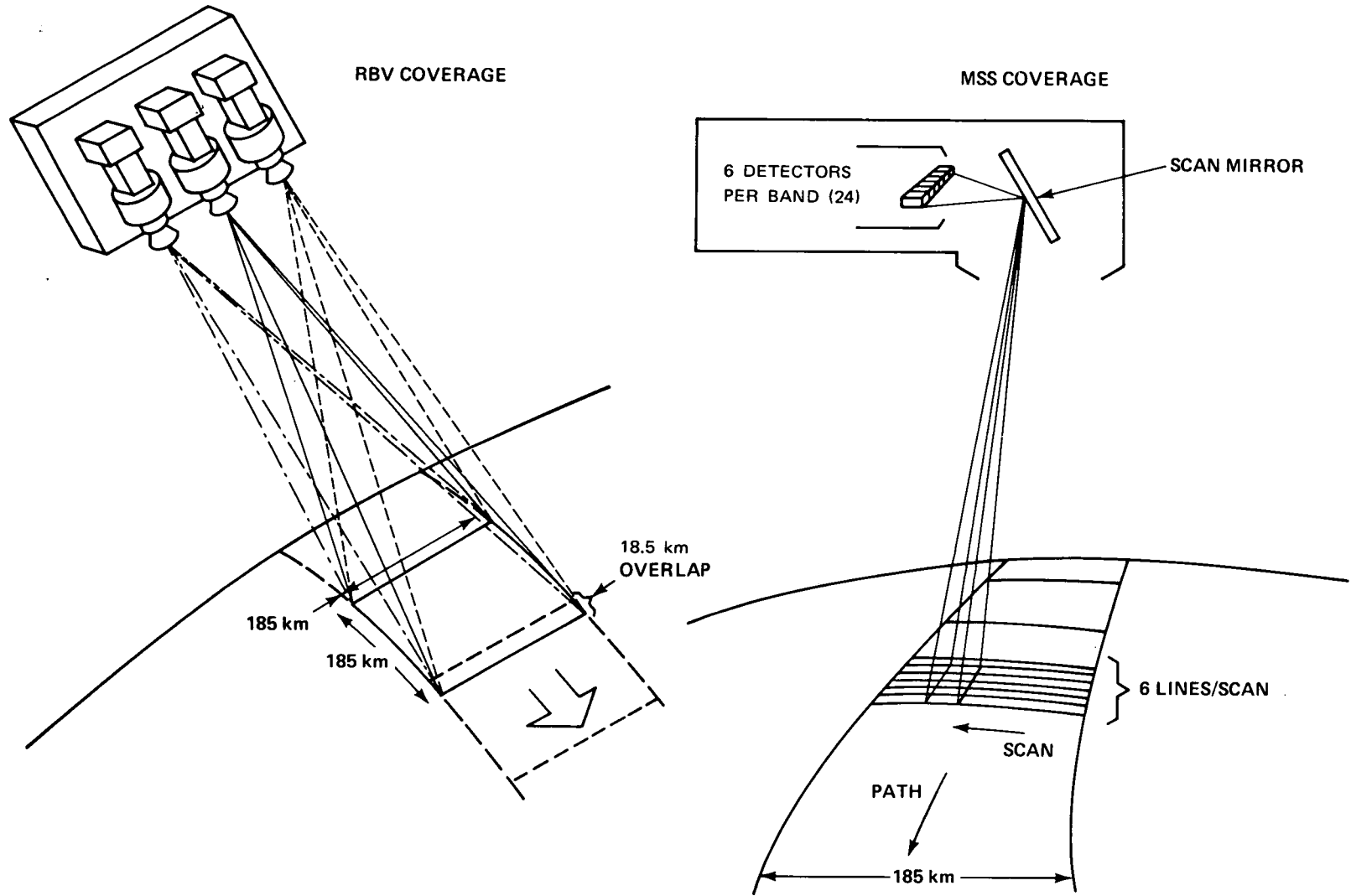
Figure 1. Payload Coverage

The RBV system operates by simultaneously shuttering at 25 second intervals three cameras, covering the .475-.83 micrometer range. Images stored on photosensitive surfaces of the camera tubes are read out by an electron beam. To provide a video signal output, each camera is read-out sequentially, requiring a video bandwidth of 3.5 MHz during read out..

The RBV is not sensitive to spacecraft attitude rates because each 185 x 185 km image is stored on the photosensitive vidicon surface in a few milliseconds. Non-linearities on the sweep circuitry of the camera read-out electronics and boresight errors in the alignment between the 3 cameras require geometric corrections on the ground that are different from those applied to the MSS images.

When operating over a ground receiving station, the MSS and RBV data are transmitted in reel time to the receiving site and recorded there on magnetic tape. For operations not in view of a receiving site, 2 wide-band video tape recorders are included as part of the payload. Each recorder records and reproduces either RBV or MSS data upon command and each has a record capacity of 30 minutes.

SPACECRAFT COVERAGE

The spacecraft operates in a circular sun-synchronous, near polar orbit at an altitude of 908 kilometers. It circles the earth every 103 minutes, completing 14 orbits per day, and viewing the entire earth every 18 days. The orbit has been selected in such a way that the ground trace repeats the earth's coverage at the same local time every 18 days to within ±18 kilometers.. A typical one day ground coverage trace is shown in Figure 2.

Figure 3 illustrates the sensor operation time required to cover the land masses of the earth as a function of season. The payloads would be required to operate between 80 and 200 minutes every day in order to completely cover the earth's land masses. Due to the fact that such coverage requirements do not exist at the present time, that the surface of the earth is on the average 50% cloud covered, that sidelap of over 50% exists at above 60° North or South latitude and that the life of the onboard tape recorder is limited, the average daily payload operation of 78 minutes per day has been selected as the basis for determining the data processing workload requirements. This includes a full real time coverage of the continental U. S. (18 minutes), and 60 minutes of tape recorded coverage. This in turn translates into a daily acquisition of 188 185 X 185 km. scenes in each of the seven spectral bands (3 RVB and 4 MSS).
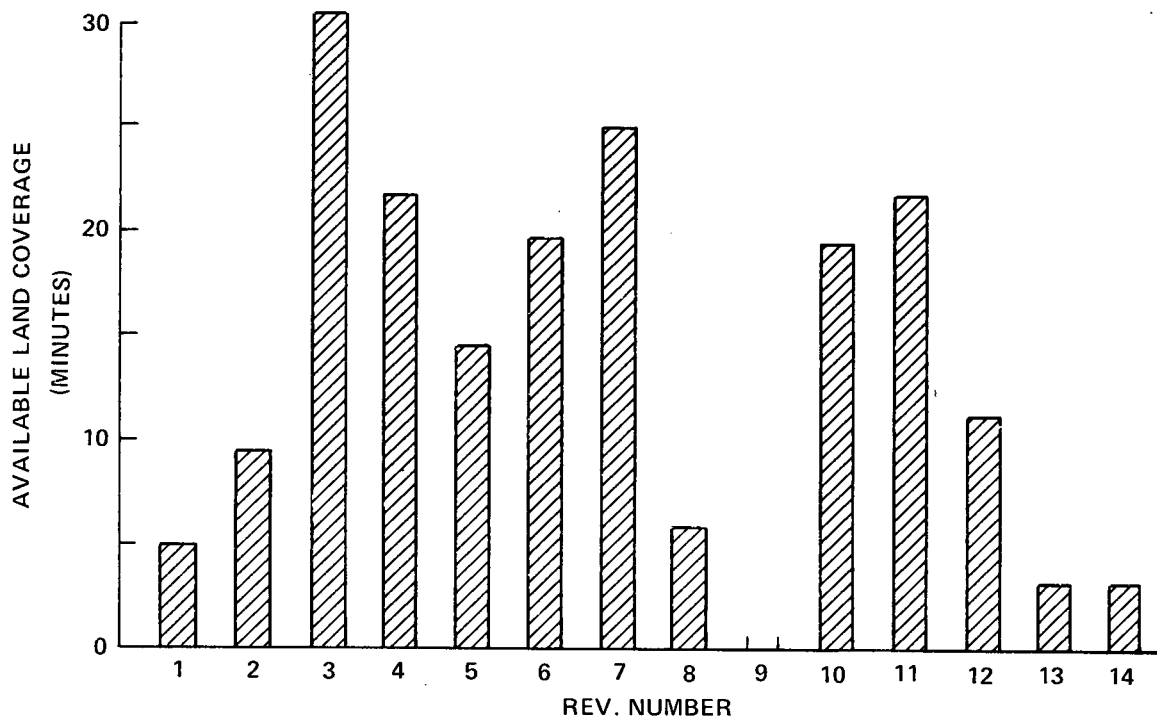
Figure 2. Orbit-to-Orbit Coverage Variation

DATA PROCESSING WORKLOAD

The 188 scenes per day, taken in 7 spectral bands generate 1,316 individual image frames per day or 3.3 million frames per year. If these data were to be handled in digital form, a storage medium with a capacity of 10^{11} bits per day or 3.6 X 10^{13} bits per year would be required.* With practical formating considerations this volume of data would require approximately 500,000 reels of standard computer magnetic tape to store the master copy. The actual number of tapes required would depend on how many copies of each image were desired. The obvious conclusion that one comes to is that the

---

*The above figures were derived as follows:

a) RBV: 4 X 10^3 lines/frame X 4 X 10^3 samples/line = 1.6 X 10^7 samples/frame X 6 bits/sample = 10^8 bits/frame X 3 frames/scene = 3 frames/scene = 3 X 10^8 bits/scene

b) MSS: 2.6 X 10^3 lines/frame (185 km swath) X 3.3 X 10^6 samples/line = 8.6 X 10^6 samples/frame X 6 bits/sample = 5 X 10^7 bits/frame X 4 frames/scene = 2 X 10^8 bits/scene

c) RBV and MSS: 3 X 10^8 + 2 X 10^8 = 5 X 10^8 bits/scene X 188 scenes/day = 10^{11} bits/day X 356 days/year = 3.5 X 10^{13} bits/year
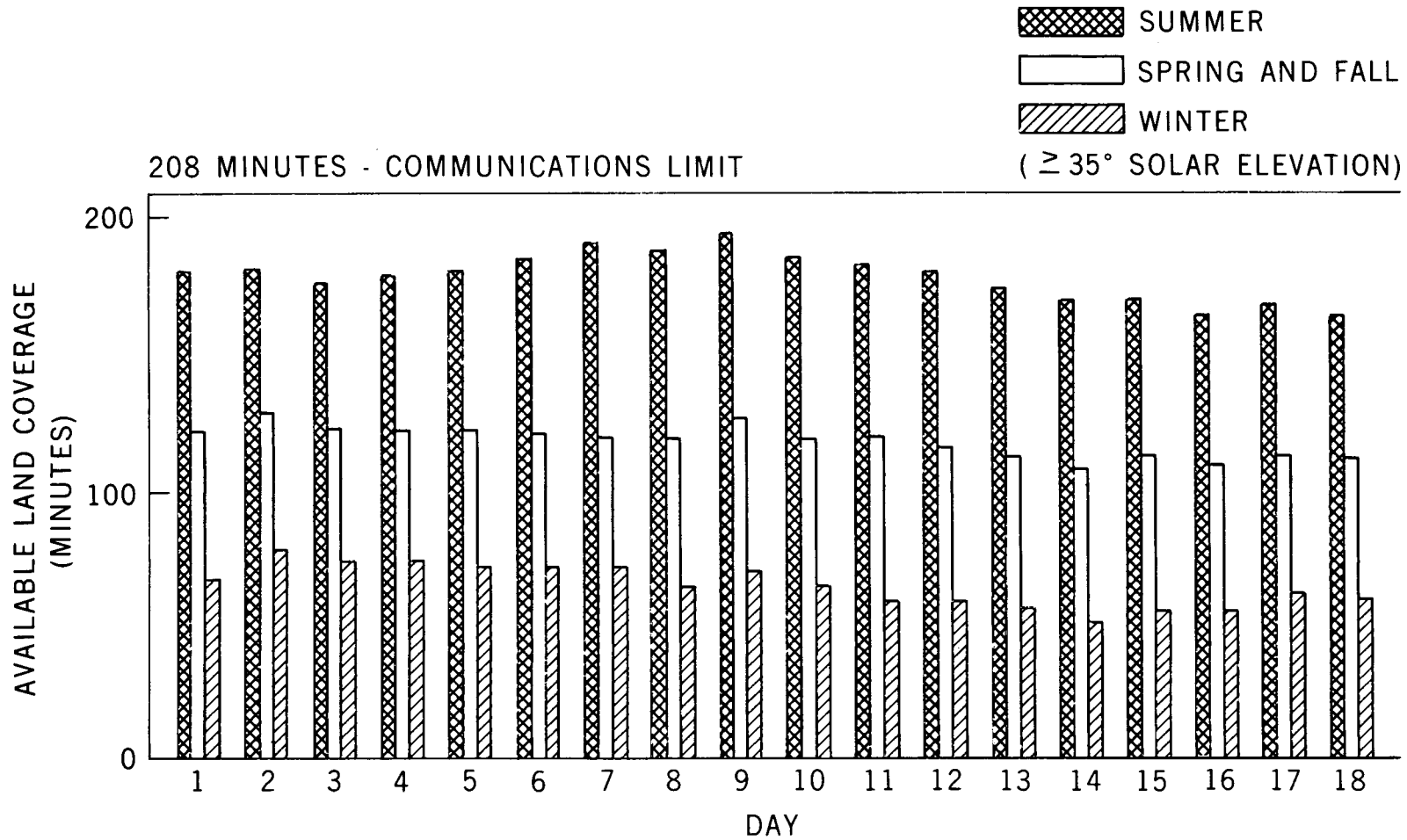
Figure 3. Daily and Seasonal Coverage Variation

storage and distribution of all ERTS-A image data cannot be done in the form of computer tapes for practical reasons. Because one deals with image data and because of the majority of investigators in the various disciplines have been in the past dealing with aerial photographs, photographic film would be a more practical medium for recording and distribution of the image data. It has been therefore planned to distribute all of the ERTS data in the form of photographs and only deliver a relatively small portion (10%) of the data in the form of digital tapes to investigators who are equipped to handle it or who are developing new techniques for utilization of digital image data.

DATA HANDLING FUNCTIONS

Prior to the description of the various data handling functions that are required for the conversion of the spacecraft-telemetered sensor voltages into user products, definition of terms is in order, since nomenclature has not been standardized in this area. Key data handling functions are defined below:

a. Data acquisition - reception of the sensor and housekeeping telemetry signals, demodulation, tape recording and transmission of these signals, tracking and commanding of the satellite.

b. Data processing - conversion of video signals to a number of standardized user products and distribution of these to the users. This function includes the application of in-flight calibrations to all data, tagging of all data with identification and location information based on spacecraft orbit and attitude, application of geometric corrections based on spacecraft ephemeris and/or use of ground control points.

c. Data analysis - All discipline-related operations, such as generation of ocean temperature maps, land use maps, enhancement of linear features, extraction of information, correlation of data from many sources, etc.

For ERTS-A existing NASA tracking stations provide the data acquisition support with the installation of special demodulation and data recording equipment. Three stations located in Fairbanks, Alaska, Goldstone, California, and Greenbelt, Maryland, will provide real time coverage for continental United States. Onboard video tape recorders will provide data recording capability for the remainder of the required world coverage.

Image processing functions such as conversion of tape-recorded video signals to photographic film, application of radiometric calibrations to the data and removal of geometric distortions from the imagery can best be performed in a central data processing facility prior to the distribution of the data

to the users. All of the required data such as spacecraft orbital parameters, in-flight and pre-flight calibration parameters are available in this central location. For this reason the data processing functions for ERTS are to be performed in a central data processing facility located at GSFC.

All data analysis functions for ERTS are planned to be performed by the investigators in their facilities. The reasons that led to this decision were as follows: the interdisciplinary nature of the program would require a large array of analysis algorithms for conversion of raw images to such products as thematic maps, edge-enhanced images and various other special products. In addition to the sheer quantity of different products that would be required, proven algorithms that would satisfy the requirements of investigators in the various disciplines do not exist at this time. Many of these will be developed by the investigators who are participating in the ERTS-A program.

The above considerations led to the implementation of an ERTS data management system shown in Figure 4. Payload video, housekeeping and
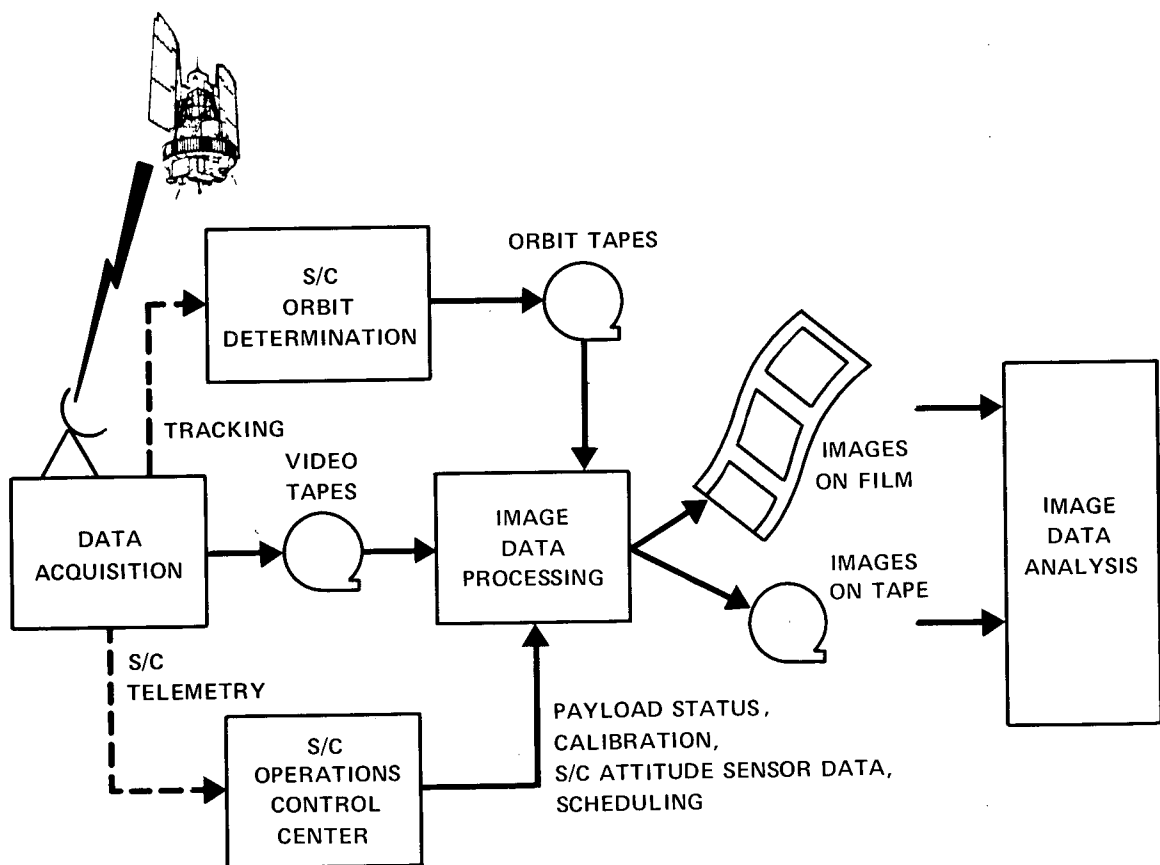
Figure 4. Image Data Flow

tracking data are acquired at the data acquisition stations. Data processing is performed in the central data processing facility at GSFC. A variety of standard image products are delivered to the user community for analysis in their facilities.

IMAGE DATA PRODUCTS

The central data processing facility converts recorded sensor signals to a variety of standard film and computer tape products. In addition to the video tapes, spacecraft housekeeping telemetry and orbit tapes are required. All of the video-taped signals are converted to 70 mm film. Radiometric and geometric corrections based on pre-flight, in-flight calibrations, spacecraft altitude and attitude derived from orbit and housekeeping tapes, are applied. The 70 mm film masters are copied, enlarged to 9 1/2" transparencies and paper prints. Sixteen mm microfilm images are also generated. A portion of the images are also presented in the form of color composites. Available bulk film products are listed in table 1.

Selected data are also formated into computer readable tapes. The RBV computer tapes are uncorrected. The characteristics and quantities of bulk tape products are shown in table 2.

Table 1

Standard Bulk Film Products
• Application of pre-flight and in-flight radiometric calibrations
• Application of geometric corrections based on S/C ephemeris data
A. All Acquired Data:
• 70 mm positive and negative transparencies
• 9 1/2 in. positive transparencies and paper prints
• 16 mm microfilm (part of Data Catalog)
B. 20% of Acquired Data:
• 9 1/2 in. (10 in.) positive color transparencies and paper prints

A portion of the images undergo additional processing which significantly improves the geometric accuracy of the images. In this process, points in the images whose location on the ground is precisely known are automatically identified and measured. This information is then used to fit the whole image to its proper location on the surface of the earth, thus improving the location accuracy. Products generated in this manner are known as precision products. Their quantities and types are shown in table 3. It should be noted that these products are available in both film and digital tape form.

The ERTS data handling system has been set up to deliver the bulk black and white film products to the user within two weeks of data acquisition, i.e.,

Table 2

Standard Bulk Tape Products
• Application of pre-flight and in-flight radiometric calibrations to multi-spectral scanner data.
• 5% of multi-spectral scanner data converted to computer readable tapes
• 1% of RBV camera data converted to computer-readable tapes

Table 3

Standard Precision Products
• Application of pre-flight and in-flight radiometric calibrations
• Application of geometric corrections based on use of ground control points
• 5% of acquired data:
-9 1/2 in. positive transparencies and paper prints
-9 1/2 in. negative transparencies
-9 1/2 (10 in.) positive color transparencies and paper prints
-computer-readable tapes

before the start of the new 18 day data acquisition cycle. This delivery cycle is constrained by several factors. Definitive orbit tapes for example are available 5 days after data acquisition. Video tapes are air mailed from the Alaska and California stations to GSFC. No attempt has been made in this program to provide data to the investigators in near real time. Two factors led to this decision: (1) the ERTS system is a research rather than an operational one, (2) the probability of the satellite being over an area where a natural disaster, for example, is taking place and where near real time data handling might be of value is only 1/18.

FUTURE REQUIREMENTS

It is difficult at this time to estimate the trend of the data handling requirements for future earth observation missions. Much experience should be gained after the launch of the first 2 ERTS satellites. It is possible, however, to predict some of the trends at this time. The trend to increase spacial and spectral resolution of sensors will continue. It is likely that only one multispectral sensor, such as the MSS, will be carried on future missions, with a higher spectral resolution, 7-8 spectral bands versus 4 on ERTS-A, with only a modest increase in spacial resolution. The 3 RBV cameras will be probably replaced with one or two panchromatic cameras and a significantly increased (factor of 4) spacial resolution. Limitations in existing RF data links will keep the down link payload telemetry in the range of 30-50 megabits per second.

On the ground, essentially all data requested by the users will be geometrically corrected to the point that registration between data points of the same area on the ground, taken on subsequent coverage cycles, will be in the order of 1 resolution element. The increased radiometric accuracy (8 bits versus 5-6 bits for ERTS) will require all-digital processing of image data for a substantially larger portion of acquired data than is the case for ERTS. This, in turn, will require development of a new high density digital data transfer medium between the central data processing facility and the investigators.

As promising data analysis algorithms are developed by the ERTS investigators, and as these algorithms are accepted by the investigator community in general, it will be possible to apply these to the data in the central data processing facility, thus eliminating the need to have the work duplicated in several investigators' laboratories.

The ERTS data handling approach, outlined in this paper, can be considered only a start of an exciting, dynamic process of improving and streamlining the flow of earth observation data to the world user community.

PARALLEL IMAGE PROCESSING FOR EARTH RESOURCES DATA

Dr. Richard LeGault, Infrared and Optics Labs,
Institute of Science and Technology, University of Michigan

ABSTRACT

Multispectral sensing has become an accepted tool for remote sensing. A major reason for the acceptance of multispectral sensing is the ability to automatically classify terrain objects. This automatic classification of terrain materials requires rather trivial computation for each resolution element but there are many resolution elements to be classified. The operational application of multispectral techniques presents a formidable computational problem.

This talk will review the current classification algorithms and preprocessing schemes with emphasis on the computational aspects. The Corn Blight Watch experience of 1971 will be used to illustrate these computational problems. A parallel data processing technique adapted to multispectral classification is postulated. A functional outline and processing times for a parallel data processing system will be presented.

THE MULTISPECTRAL APPROACH FOR PROCESSING EARTH OBSERVATIONAL DATA

Dr. David Landgrebe

Department of Electrical Engineering, and LARS, Purdue University

ABSTRACT

An alternate to image processing for analyzing the volumes of data to be gathered by earth observational satellites is possible by using so-called multispectral sensing followed by multivariant analysis techniques. This approach rests chiefly upon the use of spectral variation in the data although spatial and temporal variations can be used to derive the desired information as needed.

This approach and developments associated with it will be described and illustrated with results from aircraft scanner data and multispectral space photography.

SPACE VEHICLE-BORNE APPLICATION OF
OPTICAL DATA PROCESSING

Joseph D. Welch, General Electric Company
Valley Forge Space Center, King of Prussia, Pennsylvania

INTRODUCTION

N73-18690

Recently concern has been expressed on the capability of an advanced operational Earth resources system to effectively utilize the very large amounts of data which can be supplied by its sensing elements. This concern has related to required bandwidths of the satellite-to-Earth data link as well as to the effectiveness of the total system in providing information to the ultimate users rapidly and in a form most useful to them. One approach to achieving an effective operational system design which is deserving of investigation is that of processing much of the sensed data on-board the vehicle. This can have potential advantages relative to reducing required bandwidths as well as making more effective use of the sensing capability by permitting some of the system decision making to be accomplished by the on-board data processor.

In considering alternative techniques for on-board data processing the techniques of parallel processing of imagery data has merit which is worthy of evaluation. By "parallel data processing" of imagery data we include any technique by which every element of an image is processed simultaneously. Most data processing techniques which can be considered under this definition tend to be of an optical type. Specifically techniques of coherent and non-coherent optical data processing are applicable candidates.

This paper considers a model for vehicle-borne parallel optical data processing which might be used as a key part of an advanced Earth resources satellite mission. The subject matter of this paper is related to an investigation of "Advanced Earth Resource Information System Modeling" which the General Electric Company is presently initiating under contract to NASA (NASA Contract No. NAS 5-23090).

Before discussing the operation of the On-Board Data Processor, it is well to first note some of the typical ultimate applications which such an advanced processor might be asked to solve. Some of these functions together with typical practical uses are listed in Table 1.

The table is only a small sample of the types of operations which could be potentially possible with on-board data processing. An imaginative approach to the program can readily uncover many more potential applications.

Table 1

Typical Objectives and Examples of the On-Board Data Processing

Objectives	Typical Example
Image data compression	Instead of sending pictures of corn fields, transmit the number of acres of corn together with the percentage of healthy corn.
To transform the primary data into a form more readily useful to the practical data user	Instead of displaying cloud and ocean patterns, interpret the high probability of fish concentration areas for commercial fishermen.
To make on-board use of some of the sensed data to modify the mission program	To interpret some pre-selected outputs of certain key earth observation sensors to turn on other sensors, or to change spectral sensitivity, or to change field of view, or to change the mode of data processing, or to program a sensor or vehicle roll search, etc.
Image enhancement	Based on deterministic or self-adaptive functions; select certain images for enhancement on-board the vehicle by optical means.
To perform real-time "generic" pattern recognition	The detection of a spiral formation might provide an on-board detection of a tornado and might be used to trigger detection search and automatic alarms.
To perform real-time specific recognition	On-board automatic recognition of specific earth surface features might provide navigation as well as relative location of other observed phenomena.
Real-time spatial frequency analysis of images	Determination by spatial frequency analysis of sea state, cloud and weather patterns, patterns associated with certain geological formation, etc.

Table 1 (Cont'd)

Typical Objectives and Examples of the On-Board Data Processing

Objectives	Typical Example
Real-time spectral analysis	Agricultural crop conditions. Nature of air and water pollutants.
Image change detection	Sampled observation or change detection of major time varying events (e. g. , monitoring progress of forest fire or flood on successive orbits).

Based on considerations of these applications, it is expected that the ultimate potential benefits of such a processor could include:

1. Simpler and less expensive ground stations.

2. Lower downlink bandwidth and, consequently, lower power required on board the vehicle.

3. More rapid data availability in more convenient form.

4. Better utilization of vehicle, including all of its sensory capacity as a result of self-adaptation to the stimuli of the sensed data.

As presently conceived, an ultimate on-board data processor of this type would be an integrated entity which performs many interrelated functions. It seems appropriate to discuss approaches which appear to have merit.

For one promising approach, it is conceptually convenient to think of a typical on-board data processing system as consisting of two interrelated parts:

1. A "High Data Rate Processing Section" (e. g. , Parallel Data Processor).

2. A "Low Data Rate Processing Section".

Briefly stated, the High Data Rate Processing Section will operate, in a parallel data processing mode, to reduce the very high data rate sensor outputs to more meaningful, lower data rate outputs. The high data rate processor

receives the data from the external sensors and processes it in accordance with a program as directed by the controller function of the Low Data Rate Processor.

The Low Data Rate Section will accept these outputs plus stored and transmitted commands. It will serve as a logic module to control the operation of High Data Rate Processing Section and also to control other related vehicle subsystems and will select and encode the desired compressed data to be transmitted to earth.

It is evident that these two parts of the on-board system are interconnected by a variety of possible feedback loops.

Conceptually, the vehicle-borne part of the system might be described by the very simplified control loop of Figure 1. The essence of the system consists of advanced parallel data processing components interconnected by appropriate control and data loops.

In order to achieve the required high data rates, the on-board "High Data Rate Processing Section" will typically be an application of a parallel optical data processor with capabilities for data processing in both the spatial and spatial frequency domain.
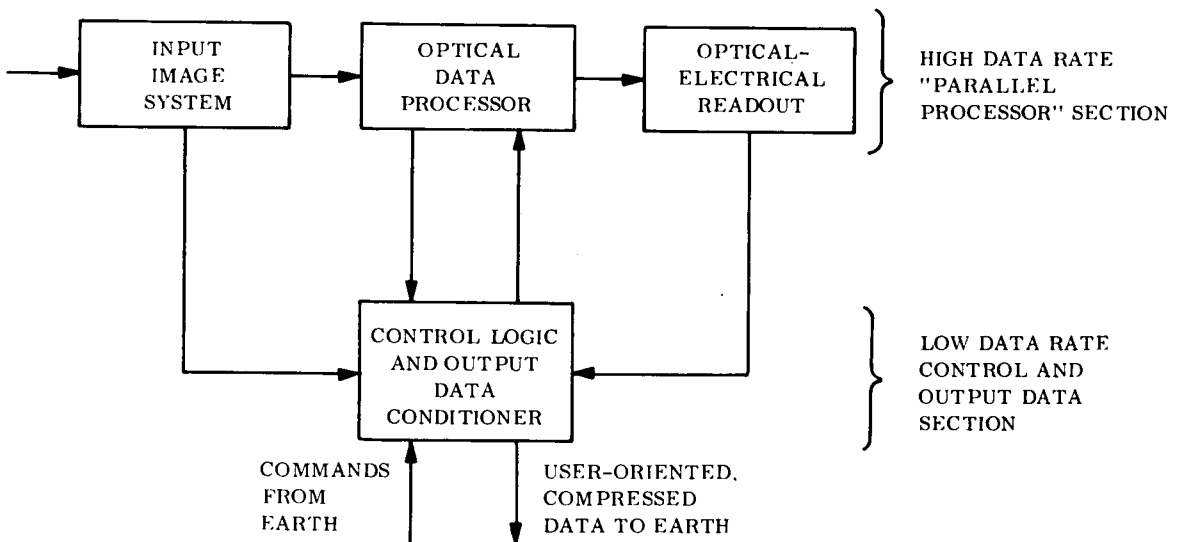
Figure 1. A Simplified Concept of the On-Board Data Processing System

Based on this premise and on the assumed existence of a flexible Low
Data Rate Processor, an overall typical system can be blocked out as shown
in Figure 2.

This system is presented merely as being typical of a general approach.
Different data needs and/or components availabilities, for example, will indi-
cate a variation in the processor. Some of the primary things which should
be mentioned concerning Figure 2 are:

- The entire system is characterized by a network of data and command
  loops interconnecting the various functional components of the system.

- Some of the system functions are performed on the earth, but for this
  advanced system, most automated functions are performed in the
  spacecraft.

- Those familiar with optical data processing will recognize the func-
  tions and components of the High Data Rate Section of the on-board
  processor.

- The Low Data Rate Section is clearly the on-board "nerve center" of
  the system.

- The system, as shown in this figure, should require no moving parts
  on the vehicle nor any sequential scanning of continuously high bit
  rate data.

- This system provides the user on the ground with the data in a form
  most usable to him with the minimum of operations required.

- The system, as shown, is presented only as an example. Many
  components and interconnecting command and data loops could be
  added, deleted, or modified based on judgments of user needs, tech-
  nical feasibility, costs, and varied opinionated engineering judgments.

- With regard to the Data Storage Unit, many points of view can be
  taken. It could be conceived as a part of either the High Data Rate
  Section or the Low Data Rate Section, more likely it will have func-
  tions in both areas.

- This figure is a nice picture—but how does it work? The answer, as
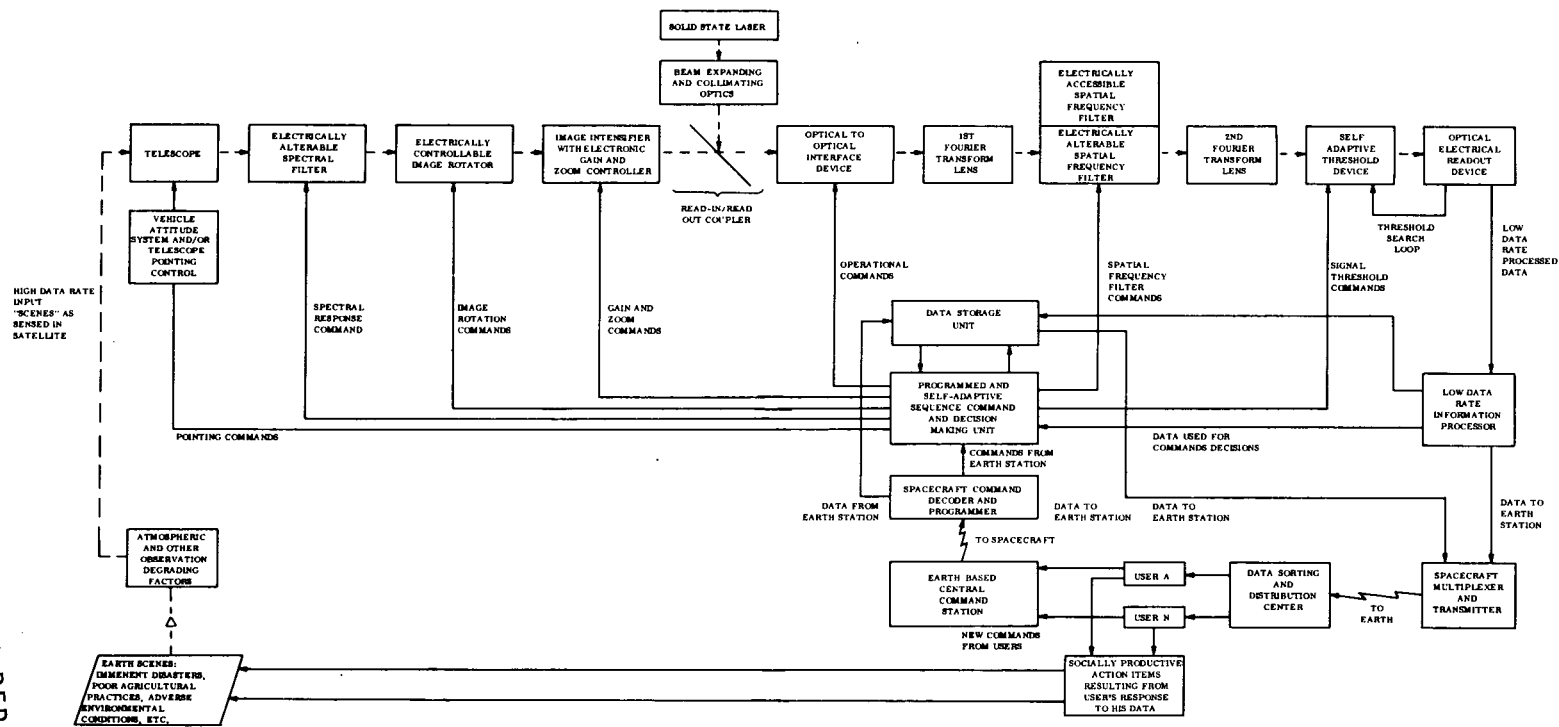 far as the overall system is concerned, is largely application-
  oriented.

Figure 2. A Typical Data Processing System

80

The most effective way of describing the concept shown is by way of some specific examples. Therefore, some cases of how a general system such as this one could operate are described:

CASE (A)

Problem

Provide to a user a spatial frequency response of an image of a specified area in a specified spectral band (as might be useful, for example, in a geological survey).

Solution

The details of the command, including its programming sequence, are assumed to be stored in the Data Storage Unit. The Command Unit provides electrical signals to components in accordance with stored or transmitted commands.

In this case the Command Unit provides appropriate electrically encoded signals to the electrically alterable spectral filter and the electrically alterable spatial frequency filters. The spectral filter assumes the desired color response. The spatial frequency filter assumes a sequenced combination of multiplicable transparent annular rings and wedges in synchronism with the integrated optical-electrical readout signal. This "output" data obtained by conventional two-dimensional Fourier transformation techniques is "tagged" synchronously to provide the desired spatial frequency information, in the desired spectral band, for purposes of encoding and transmission to the user.

CASE (B)

Problem

Recognize and locate a suspected large source of air or water pollution.

Solution

On the basis of a command transmitted from the earth station begin search operation when the space vehicle is near suspected "target". Proceed to search for the spectral response of the pollution by means of an electrically alterable narrow-band spectral filter combined with a self-adaptive threshold device. Monitor the optical electrical output signal for an unusually intense signal. This intense signal can be used to trigger a landmark correlation search by coherent optical means using a stored file of electrically retrievable matched

81

spatial frequency filters. The correlation signal detected by the optical-electrical detector, together with on-board information on the location and pointing attitude of the space vehicle can provide information on the location of the pollution source.

Furthermore, this cross-correlation interpreted in the parallel processor as a change-detector can confirm the addition of a major change (e.g., the newly observed pollution signature).

CASE (C)

Problem

Enhance selected images which were subjected to high spatial frequency contrast loss due, for example, to atmosphere effects.

Solution

Based on commanded signal, program an electrically alterable spatial frequency filter capable of "grey scale" transmissivity to assume the desired low spatial frequency suppression to compensate for high spatial frequency loss. Detect resulting signal with optical-electrical output sensor for encoding and transmission to Earth.

An interesting self-learning improvement of this may be possible by providing an idealized optically-stored MTF frame of reference on board the space vehicle as a self-adaptive guide to select the required optimum enhancement high pass spatial frequency filter function.

It is hoped that these few examples will adequately describe the approach to the overall system.

As noted before, data is provided directly to the user in a compressed form most useful to him. As indicated in this figure, it is up to the user to initiate new requests for data and to make beneficial use of the data.

OTHER VARIATIONS OF THE ADVANCED DATA PROCESSING SYSTEM

Many variations of the system not specifically incorporated in Figure 2 are possible as may be dictated by specific problems. Some specific examples are:

1. A Built-in Parallel Processing Reiteration Procedure. Such a system would be designed such that the "output" image plane could also serve

as the "input" image plane for a new iteration. This is shown in rudimentary form in Figure 3. This reiteration approach to parallel processing is analogous to its counterpart in serial processing. The reiteration logic and evaluation would be incorporated into the command and sequencer.

Applications of such a reiteration capability would include a wide range of self-enhancing, or self-learning operations where a given process is reiterated as long as improvement, according to some established and optically stored norm, is automatically observed relative to that norm.

2. A Processor which has Capability for Optically Making Spatial Frequency Filters. This possibility has application, for example, when an unexpected phenomenon is observed and when it is wished to be monitored automatically on a periodic basis to detect changes.
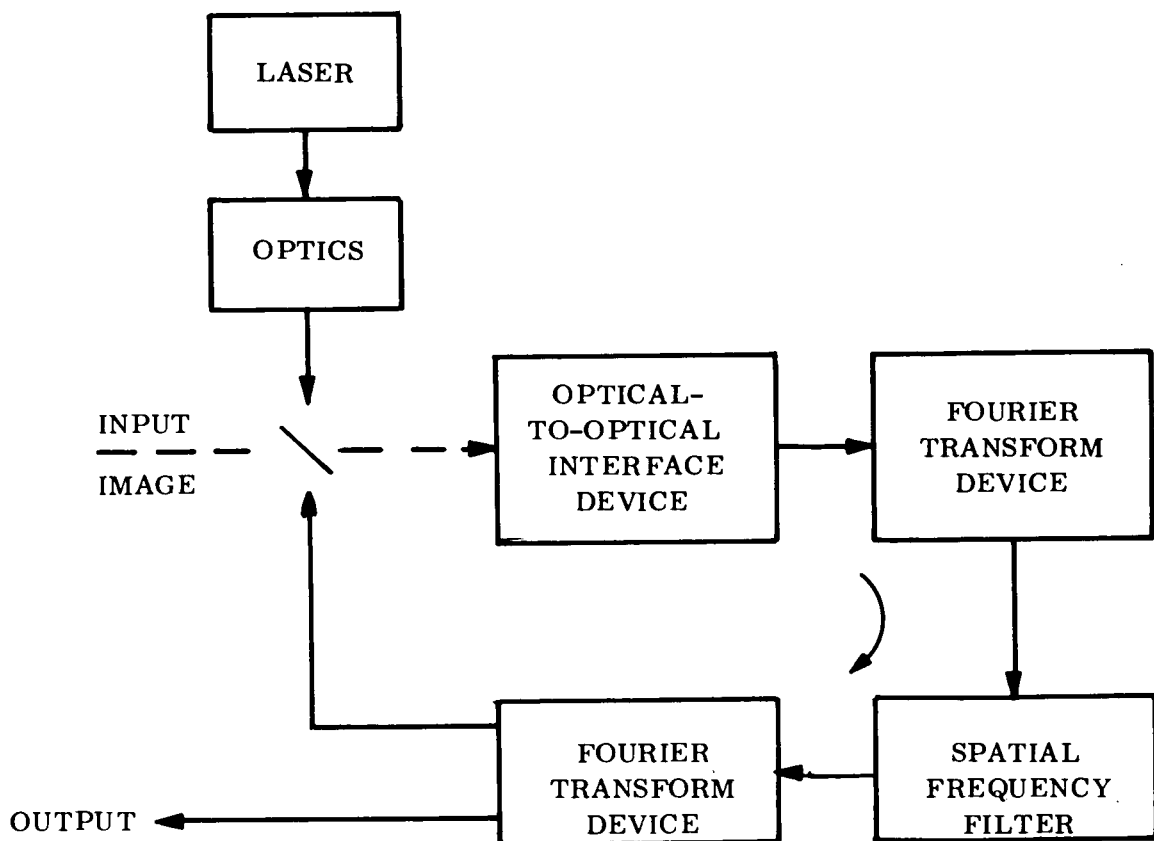
Figure 3. A Portion of an Advanced Data Processor
Showing a Reiteration Loop Operation

3. <u>Parallel Data Processing Applied to a Variety of Sensors</u>. Although we have emphasized "parallel" type of sensor inputs (e.g., image intensifiers and optical-to-optical interface devices) it is evident that optical data processing can be applied to a wide range of other sensors. In the case of serial read-in types of sensors, a channelized mode of parallel data processing may be most appropriate.

FUTURE SYSTEMS

The possible development of an advanced system based on unexpected user need and technology potentialities has been discussed. As progress in an imaginative, and yet realistic approach is made, a great analogy between advanced two-dimensional parallel processors and conventional serial digital computers can be foreseen. Entire images of the parallel processor become the analog of binary words of a serial computer. Extending this analogy to the design of parallel processing systems could lead ultimately to computers of extraordinary capabilities.

THE "OUTPUT" OF THE OPTICAL PROCESSOR

Here we consider the electro-optical readout of what appears on a defined output plane of the optical processor. Exactly what appears is a function of the specific processing task being pursued. Typically, it may be:

1. One or more correlation functions indicating the correlation response of two images.

2. A spatial frequency pattern of an image.

3. A sequence of multispectral images.

4. A selected enhanced image.

This data may be used for purposes such as:

1. An input to further optical iterative computations.

2. An input to an on-board self-programming or self-learning operation.

3. Encoding for downlink transmission.

This section is included to point out the importance of this readout operating at relatively high speed and preferably in a parallel operating mode.

THE "LOW DATA RATE PROCESSING SECTION"

Since the data rate output of the High Data Rate Processing Section will not always be high in this section, parallel data processing, although not necessarily completely ruled out, will not necessarily be a feature of this section. Indeed, at some point before transmitting the data to earth, the resultant low bit rate data will be converted to serial format.

It is likely that much of this part of the processor and its inputs and outputs will operate with low data in analog or digital form as may be appropriate to the specific function. Although the data rate of this section may be relatively low, for many missions a high capacity data storage may be required. This storage device might be logically considered part of either the High Data Rate or Low Data Rate Section of the On-Board Processor.

Consider next some of the logical operations of the Low Data Rate Processing Section. Typical examples of functions of this data processing section are:

1. Interpret ground commands and/or stored programs to select operating mode of data processing systems and operating parameters of each component.

2. Accept parallel readout of High Data Rate Section and operate on it as may be appropriately commanded.

3. Typical operation on above read-out may be:

   a. X-Y interpolation and point center detection of correlation peak.

   b. S/N evaluation of correlation function.

   c. Serializing data of certain selected spatial frequency spectral images (preparatory to encoding for downlink).

   d. Serializing of a limited number of selected enhanced images.

   e. Interpreting output data for command variations such as:

      ● Adjustment of threshold device

      ● Adjustment of gain or other "search" parameters of critical components of system

      ● Turning on or off of sensors, changing fields of view, etc.

f.   Providing automatic programming, including decision-making by
        progressive logic with respect to future operation of the system
        based on both output data and internal commands.

   4. Evaluate raw and processed data in relation to user needs and make
       decision to process data further and/or to transmit data in a selected
       format to Earth via encoder and downlink.

   5. Ultimately, to approach a self-learning functional operation such that
       a more complete automatic operation of the system is to be ultimately
       feasible.

   Although these low data rate date processing functions are expected to be
initially performed by electrical signals and solid-state components, far more
advanced techniques such as very compact thin film optical data transmission
and computing techniques should be considered for even more advanced
missions.

CHARACTERISTICS OF KEY RELATED TECHNOLOGIES
AND COMPONENTS

   An understanding of key components, their characteristics and problems
as well as some projection of their status and quantitative performance a
decade hence, is of key importance to any investigation of an "An Advanced
Earth Resources System Model".

   Most existing devices do not have all of the desired performance features
to the degree which is expected to be needed for a high capacity processor of
the type needed a decade hence. However, much effort on many related tech-
nologies is underway to continually improve components and technologies.

   In discussing these critical items we will try to list the desired features
of the specific devices. Although we will not repeat this fact for each item,
it is evident that desired potential features of all components include: low
power requirements, lightweight, small volume, and long life reliability in a
space flight environment.

OPTICAL-TO-OPTICAL INTERFACE AND OTHER INPUT
INTERFACE DEVICES

   In its most readily conceived function, this is a device which receives a
non-coherent optical input image and which is usually readout with a local
source of coherent illumination.

The term "and other Input Interface Devices" is added so as to include other types of input interface devices such as various types of passive or active radiometers which may come into greater favor in the next decade. Hopefully, even these devices will be developed having parallel data input capability.

An ideal optical-to-optical interface device should have these characteristics:

1. High sensitivity in a desired spectral band (ultimately an electrically selectable spectral response would be attractive).

2. High resolution.

3. Very rapid in-place development.

4. High modulation efficiency.

5. Very short or controllable relaxation time constants (i.e., automatic or controllable erasure).

6. Low noise characteristics.

7. High contrast ratio potential.

8. Capacity for indefinite recycling.

These various interface devices include both amplitude and phase media.

It should be noted that strides are taking place in the area of "parallel" operating image intensifiers. In some cases these can permit the practicality of an interface device which would otherwise have inadequate sensitivity. One can also foresee some realistic prospects for integrating the function of an optical-to-optical interface device and an image intensifier in a single device.

As discussed, parallel operating image intensifiers can have significant merit in permitting the use of certain optical-to-optical interface devices which may appear attractive in all respects other than sensitivity. For this reason the General Electric Company has pursued an investigation of various types of image intensifiers.

Some of the newer types of "distortionless" intensifiers appear very attractive for optical data processing.

In addition to a prime function of providing significant optical gain, certain types of image intensifiers can also provide these useful functions:

1. High speed electronic triggering (desirable for certain types of optical-to-optical interface devices which tend to be cyclic in their operation).

2. "Zoom" (or variable magnification). This feature can permit a high speed magnification change or magnification search which may be desirable for certain types of data processing operations.

ELECTRICALLY ALTERABLE SPATIAL FREQUENCY FILTERS

Reference is made here to both amplitude and phase filters as well as to complex filters. The object of these types of devices is to provide a rapid, no-moving parts means for changing spatial filters. Spatial filters of interest include simple ring and wedge amplitude filters as well as filters having much greater capability (i.e., electrically alterable complex filters).

In principle, an electrically alterable complex filter can be accomplished in various ways, most of which fall in one of these categories:

1. Electrically alterable phase medium arranged multiplicably with an electrically alterable amplitude medium.

2. Electrically alterable, carrier modulated amplitude medium.

3. Electrically alterable, carrier modulated phase medium.

These last two carrier types might be described as holographic in their approach and some question may arise as to their optimum utilization of the available space bandwidth product of a given medium.

ELECTRICALLY ALTERABLE SPECTRAL FILTERS

Most multispectral imagery to date has utilized multiple filters (as in a filter wheel), multiple sensors, or other similar devices which involve moving parts or redundant equipment. There may be considerable merit in obtaining multispectral spatial frequency images as well as more conventional multi-spectral images.

This seems to be an area for considerable investigation. The possibility of an electrically alterable spectral filter has, for example, great appeal as an element in a parallel optical data processor. If the center spectral frequency

could be tuned and also the spectral bandwidth could be adjusted electrically then this would indeed be a very powerful tool.

SPATIAL FREQUENCY FILTER SELECTION AND RETRIEVAL TECHNIQUE

This represents an alternative, or perhaps a complement to the electrically-alterable filter approach. In this present approach the spatial filter is stored optically and retrieved optically.

At least two approaches come to mind: a coded multiplexing approach and a retrieval by optical modulator.

A good example of filter multiplexing is described by Gorstein, Hallock et. al.* They have, for example, described the encoded superimposed multiplexing of at least 20 independent star field spatial frequency images. This is not by any means believed to represent a limit of the approach as imposed, for example, by the space bandwidth product of the medium. Decoding the multiplex filter can be accomplished, for example, by reading out the location of a second correlation image on the output plane. Several variations of this intriguing technique are evidently possible.

The second approach would make use of high density image type of data storage (e.g., holographic storage) coupled with nondestructive laser beam readout techniques, for example.

A certain number of high density data storage and retrieval devices are known to be under development including at least one under NASA contract.

OPTICAL-ELECTRICAL READOUT DEVICE

The function of this device is to convert an optical electrical signal appearing in some defined output plane of the parallel optical processor to an electrical signal. Consistent with the requirement for high speed parallel operation this type of device should be one which involves no moving parts or scanning of any type.

The nature of the readout device will depend on the nature of the computational operation being performed. For example, the readout of a two dimensional spatial frequency analysis could be conveniently accomplished in the

---

*Gorstein, M., Hallock, J.N., and Valge, J., "Two Approaches to the Star Mapping Problem for Space Vehicle Attitude Determination," Applied Optics, vol. 9, No. 2, Feb. 1970.

spatial frequency plane by two assemblies of solid state detector elements shaped in the form of rings and wedges to respectively provide magnitude and direction of the spatial frequency content.

Readout of more complicated images such as selected locally enhanced spatial images might ultimately be accomplished by a two dimensional solid state detector array.

IMAGE ROTATION DEVICE

In certain types of image data processing it may be desirable to provide a rotation of an input image about the optical axis of the optical data processor. One such example is where a rotation orientation or a rotation search is needed to satisfy a function of a matched spatial frequency search and recognition operation.

Another example might be a particular approach to spatial frequency analysis where it might become attractive to rotate the image about the optical axis rather than use wedge spatial filters and/or wedge electro-optical readout sensors.

Several means for accomplishing these rotations are possible including mechanically rotating the input image, or the spatial filter or rotating an image rotation prism such as a Dove prism or other similar prisms.

It would be more attractive, however, to devise a parallel electrically alterable image rotation device which requires no moving parts. Some technical approaches for accomplishing this have been conceived. It is hoped that practical techniques for accomplishing this in a compact optical data processor will become available.

ULTRA HIGH DENSITY DATA STORAGE DEVICES

Several such devices, both two dimensional and three dimensional, are known to be under development. The optical approaches appear to be dominant.

The major problems presently appear to be in read-in and read-out— particularly nondestructive read-out.

The continued successful development of these devices will be advantageous to the pursuit of advanced parallel data processing. One specific example would be the high speed storage and retrieval of spatial frequency filters.

The continued investigation of high density data storage devices is of key importance.

SUMMARY

On-board parallel optical data processing is a promising approach to the data reduction problem which will be associated with very advanced types of Earth resources missions.

ACKNOWLEDGMENT

A GENERAL APPROACH TO SOME SPIN SCAN
GEOMETRY PROBLEMS

W. Swindell
University of Arizona, Tucson, Arizona

ABSTRACT

The Pioneer F and G missions carry a spin scan imaging telescope for the purpose of obtaining two color images of Jupiter and its satellites. Although these are specific missions, the problems are general in nature and have required a general approach in their solution. First it has been necessary to create special software that can rectify the otherwise distorted image that would result from the imaging geometry. The software is completely flexible in that the shape, size, tilt and rotation rate of the viewed (ellipsoidal) object are arbitrarily variable as are the clock and cone angles, stepping rate, spin axis orientation, spin rate, sampling rate and trajectory of the imaging telescope. This program thus provides a useful tool for investigating the suitability of spin scan techniques for any flyby or orbital situation. Examples of scan maps will be shown. Second, the presence of curved scan lines (unlike TV systems) presents special problems in the image data processing with respect to enhancement and alleviation from the effects of noise. Third the curved scan lines create a special problem when it comes to filling a display matrix. The nature and method of solution of these problems will be discussed.

THE GODDARD SPACE FLIGHT CENTER PROGRAM TO DEVELOP PARALLEL IMAGE PROCESSING SYSTEMS

David H. Schaefer
Head, Computer Technology Section, Goddard Space Flight Center

My group has a program to develop hardware to accept a "real" image input, handle it as an entity in real time, and spit information—not an image, mind you—but spit information out the rear end of the system.

The title of this conference contains the phrase "parallel image processing". By our definition, parallel image processing is image processing where all points of an image are operated upon simultaneously. Our interest in parallel systems stems from the belief that, in the long run, only parallel image systems will be able to meet the very stiff speed and reliability requirements that will be demanded for image data processors aboard advanced spacecraft. Some participants at this conference have stated in discussions that the word "parallel" is simply another word for "optical."

I don't believe that this is really true. With all the promises of large scale integration one would think that LSI arrays, if they were living up to their expectations of 10 years ago, would today be able to perform many computations in parallel. We should be able to have a matrix of photo diodes directly connected to a matrix of logic and be able to perform "parallel image processing." Under our program the development of such large scale integration techniques is being encouraged.

There is another method of parallel image processing that is not optical. Here one converts an image into a modulated beam of electrons, and manipulates this with the tricks that are possible with electron optics. We are supporting the development of techniques of this sort.

Parallel image processing isn't necessarily optical processing, but, of course, optical methods are included. We want to develop both automatic non-coherent and automatic coherent optical image processors. Jim Strong, in another paper, is going to show experiments conducted here at Goddard where logical operations are performed on images. These experiments utilize non-coherent cross-correlation techniques. Dr. Husain-Abidi's work with coherent optical systems will be reported in his paper.

Under the Goddard program we want to bring all parallel image processing techniques together: electronic methods, non-coherent optical methods

and coherent optical methods. We envision hybred processors using a combination of techniques. Our program is dedicated to developing a variety of automatic parallel image processing techniques so that by the proper use of all techniques, image processing can be carried out on board spacecraft.

Our program has two facets to it:

The first facet is to develop the technologies that must be developed if we are ever going to perform the image processing tasks we talk about. Let me show you several examples. All these examples, it so happens, have their application in automatic coherent systems.

The first example of technology development is our funding of devices to convert a non-coherent input image into coherent form. Hughes Research Labs have a contract to develop a liquid crystal device that will do this job. Before this talk is over a motion picture of this converter in operation will be shown. In the following paper the device is described in detail.

We have a contract with ITEK to build a similar device. They utilize Bismuth Silicon Oxide, a material with both birefringent and photo-conductive properties. The converter has just very recently been delivered.

Electrically alterable filters for use in the Fourier transform plane have been developed by ITEK under our funding. The filters are in the form of wedges and rings. Figure 1 shows the wedge filter. The filters are liquid crystal devices, and the white areas in the figure are areas that are in the scattering mode. In the figure there are three transparent wedge pairs. In preliminary experiments these filters have proven to be most useful and we are obtaining interesting results with them.

Westinghouse has developed sensors that can electrically sense in the Fourier transform plane. These are in the form of photo-conducting rings and wedges.

Along with developing technology, we are also developing the theory and methods of using these new systems.

For instance, Yale University, under Dr. Richard Barkers direction, is undertaking both materials work and work in optical techniques, including techniques of performing spectral analysis in a parallel manner.

Dr. Sing Lee, of Carnegie Mellon, has a grant from us to investigate advanced methods of coherent processing.

A rather small contractual arrangement with Avco Corporation has been recently concluded. We asked them to come up with a Fourier transform filter hologram that would recognize any kind of a spiral. If the image input is a spiral, you get an output. If the image input is something other than a spiral, you aren't supposed to get any output. This was a small effort and the results are not spectacular, but they are interesting. This work, we feel, will lead to a way of recognizing objects described in generic terms.

Joe Welch yesterday indicated that General Electric has a contract to model advanced Earth Resource information systems. This contract is just starting. Hopefully, it will indicate what kind of devices we are going to ultimately need for certain Earth Observation tasks.

We are giving assistance to Fred Billingsley of JPL. He is going to take some of his serial algorithms and convert them into parallel algorithms so that certain of his operations can be performed in a parallel manner.
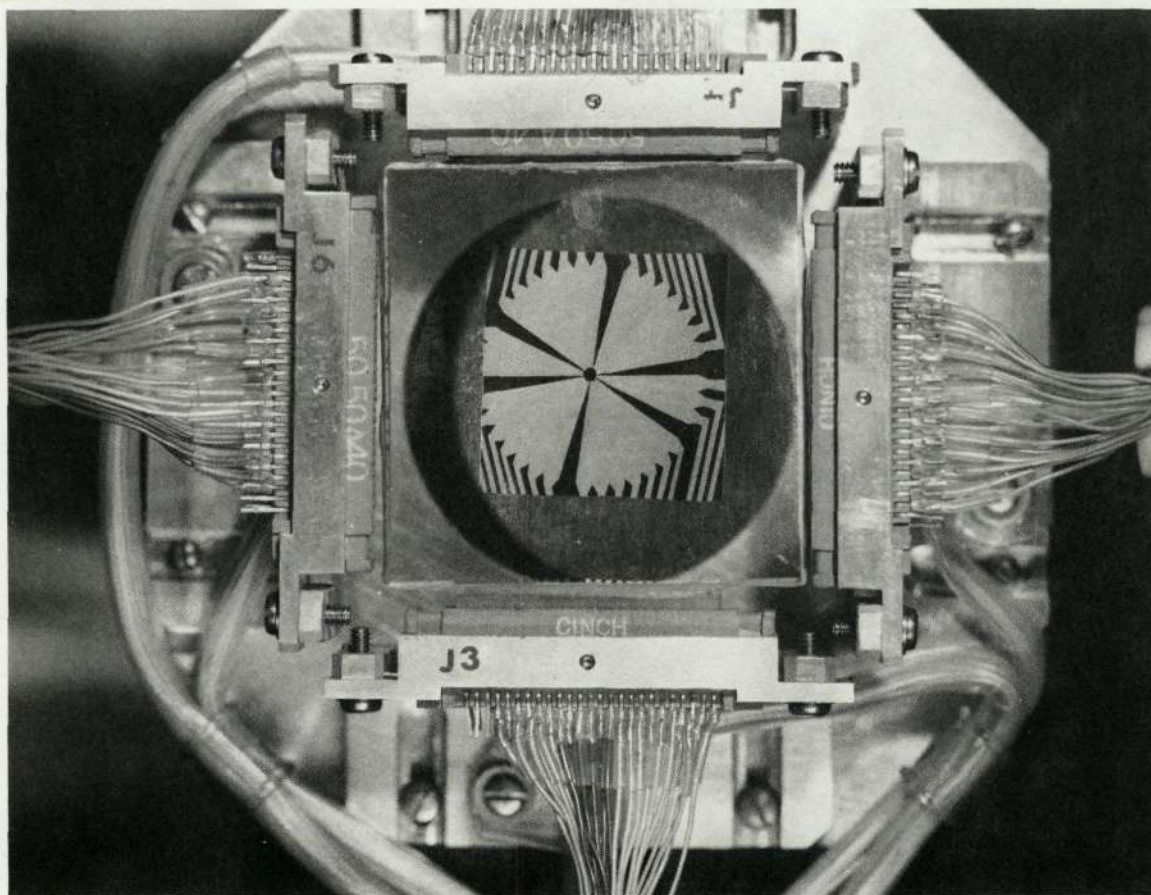

Figure 1. Liquid Crystal Electrically Alterable Wedge Filter
for Use in Fourier Transform Plane.

This morning I was wondering how to give you a progress report of how far along we are in developing real-time parallel image processing systems. It seemed like the best thing was to show you a system that we have built up in our lab using some of the devices that we have gotten from the people who have been doing hard work for us. We are going to talk about a very primitive coherent optical system.

Our aim, as I said, is to have, as input, an image, and to obtain as output, information.

For the system we are going to demonstrate, our "image in" is simply a black ruler (figure 2). The "information out" is a whistle indicating that the ruler is horizontal.
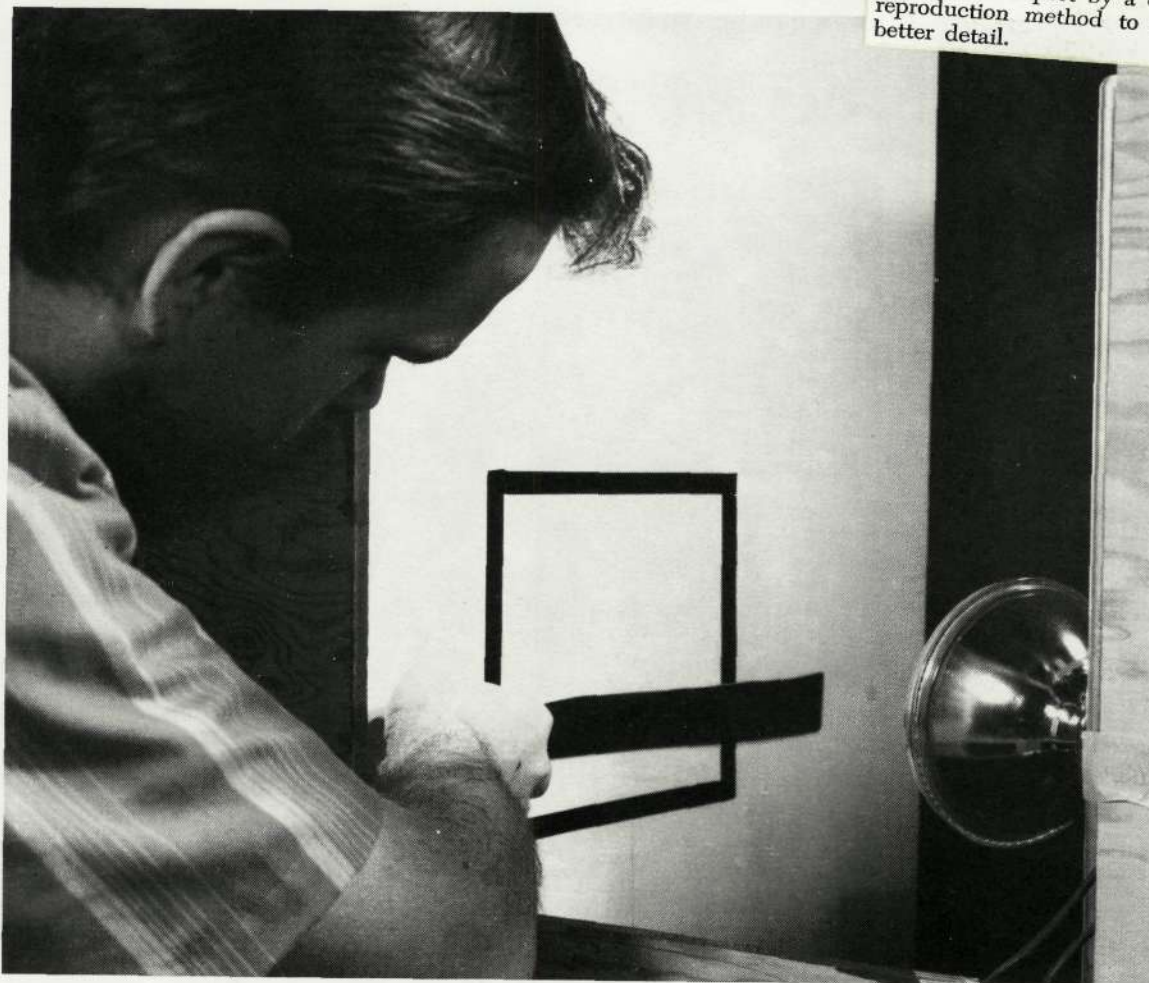
Figure 2. "Input" to Experimental System

The first step is to focus the image on an image intensifier tube. In this particular experiment we were anxious to show that an image intensifier could be used to activate the non-coherent-to-coherent converter.

The image of the stick on the output of the image intensifier tube goes through a beam splitter and is then focused on the interesting looking gadget at the right in figure 3. This piece of hardware is what we call our "OTTO" device for "optical-to-optical"—with a slight stutter. As you realize, this is the device that is going to change the non-coherent image into a coherent image. The laser is out of the picture at the right. The laser beam travels from the right, through the OTTO device and beam splitter, and on to the lens system at the left of the figure.

Dr. Jacobson in the next paper is going to fully describe the OTTO device. Let me give you a very general description. It is a liquid-crystal cadium-sulfide sandwich. In the areas upon which non-coherent light falls the cadium
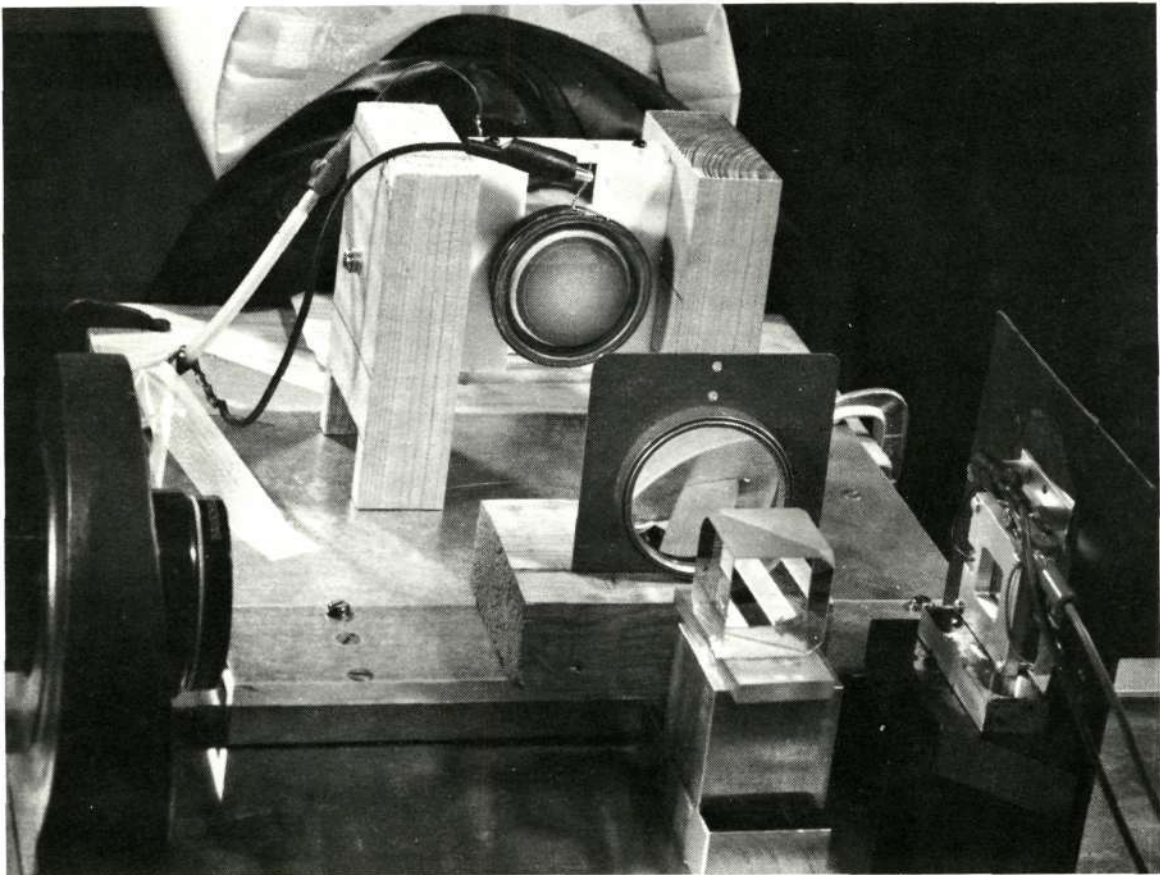

Figure 3. Experimental Setup. The OTTO Device At the Right Hand Side of Figure

sulfide becomes a conductor making the liquid crystal behind that particular area a scatterer. Other areas remain good light transmitters. Coherent light is, therefore, scattered out of the system in areas of non-coherent illumination. The output is, because of this, the negative of the input image. The non-coherent black stick on a white background is converted to a coherent red (from the He-Ne laser) stick on a black background.

After conversion the Fourier transform of the scene is formed and focused on the photoconductor wedge sensor shown in figure 4. Whenever the stick is horizontal, no matter how it is translated up, down, or sideways, the Fourier transform will be a vertical line. By monitoring the two vertical wedges we have an electrical indication of when the stick is horizontal. The output from the two vertical wedges activates the whistle.

We have here a parallel image processing system where the input is a non-coherent image, processing is performed in the coherent optical realm, and the output is an electrical signal. Our prime reason for putting this together was to exercise the OTTO device in a very simple system.

The sound motion picture that follows will show the system in operation. Certain limitations of our presently available devices, especially the limitations due to the slow time response of the OTTO devices on hand, will be evident to you. The movie will, however, show our first attempt at building a real-time parallel processor using coherent techniques. It is our hope and belief that from such modest beginnings we will be able to develop hardware that will help the country in its many image processing tasks of the future, be these tasks on the ground or aboard spacecraft.
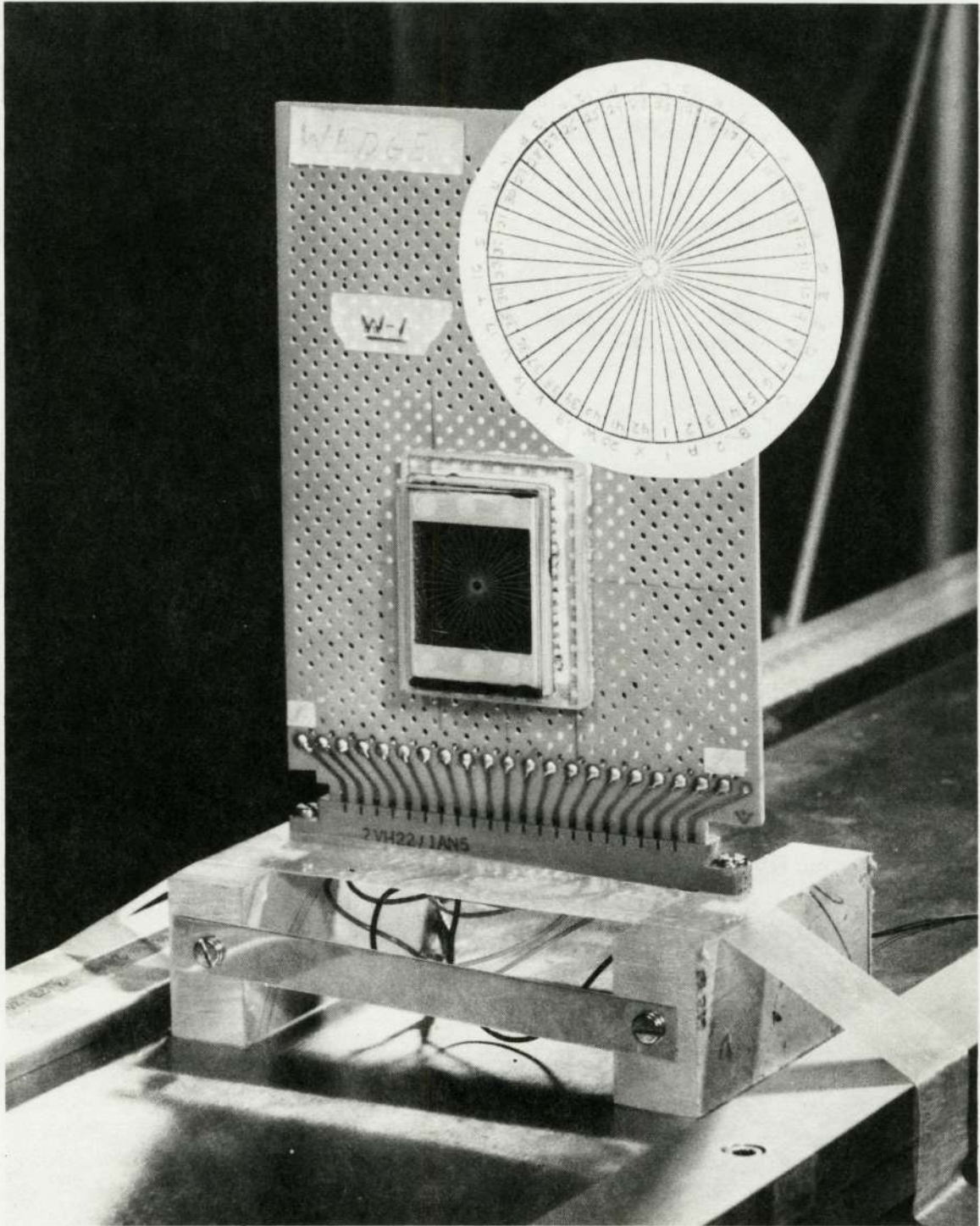
Figure 4. Photoconductor Wedge Sensor

101

THE LIQUID CRYSTAL LIGHT VALVE, AN OPTICAL-TO-OPTICAL INTERFACE DEVICE

A. D. Jacobson, T. D. Beard, W. P. Bleha
J. D. Margerum, and S. Y. Wong
Hughes Research Laboratories, Malibu, California 90265

INTRODUCTION

N73-18692

The subject of this discussion is a new device which is called, generically, a photoactivated liquid crystal light valve.[1] But it is more affectionately known as OTTO, which is an acronym for optical-to-optical interface device.

FIGURE 1—STYLIZED SCHEMATIC OF OTTO IN USE

Very briefly, as shown in Fig. 1, the device is designed to transfer an optical image from a noncoherent light beam to a spatially coherent beam of light—i.e., a laser—and to do it in real time. The purpose for doing this sort of transfer operation is to input the optical image from the real (i.e., sunlit) world or the world of CRT's into the highly refined laser illuminated world of a coherent optical data processor. In the past this task has been carried out primarily using silver halide film.[2] From most standpoints, silver halide film is ideal for this purpose. It has high resolution, excellent contrast, adequate dynamic range, sensitivity and durability. Its main drawback, however, is that it requires wet, chemical processing. From an operational standpoint, this requirement is an overwhelming limitation. Primarily because it requires intolerable time delays between exposure and use—from tens of seconds up to substantial fractions of an hour depending on the type of film and the type of processing. In order to build practical systems for most applications it is crucial that the data input operation be performed much faster than can be done with conventional film. In fact, we feel that the absence of a real or quasi real-time input device has been one of the major factors impeding the development and use of coherent optical data processing systems. Unfortunately, it has proven to be very difficult to find a practical device (with emphasis on the word "practical") that offers both real-time performance as well as the full spectrum of optical qualities required by coherent optical data processing systems. In fact, to our knowledge, there still is no such device available on an off-the-shelf basis. The device that we describe below is a new candidate for that role.

LIGHT VALVES
DEVICES WHOSE LIGHT TRANSMISSION CHARACTERISTICS CAN BE CONTROLLED ON A POINT-BY-POINT BASIS
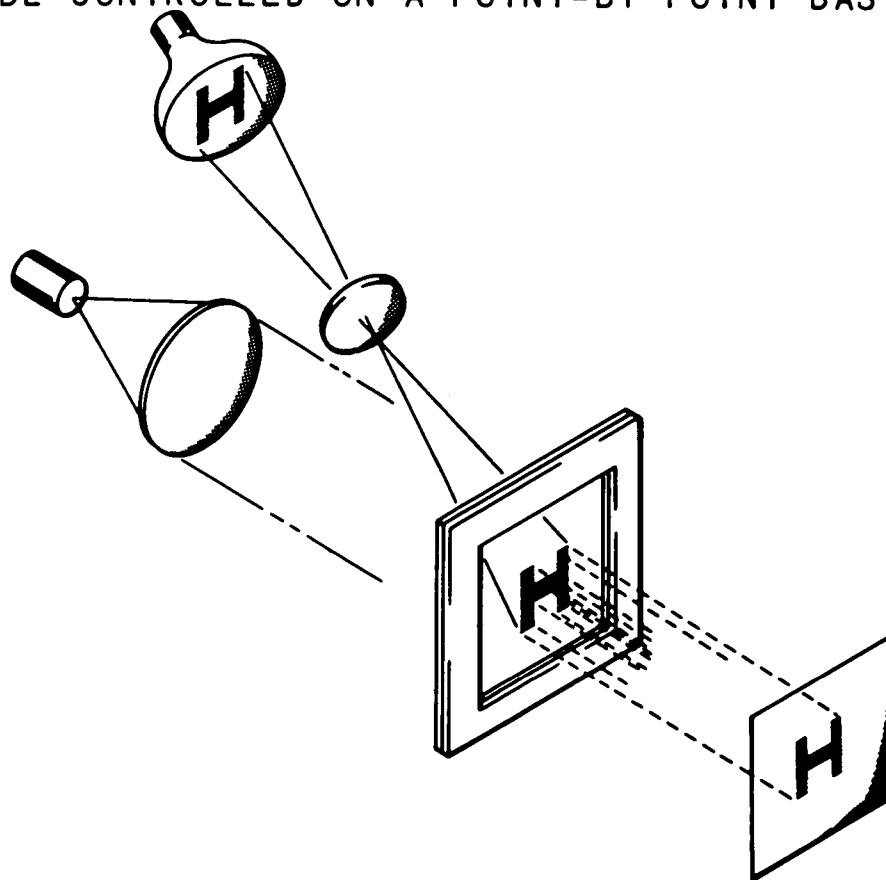

Figure 1. Stylized Schematic of OTTO in Use

FIGURE 2—SCHEMATIC OF LIQUID CRYSTAL CELL

Figure 2 shows a schematic view of OTTO. The cell consists of a thin film photoconductor in contact with a thin layer of liquid crystal. Typically, these layers are 10-20 μ thick. The photoconductors and liquid crystal layers are sandwiched between transparent electrodes across which a dc voltage is impressed. The entire sandwich of layers is enclosed in glass. In order to understand the operation of the device it is necessary to consider the electro-optical character of liquid crystals.

FIGURE 3—LIQUID CRYSTAL STRUCTURE SCHEMATIC

Figure 3 illustrates the structure of the three basic types of liquid crystal.[3] In the nematic type, the cigar shaped liquid crystal molecules have

APPLIED
VOLTAGE

GLASS PLATES

CONDUCTIVE
NESA-COATINGS

LIQUID CRYSTAL

IMAGING
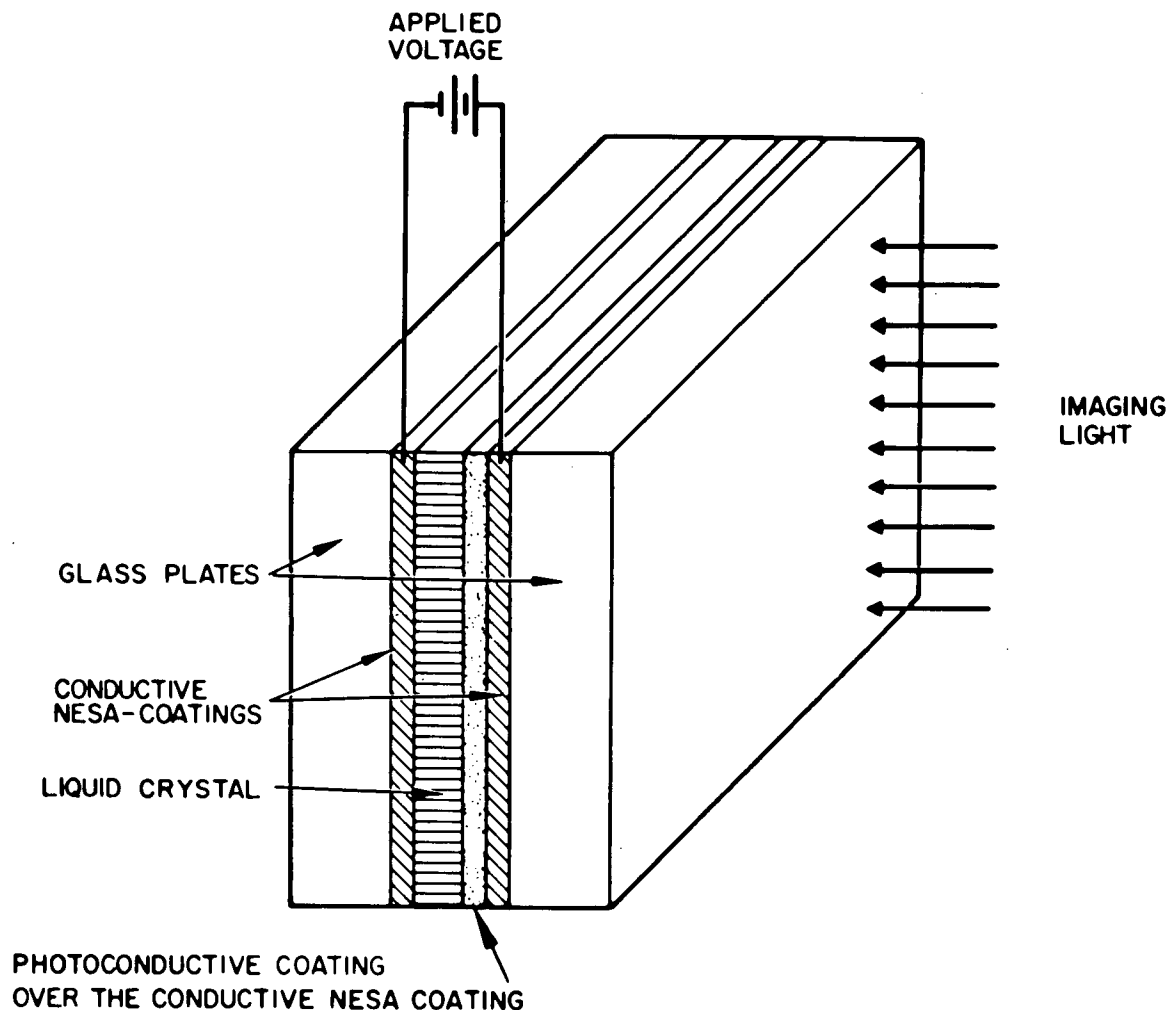LIGHT

PHOTOCONDUCTIVE COATING
OVER THE CONDUCTIVE NESA COATING

Figure 2. Schematic of Liquid Crystal Cell

a single axis along which they prefer to align. In the other two directions, there is no such preferred direction of alignment. In the case of cholesteric liquid crystals there is a second level of alignment. This type of liquid crystal organizes itself in layers. Within each layer there is nematic-type alignment. The nematic axis rotates from layer to layer thereby creating the spiral or helical structure that characterizes the cholesteric liquid crystal. The smectic liquid crystal is still more ordered in that the molecules form layers and all layers are aligned with respect to each other. In the OTTO device, we use nematic liquid crystals and we operate them in the dynamic scattering mode. The phenomenon of dynamic scattering is illustrated in Figure 4.[4,5]
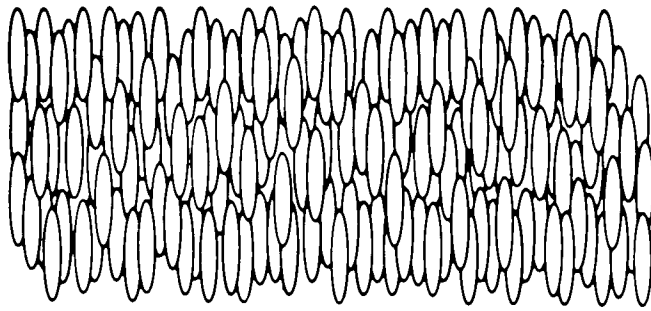
(a) Nematic liquid crystals
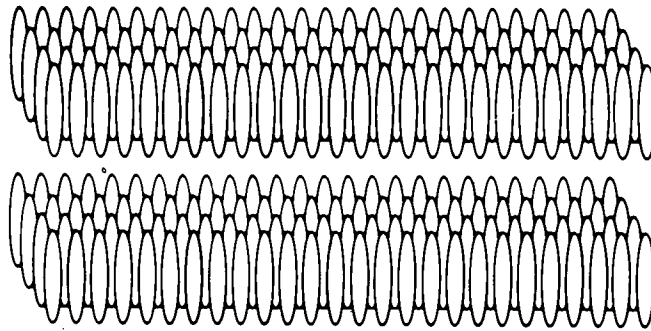
(b) Smectic liquid crystals
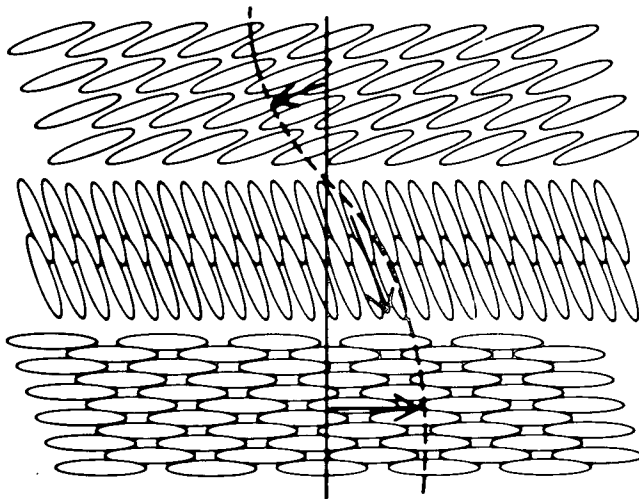
(c) Cholesteric liquid crystals

Figure 3. Liquid Crystal Structure Schematic

FIGURE 4—DYNAMIC SCATTERING

Basically, dynamic scattering is characterized by the formation of small (about 1 μ) domains of aligned liquid crystal material that are in turbulent motion with respect to one another. These domains scatter light and therefore can be used to modulate a laser beam. The domains arise as shown in Fig. 4. A dc voltage applied across the liquid crystal layer aligns the liquid crystal molecules. As the voltage is increased current starts to flow due to the presence of impurities in the liquid crystal. At sufficiently high voltages, the charge carriers disrupt the aligned liquid crystal into the scattering domains that characterize dynamic scattering. Due to the strength of the elastic bonding between the liquid crystal molecules there exists a threshold voltage (on the order of ten volts) below which no scattering occurs. With those few remarks as background, it is now possible to explain the operation of the OTTO.

Referring to Fig. 2, we can explain the principle of operation of the cell in the following way. The photoconductor is fabricated so that its impedance in the dark state is substantially higher than that of the liquid crystal. Thus, when the photoconductor is not illuminated it accepts most of the voltage drop thereby maintaining the liquid crystal below its threshold for dynamic scattering. When light falls on the photoconductor, its impedance drops well below that of the liquid crystal and the voltage switches over to the liquid crystal to exceed the threshold for dynamic scattering. This process occurs locally. The transverse impedance both of the liquid crystal and of the photoconductor are so high that there is virtually no loss of resolution due to transverse spreading of either the photocurrent or of the turbulent scattering. As a result,

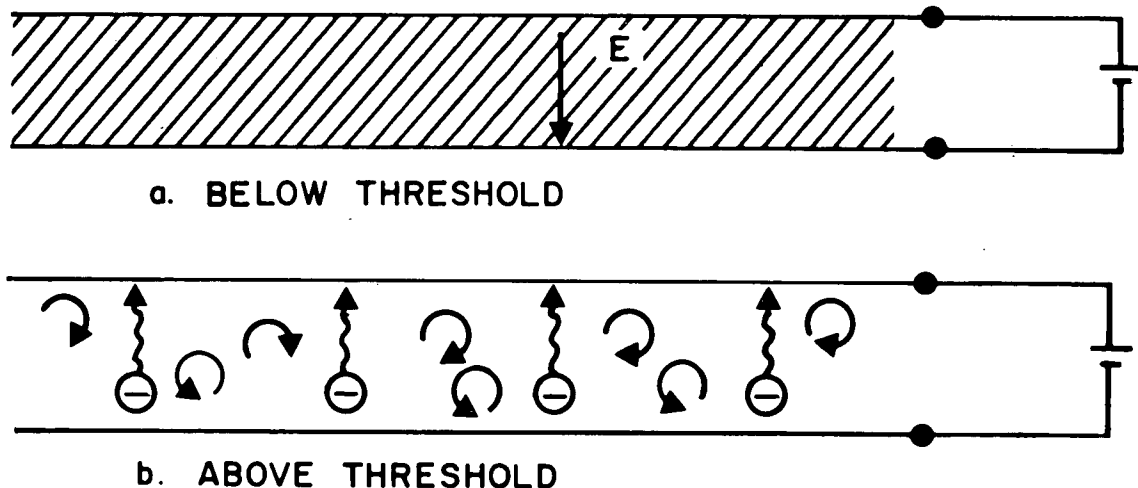a. **BELOW THRESHOLD**

b. **ABOVE THRESHOLD**

Figure 4. Dynamic Scattering

the resolution of the excitation process is approximately equal to the thickness of the liquid crystal layer. Since the liquid crystal layer is approximately as thin as typical photographic emulsions, these cells have photographic quality resolution. Thus, if we excite the photoconductor with an image—i.e., a 2-D distribution of light intensity variation—the cell will transform this light into an identical scattering image which can then be picked up with a second beam of light. In the case of the OTTO, the photoconductor is excited with noncoherent light and the scattering image is sensed with spatially coherent laser light.

FIGURE 5—PRINCIPLES OF OPERATION OF THE OTTO

Figure 5 shows how this process is carried out without destroying the spatial coherence of the laser light.[6] Consider two pencils of rays of laser light—one that strikes a portion of the cell that is in its scattering state and one that strikes the cell at a location where it is not scattering. If we place a lens and aperture each a focal length apart, then the undisturbed light passes through the aperture and can be reimaged on the output plane, whereas the scattered light is recollimated by the first lens and is blocked from appearing at the output plane. The point to note is that apart from a noise background which primarily affects contrast, all of the scattered light is blocked from the output plane. Only unscattered light reaches the output plane to form the image, thereby insuring that the output is fully coherent.
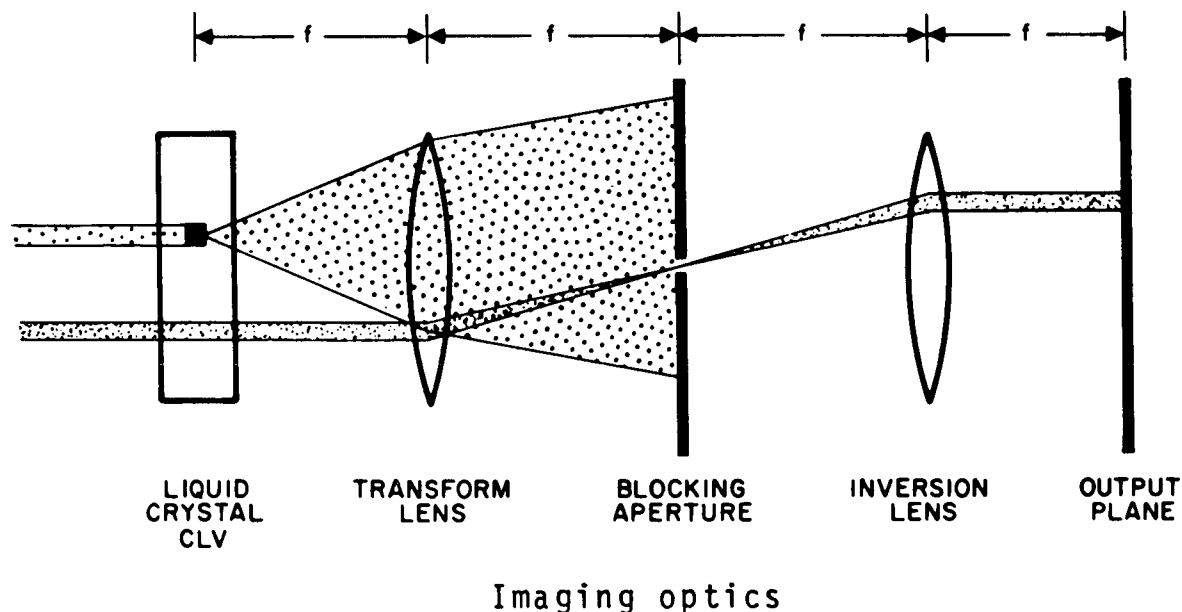

Imaging optics

Figure 5. Principles of Operation of the OTTO

FIGURE 6—SYSTEM SCHEMATIC

Figure 6 shows a schematic of the system that we use to operate the cell. The horizontal portion of this system is the optical data processor. It consists of a laser, a beam spreader, a recollimating lens, a 90 Hz light chopper (to avoid measuring light levels at dc), the OTTO, and the optical system for forming the amplitude image from the scattering image. Spatial filters for data processing would be placed just to the right of the blocking aperture. The vertical leg contains the write beam. It is illuminated with noncoherent light that is focused onto the photoconductor of the OTTO via the pellicle beamsplitter.

FIGURE 7—PHOTO OF TEST SETUP

Figure 7 shows a photo of the experimental setup. As could be seen from the schematic (Fig. 6) the laser light passes through the photoconductor. The reason it doesn't "write up" the photoconductor on its way to the output plane can be seen in Fig. 8.
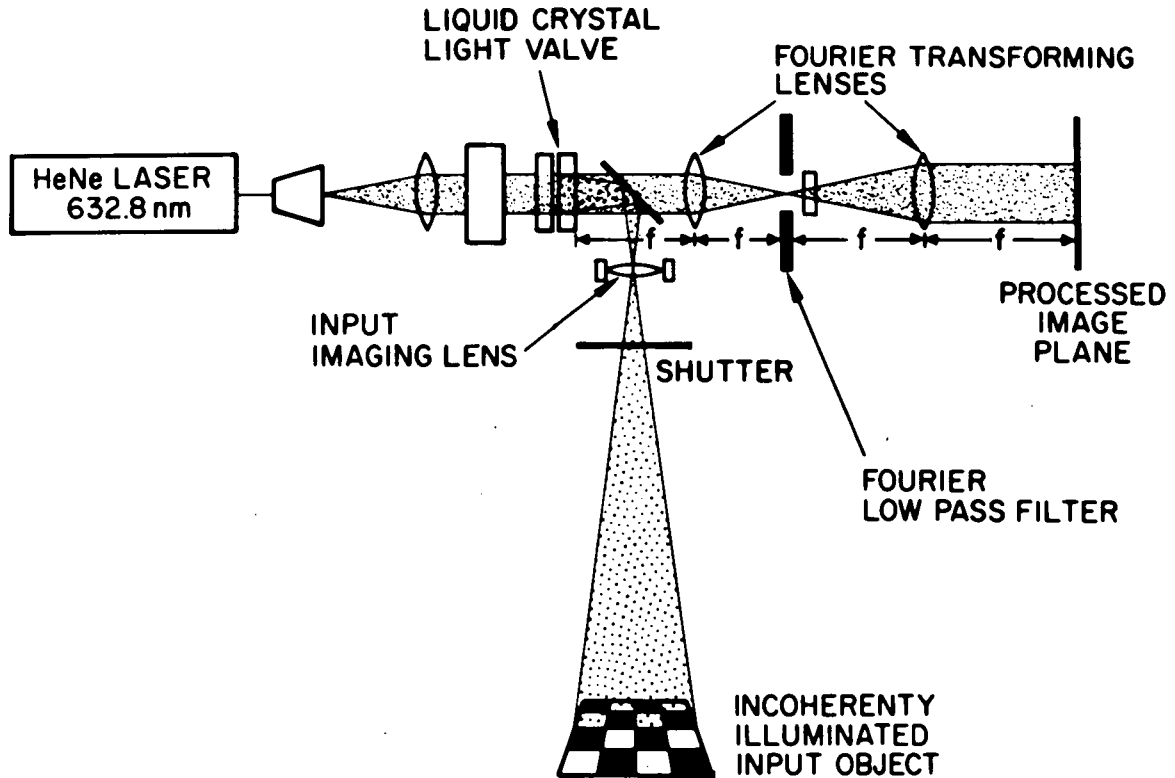
Figure 6. Schematic Diagram of Liquid Crystal Light Valve Optical Processor
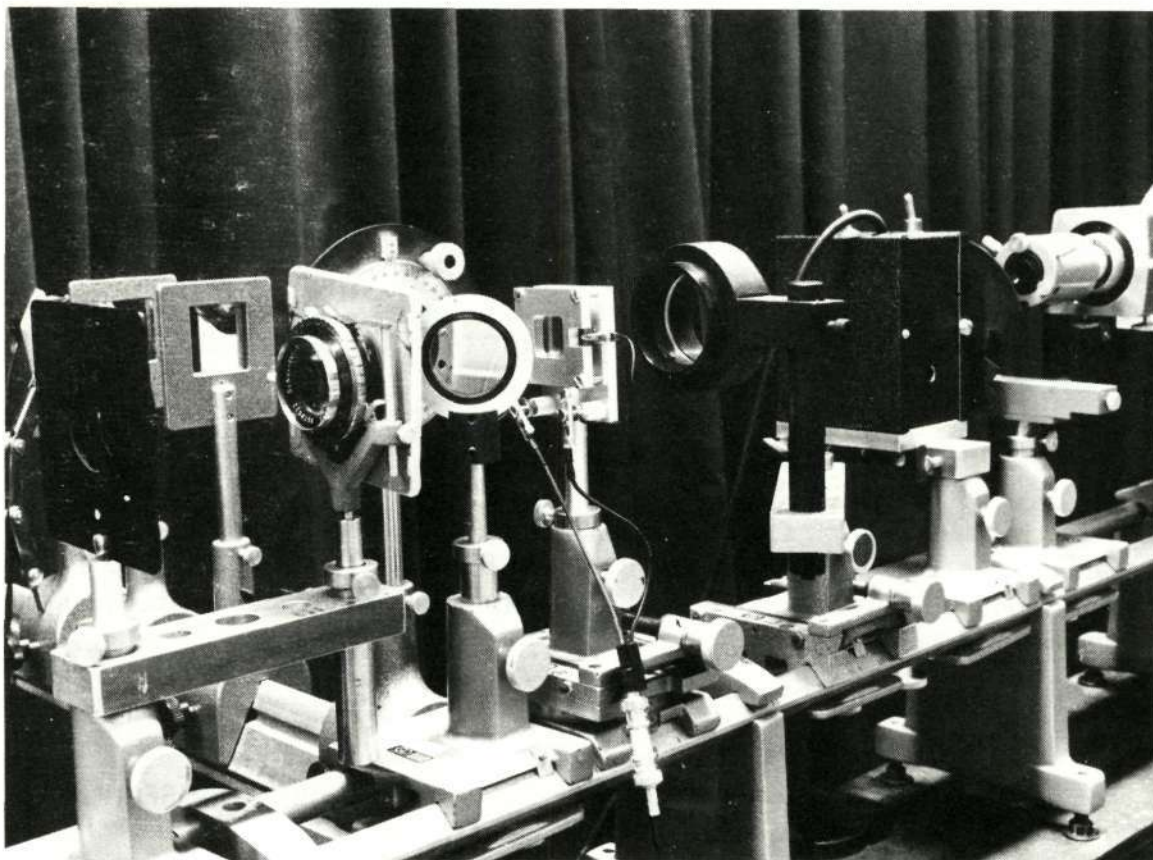
109

Figure 7. Test Setup

FIGURE 8—CDS SENSITIVITY CHARACTERISTICS

This figure shows the absorption characteristics of CdS, the photoconductor that is used in the OTTO, as a function of wavelength. The heavy curve shows this characteristic in the absence of liquid crystal and the dashed curve shows it in the presence of liquid crystal. Consider first the dashed curve. In the presence of liquid crystal, the sensitivity of the CdS to HeNe laser light is down by two orders of magnitude compared with that at the peak sensitivity of the CdS at 5000 Å in the green. This is the reason that we can pass the laser light through the photoconductor without exciting the cell. Figure 8 illustrates a second very important characteristic of CdS in this application; viz, the presence of the liquid crystal significantly alters the sensitivity characteristics of the CdS. The spectral response of the CdS in the presence of liquid crystal is lifted in the blue and falls off more rapidly in the red. Both effects enhance the performance of the device. In the presence of liquid crystal the CdS is

110
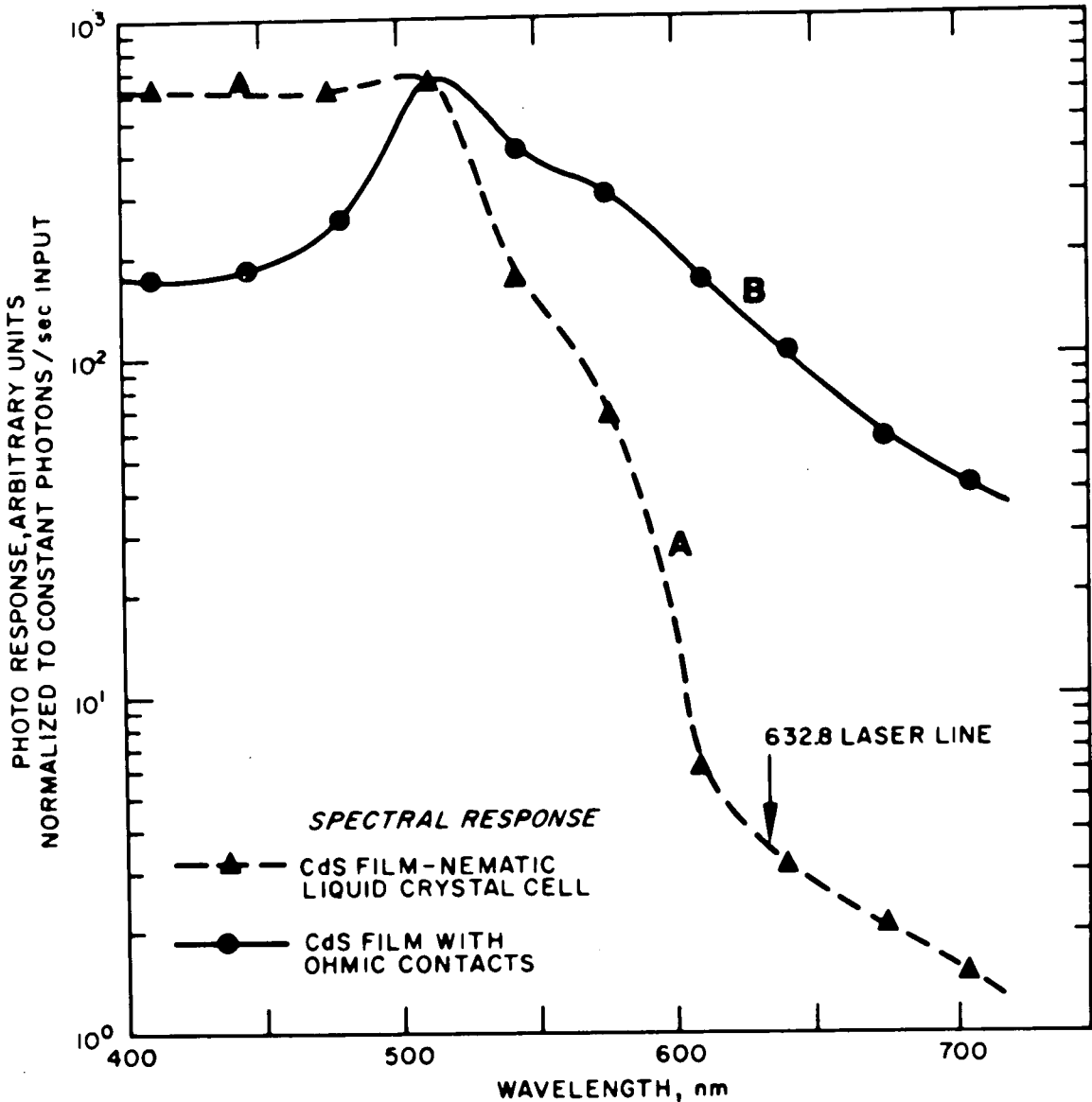
Figure 8. CDS Sensitivity Characteristics

substantially more sensitive to the noncoherent write beam and substantially less sensitive to the coherent read beam. This effect is due to the formation of a diode-like, depletion region in the vicinity of the interface between the liquid crystal and the CdS. This depletion region also increases the dark impedance of the CdS. As a result, it makes the impedance match between the CdS and the liquid crystal more nearly ideal than would be thought possible simply on the basis of the bulk resistivity of the CdS alone.

111

FIGURE 9—OTTO CHARACTERISTICS

Figure 9 summarizes the operating characteristics of the OTTO. It is a reasonably high resolution, very sensitive, somewhat slow, high efficiency and low operating voltage device. The ac voltage is applied to speed up the cell and to promote uniformity of scattering.

FIGURE 10—OUTPUT PLANE PHOTO

Figure 10 shows some imagery recorded with the OTTO. This is a photograph of the output plane image for the case of a checkerboard input image. This was recorded in laser light. The input image was created with non-coherent light from a tungsten lamp with the system shown in Fig. 7.

FIGURE 11—BLOWN UP VERSION OF OUTPUT PLANE PHOTO

Figure 11 shows a blown up version of the image shown in Fig. 10. The input image had 90 squares across a one-inch field. Note the sharp edges of the dark areas. This edge detail is obtained by virtue of the high resolution capability of the OTTO.

RESOLUTION	70 lines per mm
SENSITIVITY	1 $\mu W/cm^2$ @ 510 nm
CONTRAST RATIO	500:1
EXCITATION TIME	100 msec
DECAY TIME	100 msec
COHERENT LIGHT THROUGHPUT	95%
OPERATING VOLTAGE	40 VDC plus 27 VRMS @ 20 KHz

Figure 9. OTTO's Performance Characteristics
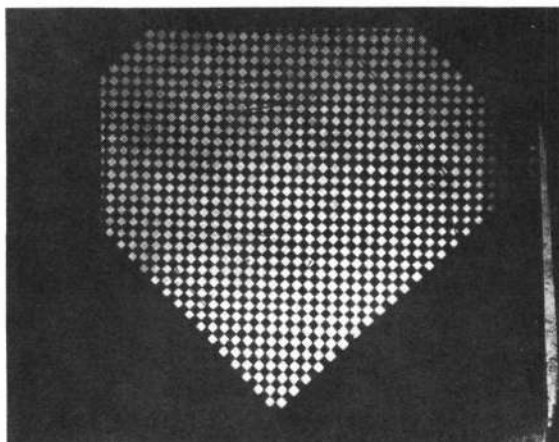
Figure 10. Output Plane
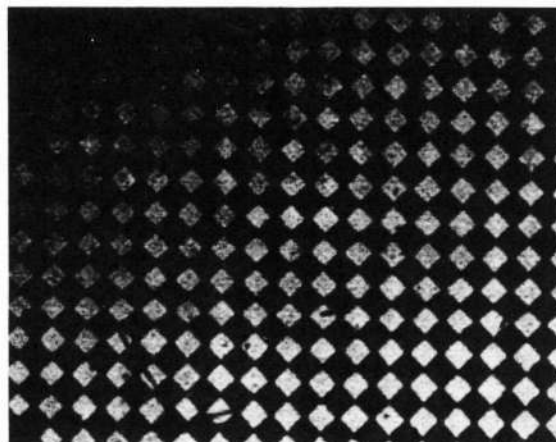
Figure 11. Blown Up Version of
Output Plane

REFERENCES

1. J. D. Margerum, et al, Appl. Phys. Letters, Vol. 13, Pg. 51 (1970).

2. E. N. Leith, Photo. Sci. & Engr., Vol. 6, Pg. 75 (1962).

3. G. W. Gray, "Molecular Structure and the Properties of Liquid Crystal,"
    Academic Press, London (1962).

4. G. H. Heilmeier and L. A. Zanoni, Appl. Phys. Letters, Vol. 13,
    Pg. 132 (1968); Proc. IEEE, Vol. 57, Pg. 34 (1969).

5. S. Y. Wong and J. D. Margerum, "On the Question of Dynamic Scattering
    and Guest-Host Alignment—A Molecular Approach," presented at Amer.
    Chem. Soc. Informal Symposium on Liquid Crystals, Washington, D.C.,
    Sept. 1971.

6. R. B. MacAnally, Appl. Phys. Letters, Vol. 18, Pg. 54 (1971).

THE SYNTHESIS OF COMPLEX SPATIAL FILTERS
FOR COHERENT OPTICAL DATA PROCESSING

Sing H. Lee, Department of Electrical Engineering
Carnegie-Mellon University, Pittsburgh, Pennsylvania 15213

INTRODUCTION

N73-18693

The fundamental advantages of coherent optical processors are their information processing capacities and speed. Comparing with their incoherent counterparts coherent processors are also more flexible in that they can perform "complex" spatial filtering.

The key elements in coherent optical processors are the spatial filters. Therefore, in order to realize the full potential of coherent processors much work should be devoted to the synthesis of and the production techniques for them. In this paper, some recent work on filter synthesis will be summarized, and the implications in optical computation, image processing (enhancement), image restoration (deblurring) and image detection examined. In addition, some advances on the production techniques for the spatial filters will be briefly reviewed. This would include the extension of Vander Lugt's filters to the multiply-exposed filters,[1-4] the binary filters,[5-7] the phase only filters,[8] and the introduction of nonlinear filters.[17]

FILTERING FUNCTIONS

For Optical Computations

On filter synthesis we shall first discuss filters for optical computations. The most fundamental linear operations in optical computations are translation, addition, subtraction, differentiation and integration. The filtering functions, which can perform these computation operations, are surprisingly simple, and consist of no more than a proper collection of sinusoidal gratings.

Optical Translation. Given an optical pattern function in the input plane of a coherent processor, its image which appears in the first diffraction order can be translated with respect to the optical axis in the output plane by controlling the grating spacing of a (sinusoidal) diffraction grating set in the filtering plane (Fig. 1). The higher the frequency of the grating is, the farther away from the optical axis the diffracted images will be.
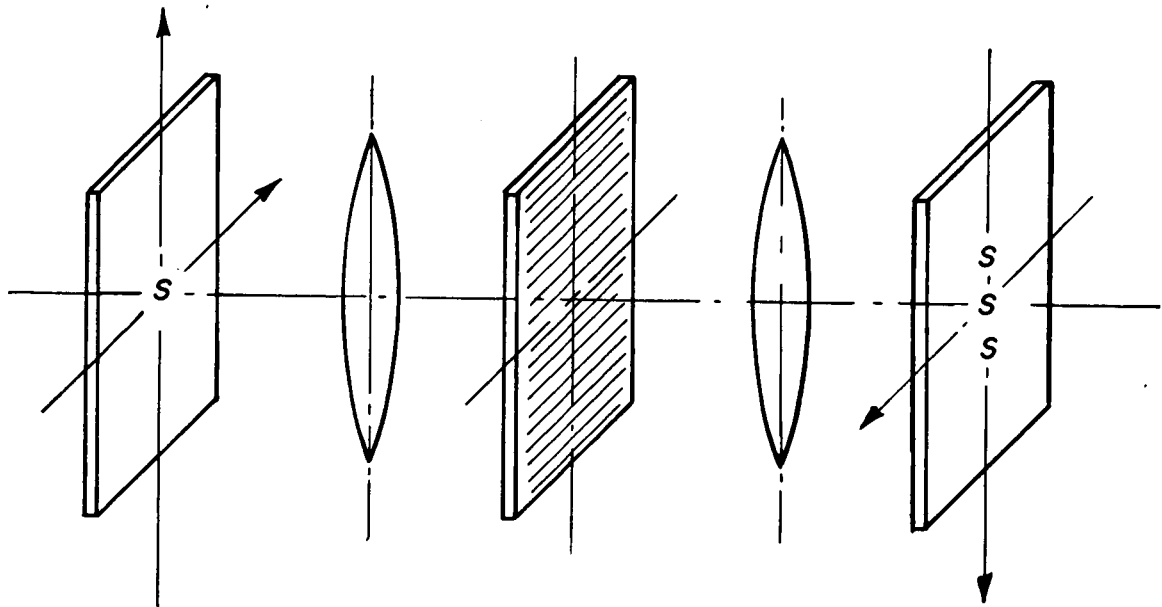
Figure 1. Optical Translation
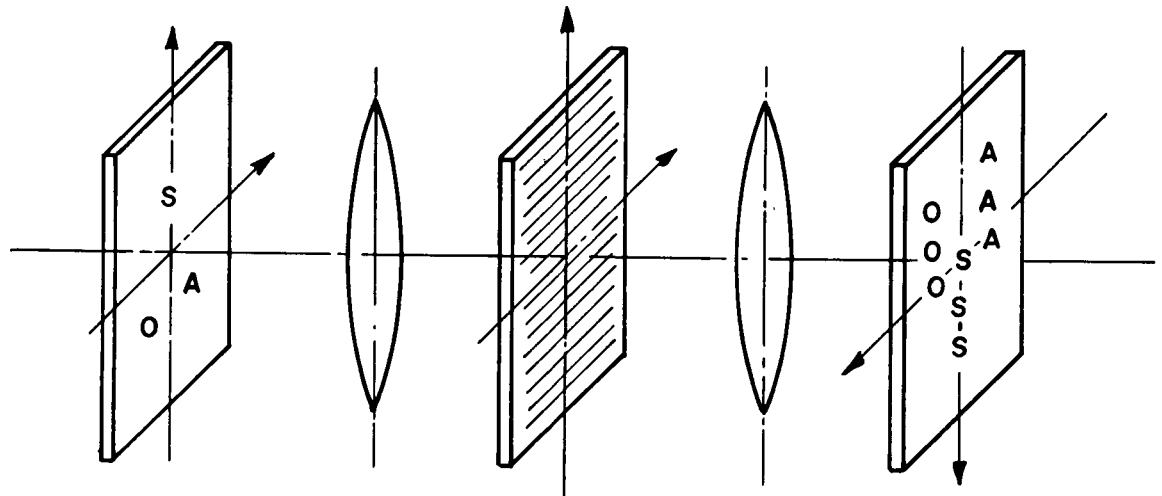
Figure 2. Optical Addition and Subtraction

Optical Addition and Subtraction. Consider the shifting in position of a
pattern function in the input plane (Fig. 2). Since a coherent optical system is
space-invariant, its image in the output plane will be shifted in position also.
That is, the image of the letter "S" in the input plane, which is shifted upward
with respect to the optical axis, will appear shifted downward with respect to
the optical axis in the output plane. Similarly, the image of the letters "OA",

116

which is shifted downward in the input, will appear shifted upward in the output. Notice that in the central region of the output plane the image of the letter "S" overlaps with the image of the letter "OA", if the frequency of the grating in the filtering plane is chosen properly to correspond to the separation between the two input pattern functions. Furthermore, in the overlapping region, the two images will interfere constructively (or add) if the grating function is a co-sinusoidal one with maximum transmittance at the optical axis as illustrated in Fig. 3(a). On the other hand, the two images will interfere destructively (or subtract) if the grating function is a sinusoidal one with minimum transmittance at the optical axis (Fig. 3(b)).

Optical Differentiation and Integration. To differentiate a pattern function, the method of finite differences can be applied. According to the concept of finite differences, the differentiation of a pattern function can be arbitrarily closely approximated by taking the difference between two images, one of which is shifted with respect to the other by an arbitrary small distance. To generate the two images in the output from one pattern function in the input, two gratings

(a)   (b)
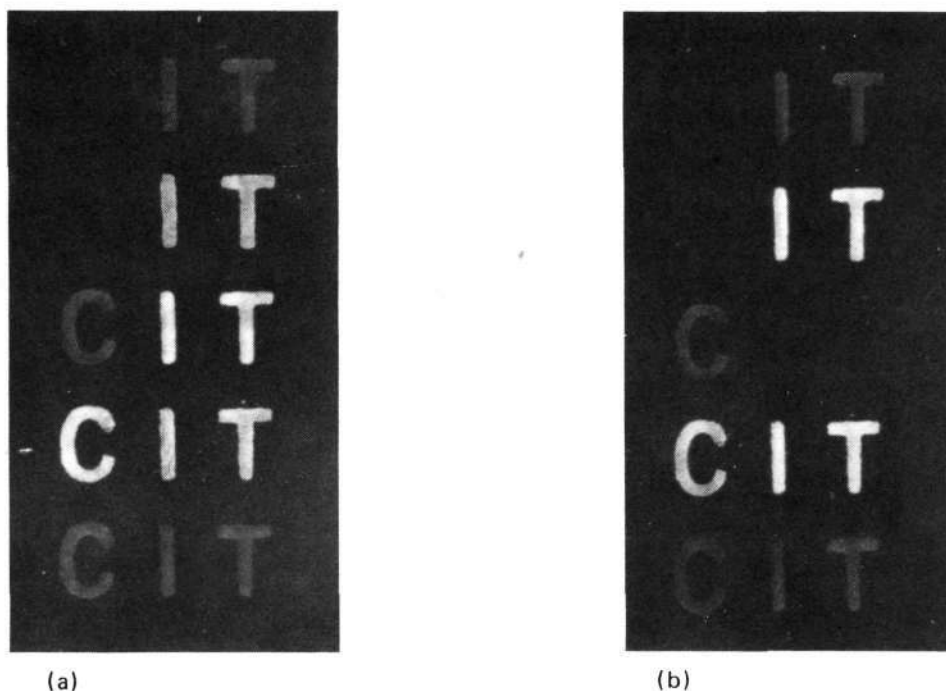
Figure 3. (a) Complex Amplitude Addition. The pattern function
           "IT" is added onto that of "CIT" in the central region of
           the output plane; (b) Complex Amplitude Subtraction.
           The pattern function "IT" is subtracted from that of "CIT"
           in the central region of the output plane.

in the filtering plane will be necessary. The small displacement of one image from the other can then be obtained by choosing the two gratings of slightly different frequencies. The difference (or the subtraction) between the two images will then be ensured, when one of the grating functions has maximum transmittance at the optical axis and the other minimum transmittance at the optical axis. Figure 4(b) illustrates the differentiation along the horizontal direction of the pattern function of Figure 4(a).

For more complex or higher order differentiations (Fig. 5), more gratings will be needed in the finite difference approach. But, gratings are usually fairly easy to make.

To integrate a pattern function, if one can accept the fact that the integration of a function is simply the sum of many of its images shifted by various amounts, it becomes obvious that a collection of gratings of various spatial frequencies will also provide the desired integration result in the output. To summarize, filtering functions consisting of composite gratings can be utilized to perform a number of fundamental computational operations. Once these composite gratings are prepared, they can operate on any new input pattern
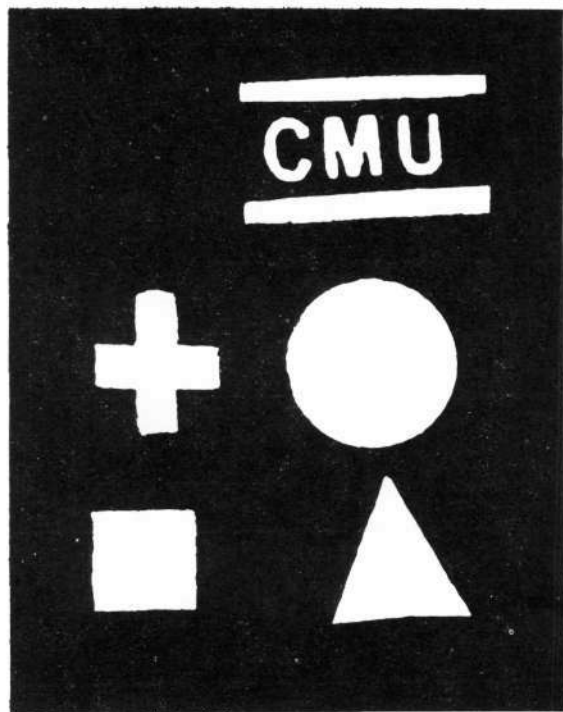

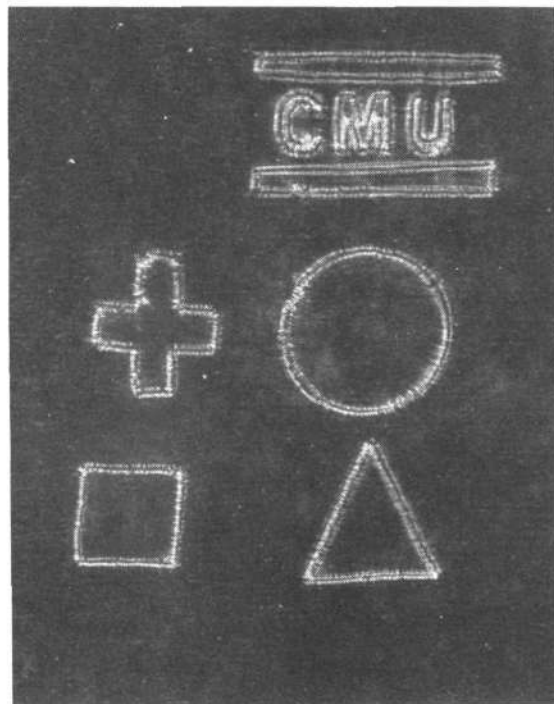Figure 4a. The Object Pattern for Differentiations

Figure 4b. Experimental Result for $\partial f / \partial x$

information. Hence, they are well suited to the role that a coherent processor can play as a computer.

A different perspective on performing optical computations by composite gratings can be visualized when the Fourier transform of a sinusoidal grating is recognized as the sum of two delta functions. Optical processing with such a grating performs in effect the correlations of the two delta functions and the input pattern. Only one of the correlations normally contributes to the desired processed result. This is evident from the earlier discussions and examples, which show that only one diffraction order from each grating contributes to the processed result. Therefore, when processing with composite gratings, the correlation functions of the input pattern and one of the delta functions associated with each "component" grating (in the composite grating) interfere among one another and give rise to the processed output. Mathematically, the computational operations can be expressed in the following forms.

$$\text{Translation} \quad f(x+a,y) = f(x,y) * \delta(x-a,y) \tag{1}$$

$$\text{Addition} \quad f(x,y) + g(x,y) = f(x-a,y) * \delta(x+a,y) + g(x+a,y) * \delta(x-a,y) \tag{2a}$$
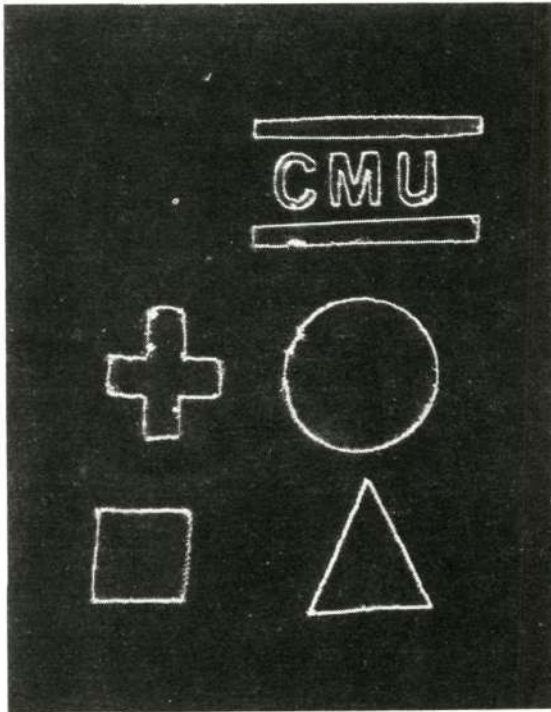

Figure 5a. Experimental Result for $\partial f/\partial x + \partial f/\partial y$
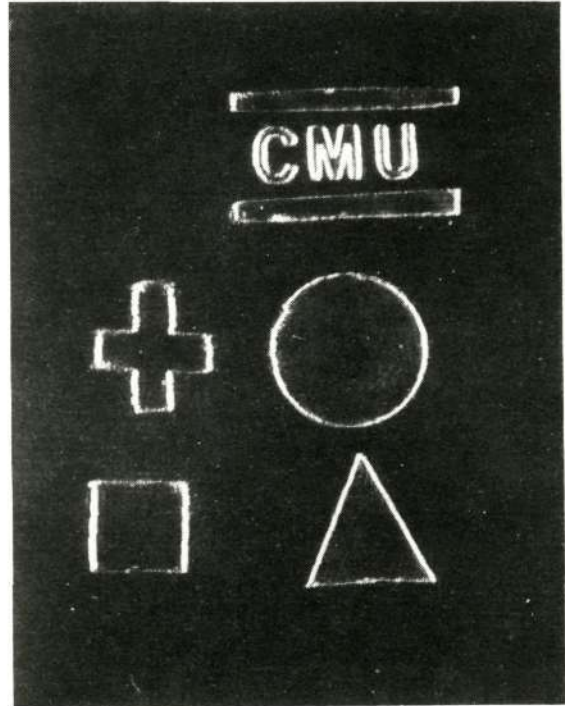
Figure 5b. Experimental Result for $\partial^2 f/\partial x^2 + \partial^2 f/\partial y^2$

Subtraction $\quad f(x,y) - g(x,y) = f(x-a,y) * \delta(x+a,y) + g(x+a,y) * \delta(x-a,y)\, e^{i\pi}$ (2b)

Differentiations

$$\frac{\partial f}{\partial x} = \lim_{h \to 0} \left[\frac{1}{h} \, f(x,y) * g_1(x,y) \right]$$

$$g_1(x,y) = \delta(x+h,y) - \delta(x,y);$$ (3a)

$$\frac{\partial f}{\partial y} = \lim_{h \to 0} \left[\frac{1}{h} \, f(x,y) * g_2(x,y) \right]$$

$$g_2(x,y) = \delta(x,y+h) - \delta(x,y);$$ (3b)

$$\frac{\partial f}{\partial x} + \frac{\partial f}{\partial y} = \lim_{h \to 0} \left[\frac{1}{h} \, f(x,y) * g_3(x,y) \right]$$

$$g_3(x,y) = \delta(x+h,y) + \delta(x,y+h) - 2\delta(x,y)$$ (3c)

$$\frac{\partial^2 f}{\partial x^2} + \frac{\partial^2 f}{\partial x^2} = \lim_{h \to 0} \left[\frac{1}{h^2} f(x,y) * g_4(x,y) \right]$$

$$g_4(x,y) = \delta(x+h,y) + \delta(x-h,y) + \delta(x,y-h) + \delta(x,y+h) - 4\delta(x,y)$$ (4)

$$\frac{\partial^2 f}{\partial x \partial y} = \lim_{h \to 0} \left[\frac{1}{h^2} \, f(x,y) * g_5(x,y) \right]$$

$$g_5(x,y) = \delta(x+h,y+h) + \delta(x,y) - \delta(x,y+h) - \delta(x+h,y)$$ (5)

Integrations: $\qquad \displaystyle\int_{-\infty}^{X} f(\xi,\eta)d\xi = f(x,y) * u(x,0)$ (6a)

$$\int_{-\infty}^{X} \int_{-\infty}^{y} f(\xi,\eta)d\xi \, d\eta = f(x,y) * u(x,y)$$ (6b)

where the symbol * denotes the correlation operation, $u(x,0)$ is a slit function and $u(x,y)$ a step function.

For Image Enhancement

In image enhancement there are two situations often encountered. One situation requires an image to be smoothed in order to suppress noise that may be presented in it. The other requires an image to be sharpened in order to extract contours and edge details. As in the last section and the sections that follow, we again concentrate our attentions on the methods that can be implemented by a coherent processor.

Smoothing

a. <u>Band-pass Spatial Frequency Filtering.</u> Lowpass and bandpass spatial filtering are the simplest methods in suppressing noise, when the spatial frequency characteristics of noise is substantially different from that of the picture. The filtering functions in this kind of filtering, as is well-known, consists of stops (or zeroes) in those frequency regions, where noise gives most contribution.

b. <u>Averaging over a Neighborhood.</u> One can also smooth a picture by simply replacing its value at each point by the average of the values over a neighborhood of the point. This method of smoothing is, therefore, just the correlation of the picture with an aperture of an area over which the values are averaged, and can be considered as a processing operation similar to that described by integration.

c. <u>Averaging of Multiple Images.</u> Another method for improving the signal-to-noise ratio of a picture is by averaging a set of independent, noisy images of a picture. In principle the averaging can be done by optical summation as described above, though in practice the constraint on the quality of the optical system should be considered in using this method.

<u>Sharpening.</u> Just as one can smooth a picture in a variety of ways, so there are many ways to sharpen a picture. For example, highpass spatial filtering or some sort of differentiation operation (such as the gradient and the Laplacian operations) can enhance a picture by extracting contours and edge details. Thus, the filtering functions for differentiation operations described earlier for computational purpose are also useful here in image enhancement.

For Image Restoration

There are many methods to restore a degraded image.[9-12] But, in this section we shall continue our attempt with composite gratings to illustrate that

when they are properly synthesized, they can play an important role, as they have in optical computations and image enhancement.[13] (Note once again that processing with a filter of composite gratings is the same as processing the input pattern function (in this case a degraded image) by correlating it with a collection of delta functions.)

To begin, the simple case of an image degraded by N multiple exposures will be considered. Between exposures the object illuminance is displaced by a distance Δ relative to the recording medium.

In this case the degraded image g_1 can be expressed as

$$g_1 = f * h_1, \tag{7}$$

where

$$h_1 = \sum_{n=0}^{N} a_n \delta(x-n\Delta), \tag{8}$$

and a_n corresponds to the intensity of the nth exposure. Our objective is to synthesize a processing function, p, consisting of a set of delta functions so that when this processing function correlates with $g_1(x,y)$, the image function $f(x,y)$ can be retrieved within a certain area of interest. We let

$$p(x,y) = \sum_{m=0}^{M} b_m \delta(x-m\Delta), \tag{9}$$

where b_m may take on any values, positive, negative, or even zero. Correlating $g_1(x,y)$ with $p(x,y)$ gives

$$g_1(x,y) * p = f * h_1 * p.$$

$$= f * \sum_{m=0}^{N} \sum_{m=0}^{M} a_n b_m [x-(n+m)\Delta]. \tag{10}$$

The correlation $(h_1 * p)$ is illustrated in Figure 6 where we have in the mth row the mth delta function associated with $p(x,y)$ correlating with the blurring function h_1. It is clear from this figure that the condition for $(g_1 * p)$ be equal to $f(x,y)$ within the region $|x| \leqslant (q/2)\Delta$ requires

$$a_0 b_0 \qquad\qquad\qquad\qquad = 1$$

$$a_1 b_0 + a_0 b_1 \qquad\qquad\qquad = 0$$

$$a_2 b_0 + a_1 b_1 + a_0 b_2 \qquad\qquad = 0$$

$$\vdots$$

$$a_{q-1} b_0 + a_{q-2} b_1 + \ldots + a_0 b_{q-1} = 0.$$

This set of conditions or equations allow us to determine the processing function $p(x,y)$, or equivalently the coefficients b_m. Writing the set of equations into the matrix form, we have

$$\underset{\sim}{A}\,\underset{\sim}{b} = \underset{\sim}{c}, \qquad\qquad\qquad (11)$$

where

$$\underset{\sim}{A} =
\begin{pmatrix}
a_0 & 0 & \ldots\ldots & 0 \\
a_1 & a_0 & 0\ldots\ldots & 0 \\
\cdot & \cdot & \ldots\ldots\ldots\ldots \\
\cdot & \cdot & \ldots\ldots\ldots\ldots \\
a_{q-2} & a_{q-3} & \ldots\ldots a_0 & 0 \\
a_{q-1} & a_{q-2} & \ldots\ldots a_1 & a_0
\end{pmatrix}$$

$$\underset{\sim}{b} =
\begin{pmatrix}
b_0 \\
b_1 \\
\cdot \\
\cdot \\
\cdot \\
b_{q-2} \\
b_{q-1}
\end{pmatrix}
\quad \text{and} \quad
\underset{\sim}{c} =
\begin{pmatrix}
1 \\
0 \\
\cdot \\
\cdot \\
\cdot \\
0 \\
0
\end{pmatrix}$$

Since the matrices $\underset{\sim}{A}$ and the vector $\underset{\sim}{c}$ are known, the vector $\underset{\sim}{b}$ can easily be determined by matrix inversion, $\underset{\sim}{b} = \underset{\sim}{A}^{-1}\,\underset{\sim}{c}$. As an example, consider an image

123
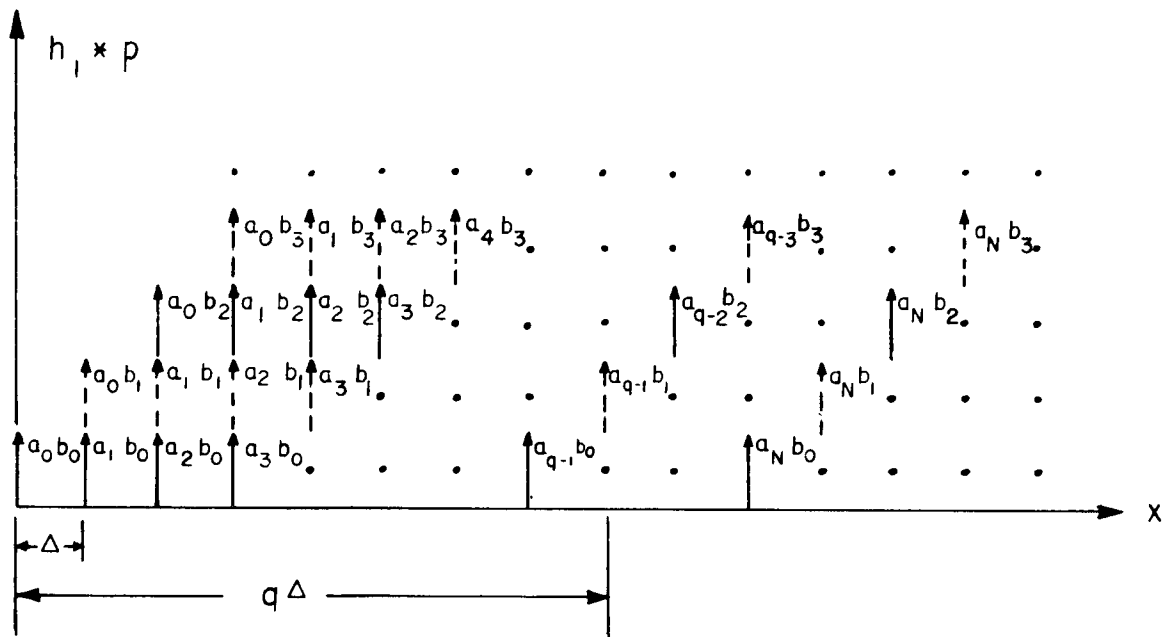
Figure 6. The Correlation of h_1 (x,y) and p(x,y)

degraded due to the malfunctioning of a camera such that the recorded image has four exposures. Between exposures there is a relative displacement Δ between the object illuminance and the film. If all four exposures are identical, $h_1(x,y)$ then becomes the function as shown in Figure 7a. Further, if f(x,y) is to be restored from g(x,y) at least within a region of width 4Δ, the vector $\underset{\sim}{c}$ becomes

$$\underset{\sim}{c} = \begin{pmatrix} 1 \\ 0 \\ 0 \\ 0 \end{pmatrix} \tag{12a}$$

From our matrix formulation the vector b is found to be

$$\underset{\sim}{b} = \underset{\sim}{A}^{-1} \underset{\sim}{c} = \begin{pmatrix} 1 \\ -1 \\ 0 \\ 0 \end{pmatrix} \tag{12b}$$

Figure 7. (a) The PSF for an Image of Four Exposures;
(b) The Processing Function Synthesized from the Matrix Formulation
for the Restoration of an Image of Dimension up to 4Δ Along
the x-Direction;
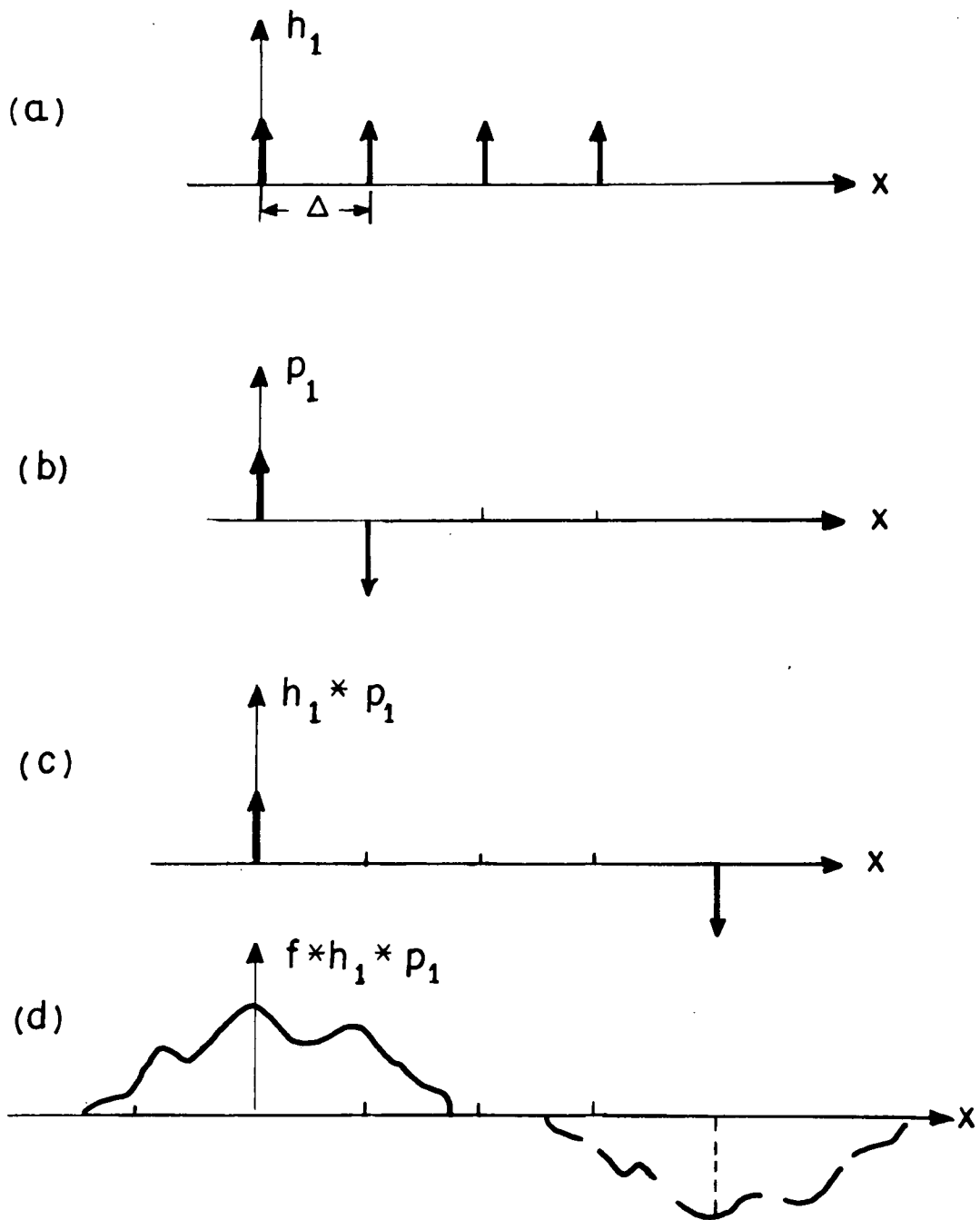(c) The Result of Correlating h_1 with p_1;
(d) The Processed Result of $g_1(x,y)$ by $p_1(x,y)$.

The solution for $\underset{\sim}{b}$ leads to the processing function $p_1(x,y)$ as shown in Figure 7b. It is clear that an image of dimension up to 4Δ along the blurred direction has been restored as intended (Fig. 7c, 7d). Figure 8 shows one of our experimental results obtained using the processing function $p_1(x,y)$. If an image of dimension larger than 4Δ, but smaller than 8Δ, is to be retrieved from a record degraded by the same PSF as in the last example, similar analysis shows that $\underset{\sim}{c}$ now becomes

$$\underset{\sim}{c} = \begin{pmatrix} 1 \\ 0 \\ 0 \\ 0 \\ 0 \\ 0 \\ 0 \\ 0 \end{pmatrix} \tag{13a}$$

The solution for $\underset{\sim}{b}$ is

$$\underset{\sim}{b} = \begin{pmatrix} 1 \\ -1 \\ 0 \\ 0 \\ 1 \\ -1 \\ 0 \\ 0 \end{pmatrix} \tag{13b}$$

The processing function $p_1'(x,y)$ corresponding to this solution of $\underset{\sim}{b}$ is as illustrated in Figure 9. Comparison between Figures 7 and 9 indicates that the addition of another pair of delta functions (one positive, the other negative) to $p_1'(x,y)$ helps to move the ghost image away such that a $f(x,y)$ of relatively
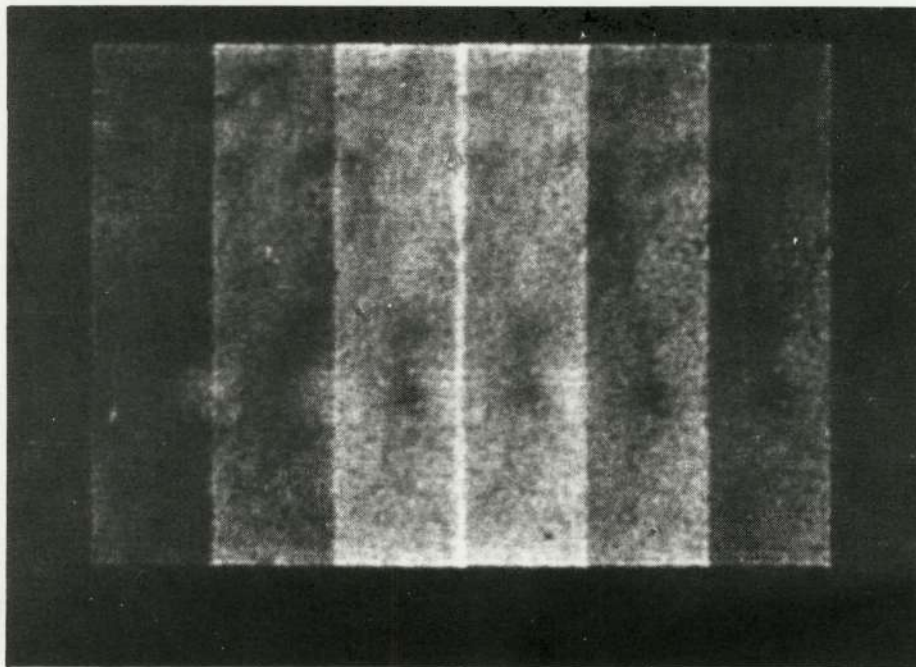
(a)
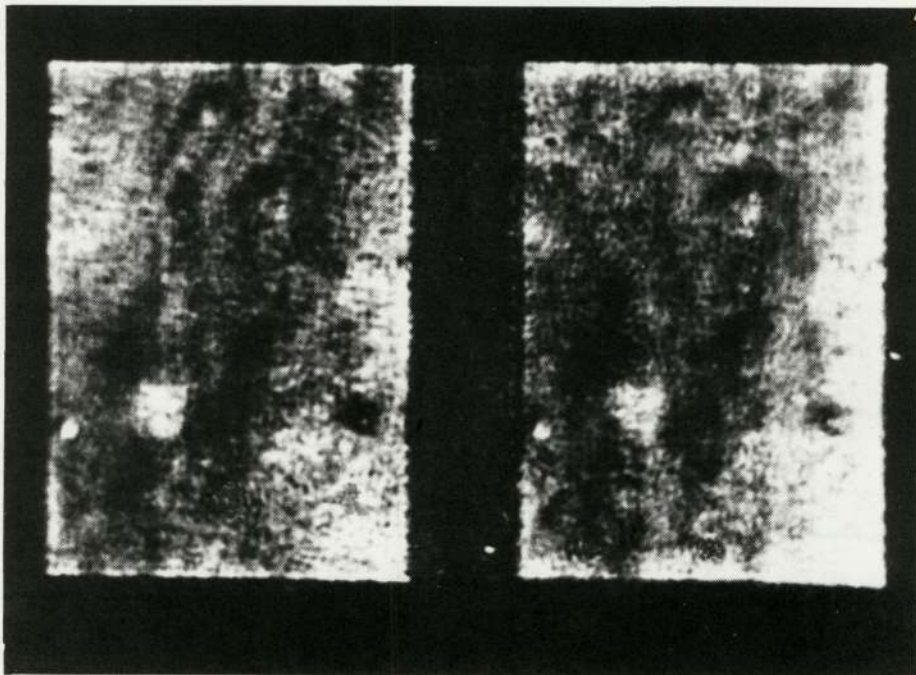
(b)

Figure 8. Image Restoration. (a) An image of a portion of the Moon degraded by malfunctioning of the camera shutter; (b) A photo of the output obtained from the restoration scheme described in text.

Figure 9. Same as Figure 7 except that the processing function, $p_1'(x,y)$ is synthesized for the restoration of an image of dimension up to 8Δ.

larger dimensions can be recovered. In extension, by adding more pairs of delta functions one would be able to restore a f(x,y) of even larger dimensions. It should be pointed out that since the coefficients a_n, b_n in our approach are not restricted to equal magnitudes, the multiple exposures in g(x,y) need not be equal for restoration to take place.
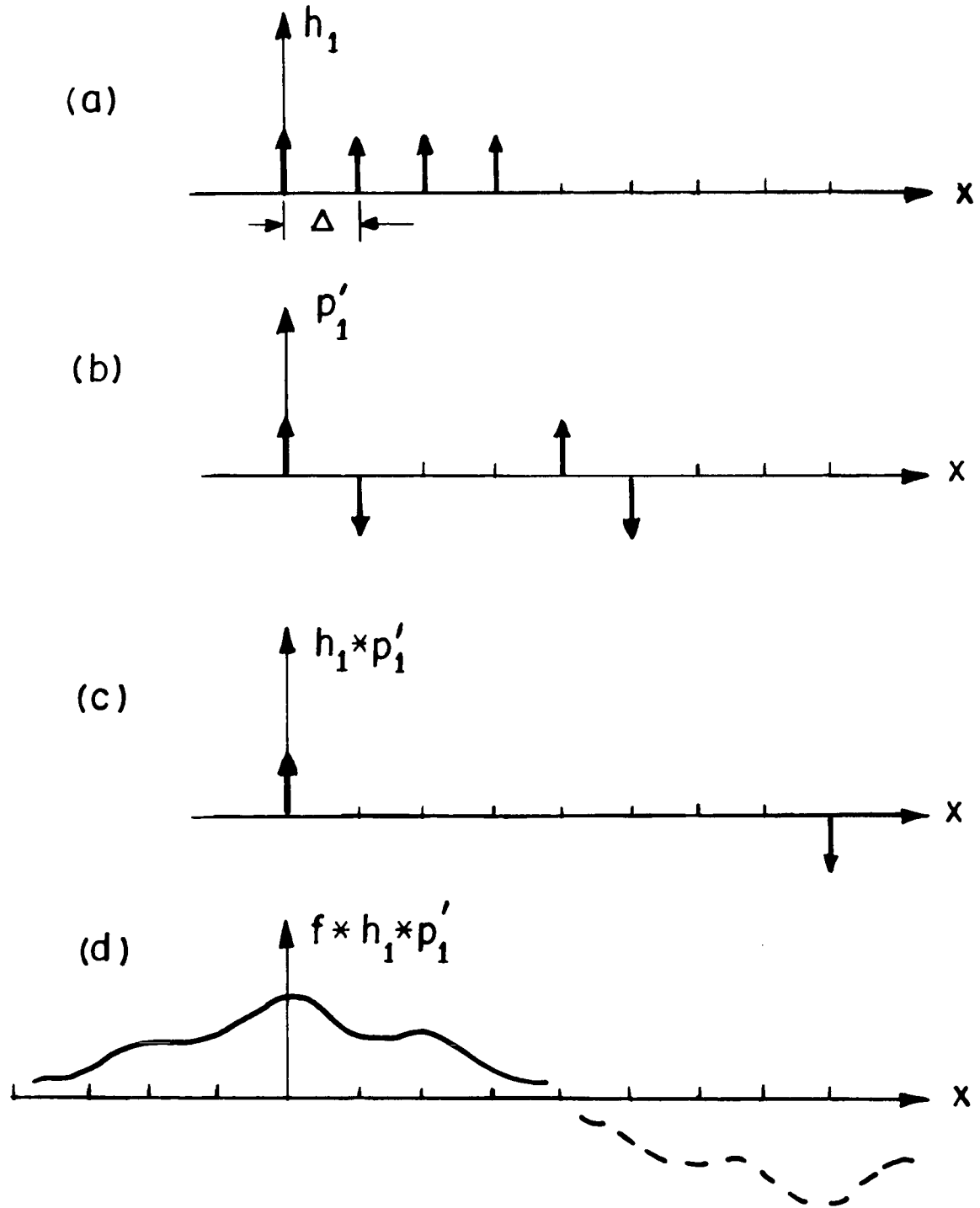
Next, let us consider images degraded by linear smear. The PSF for linear smear degradation, h_2, is a rectangular function of width Δ' (Fig. 10a). Since a rectangular function is a limiting case of h_1 in Figures 7 and 9 when Δ is allowed to approach ϵ, an arbitrary small distance, but $(N-1)\Delta$ is kept constant at Δ' by increasing N, the solution for the processing function $p_2(x,y)$ can be deduced from the solution $p_1(x,y)$ obtained earlier for the multiply-exposed type of degradation. Hence, $p_2(x,y)$ of Figure 10b is deduced from $p_1(x,y)$ and $p_2'(x,y)$ of Figure 10e from $p_1'(x,y)$ for the restoration of linearly smeared images of dimensions up to Δ' and $2\Delta'$ respectively. As is obvious $p_2(x,y)$ and $p_2'(x,y)$ are merely collections of doublets. In extension, one can also show that the restoration function for linear acceleration and deceleration type of degradation with a blurring function of a triangle is the differentiation of doublets.

For Image Detection

Image detection with coherent light has most often based on matched filtering.[14-16] By way of definition, a linear filter is said to be matched to the particular signal f(x,y) if its impulse response g(x,y) is given by the complex conjugate of f(x,y),,

$$g(x,y) = f^*(-x,-y), \tag{14}$$

Matched filtering works very well, when it is used to detect an image among many which bear little resemblance. But, for similar images, different types of filtering with better discriminating capabilities appear to be needed. Two simple approaches have been studied with this intention in mind. One makes use of the gradient correlation,[2] and the other make use of the subtraction-correlation.[3]

The Gradient Correlation. The gradient correlation recognizes or detect the input signal by its perimeter or outline, in contrast to the correlation of the signals themselves recognizes it by area. Mathematically the gradient correlation is represented by

$$s(x,y) = \iint \operatorname{grad} f(x',y') \operatorname{grad} f^*(x'-x,y'-y)\, dx'dy'$$
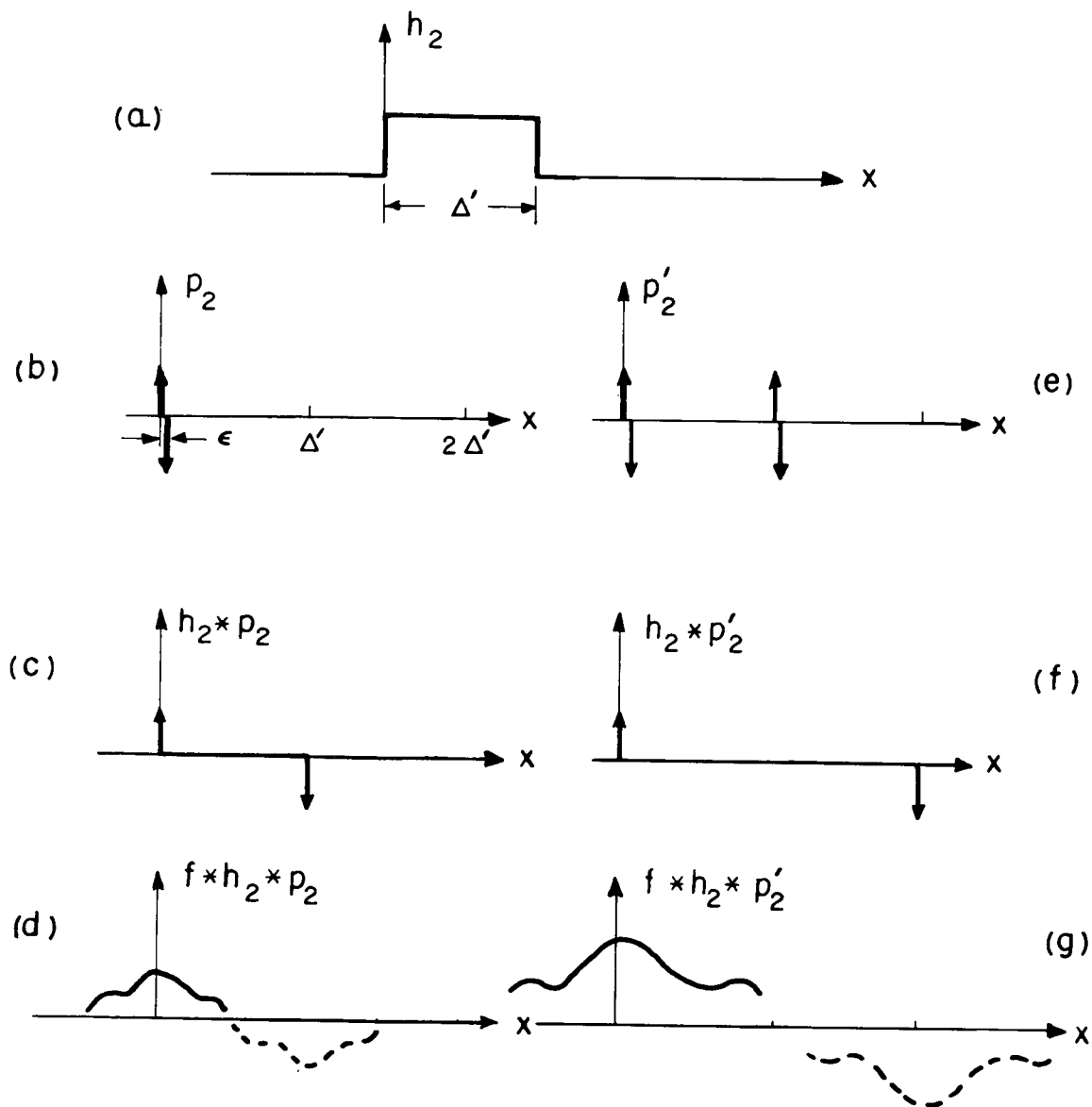
Figure 10. (a) Linear–Smear Degradation; (b) The Processing Function for the Restoration of an Image of Dimension up to Δ' (c) The Result of Correlating h_2 by p_2; (d) The Processed Result of $g_2(x,y)$ by $p_2(x,y)$; (e)–(g) same as (b)–(d) except that the processing function $p_2'(x,y)$ is synthesized for the restoration of an image of dimension up to $2\Delta'$.

$$= \left[(\partial^2 \delta / \partial x^2) + \left(\frac{\partial^2 \delta}{\partial y^2} \right) \right] * f * f \tag{15}$$

Expressing the Laplacian operation on the delta function in terms of a difference equation as was done earlier on optical computations,

$$(\partial^2 \delta / \partial x^2) + (\partial^2 \delta / \partial y^2) \cong \lim_{h \to 0} \left\{ \left(\frac{1}{h^2} \right) \; [\delta(x+h,y) + \delta(x-h,y) \right. \tag{16}$$
$$\left. + \delta(x,y+h) + \delta(x,y-h) - 4\delta(x,y)] \right\}$$

we have

$$s(x,y) = \lim_{h \to 0} \left\{ \left(\frac{1}{h^2} \right) \; [f(x+h,y) + f(x-h,y) + f(x,y+h) \right. \tag{17}$$
$$\left. + f(x,y-h) - 4f(x,y)] \right\} * f(x,y).$$

The filtering function which achieve gradient correlation is

$$G(u,v) = \lim_{h \to 0} \left\{ \left(\frac{1}{h^2} \right) \; [\exp(-i2\pi \vec{u} \cdot \vec{h}_1) + \exp(i2\pi \vec{u} \cdot \vec{h}_1) \right. \tag{18}$$
$$\left. + \exp(-i2\pi \vec{v} \cdot \vec{h}_2) + \exp(i2\pi \vec{v} \cdot \vec{h}_2) - 4] \right\} F^*(u,v)$$

Figure 11(a) illustrates the impulse response of such a filter which has been synthesized for the character T. It is to be compared with the impulse response of a matched filter (Fig. 11b). Figure 12 shows the response of the two filters to the letters C, I, T. Clearly, the gradient correlation filter gives better detection discrimination between the similar images of I and T, when the intensity profiles across the central part of the correlation functions are examined on an oscilloscope display.

The Subtraction Correlation. The concept of employing the subtraction operation to extract a desired feature which characterizes an image and utilizing the correlation operation to detect it is quite straightforward. To implement

131

Figure 11a. Impulse Response of a
Gradient Correlation
Filter for the Letter T
Synthesized by a Multi-
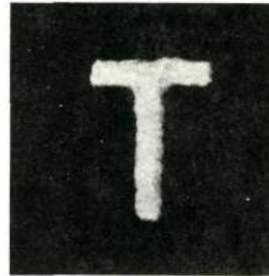ple Exposure Technique

Figure 11b. Impulse Response of a
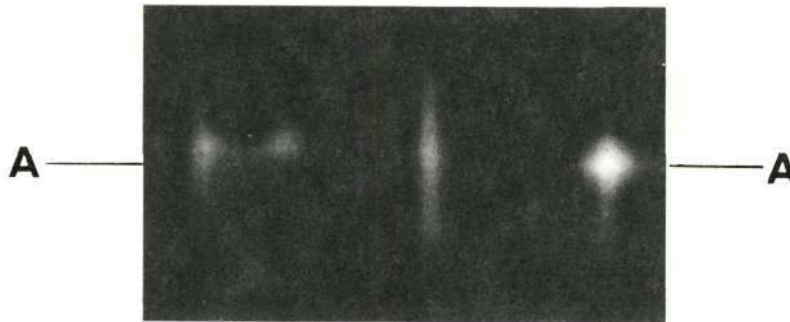Matched Filter for the
Letter T

Figure 12a. Correlation for the Input Letters CIT Using a
Gradient Correlation Filter of the Letter T
Synthesized by a Multiple Exposure Technique
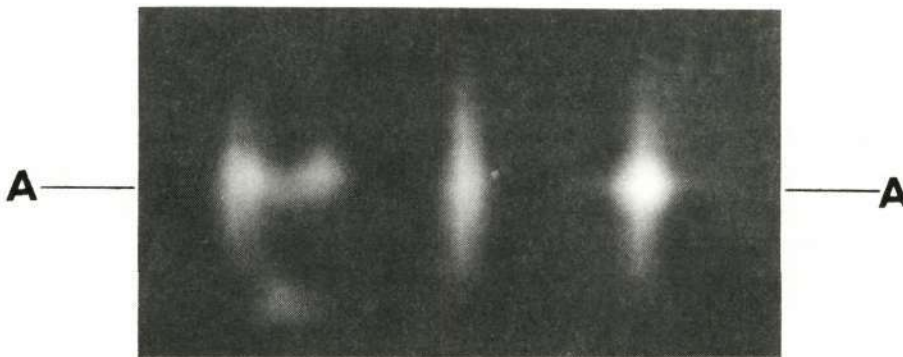
Figure 12b. Correlation for the Input Letters CIT Using
a Matched Filter of the Letter T
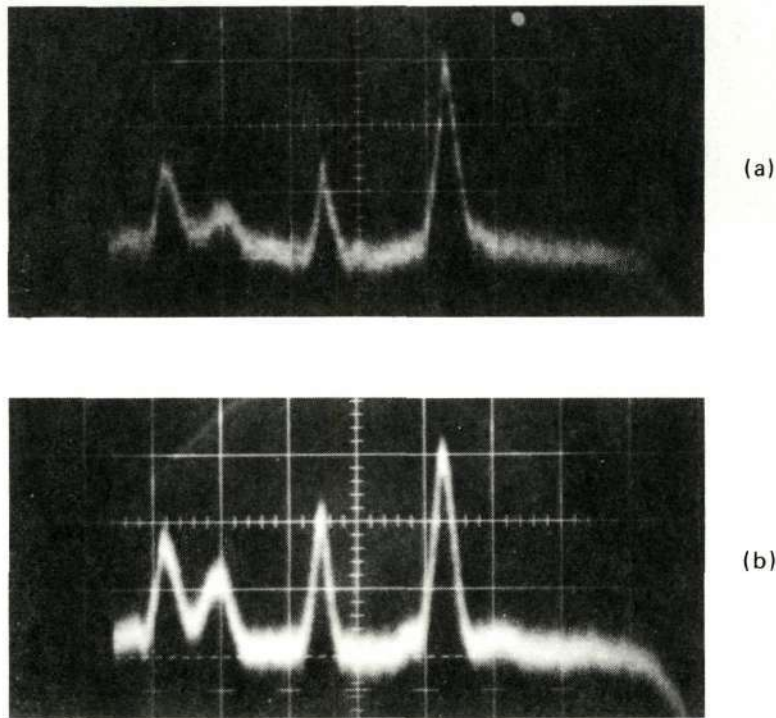
Figure 12c. Intensity Profiles Across the Center Lines of the Correlation Patterns for Input Letters CIT and (a) the Gradient Correlation Filter (b) The Matched Filter of the Letter T

it optically in a single-stage coherent processor, one feasible and convenient method is to display both image functions simultaneously in the input plane, one centered at say b_1 distance from the optical axis, the other at b_2 from the optical axis. A spatial filter bearing the information of

$$t(\vec{v}) = F_1^*(u,v) \, [\exp(i2\pi\vec{v}\cdot\vec{b}_1) - \exp(i2\pi\vec{v}\cdot\vec{b}_2)] \qquad (19)$$

will be needed, where $F^*(u,v)$ stands for the complex conjugate of the Fourier transform of the feature to be detected. For example, we wish to distinguish R from P. The feature to be extracted from this letter pair is then the tilted stroke. Figures 13 and 14 illustrate the experimental result of our combined subtraction and correlation procedure when the inputs correspond to R and P, and P and P respectively. The presence and absence of the feature of interest in the central region of the output plane is obvious and can be easily detected.

Figure 13. The Output of a Coherent System with a Subtraction-Correlation Filter. Patterns from left to right are $f_2 * f_1$, $(f_2 - f_3) * f_1$, and $f_3 * f_1$ where f_1 stands for the tilted stroke, f_2 the character R, and f_3 the character P.
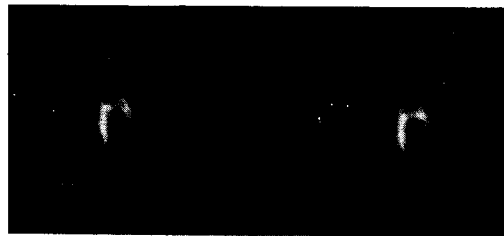
Figure 14. The Output of a Coherent System with a Subtraction-Correlation Filter. Patterns from left to right are $f_2 * f_1$, $(f_2 - f_3) * f_1$, and $f_3 * f_1$, where f_1 stands for the tilted stroke and both f_2 and f_3 are the character P.
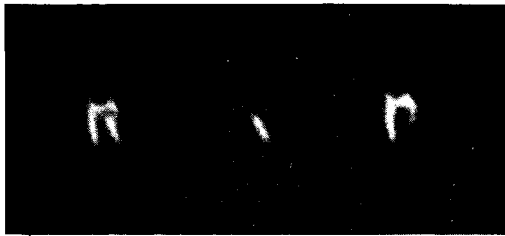
FILTER PRODUCTION

The Multiply-Exposed Filter

Normally, Vander Lugt's interferometric method is very convenient to employ in complex filter production (Fig. 15). However, on a number of occasions as we have seen earlier that composite filtering functions consisting of a collection of gratings or a sum of several complex functions do arise. For these occasions there is a need to extend Vander Lugt's technique to include multiple exposures. As an example, the gradient correlation filter of Eq. (18) is to be produced. Since the filtering function for gradient correlation consists of five terms, five exposures will be necessary. In these exposures the same reference wave is to interfere with the Fourier transforms of f(x,y), but before each subsequent exposure is made, the position of f(x,y) will be shifted slightly by the amount h. Note also that one of the exposures should be four times stronger or longer than the others, and the negative sign can be introduced by shifting the film plate by half a fringe relative to its position for the other exposures. The impulse response of a gradient correlation filter for the letter T has been shown earlier in Figure 11(a).

The Binary Filter

Another method of producing a complex filter employs the digital computer to provide a binary filter (Fig. 16). Binary filters work on the optical diffraction phenomena of slits. The important procedures involved here are (1) to
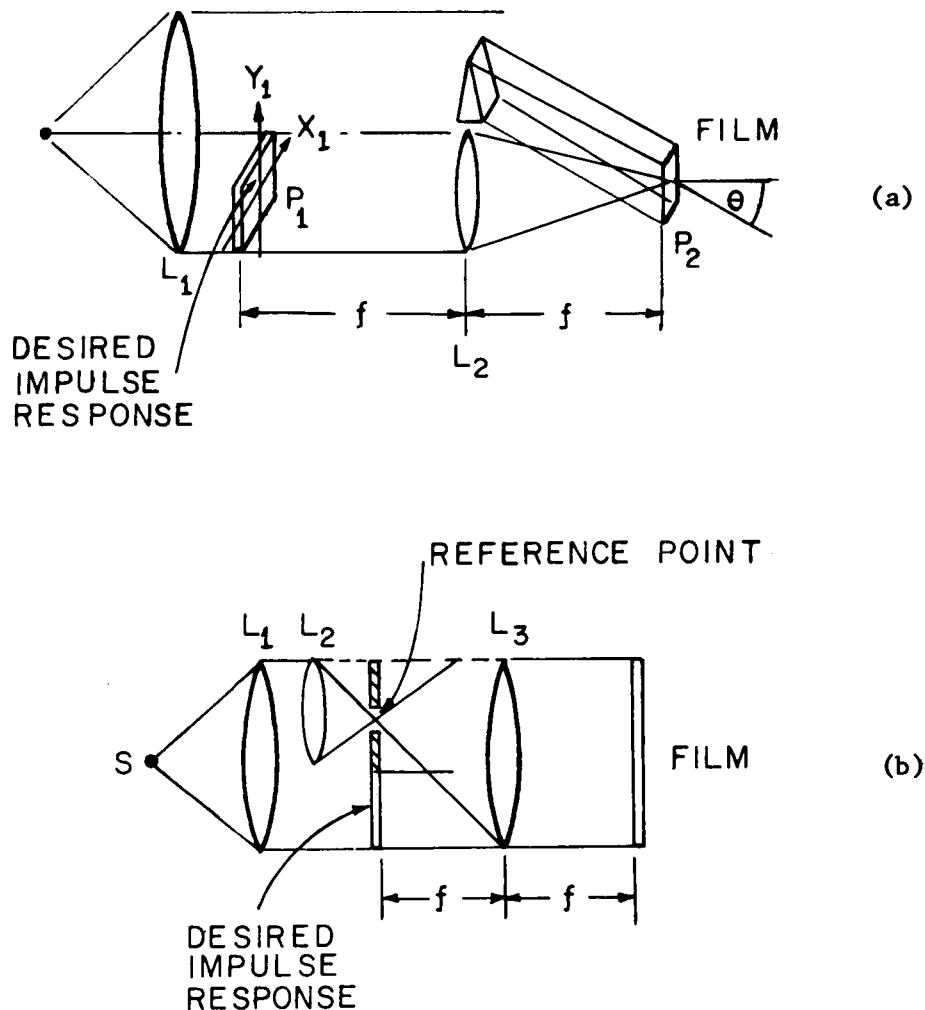
Figure 15. Two Interferometric Systems for Producing the
Frequency Plane Mask — the Vander Lugt Filter

$$\alpha = \frac{\sin\theta}{\lambda}$$

sample the filtering function at periodic lattice points, (2) determine the dimensions of the transparent slits so that the amount of light passing through them are proportional to the magnitudes of amplitude transmittance called for by the filtering functions at those points sampled, (3) shift the position of each slit by an amount proportional to the phase angle of the filtering function at that point, (4) photoreduce the plotter output from the computer.

In Lohmann's method[5,6] the phase angles of the filtering function at the sampled points are quantized. Since phase quantization introduces noise in
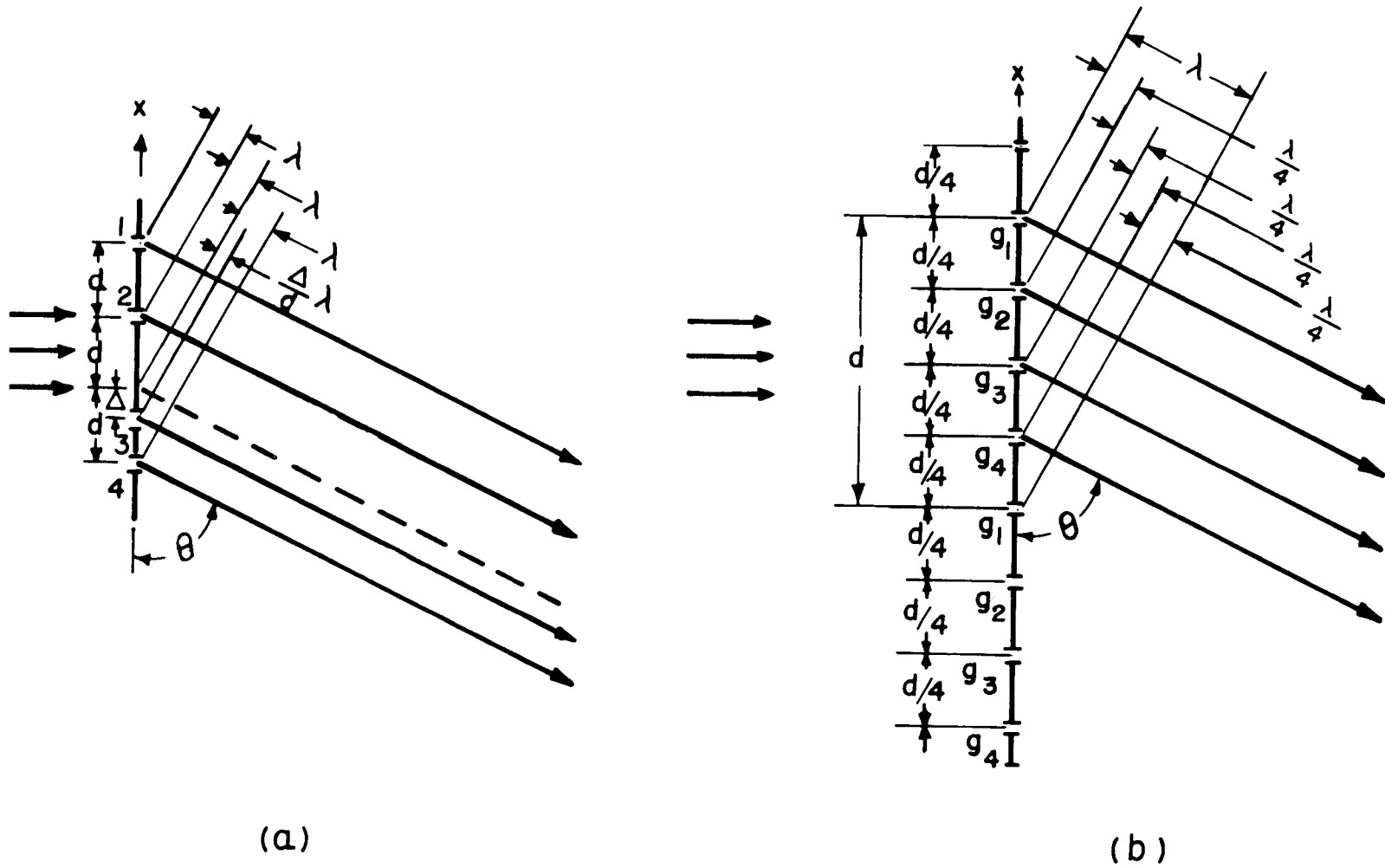
Figure 16. Binary Filters (a) Lohmann's Method, (b) Lee's Method

the impulse response of the filter, W. H. Lee[7] has suggested an alternative method to overcome this problem. But, Lee's method requires somewhat more computer time.

The Phase-Only Filter

In place of a slit for each sampled point, light can also be diffracted into a desired diffraction order by a high frequency grating. Then the intensity of light diffracted can be controlled by the density of the grating and the phase angle by shifting the grating. To improve efficiency of the hologram filter the grating can be bleached to give a phase-only filter.[8]

Comparing the multiply-exposed filter with the computer generated binary or phase-only filters, one notes that while all are useful filter production techniques, filters made on an optical bench generally give better signal to noise ratio because they contain more information (or physically larger) than those generated by computers. On the other hand, the maximum number of multiple exposures that can be practically made is not unlimited. Hence, if a filtering function is any more complicated than those we discussed earlier, it might be easier to produce it by computer.
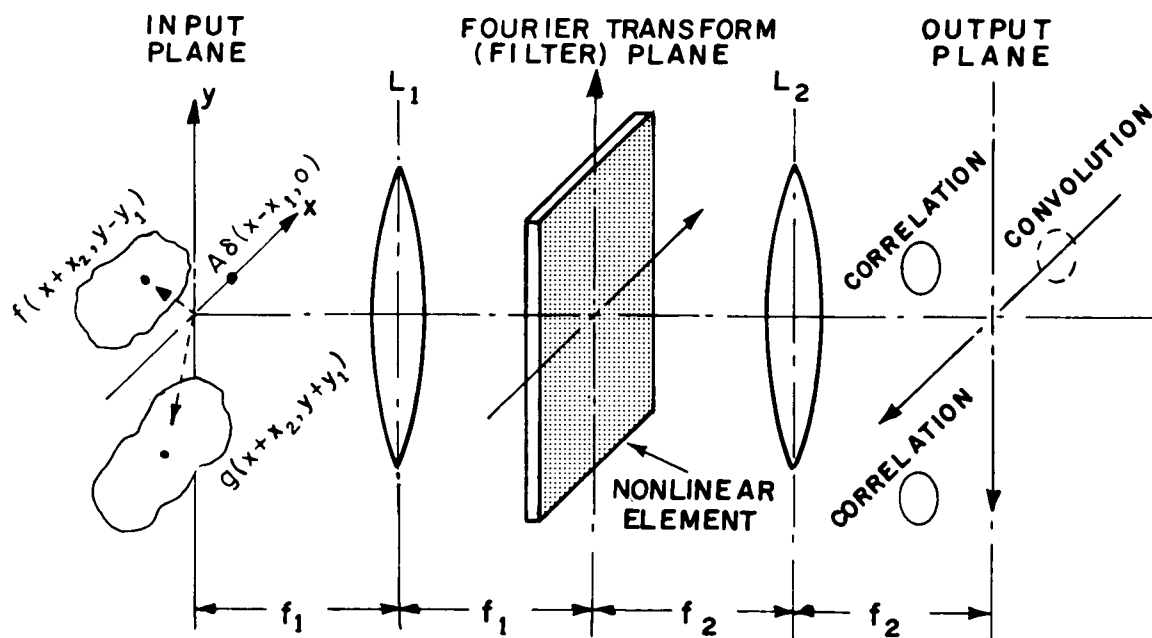
Figure 17. An Optical System that Performs Linear Operations with a Nonlinear Element

The Non-Linear Filter

So far most optical complex filterings have been performed only with filters produced by any one of the three techniques just described. Recently we have been investigating the possibility of performing filtering without having to go through the process of preparing the filters. One promising scheme that we have found[17] is shown in Figure 17. In the scheme always the same filtering element is supposed to be used, while different filtering operations are to be performed. The processing functions, g, must then be placed also in the input plane together with the images to be processed, f. In order for the Fourier transforms of the two functions, f and g to interact and multiply with each other, so as to yield the result of convolution, correlation or other linear operations, we need to choose in the filtering plane a nonlinear element with amplitude transmittance characteristic proportional to the intensity incident on it. Further, in order for the convolution and correlation functions to be physically separated from other undesired outputs in the output plane, we introduce a reference delta function in the input plane. Preliminary experimental results using this scheme is very encouraging. But, we can not elaborate anymore on it now. It is planned, however, that a paper with details of analysis and more experimental result on this scheme will be submitted to the OSA meeting come this fall.

ACKNOWLEDGMENTS

REFERENCES

1. S. K. Yao and S. H. Lee, J. Opt. Soc. Amer. <u>61</u>, 474, (1971).

2. K. J. Petrosky and S. H. Lee, Appl. Opt. <u>10</u>, 1968, (1971).

3. S. K. Yao and S. H. Lee, Appl. Opt. <u>10</u>, 1154, (1971).

4. S. H. Lee, S. K. Yao and A. G. Milnes, J. Opt. Soc. Amer. <u>60</u>, 1037, (1970).

5. B. Brown and A. W. Lohmann, Appl. Opt. <u>5</u>, 967, (1960).

6. A. W. Lohmann and D. P. Paris, Appl. Opt. <u>7</u>, 651, (1968).

7. W. H. Lee, Appl. Opt. <u>9</u>, 639, (1970).

8. J. P. Kirk and A. L. Jones, J. Opt. Soc. Am. 61, 1023, (1971).

9. G. W. Stroke, Phys. Lett. 27A, 405, (1968).

10. A. W. Lohmann and H. W. Werlich, Phys. Lett. 25A, 570, (1967).

11. D. A. Ansley, Electro-Optical System Design, July/August 26, (1969).

12. J. L. Horner, Appl. Opt. 9, 167, (1970).

13. D. P. Jablonowski and S. H. Lee, to be presented in the 1972 Spring Meeting of the Optical Society of America, New York, New York.

14. A. Vander Lugt, IEEE Trans. Inform. Theory IT-10, 139, (1964).

15. A. Kozma and D. L. Kelly, Appl. Opt. 4, 387, (1965).

16. J. W. Goodman, Introduction to Fourier Optics (McGraw Hill, New York, 1968), Sec. 7.6.

17. S. H. Lee and K. T. Stalker, to be published.

DESIGN CONCEPTS FOR AN ON-BOARD COHERENT OPTICAL IMAGE PROCESSOR

Dr. Akram S. Husain-Abidi,[*] Research Associate,
National Academy of Sciences/Goddard Space Flight Center

INTRODUCTION

Optical data processing techniques have been known for the past one hundred years and are the oldest documented techniques for information processing. The research and development work of the past fifteen years has given a new impetus to this field. A number of techniques such as those for diffraction pattern analysis, amplitude and complex spatial filtering, matched filtering and auto and cross correlation are now fairly well understood. The inherent two dimensional nature of the optical system makes them superior to electronic counterparts which take the information sequentially or on bit by bit basis, and are inherently one dimensional.

In particular, the need for parallel image data processing techniques for analysis, synthesis and extraction of information arises from the fact that an enormous amount of pictorial type data about the earth's features will be acquired by NASA's future Earth Resources satellites. To make good use of this data for earth's agricultural, geological, hydrological, geographical, oceanographical and environmental conditions, an efficient and timely processing of data is necessary. The use of coherent optical techniques is one of many techniques that will be an aid in handling this problem. On-board spacecraft image data processing systems will be very useful because they will allow transmission of processed data rather than raw data, resulting in an enormous saving of transmitter bandwidth.

HISTORICAL DEVELOPMENT OF OPTICAL DATA PROCESSING TECHNIQUES

In 1873, Abbe[1] in his classical paper reported a number of experiments in which he manipulated the diffraction pattern produced by specimens in a microscope system. The main aim of his work was to improve the resolution in microscopes. These experiments were performed to seek the explanation of the observation that, "a large angular aperture results in a more brilliant

---

[*]Air Headquarters, Peshawar, Pakistan.

image of higher resolution than small angular apertures—even though the cone of the light emanating from the light source fills only a very small portion of the aperture, leaving the remainder seemingly unused as dark space". After a number of experiments he discovered that the influence of angular aperture is due to diffraction phenomenon. Porter[2] following Abbe's work and realizing that a complete mathematical development has never been published, presented a paper in 1905, in which he reported a number of band pass type spatial filtering experiments and treated the phenomenon by means of a simple application of the Fourier Theorem. Zernike[3] in 1932 proposed a technique for converting spatial phase modulation to spatial intensity modulation. This technique was also based on Abbe's theory and is known as the, "Phase Contrast" technique. Gabor[4] in 1948 presented the idea of wave-front reconstruction. He described the theory and performed experiments to demonstrate that a recorded diffraction image could be reconstructed to a normal image. Due to the lack of suitable coherent light sources at that time, the full potential of this technique was not realized. This was a unique two step method of optical imagery. In 1952, Elias[5], et al. published a paper in which they pointed out that some optical systems are analogous to electronic filter circuits. Elias[6] in another paper published in 1953 illustrated the application of a few mathematical techniques originally developed for electrical communication theory to optical problems.

The work of Maréchal and Croce[7] first published in 1953 was mainly concerned with the improvement of photographs. By using coherent optical data processing techniques they were able to suppress a given periodicity in the image, improve the details and the contrast of the details and to remove the spherical aberration and astigmatism from a recorded image. A year later in 1954 Cheatham and Kohlenberg presented a paper emphasizing that many optical systems perform a linear transformation of an object plane equivalent of the one dimensional time transformation performed by a linear electrical filter, many mathematical techniques developed for treating linear electrical filters can be used to study the optical systems. They also presented the methods of synthesizing optical filters.

O'Neill[8] in 1956 published a comprehensive paper in which detailed theoretical and experimental results were presented that demonstrate the analogy between optical and electrical filtering. In 1959, Cutrona[9], et al. published a paper in which they described the configurations and the properties of multichannel coherent optical signal processing system. It was pointed out that the two dimensional nature of optical systems makes them very attractive to supplement or even to replace complex electronics systems for performing a number of linear mathematical operations. Van Heerden[10] in a paper published in 1963 presented the theory of an "Intensity Filter" for the focal plane

of an imaging system. Projected capabilities of this filter in a recognition system were also explored.

Slabodin[11] in his communication also published in 1963 presented an optical technique for correlating electronic signals in realtime.

In 1964,[12] Vander Lugt introduced a unique technique for synthesizing complex spatial filters. The salient feature of this technique was the transformation of phase and amplitude information into intensity information so that they can be recorded on a photographic plate. Modified Mach-Zehnder and Rayleigh interferometric arrangements were used for the synthesis of these filters. The introduction of this technique was largely responsible for a re-evaluation of the coherent optical spatial filtering techniques for recognition and detection purposes.

The works of Stroke[13] and co-workers and Lohmann[14] and co-workers has also benefited the various aspects of optical data processing.

THE COHERENT OPTICAL DATA PROCESSING SYSTEM AND EXPERIMENTAL RESULTS

Figure 1 illustrates the conventional configuration of an optical system normally used for coherent optical data processing. Light from a He-Ne laser radiating at a wavelength of 632.8 nm is brought to a point focus by a microscope objective. A pinhole is placed in this focal plane to eliminate laser beam

1. He-Ne GAS LASER
2. MICROSCOPIC LENS
3. PIN HOLE
4. COLLIMATING LENS
5. INPUT PLANE
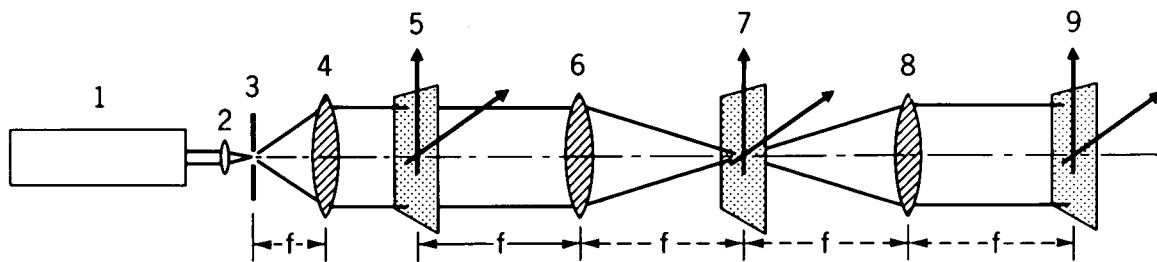
6. FOURIER TRANSFORMING LENS
7. FOURIER TRANSFORM PLANE
8. IMAGE RECONSTRUCTING LENS
9. IMAGE RECONSTRUCTION PLANE

Figure 1. Conventional Configuration of a Coherent Optical System

noise and to exclude stray light. Another lens is placed a focal length away from a converging lens. This lens in its focal plane produces the Fraunhofer diffraction pattern of the input information in two dimensions. This diffraction pattern has all the characteristics of a two-dimensional Fourier transform of the light distribution in the input information. If an arbitrary function is introduced in the input plane, a two-dimensional spectrum of that function is obtained in the Fourier transform plane. If a complex spatial filter is placed in the Fourier transform plane, the system can be used for autocorrelation or cross-correlation.

This optical system works well in the laboratory environment. Aboard spacecraft, however, this system has two main drawbacks. The first is the low efficiency and bulkiness of the gas laser, and the second is the lens system. Disadvantages of lens systems are front surface reflections, which are unavoidable, and the requirement for axial symmetry of the system (i.e., the optical system with lenses cannot easily be folded).

A solid-state GaAs laser diode has been used to overcome the first drawback. This laser is at least ten thousand times better in efficiency and probably the same order of magnitude smaller in overall volume. Furthermore, since a GaAs laser can be treated as a point source, the system does not require the microscopic lens and pinhole spatial filter minimizing optical alignment problems.

To overcome the second problem, paraboloidal mirror segments are used. It has been found that paraboloidal mirror segments not only overcome the axial symmetry problems but have a number of significant advantages over lenses. Let us start by considering the problems associated with lenses.

The quality and resolution of Fourier transform functions in the focal plane of a lens is very much affected by the lens aberrations and the optical refracting material. The three types of aberration that are primarily responsible for the degradation of the Fourier transforms are spherical aberration, astigmatism, and coma.

Besides overcoming these aberrations, other critical problems with lenses consists of the choice of the optical material. For an ultrahigh-quality lens suitable for data processing, the optical material should be:

(1) homogeneous to a very high degree. (It is important that the refractive index of the lens be constant throughout.)

(2) free from thermal and mechanical strains.

(3)   optically isotropic (i.e., the index of refraction at any point must be constant regardless of the direction in which the radiation is passing the point).

Therefore, for a good optical system with lenses, it is necessary to rectify all the aberrations and to insure the selection of proper optical material. Both of these requirements are extremely difficult and costly to satisfy.

Let us now consider the paraboloidal mirror as a linear element in an optical data processing system. Referring to figure 2, light rays entering from the right parallel to the z axis are reflected from the mirror and intersect the z axis at the focal point f. The relationship between the incident and reflected scalar light fields at any point in the (x,y,z_0) plane can be described in terms of a transfer function, $t(x,y,z_0)$. For mirrors (as well as for lenses) the transfer function is strictly a phase function, and we have

$$t(x,y,z_0) = e^{j\emptyset(x,y,z_0)}$$ (1)
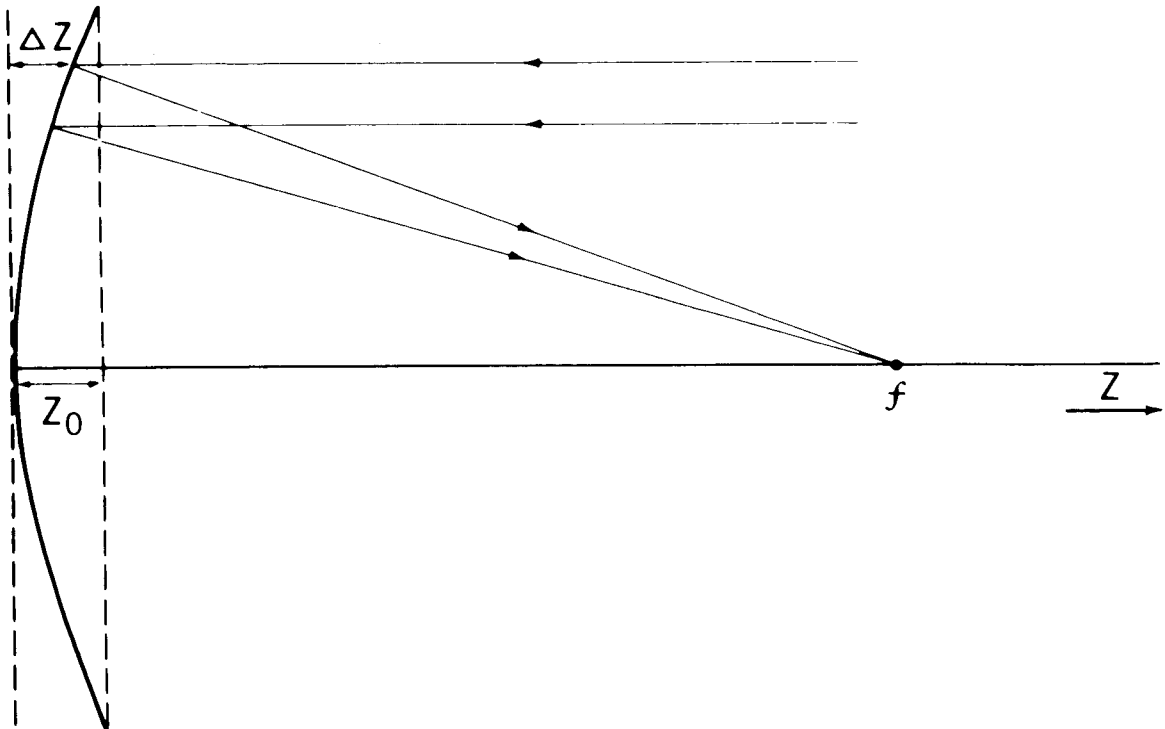
$$= e^{jk\Delta(x,y,z_0)}$$

Figure 2. Transfer Function for Parabolic Mirror

where $\phi(x,y,z_0)$ is the phase difference in radians between the incident and reflected fields, k is the wave number $2\pi/\lambda$ and $\Delta(x,y,z_0)$ is the difference in pathlengths between the incident and reflected waves.

Again referring to figure 2, we see that the total path difference is

$$\Delta(x,y,z_0) = 2(z_0 - \Delta z) \tag{2}$$

(This assumes no ray bending to the left of the (x,y,z_0) plane, analogous to the thin-lens approximation in lens analysis.)

Now from the equation for a paraboloid of revolution,

$$\Delta z = \frac{x^2 + y^2}{4f} \tag{3}$$

Therefore,

$$t(x,y,z_0) = e^{jk\Delta(x,y,z_0)}$$

$$= e^{[j2kz_0]} \, e^{-jk\left[\frac{x^2 + y^2}{2f}\right]} \tag{4}$$

In the case of a spherical thin lens, if the paraxial approximation is made, i.e., if we consider only light rays close to the lens axis, the transfer function is found to be

$$t(x,y,z_0) = e^{[jknz_0]} \, e^{-jk\left[\frac{x^2 + y^2}{2f}\right]} \tag{5}$$

Here $\underline{n}$ is the index of refraction of the lens material, and $\underline{z}_0$ is the lens thickness along the optical axis. It is important to note that the focal length $\underline{f}$ of a lens is a function of the index of refraction of the lens material.

Referring to the derivation of the transfer function, several points can be made for the parabolic mirror as a system element. First, since the focal length $\underline{f}$ of a mirror is not a function of index of refraction, the parabolic mirror system will not have the chromatic aberration that is inherent in the lens system. Secondly, all the light rays parallel to the z axis will intersect the point $\underline{f}$ for a parabolic mirror, while only the paraxial rays will intersect the focal point for a spherical lens. This means that the parabolic mirror is inherently free from spherical aberrations (while the lens, of course, is not).

146

The absence of paraxial approximation for mirrors has several practical advantages. One is that the aperture of the optical signal being processed can be larger for a parabolic mirror than for a lens of the same diameter. More important, off-axis segments of a parabolic mirror will have the same transforming properties as the original mirror. Thus one can construct a folded optical processing system.

Two other aberrations also deserve some attention. Let us consider astigmatism. This aberration occurs when the incoming light rays make a large angle with the z axis of a mirror. This is not a serious drawback, however, since for most optical signal processing, the incoming light is a coherent plane wave whose rays are parallel to the z axis. Furthermore, all interelement light paths can be kept at very small angles with respect to the element axis. Astigmatism therefore can be made negligible in a parabolic processing system.

The second aberration is coma, the aberration that occurs for light rays at small angles to the z axis. In experiments using parabolic mirrors as Fourier transforming elements, the effects of coma were not observable at the normal working angles.

Figure 3 illustrates an optical data processing system using paraboloidal mirror segments. The coherent light source (1) is a p-n gallium arsenide laser diode with an effective radiating area of 0.0015 mm^2. The laser operates at room temperature at a wavelength of 900 nm. It is placed in the focal plane of the paraboloidal mirror (3). The coherent light (2) from the laser diverges and typically forms a 30° angle. Since the coherent light source is almost a point source and since it is in the focal plane of the paraboloidal mirror (3), the light reflected from the paraboloidal mirror segment (4) is collimated.

To perform a two-dimensional spectrum analysis, the information to be analyzed is produced in transparency form (either by taking a photograph or by other means). The transparency (6) is placed in the collimated beam (5), a focal length away from the paraboloidal mirror (7). The paraboloidal mirror segment (8) converts the information of the transparency into a diffraction pattern that has all the properties of a Fourier transform in the plane (10) centered at the point (9) which is the focal point of the paraboloidal mirror (7). The information in the diffraction pattern can be converted into electrical signals by placing an appropriate photon detector (11) in the plane (10). The photon detector can be of any suitable geometry such as in the form of wedges or concentric rings.

Spatial filtering can also be performed in the plane (10). For example, the two basic types of filtering, bandpass and bandstop, can be performed by having
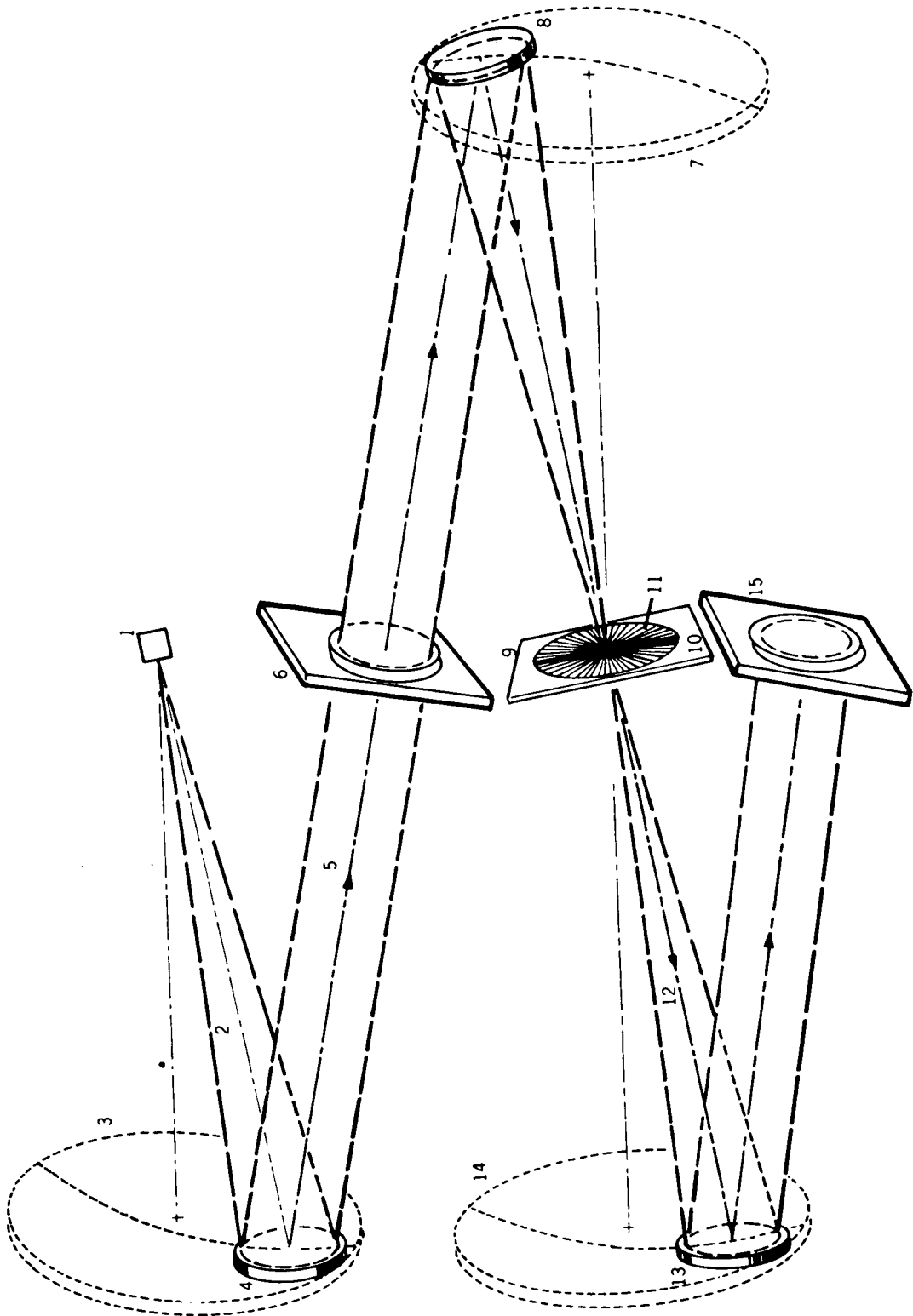
Figure 3. Optical Data Processor

a transparent or an opaque region at a desired place in the plane (10). Optical filters in the form of wedges, annuili or opaque disks are used in the plane (10) (electrically alterable filters of this type has recently been delivered to us). The light transmitted through the filter–detector (11) is reflected by a paraboloidal mirror segment (13) of paraboloid (14), placed a focal length away from the plane (10). The input information is reconstructed at the plane (15), which is a focal length away from the paraboloidal mirror (14).

Figure 4 shows how the system could be housed in an enclosure 15 cm long, 9 cm high, and 4 cm wide. Experimental performance of the paraboloidal mirror segment system was evaluated by first monitoring the Fourier transform function in the focal plane of the mirror segment using a He-Ne laser. The following figures show some Fourier transforms obtained with a parabolic mirror. As examples of single simple shapes, Figure 5 shows the Fourier
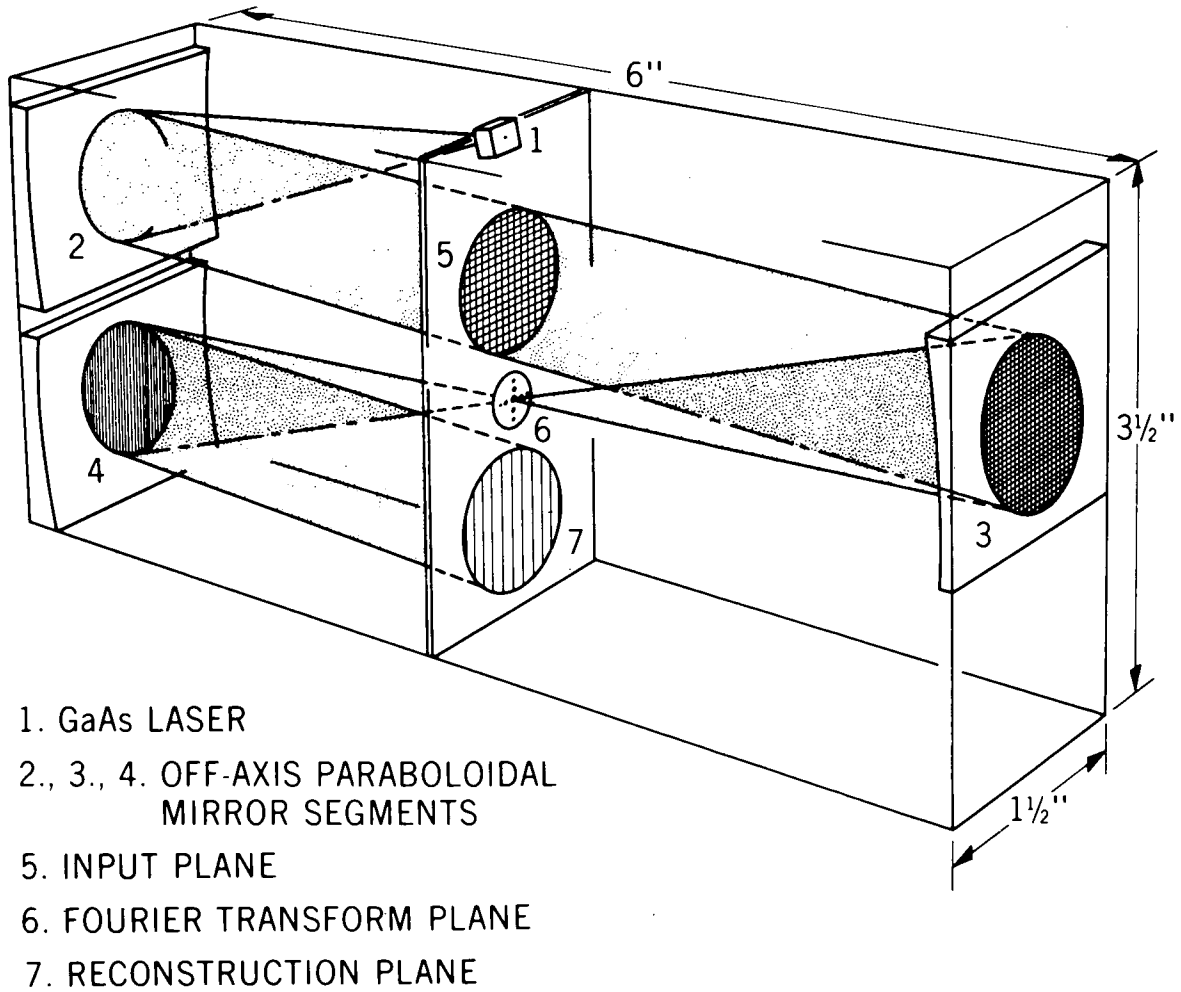

1. GaAs LASER
2., 3., 4. OFF-AXIS PARABOLOIDAL
           MIRROR SEGMENTS
5. INPUT PLANE
6. FOURIER TRANSFORM PLANE
7. RECONSTRUCTION PLANE

Figure 4. OPDIC Computer

| FOURIER TRANSFORM OF A CIRCULAR APERTURE | FOURIER TRANSFORM OF A RECTANGULAR APERTURE | FOURIER TRANSFORM OF A TRIANGLE |

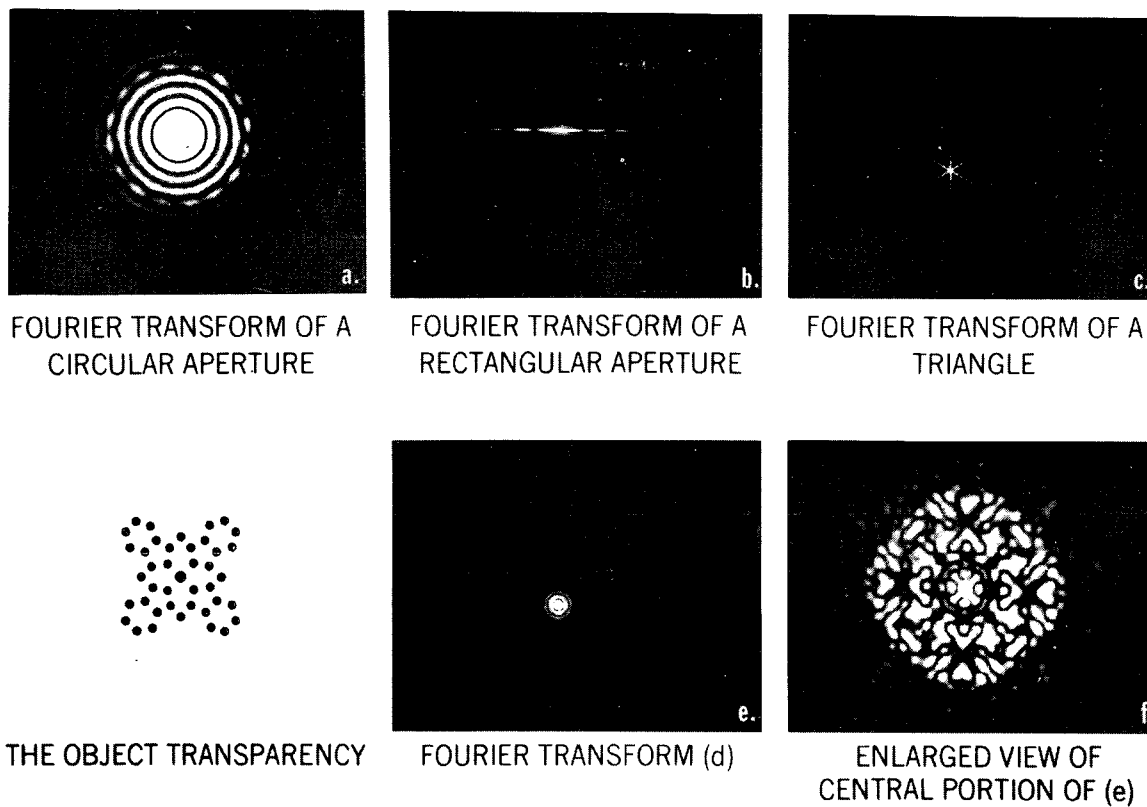| THE OBJECT TRANSPARENCY | FOURIER TRANSFORM (d) | ENLARGED VIEW OF CENTRAL PORTION OF (e) |

Figure 5. Examples of Fourier Transforms Generated by Parabolic Mirrors

transforms of a circular, a rectangular, and a triangular aperture. The well known Airy disk can be seen distinctly in the center of the transform of the circular aperture. Figure 5 (d through f) also illustrates an example of multiple simple shapes.

The Fourier transform which is a two dimensional distribution of light can be sampled to obtain information for decision making purposes. The sampling process is simply measuring the amount of light energy falling within a specific area and is normally performed by constructing a set of windows of some suitable shapes. By mechanically or manually changing the position of the window and monitoring the amount of light in a particular position, a set of measurements called the "sample signature" can be obtained.

To overcome the problems of mechanical and manual positioning of the sample windows and to decrease the time normally required to produce a sampling signature we have designed a solid state silicon p-n junction device. This device is being used in Fourier transform plane and converts the two dimensional light distribution into an analog electrical signal.
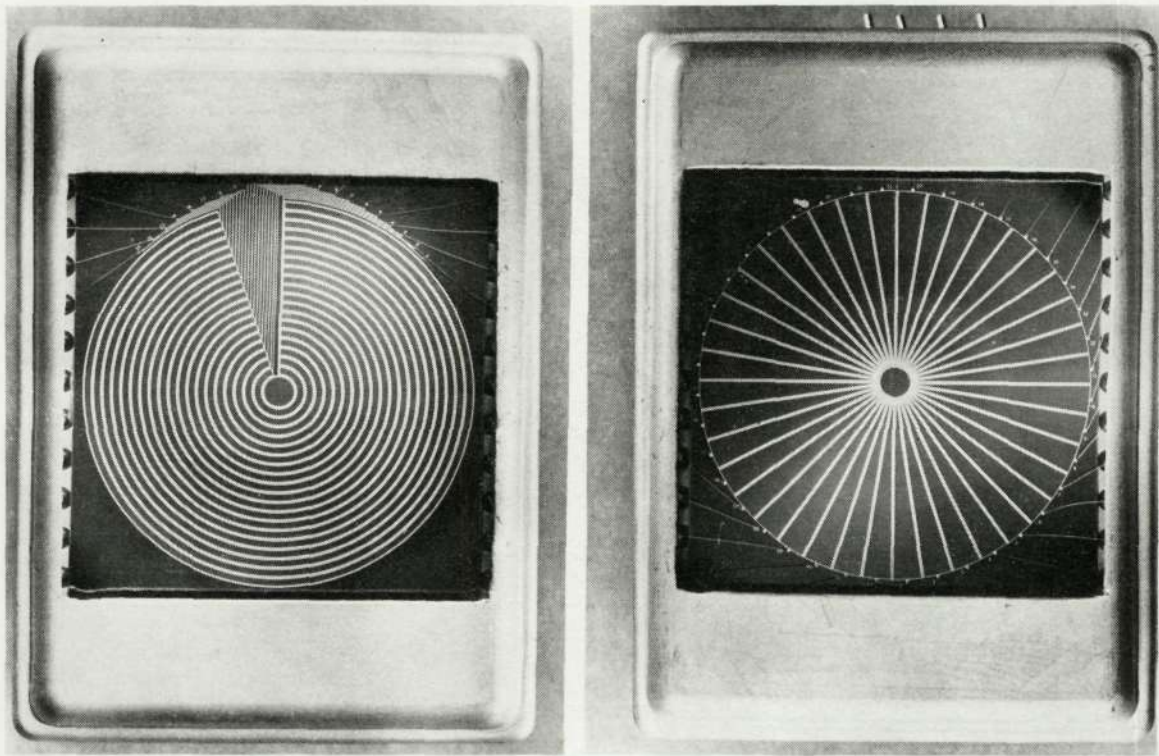
Figure 6. Fourier Plane Photosensors

Two types of photosensors have been designed. The first is in the form of nineteen concentric rings surrounding a two millimeter circle, and is shown in Figure 6(a). The width of effective sensitive area of each ring is 0.016" and the separation between the two rings is 0.009". The second detector is in the form of forty wedges of 9°, separated by 0.008", and the diameter of the central circle was 2 mm. Both detectors are one inch in diameter. Figure 6(b) shows the wedge type detector.

Two simple experiments were performed. In the first experiment a transparency of the letter "U" was placed in the input plane. The resulting Fourier transform is shown in Figure 7(b). The output voltages on the ring and wedge detectors were sampled sequentially and displayed as a histogram on an oscilloscope. These histograms are shown in Figure 7(c and d). Note that the high peaks in the wedge detector output corresponds to the straight side of the "U". In the second experiment the cloud cover picture was used as an input transparency and is shown in Figure 8(a). The resulting Fourier transform and the histograms are shown in Figure 8(b, c, and d). The two broad peaks in the wedge detector histogram corresponds to the directionality of the clouds in the input transparency.

151
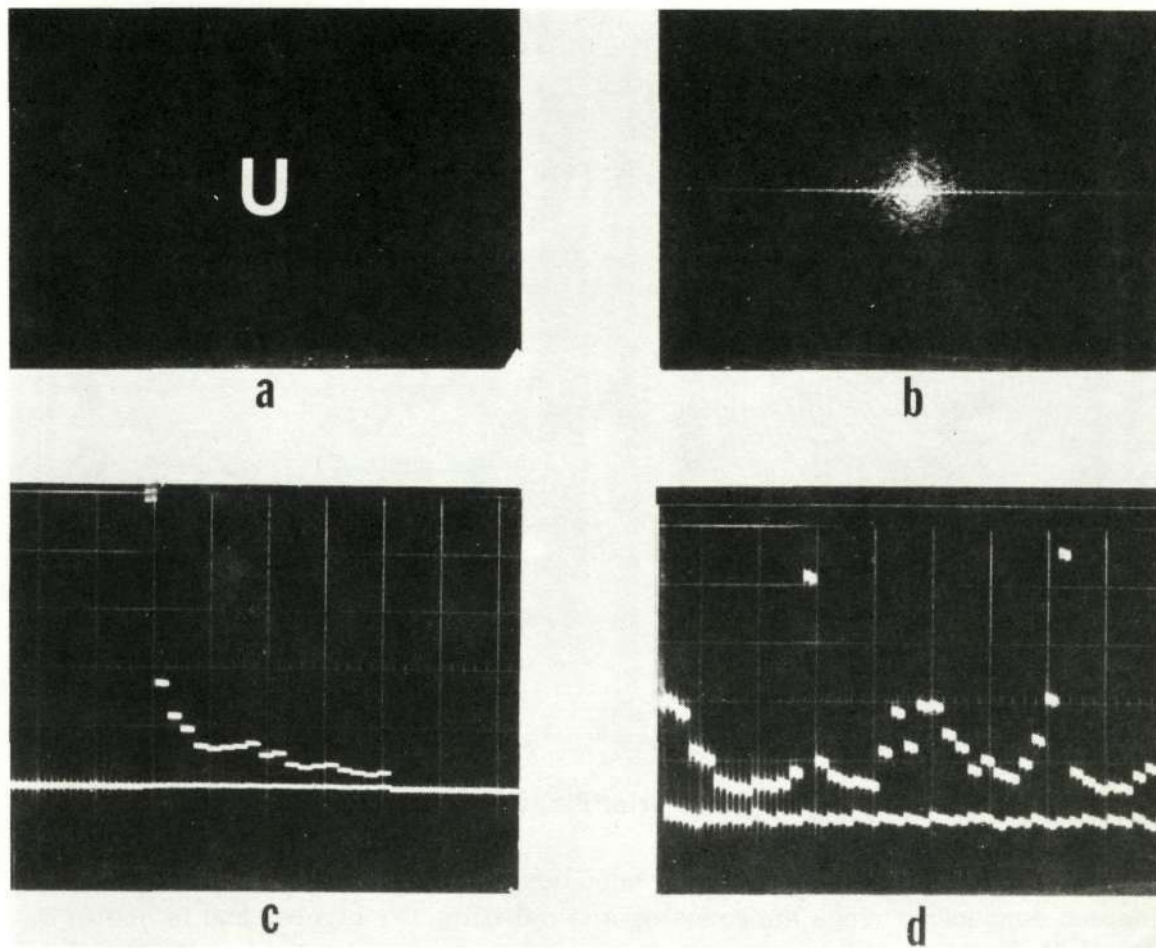
Figure 7. Photosensor Outputs for Letter "U"

Figure 9 shows an example of spatial filtering. The Fourier transform of a triangle and its reconstructed image are shown in figure 9 (top). To filter out one of the sides of the triangle, a narrow wedge was placed in the Fourier transform was blocked. The effect of blocking the Fourier component is shown in Figure 9 (bottom), where it can be seen that the reconstructed image is without one side. The missing side has been filtered, or more correctly, suppressed in the Fourier transform plane.

Figure 10 shows another example of spatial filtering. In this experiment a He-Ne gas laser was used as a source of coherent radiation mainly because the resolution of the image converter tube used in the image reconstruction plane was very low. A wire grid was chosen as an object (fig. 10a). The Fourier transform of this object is shown in figure 10b. For spatial filtering purposes, a slit was placed in the Fourier transform plane so that only the vertical
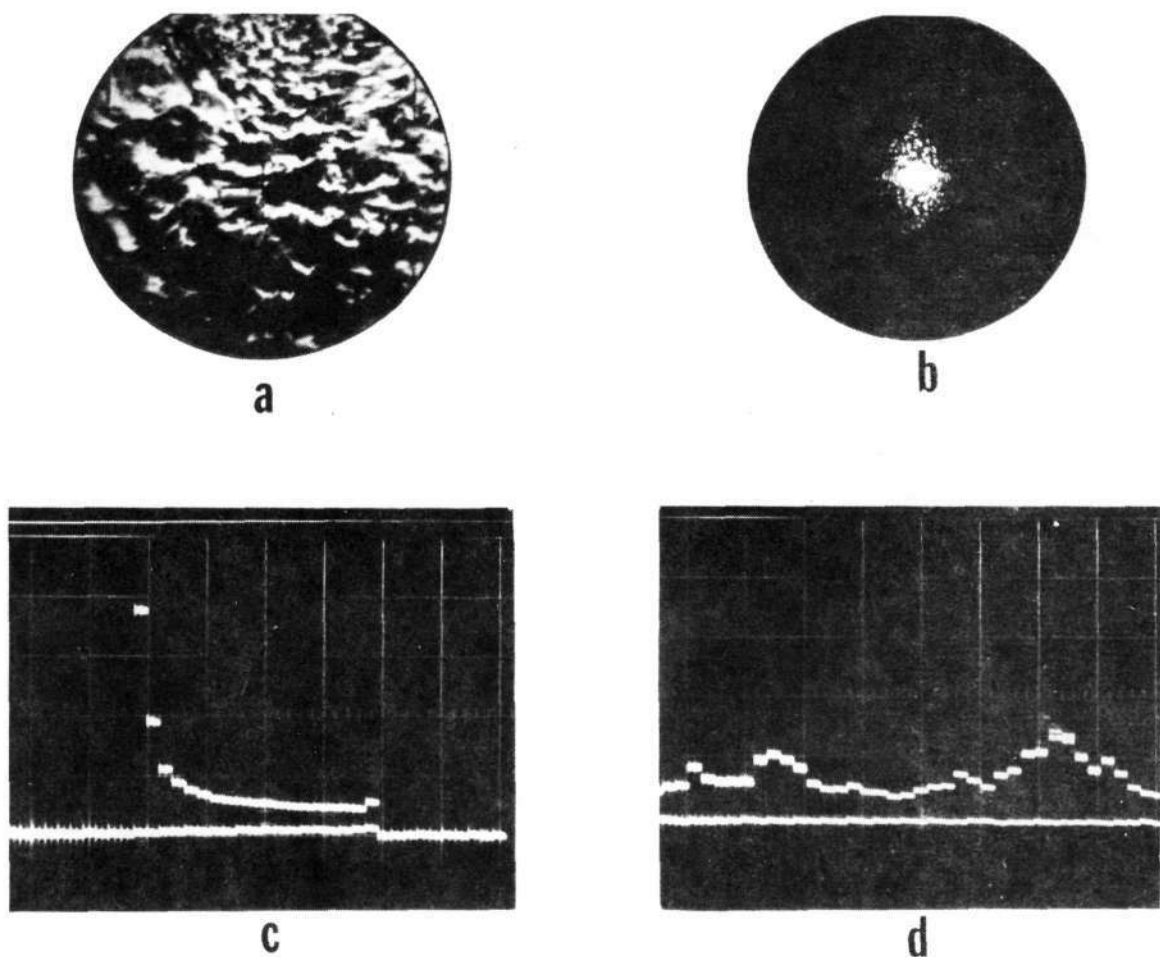
Figure 8. Photosensor Outputs for Cloud Cover Input

structure of the Fourier transform was allowed to pass through the Fourier transform plane. The reconstructed filtered image (fig. 10c) is without any vertical information. Figure 10d shows the reconstructed image without any spatial filtering.

Optical correlation experiments using paraboloidal mirror segments were also performed. Figure 11 illustrates the optical correlator. The input transparency was placed in the input plane. A Fourier transform hologram was recorded in complex spatial filter plane. The photographic film was developed and placed back in exactly the same place it occupied during the exposure. The reference beam was blocked and the hologram was illuminated by the signal beam only.

Another off-axis paraboloidal mirror segment was used to Fourier-transform the field transmitted by the hologram. The correlation plane, which is located

IMAGE IN FOURIER TRANSFORM PLANE → **RECONSTUCTED INPUT IMAGE**

SPATIAL FILTER → **RECONSTRUCTED FILTERED IMAGE**
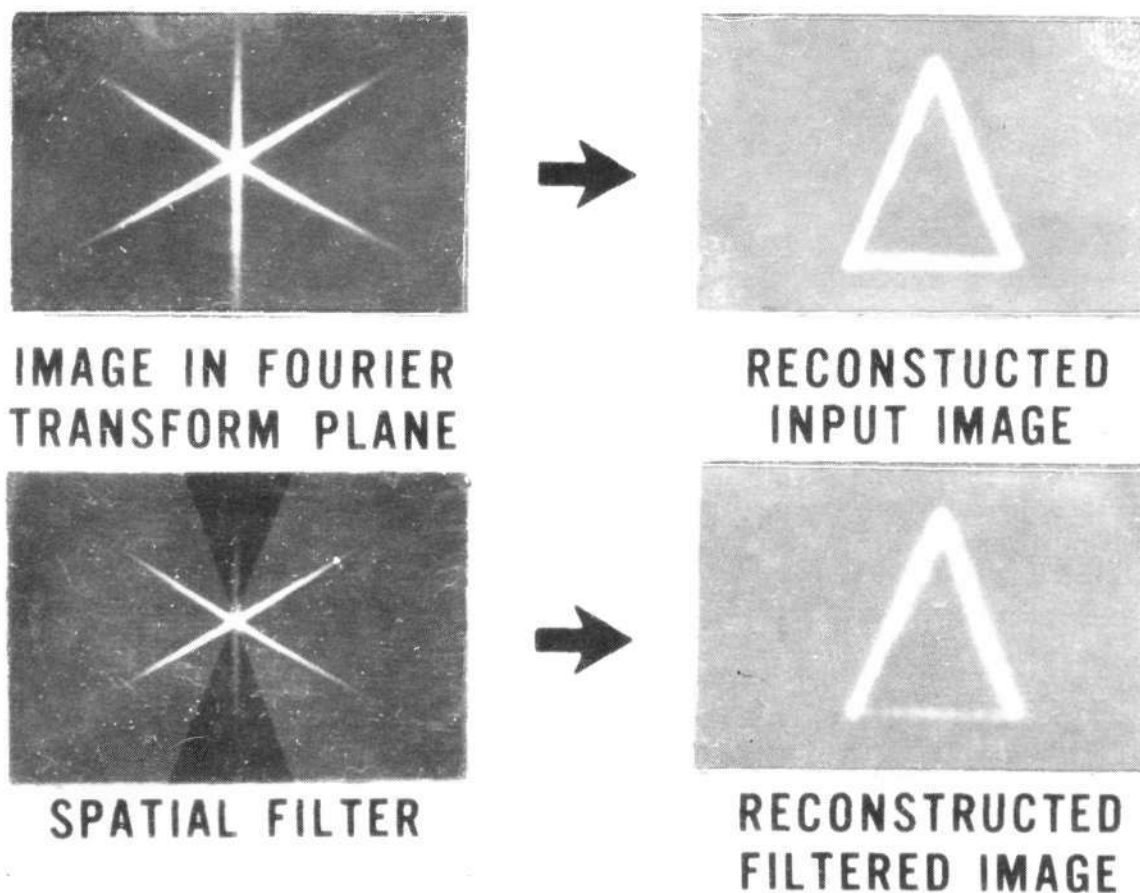
Figure 9. Spatial Filtering With Paraboloidal Mirror Segments and Gallium Arsenide Laser

a focal length away from the off-axis mirror segment, displays the convolution function geometrical image, and correlation function. The autocorrelation has a bright central peak of the autocorrelation function can be seen. Correlation experiments using a real time optical input device known as "OTTO" were also performed. (This device will be described in a later paper by Dr. Jacobson.)

Figure 13 shows the conceptual design of a coherent optical system with a non-coherent image input. The image of the desired part of the earth impinges through a beam splitter onto a noncoherent to coherent conversion (OTTO) device. The collimated light beam passes through the OTTO device and after being reflected from a paraboloidal mirror segment forms the Fourier transform of the input image. By using a beam splitter the Fourier transform can be electrically sampled using special purpose detectors. By placing electrically alterable Fourier transform plane filters in the Fourier transform plane various features of the image can be detected, enhanced or suppressed. By placing
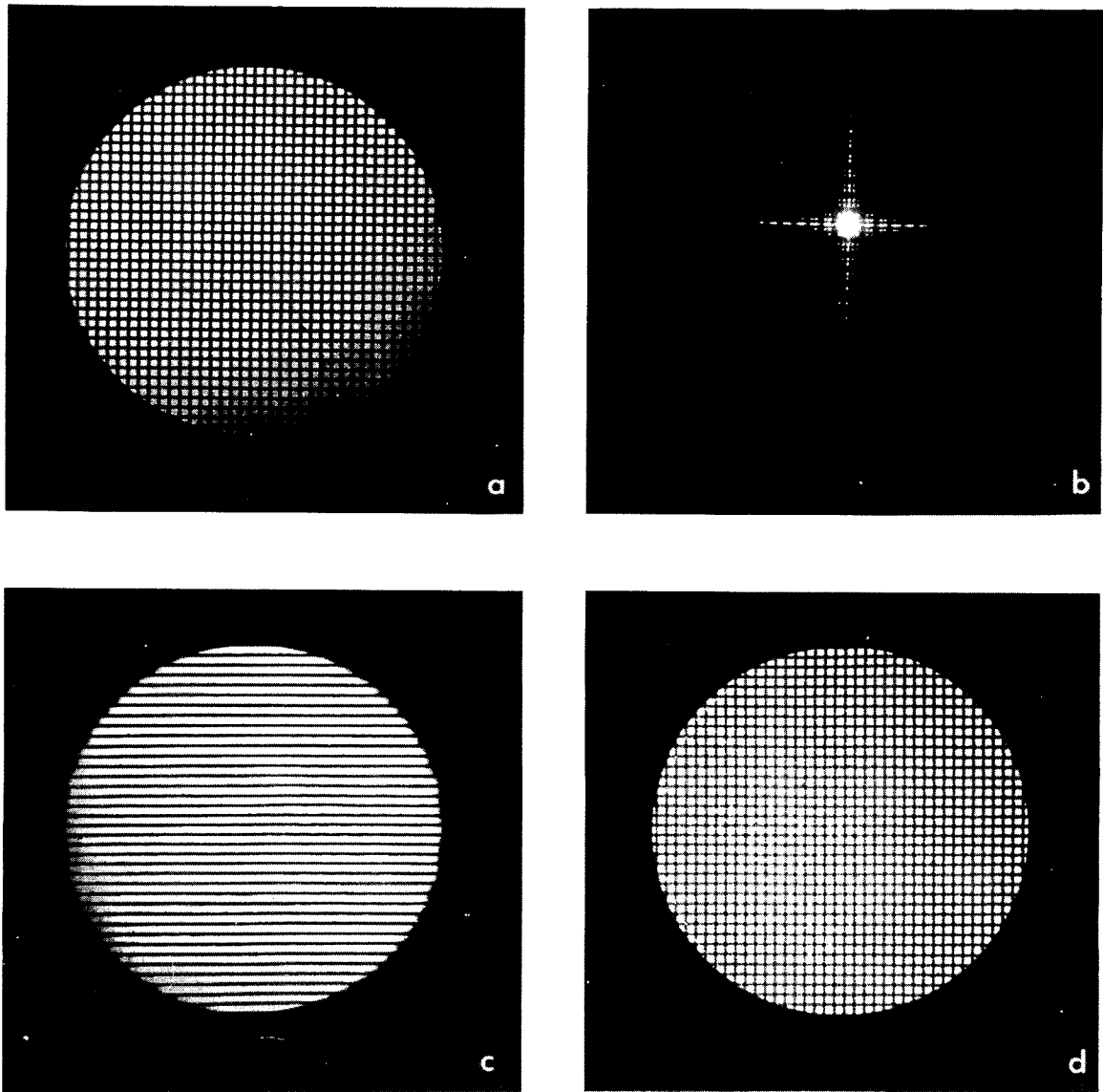
Figure 10. Spatial Filtering Experiments Using Paraboloidal Mirror Segments,
(a) Wire grid in a circular aperature (the object transparency),
(b) Fourier Transform of (a),
(c) Filtered Reconstructed Image,
(d) Unfiltered Reconstructed Image

1 He Ne LASER
2 MICROSCOPE LENS
3 6 MICRON PIN HOLE
4 COLLIMATING
   PARABOLIC MIRROR
5 FRONT SURFACE
   MIRROR
6 FOCUSING PARABOLIC
   MIRROR (OFF AXIS
   SEGMENT)
7 INPUT PLANE
8 FRONT SURFACE
   MIRROR
9 FRONT SURFACE
   MIRROR
10 OFF AXIS
   PARABOLOIDAL
   MIRROR SEGMENT FOR
   FOURIER
   TRANSFORMING
11 COMPLEX SPATIAL
   FILTER PLANE
12 OFF AXIS
   PARABOLOIDAL
   MIRROR SEGMENT FOR
   FOURIER
   TRANSFORMING
13 CORRELATION PLANE

Figure 11. Optical Correlator Using Paraboloidal Mirror Segments
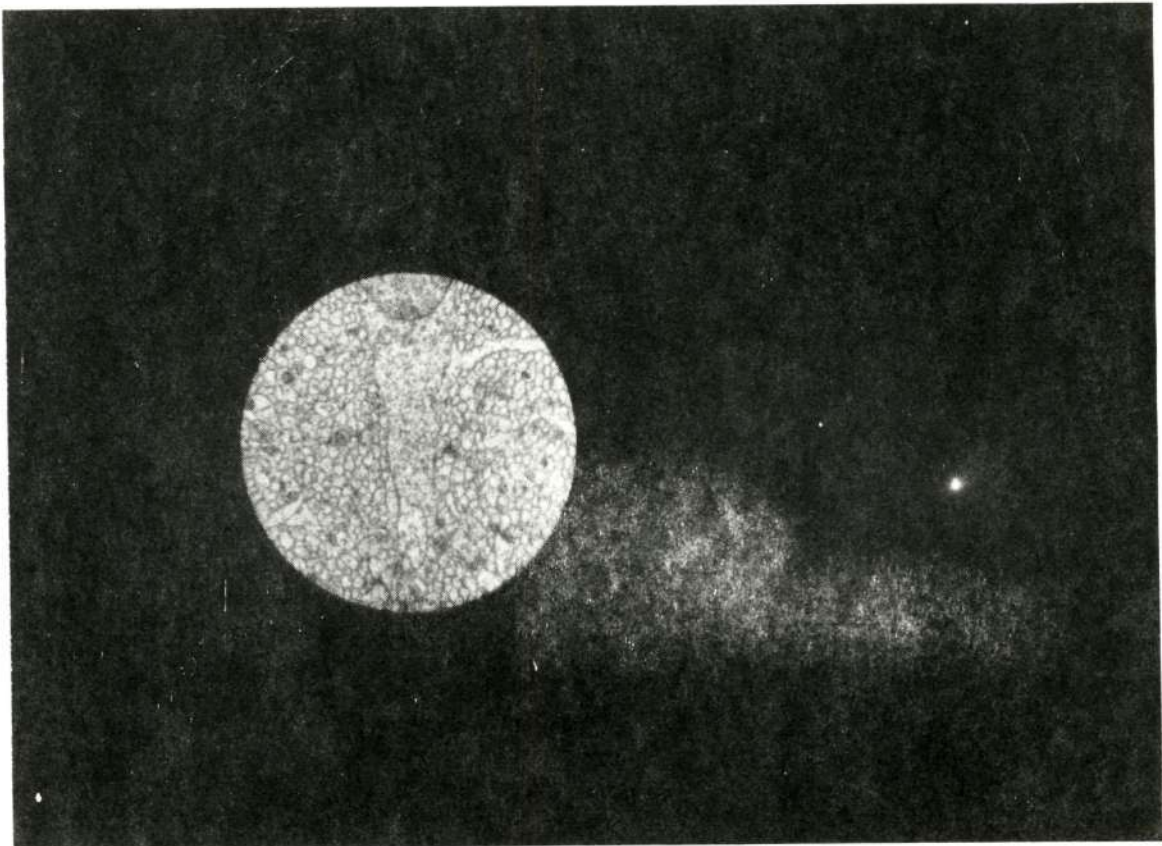
Figure 12. Optical Correlation Experiment

156
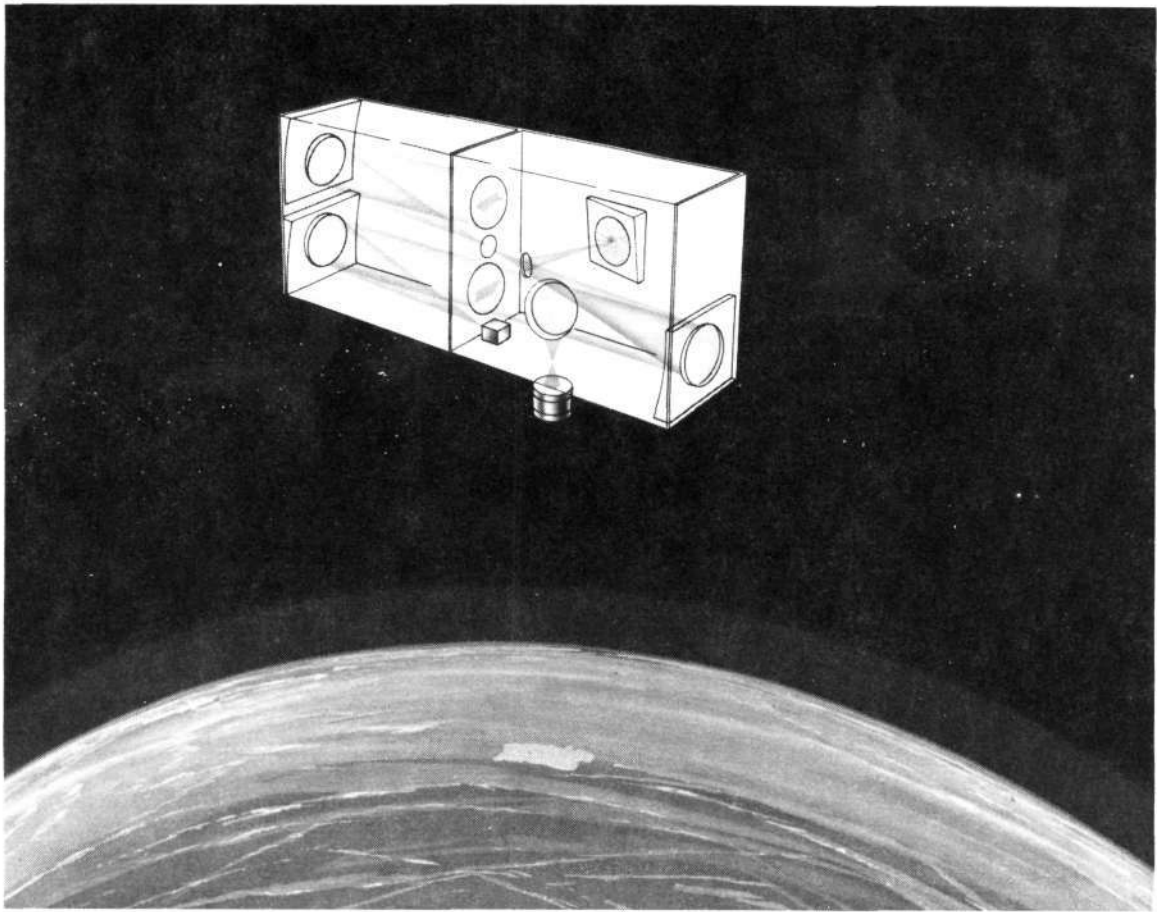
Figure 13. Conceptual Design of a Coherent Optical System
With a Non-coherent Image Input

complex spatial filters in this plane correlation between two images can be performed. Suitable sensing devices in the reconstructed image plane can provide an electrical signal as the output of the system.

In conclusion, the results obtained so far indicate that a low power rugged, compact coherent optical data processing system suitable for on-board spacecraft use can be constructed.

ACKNOWLEDGMENTS

E

REFERENCES

1. Abbe, E. Archiv fur Mikroskopischon Anatomie, Vol. 9, p. 413, 1873

2. Porter, A. B. Philosophical Magazine, Vol. 11, p. 154, 1906

3. Zernike , F. A. Tech. Phys. , 16, p. 454, 1935

4. Gabor, D. Nature, 161, p. 777, 1948; also, Proc. Roy. Soc. A 197:454, 1949 and Proc. Roy. Soc. B64, 449, 1951

5. Elias, P., et al. , J. Opt. Soc. Am. , 42, 127, 1952

6. Elias, P. J. Opt. Soc. Am. , 43, p. 229, 1953

7. Croce, P. and Marechal, A. , Compt. Rend. 237, 706 (1953)

8. O'Neill, E. L. IRE Trans. of the Professional Group on Information Theory, IT-2, No. 2, p. 56, 1956

9. Cutrona, L.J. , et al. , IRE Trans. Auto. Control, AC-4, No. 2, p. 137, 1959

10. Van Heerden, P. J. , Appl. Opt. 2, 287 (1963)

11. Slebodin, L. Proc. I.E.E.E., Vol. 51, p. 1782, 1963

12. Vander Lugt, A. IEEE Trans. Information Theory, vol. IT-10, p. 139, 1964

13. Stroke, G.W. An Introduction to Coherent Optics and Holography (Academic Press, New York, 1966)

14. Lohmann, A.W. , et al. , Phys. letters, 25A, p. 570, 1967

PARALLEL IMAGE LOGICAL OPERATIONS
USING CROSS-CORRELATION

Dr. James P. Strong, III
Goddard Space Flight Center, Greenbelt, Maryland

INTRODUCTION

The Goddard Space Flight Center program to develop parallel image processing methods has as a basic tenet the concept of an image as input, information as output. One of the most basic types of information contained in an image is the number of objects in the image. In a binary or two-level image, this amounts to the number of connected areas in the image. Algorithms for such counting are known. These algorithms require a succession of logical operations on images. This paper will present methods of performing such operations in a parallel manner using non-coherent optical techniques.

LEVIALDI'S ALGORITHM FOR COUNTING

A parallel algorithm for counting areas in a binary image has been developed by S. Levialdi.[1] This algorithm is an iterative operation where the white areas are shrunken by incremental amounts until they become single points. At each shrinking iteration, isolated points are detected and counted. This algorithm is illustrated in Figure 1. For the input image shown, it takes 16 shrinking steps to count the areas. The algorithm considers an image as a matrix array and an isolated point is defined as a white point whose nearest neighbors (adjacent and diagonally) are all black. In the input image, there are seven connected areas, three of which are isolated points. In the algorithm, these are counted and the shrinking operation is then applied forming the first iteration. The shrinking and counting operation is continued until all areas have disappeared.

The necessary requirement of Levialdi's algorithm is that in shrinking areas any area will eventually be shrunken to a single isolated point so that there is only one isolated point corresponding to any connected area. The shrinking function which transforms the image at each iteration of the algorithm into the image at the next iteration is shown in Figure 2. Here, image A is transformed into image B. Each point in image B is a function of a 2 x 2 element neighborhood of points in image A. The equation of a typical point b_{ij} is given by:

$$b_{ij} = (a_{ij} \wedge a_{i,j-1}) \vee (a_{ij} \wedge a_{i+1,j-1}) \vee (a_{ij} \wedge a_{i+1,j}) \vee$$

$$(a_{i,j-1} \wedge a_{i+1,j}) \tag{1}$$

In order to count the isolated points at each iteration of the algorithm, an image containing only the isolated points in each iteration must be obtained. This image, C, can be obtained from an image, B, at a given iteration according to the equation:

$$c_{ij} = \overline{b}_{i-1,j-1} \wedge \overline{b}_{i-1,j} \wedge \overline{b}_{i-1,j+1} \wedge \overline{b}_{i,j-1} \wedge$$

$$\overline{b}_{i,j+1} \wedge \overline{b}_{i+1,j-1} \wedge \overline{b}_{i+1,j} \wedge \overline{b}_{i+1,j+1} \wedge b_{ij} \tag{2}$$
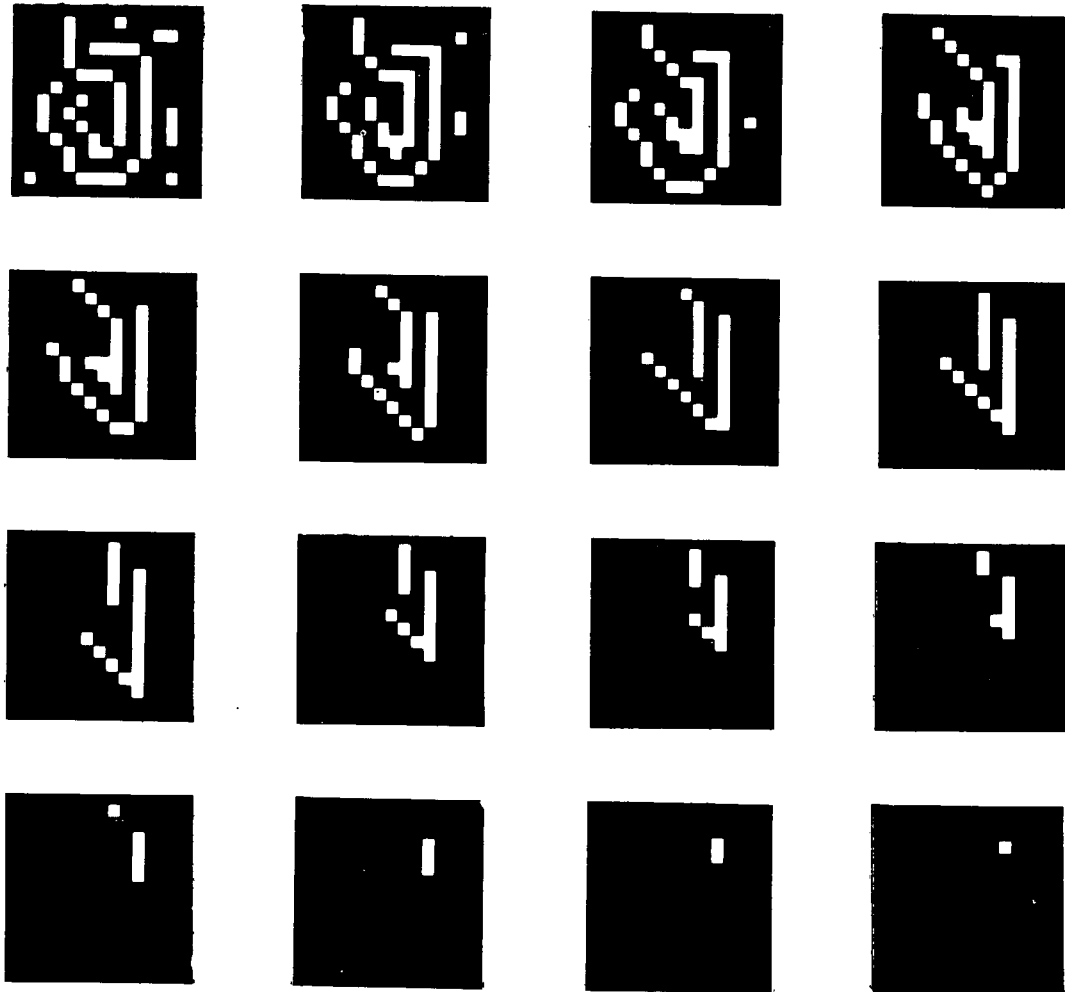

Figure 1. Shrinking Steps of Leviadi's Algorithm. Input image is at upper left-hand corner and last isolated point is in lower right-hand corner.

160

$$b_{12} = a_{11} a_{12} \vee a_{22} a_{12} \vee$$
$$a_{21} a_{12} \vee a_{11} a_{22}$$
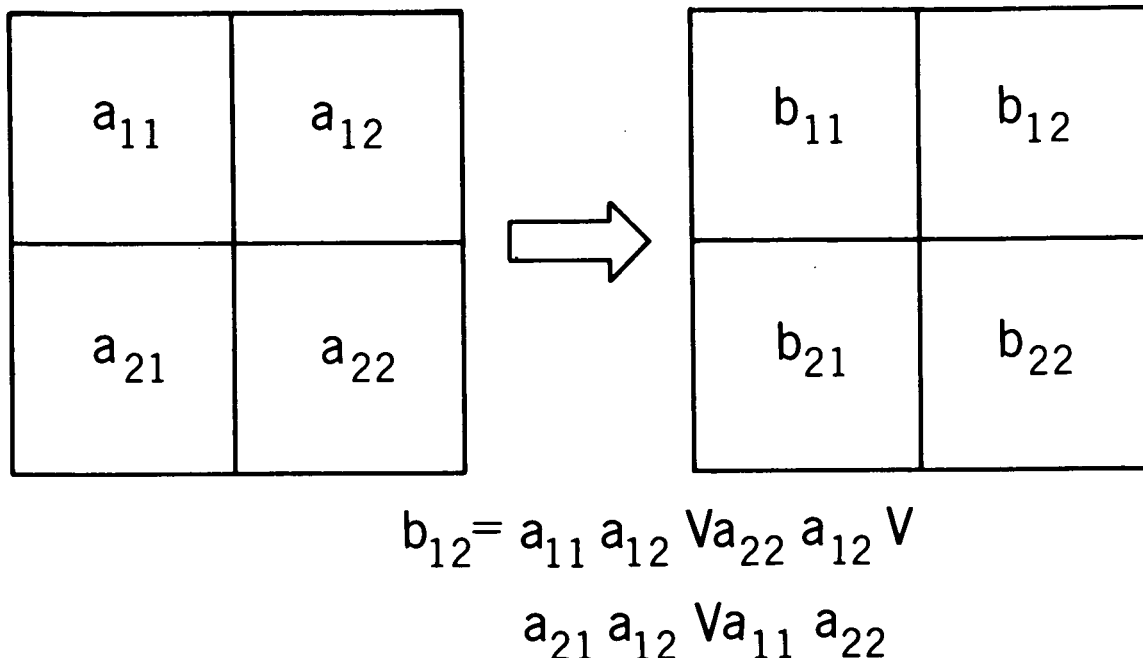
Figure 2. Function for Shrinking the Image at One Iteration Into the Image at the Next Iteration

where c_{ij} is a typical point in image C. The remainder of this paper concerns optical techniques for performing binary image operations which may be used to generate the images defined by Equations 1 and 2.

OPTICAL TECHNIQUES FOR BINARY OPERATIONS

The addition of two images is one of the most straight-forward optical techniques available. One simply superimposes two projected images on a screen. Addition of two binary images can be used to perform either the "or" operation or the "and" operation. Assume that an input consists of two binary images where white has brightness "1" and black has brightness "0". If the two images are superimposed, a new image of three gray levels is formed, the levels being 0, 1, and 2. "Thresholding" the new image such that all areas greater than 1/2 become white and those less than 1/2 become black gives the "or" of the two images. If the threshold is set at 1-1/2, the result is the "and" of the two images.

Equation 1 defined each point in a new image as a function of a neighborhood of points in another image. Corresponding to Equation 1, the whole

image can be obtained as a function of shifted versions of another image by the equation

$$B = (A \wedge A_{10}) \vee (A \wedge A_{11}) \vee (A \wedge A_{01}) \vee (A_{01} \wedge A_{10}) \tag{3}$$

Using this nomenclature, "A" is the unshifted image and A_{xy} is image A shifted by x elements to the right and y elements up ($-x$ and $-y$ would indicate left and down, respectively). Since image B is defined as a series of "and" and "or" operations, a series of optical addition, thresholding and storing operations can generate image B from shifted versions of image A. In order to see how shifted versions of an image might be obtained, consider an image formed on the back plane of a pinhole camera. If the pinhole is moved up or down relative to an initial position, the image (though inverted) will move up or down relative to an initial position. If another pinhole were punched in the front of the camera, two images would be superimposed on the back plane, one shifted relative to the other, corresponding to the positions of the two pinholes. Thus, to add two shifted versions of an image, two pinholes can be punched in the front of the camera corresponding to the desired shifts. If the image in front of the pinhole were binary and two pinholes were used, the image on the back plane of the camera could be "thresholded" as described previously, creating the "and" or "or" of two shifted versions of the input image. To generate the image defined by Equation 3, four pinholes arranged in a 2 x 2 array would be needed, generating images $A, A_{01}, A_{10},$ and A_{11}. The pinholes would be capable of being opened or closed. In performing the operation, two pinholes would be opened at a time corresponding to the four "anded" pairs of images. At each step the superimposed images on the back plane would be "anded" by thresholding at 1-1/2 and the resulting image would be stored. Then the four stored images would be "ored" by superimposing all four images and thresholding the resulting image at 1/2.

This operation requires several steps. A slightly different technique will perform this operation in one step. Equation 3 can be converted to the following threshold logic equation[2]:

$$B = 1 \text{ where } (3A + 2A_{01} + 2A_{10} + A_{11}) > 3,$$

$$B = 0 \text{ otherwise.} \tag{4}$$

which says that image B is 1 (white) at points where the summation of shifted images is greater than 3 and is 0 (black) where the summation is three or less. This equation may be easily verified using a truth table. The summation of shifted images within the parenthesis can be obtained again using the pinhole camera technique. The same 4 pinholes as described previously are used. The two pinholes generating A_{01} and A_{10} are attenuated such that 2/3 of the light gets

through. The pinhole for A_{11} is attenuated such that $1/3$ gets through and the shifted pinhole for "A" is not attenuated. This corresponds to the coefficients of 3 for "A", 2 for A_{10} and A_{01} and 1 for A_{11}. If the image in the back plane of the "multiple pinhole" camera is "thresholded" such that all areas greater than 3 become white and all areas 3 or less become black, one has generated image B from image A in a single step.

The summing of shifted versions of an image using the "multiple pinhole" camera is, in effect, taking the mathematical cross-correlation between that image and the "weighted" pinhole pattern.[3] The image on the back plane of the camera is the cross-correlation function. Thus, the "multiple pinhole" camera is an image cross-correlator.

A laboratory experiment using the "multiple pinhole" camera was set up to perform the operation in Equation 4. In this experiment, however, for illumination purposes, the positions of the input image and pinholes were reversed. That is, in place of the input image was an array of pinholes and in place of the pinholes was a transparency of the binary image. The cross-correlation function is the same in either case. This cross-correlator is diagrammed in Figure 3. The pinhole array is image A and the binary image is image B. The scale indicated for image B relative to image A produces the correct increments of image shifting. The pinhole array used in the experiment
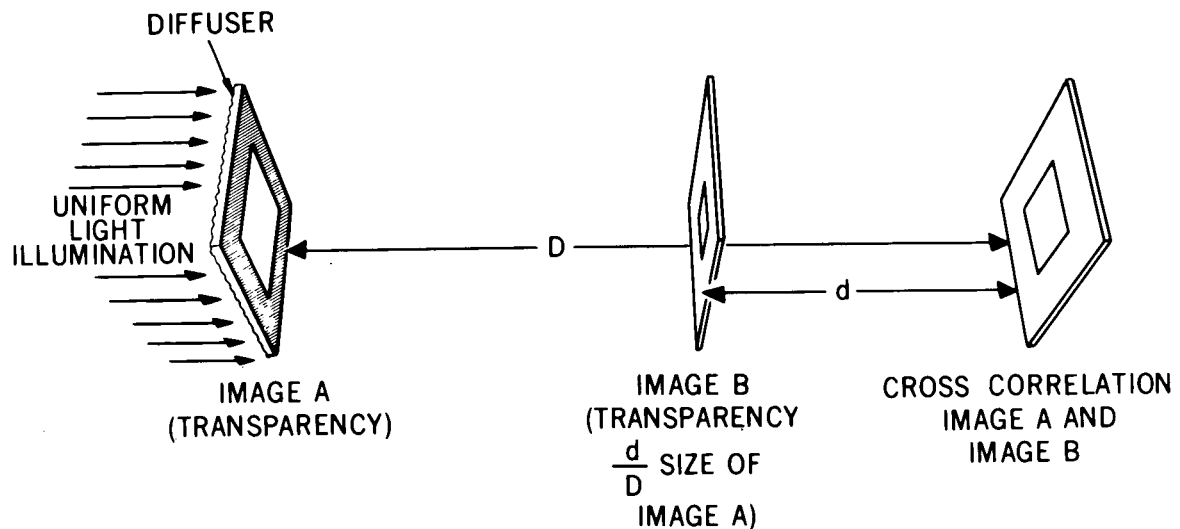

Figure 3. Cross-Correlator for Shifting Images. Sum of shifted images appears in cross-correlation plane.

was actually the array of square aperatures shown in Figure 4. This allowed the simple shading technique shown to be used to give accurate relative attenuation.

An example of the imagery obtained in this experiment is shown in Figure 5. The input image (upper left) is cross-correlated with the array in Figure 4 producing the cross-correlation function in the upper center of Figure 5. Below this function are the numerical values associated with the gray levels. "Thresholding" the cross-correlation function at 3-1/2 would produce the desired shrunken image (upper right). A device for doing this thresholding over an entire image does not presently exist. However, a device that has been developed by Hughes Research Laboratories designed to spatially modulate a laser beam (called the OTTO device) has a steep gamma curve and, therefore, an attempt was made to use this device as an image thresholder.

The experimental setup is shown in Figure 6. Here, the multiple pinhole camera system to the left formed the cross-correlation function on an image intensifier tube. The output of the tube was then focused onto the surface of the OTTO device which was read out with the laser beam. The gain of the image intensifier tube was adjusted until thresholding occurred at about 3-1/2. Figure 7 shows the results. The image on the top left was cross-correlated with the pinhole array in Figure 4 producing the cross-correlation function in

NUMERICAL
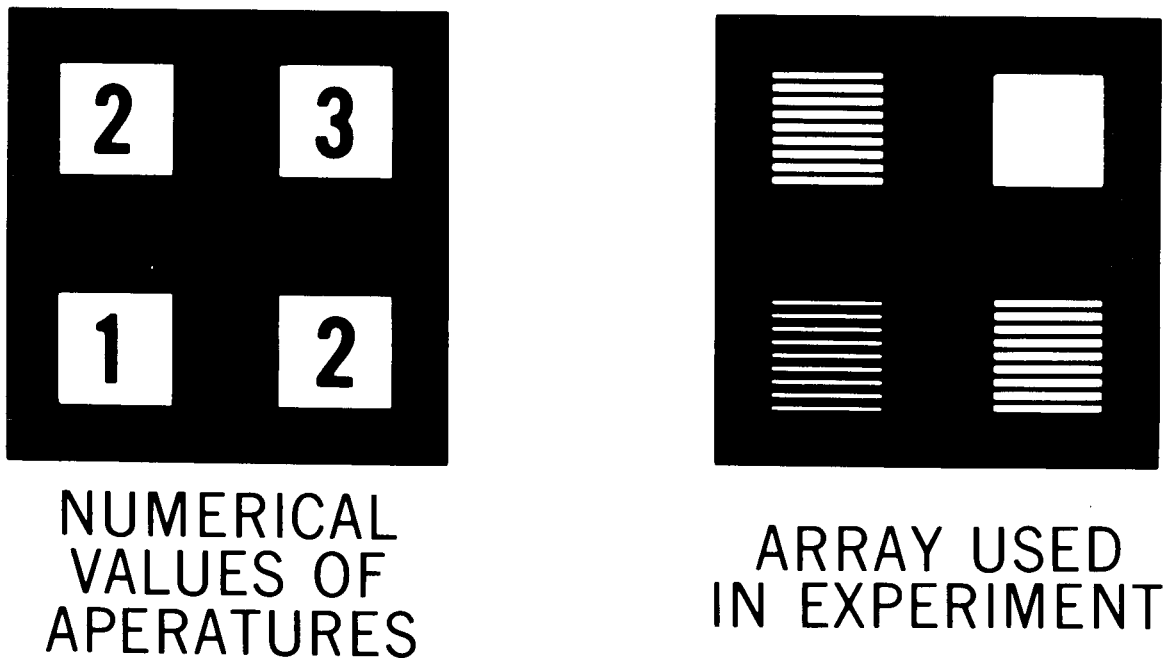VALUES OF
APERATURES

ARRAY USED
IN EXPERIMENT

Figure 4. "Attenuated Pinhole Array" for Shrinking

the top center. The desired thresholded result is at the top right. The output of the OTTO device (which is a negative) is seen in the lower part of Figure 7. This was basically a feasibility experiment and no attempt was made to assure uniform sensitivity or illumination over the surfaces of either the image intensifier or the OTTO device. The OTTO device was an interim device loaned by Hughes for evaluation.

A MORE COMPLEX OPERATION

The results shown in Figure 7 show that the OTTO device can do some "thresholding" between the levels of 3 and 4 but not very effectively. However, the device will "threshold" effectively between the levels of 0 and 1. That is, it can be made to "saturate" at the lowest incremental brightness level above
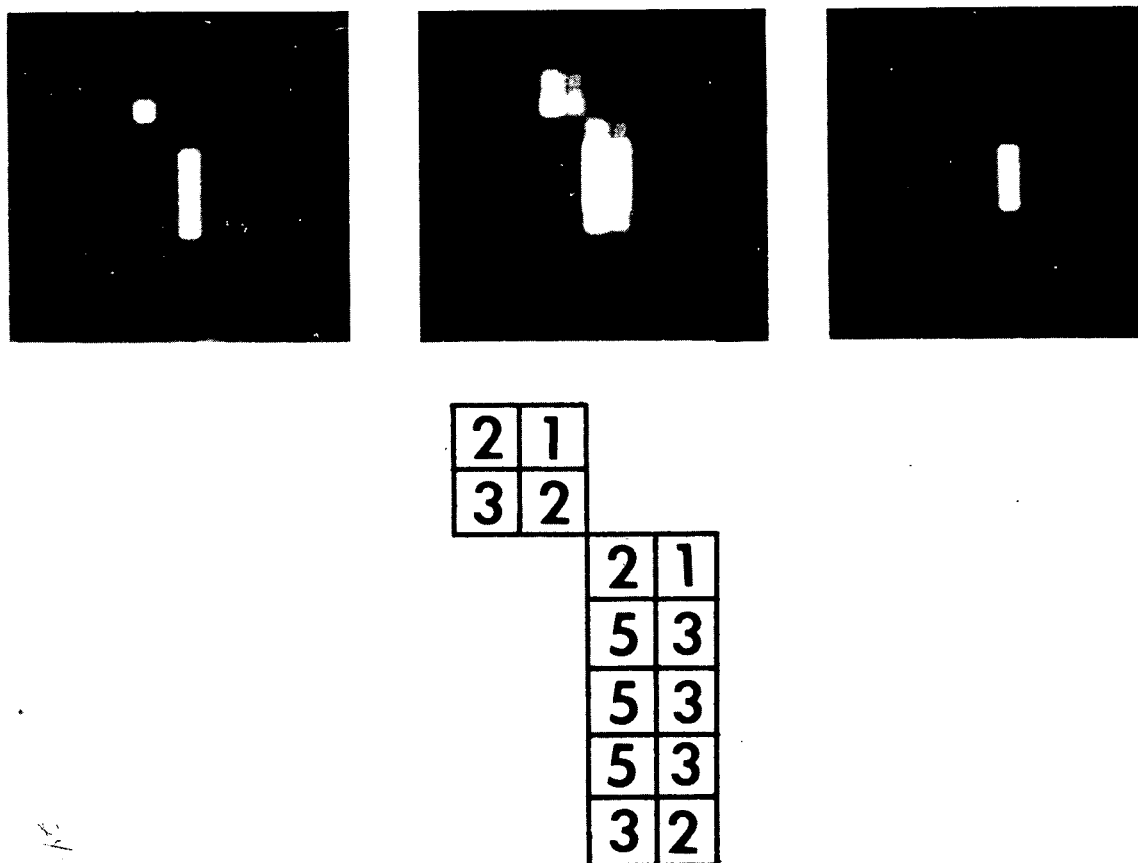

Figure 5. Demonstration of Summing of Shifted Images Using Multiple Pinhole or Cross-Correlation Technique. Input image is at upper left. Summation of shifted images is at upper center. Results of thresholding is at upper right.

DIFFUSER

UNIFORM
LIGHT
SOURCE

PINHOLE
ARRAY

LASER

OTTO

IMAGE
INTENSIFIER

IMAGE

CROSS
CORRELATION
FUNCTION AT
INPUT OF IMAGE
INTENSIFIER

THRESHOLDED
CROSS
CORRELATION
FUNCTION
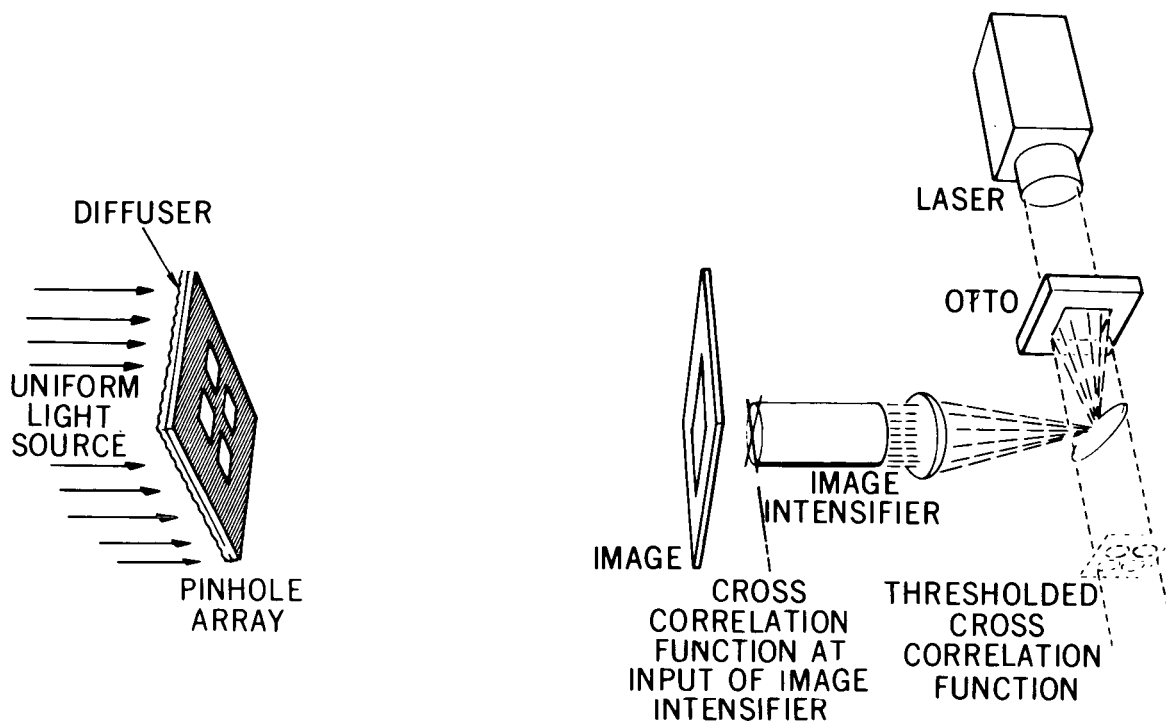
Figure 6. Optical System for Shrinking Image

zero. Using this property, the following experiment was performed which pro-
duced the image of isolated points necessary in Levialdi's counting algorithm.

Corresponding to Equation 2, an image, C, containing only the isolated
points in another image, B, can be obtained from shifted versions of image B
using the following function:

$$C = \overline{B}_{1,-1} \wedge \overline{B}_{0,-1} \wedge \overline{B}_{-1,-1} \wedge \overline{B}_{1,0} \wedge \overline{B}_{-1,0} \wedge \overline{B}_{1,1} \wedge$$

$$\overline{B}_{0,1} \wedge \overline{B}_{-1,1} \wedge B$$

where $\overline{B}$ is the negative of image B. In the experiment, it was more convenient
to use $\overline{C}$ which can be written as:

$$\overline{C} = B_{1,-1} \vee B_{0,-1} \vee B_{-1,-1} \vee B_{1,0} \vee B_{-1,0} \vee B_{1,1} \vee$$
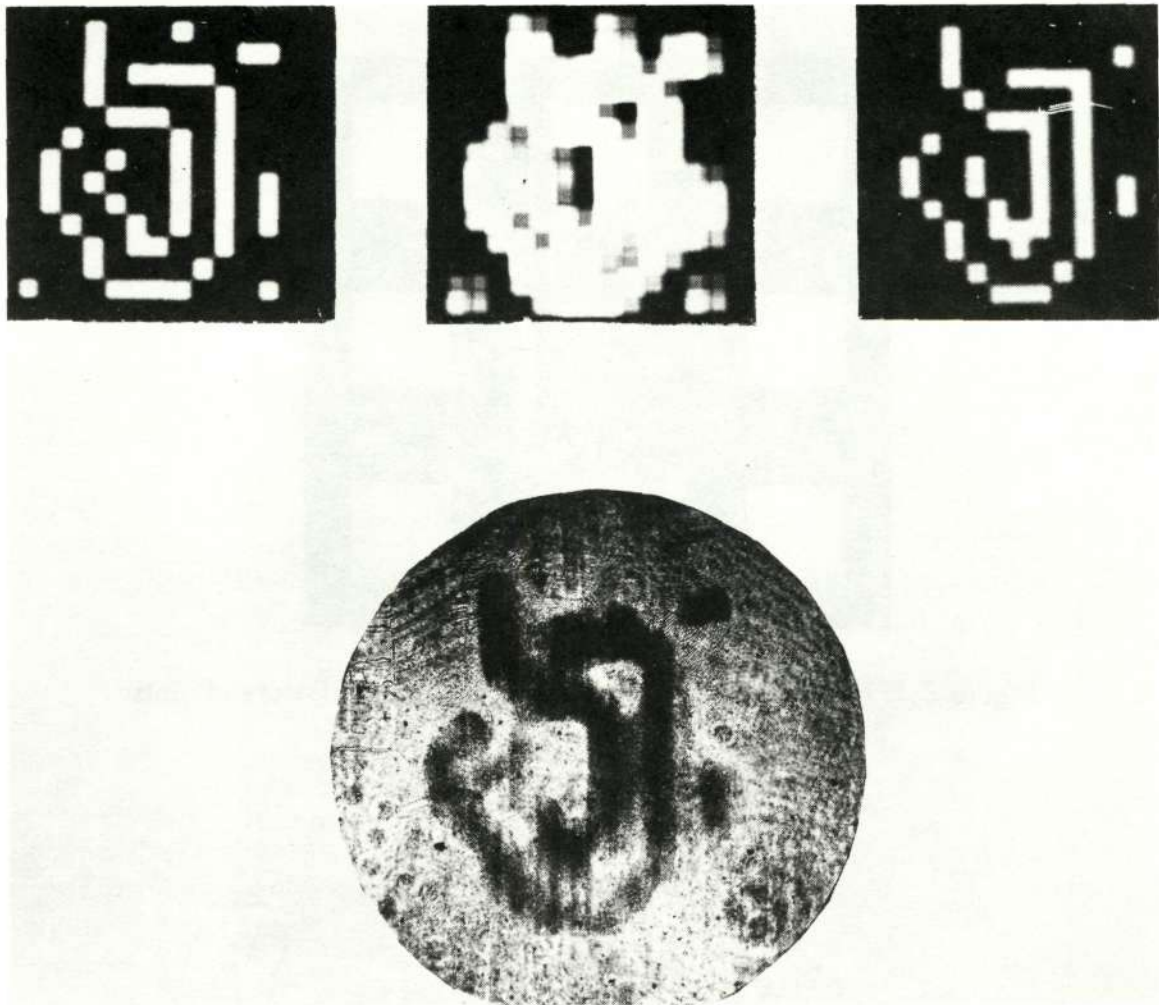
$$B_{0,1} \vee B_{-1,1} \vee \overline{B}$$

Figure 7. Thresholding of Cross-Correlation
Function Between Levels of 3 and 4
Using OTTO device

This equation when converted to threshold logic becomes:

$$\overline{C} = 1 \text{ where } (B_{1,-1} + B_{0,-1} + B_{-1,-1} + B_{1,0} + B_{-1,0} + B_{1,1} + B_{0,1} + B_{-1,1}) + \overline{B} > 0$$

$$\overline{C} = 0 \text{ elsewhere} \tag{5}$$

The first step in the experiment was to sum the shifted versions of image B within the parenthesis in Equation 5. This was done by cross-correlating image B with the pinhole array shown in Figure 8. The experimental setup is illustrated in Figure 9 where the pinhole array illuminated the transparency of

167

Figure 8. "Pinhole Array" for Generating Image of Isolated Points

Figure 9. Optical System for Generating Image of Isolated Points

image B forming the cross-correlation function or summation of shifted images on the input of an image intensifier tube. A negative transparency of image B was projected onto the image intensifier input so that it add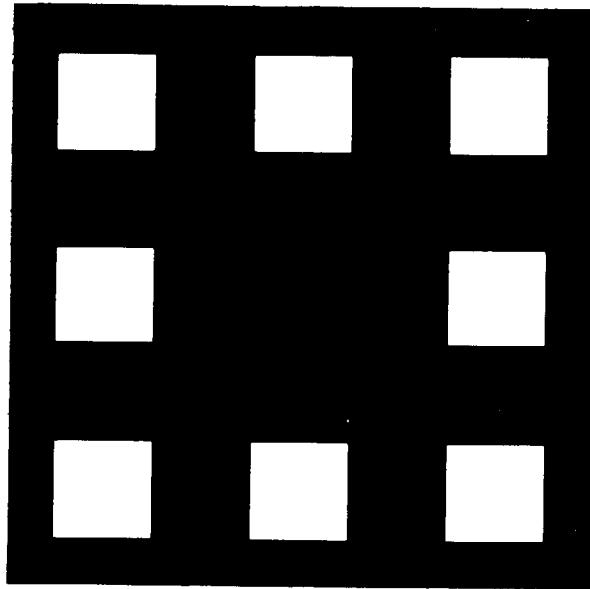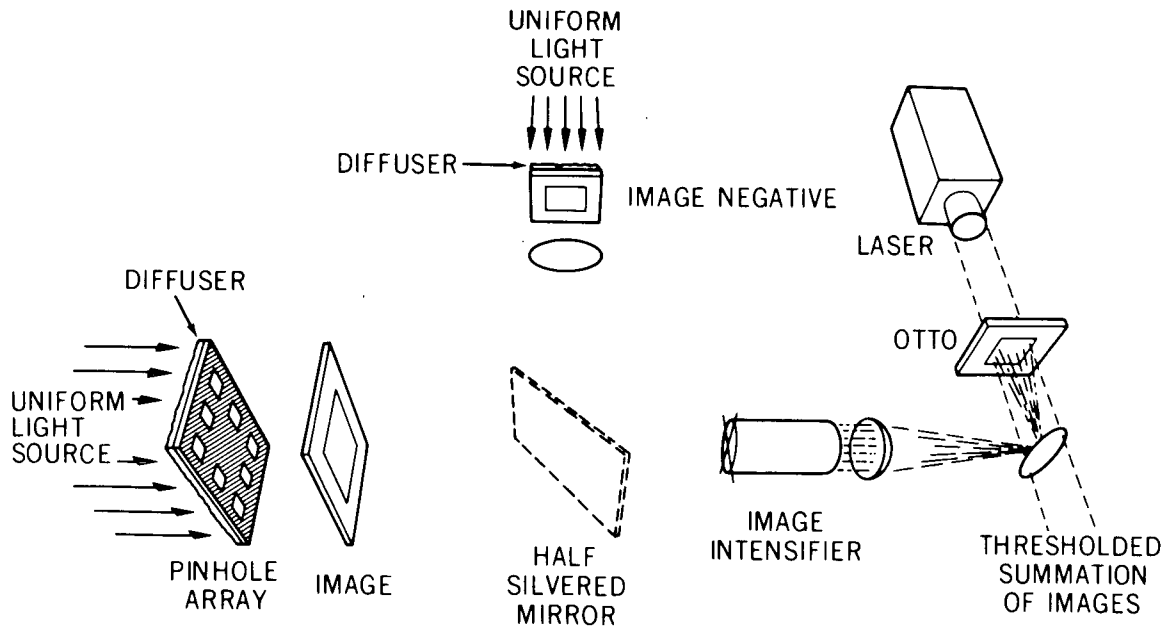ed to the summation of shifted images. This corresponds to the $\bar{B}$ term in Equation 5. The output of the image intensifier tube was focused onto the input of the OTTO device. Here the total summation of images was thresholded at about 1/2 and, since the OTTO device produces a negative, the laser read out image C. Figures 10 and 11 show results. Figure 10a shows an input image with one isolated point. In 10b there is shown the cross-correlation function between the input image and the pinhole array, and 10c shows the isolated point in the output of the OTTO device. Figure 11 shows the same results when the input image was the input image of Figure 1 with 3 isolated points.
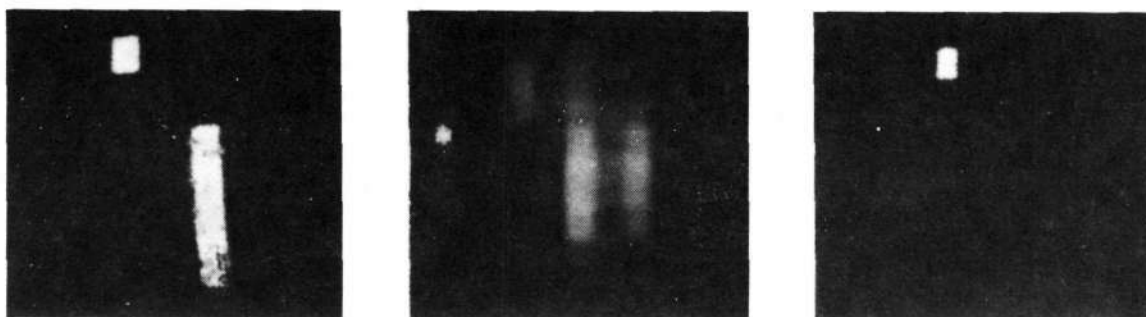
Figure 10. Detection of a Single Isolated Point. (a) Input Image, (b) Cross-Correlation Function Between Input Image and "Pinhole Array" of Figure 8, (c) Isolated Point Output of OTTO Device
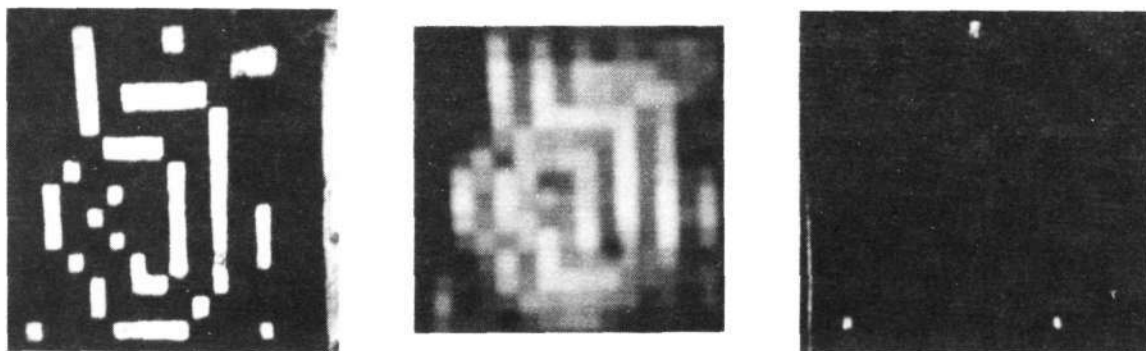
Figure 11. Detection of Multiple Isolated Points: (a) Input Image, (b) Cross-Correlation Function Between Input Image and "Pinhole Array" of Figure 8, (c) Isolated Points in Output of OTTO Device

CONCLUSIONS

This work has described very simple optical techniques for performing complex binary operations on images. In cases where binary equations can be converted to single threshold logic equations, a single cross-correlation operation can take the place of multiple image shifting, "anding", "oring" and storage operations.

REFERENCES

1. Levialdi, S.: "On Shrinking Binary Picture Patterns," Communications ACM, 1970.

2. Hu, S. T.: Threshold Logic, University of California Press, Berkeley and Los Angeles, California, 1965.

3. Rosenfeld, A.: Picture Processing by Computer, Academic Press, New York, London, 1969.

DIGITAL HOLOGRAPHIC LOGIC

K. Preston, Jr.
The Perkin-Elmer Corporation, Norwalk, Connecticut 06856

INTRODUCTION

Optical computers ordinarily operate in an analog mode where signals introduced into the computer take on continuous values. The computing rate achievable in such computers is given by

$$R_c = \frac{\epsilon \eta P}{h\nu(S/N)^2}$$

(1)

where ϵ is the optical transfer efficiency, η is the quantum efficiency of the output detector, P is the optical input power, h is Planck's constant, ν is the optical frequency, and (S/N) is the desired rms output signal to noise ratio.

For typical values such as $\epsilon = 0.5$, $\eta = 0.1$, P = 1.0 watt, $\nu = 10^{15}$ Hz, S/N = 10, R_c is of the order of 10^{14} multiplications per second. Accuracy, however, is low. In ordinary optical systems the accuracy level is 5 bits, but with extreme care in both optical design and lens element fabrication, 7 to 8 bit accuracy may be achieved (1).

Ordinarily the dynamic range in the optical analog computer is 40 db (13-bits). Again, with extreme care in design, fabrication and assembly 60 db (20-bits) may be reached. In comparison with the electronic digital computer, where in many cases 128 bits accuracy is available for double precision arithmetic, the optical analog computer is far from competitive.

However, it is possible for optical computers to achieve high accuracy by operating in a digital mode using signal levels which are restricted to the binary values (0 and 1). The purpose of this paper is to describe experiments conducted at Perkin-Elmer demonstrating the feasibility of an optical digital computer. The program of this computer is entered holographically. This would be done under control of an electronic digital control unit (see Figure 1). The digital control unit would store the program and would also act as a storage medium for binary number arrays. These arrays would form the input to the optical computer and similar arrays would be retrieved from the optical computer when calculations were completed.

In order to satisfactorily combine the relatively slow electronic digital control unit with the optical computer, it is necessary that the optical computer iterate through many stages of a calculation before either requesting more data

F
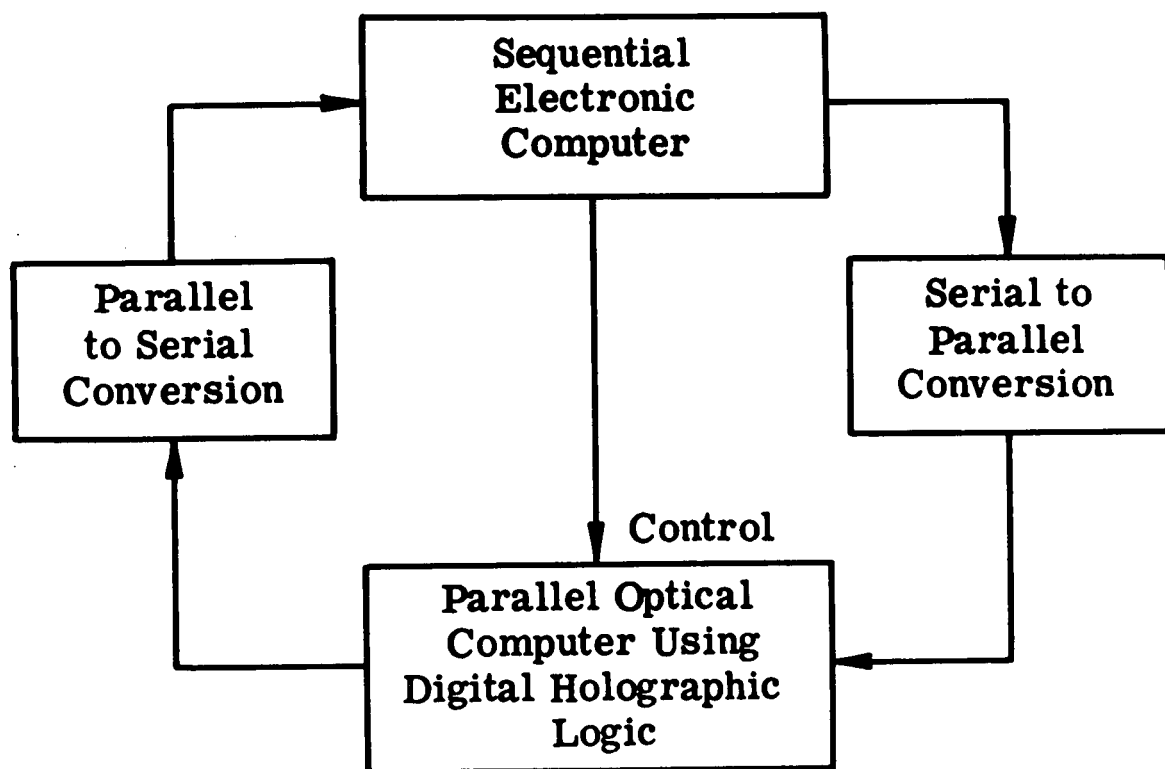
Figure 1. Block schematic showing connections between the electronic control computer and the parallel optical computer for use in performing digital logic holographically.

at its input or transferring results from its output. The optical computer would thus be built from a concatenation of blocks of the type shown in Figure 2. The block shown in this figure consists of a combination of optical-to-optical conversion devices (OTTO's) interspersed with computing elements consisting of lens pairs and holograms.

This paper discusses the characteristics of the block shown in Figure 2. First the holographic operation is reviewed from the Fourier transform viewpoint. The paper then describes the formation of holograms for use in performing digital logic, illustrates the operation of the computer with an experiment in which the binary identity function is calculated, then discusses devices for achieving real-time performance, and describes an application in pattern recognition using neighborhood logic.

HOLOGRAPHY

Figure 3 shows a schematic representation of the first stage of the block shown in Figure 2. This block makes use of the lens in taking the Fourier
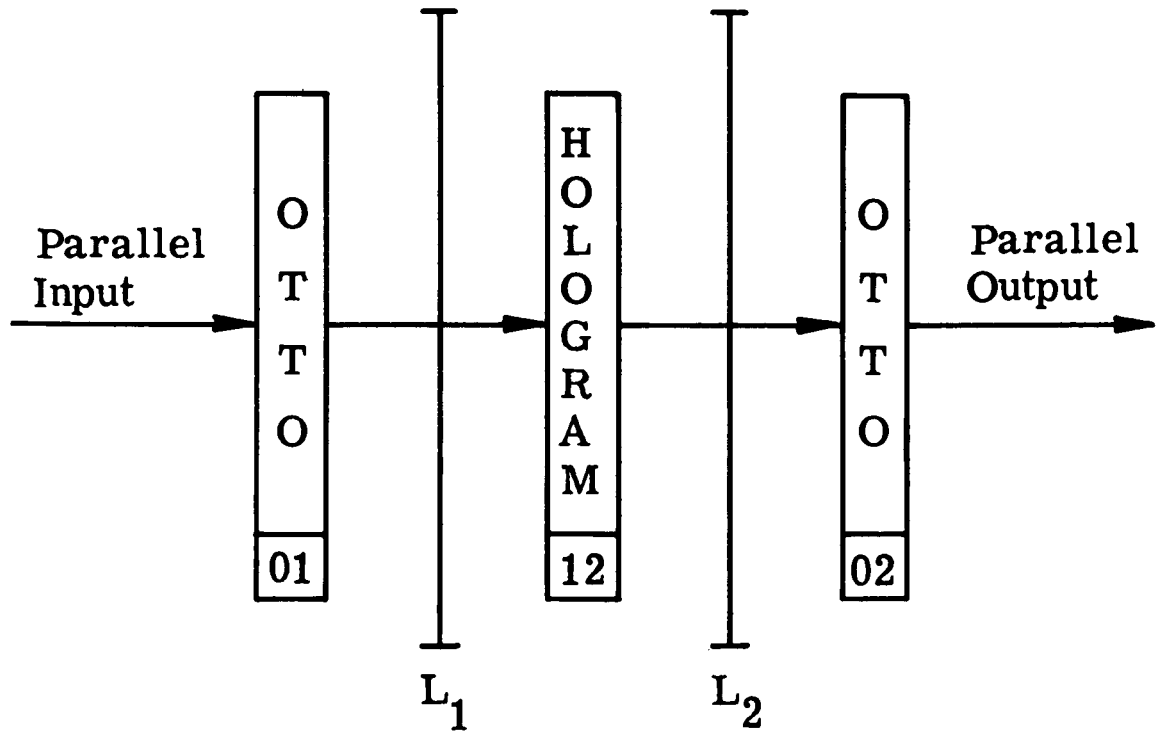
Figure 2. Schematic arrangement of the basic building block of the holographic logic computer. Two optical to optical transducers, one hologram, and two Fourier transform lenses are required.

transform. The x_1 plane is the input plane, L_{12} is the transform lens, and the x_2 plane is the Fourier transform plane. These planes are separated by two focal lengths. The lens action of the transform lens is given in the below equation (2).

$$E(x_2) = \int E(x_1) e^{-j\omega_x x_1} dx_1 \tag{2}$$

where $E(x_1)$ is the electric field distribution in the input plane, $E(x_2)$ is the electric field distribution in the output plane and $\omega_x = 2\pi x_2/\lambda F$ where λ is the optical wavelength and F is the focal length of L_{12}.

Assume that the x_1 plane contains a spatial light modulating device whose light modulating elements are discrete and regular in position. One such element is located at x_a. Light emanating from this point may be considered to be a positional delta function which is transformed into a plane wave in the x_2 plane as follows.

$$E(x_2) = \int \delta(x_1 - x_a) e^{-j\omega_x x_1} dx_1 = e^{-j\omega_x x_a} \tag{3}$$

173
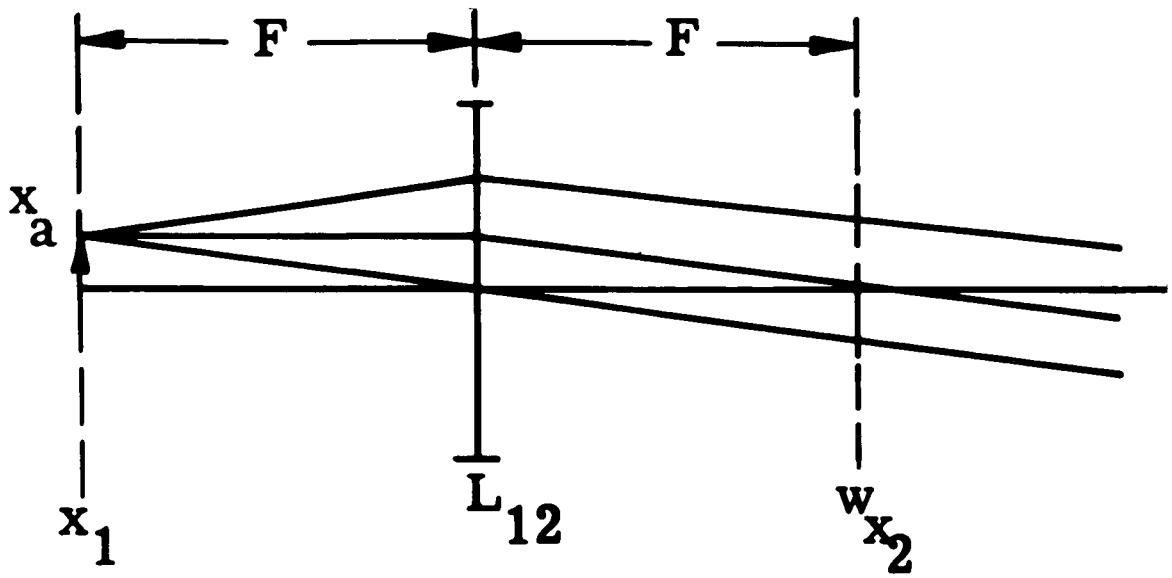
$$E\left(w_{x_2}\right) = \int E\left(x_1\right) e^{-jw_{x_2}x_1} dx_1$$

$$w_{x_2} = 2\pi x_2 / \lambda F$$

$$\delta\left(x_1 - x_a\right) \longrightarrow e^{-jw_{x_2}x_a}$$

Figure 3. Analytical relationship between a discrete input at x_a in the input plane and the associated plane wave in the Fourier plane created by the transform lens L_{12}.

When the second lens of the block is introduced, the block is complete and the configuration is as shown in Figure 4. The lens L_{23} takes a Fourier transform with the result appearing in the x_3 plane. The reader should note that, since lenses in optical computers take successive Fourier transforms, the

174

$$\delta\left(x_1 - x_a\right) \longrightarrow e^{-jw_{x_2}x_a} \longrightarrow \delta\left(x_3 + x_a\right)$$
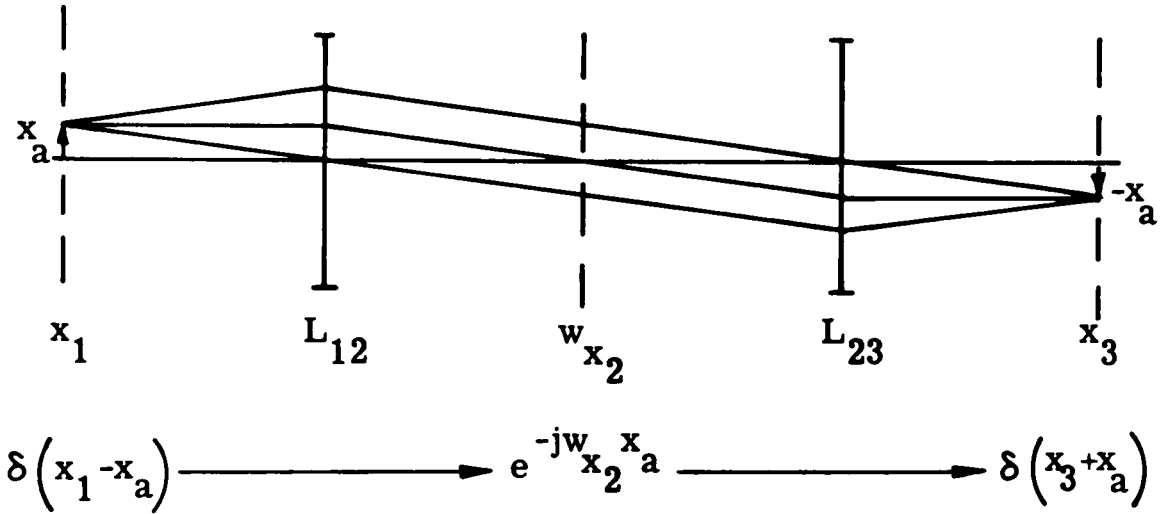
Figure 4. Analytical relationship between the discrete input at x_a in the input plane and its image at $-x_a$ in the output plane when two successive Fourier transforms are taken using lenses L_{12} and L_{23}.

inverse of the input function appears at the output, namely, a delta function not at x_a but at $-x_a$. This is expressed in the following equations

$$E(x_3) = \int E(x_2)e^{-j\omega_x x_2}\, dx_2$$

$$= \int e^{-j\omega_x'(x_3 + x_a)}\, dx_2$$

$$= \delta(x_3 + x_a)$$

where $\omega_x = 2\pi x_3 / \lambda F$ and $\omega_x' = 2\pi x_2 / \lambda F$.

In order to form a hologram and illustrate its operation upon an input delta function at x_a consider the configuration diagrammed in Figure 5. Two discrete inputs are provided: one at x_a; one at x_r. Lens L_{12} carries out the Fourier transform of these two delta functions to produce the electric field distribution

$$E(x_2) = e^{-j\omega_x x_a} + e^{-j\omega_x x_r} \tag{5}$$

175

$$\delta\left(x_1 - x_a\right) \longrightarrow e^{-jw_{x_2}x_a}$$

$$\delta\left(x_1 - x_r\right) \longrightarrow e^{-jw_{x2}x_r}$$

$$H_{ar} \equiv E\left(w_{x_2}\right) E^*\left(w_{x_2}\right)$$

$$= 2\left[1 + \cos w_{x_2}\left(x_r - x_a\right)\right]$$
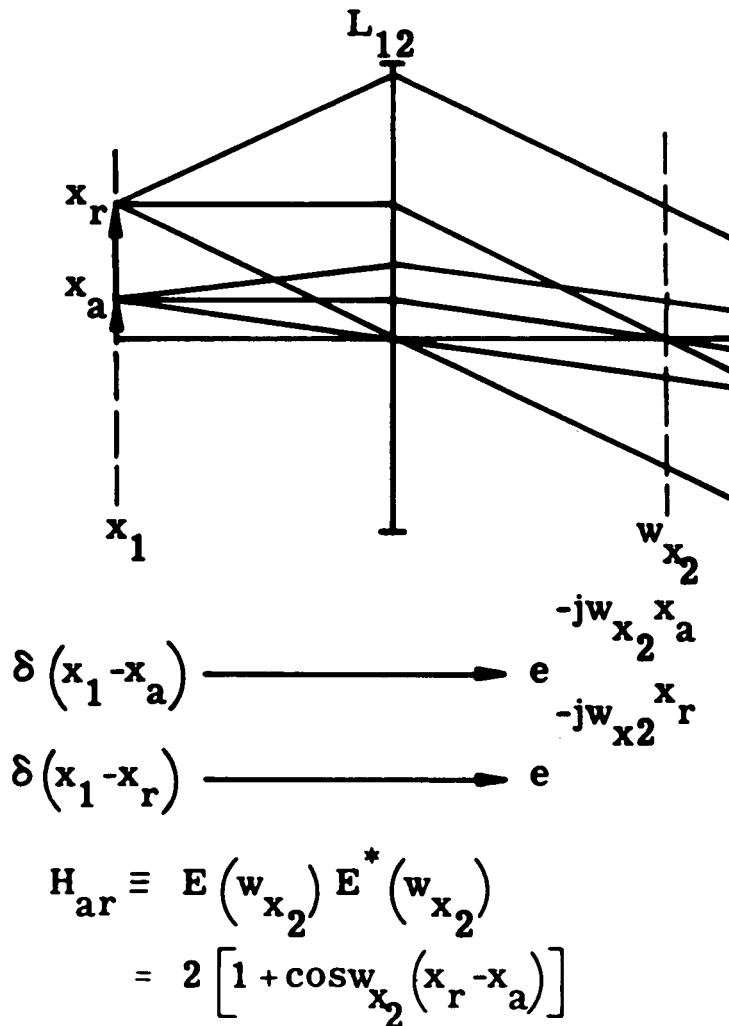
Figure 5. Equations describing the generation of a hologram in the Fourier plane using a discrete input at x_a and a reference at x_r in the input plane.

An energy detector placed in the x_2 plane records the hologram H_{ar} given as follows

$$H_{ar} = E(x_2)E^*(x_2) = 2[1 + \cos \omega_x(x_r - x_a)] \tag{6}$$

Note that this hologram consists of a bias term plus a cosinusoidal term whose spatial frequency is proportional to the quantity $(x_r - x_a)$.

When this hologram is placed in the optical computer and a discrete input occurs at x_a, the result is as shown in Figure 6. Once again the lens L_{12} generates a plane wave in the x_2 plane in which the hologram H_{ar} is located. The
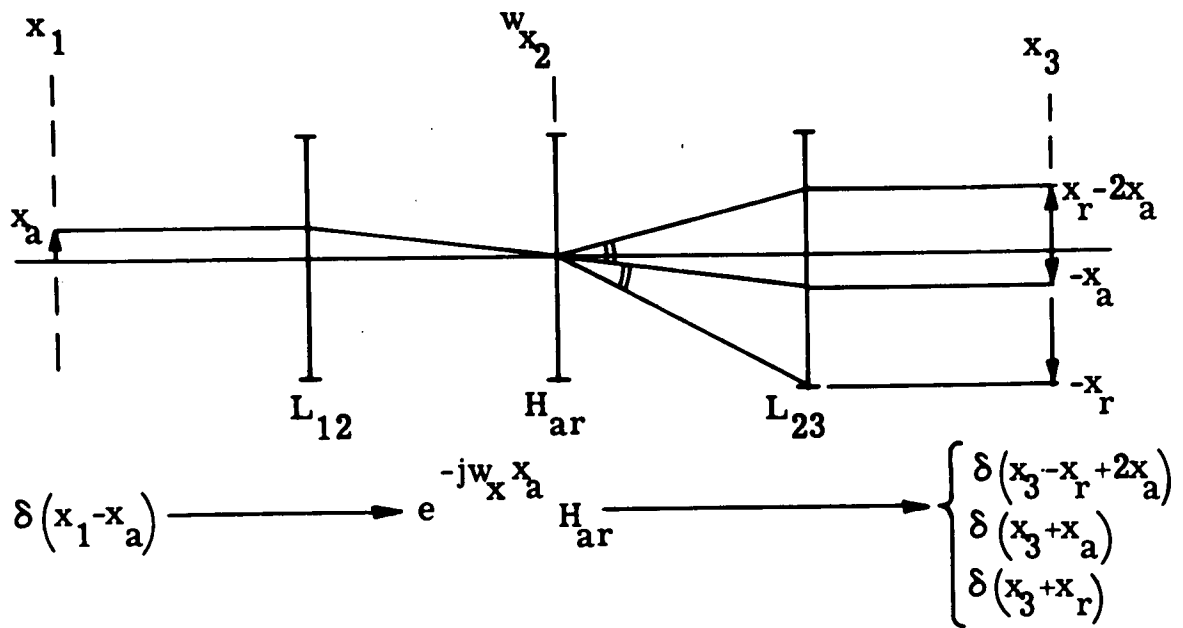
Figure 6. Schematic showing the results when a discrete input at x_a is used in conjunction with a hologram H_{ar} in the Fourier plane to produce three discrete outputs in the output plane.

plane wave interacts with H_{ar} in such a way that three plane waves are created which are transformed by L_{23} into three delta functions according to the below equation

$$E(x_3) = \int \left[2 + e^{j\omega_x(x_r-x_a)} + e^{-j\omega_x(x_r-x_a)} \; e^{-j\omega_x x_a} \; e^{-j\omega_x x_2} \, dx_2 \right]$$

$$= \int \left[2e^{-j\omega'_x(x_3+x_a)} + e^{-j\omega'_x(x_3+x_r)} + e^{-j\omega'_x(x_3-x_r+2x_a)} \; dx_2 \right] \qquad (7)$$

$$= 2\delta(x_3 + x_a) + \delta(x_3 + x_r) + \delta(x_3 - x_r + 2x_a)$$

The reader familiar with matched filter theory will recognize that the delta function at $-x_r$ is the peak of the correlation function generated by H_{ar} acting as a matched filter in the frequency domain (3).

Another way of diagramming the action of H_{ar} is shown in the left hand portion of Figure 7. This simplified diagram indicates only the input plane (horizontal line at top) and the output plane (horizontal line at bottom). The action of the entire lens system in combination with H_{ar} is shown merely by the downward

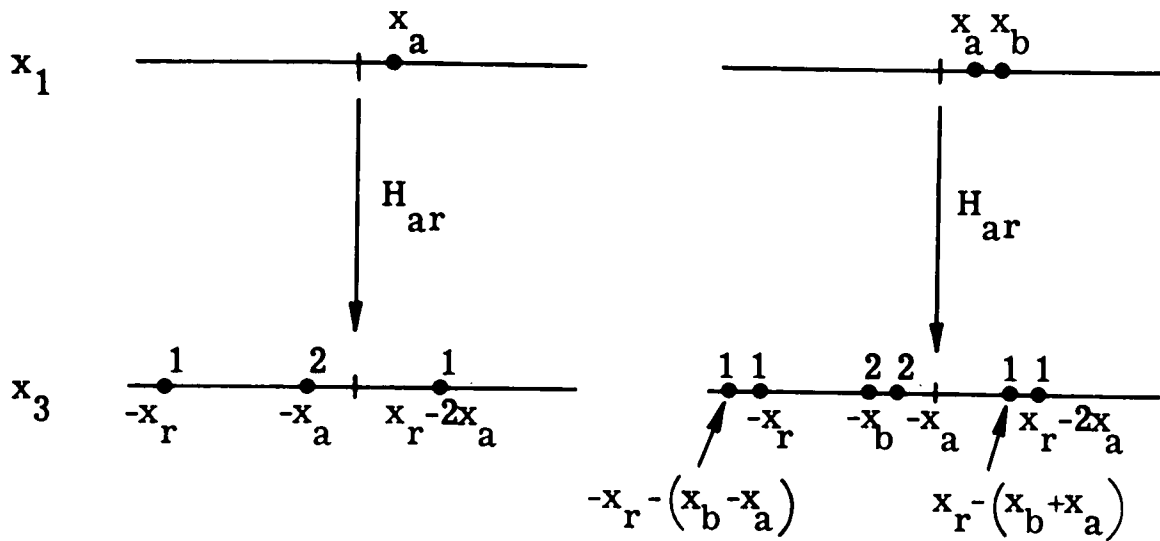Figure 7. Abbreviated schematics showing (left hand drawing) the result given in Figure 6 and (right hand drawing) result when using two discrete inputs in the input plane at the points x_a and x_b.

directed arrow. On the line representing the output plane the numerics indicate the electric field strength of three delta functions. Note that the electric field strength at $-x_a$ is twice that of the other two delta functions.

HOLOGRAPHIC LOGIC

In performing holographic digital logic it is important to understand how the hologram interacts with light emanating from a multiplicity of discrete inputs in the x_1 plane. The right hand portion of Figure 7 shows what occurs when a second input is added at x_b. New delta functions appear in the output plane separated by the distance $(x_b - x_a)$ from the other delta functions. They are of identical electrical field strength and of equal phase if we assume that the input at x_b has strength and phase equal to that at x_a.

In order to perform digital logic holographically it is necessary to combine at one point in the output plane energy emanating from two discrete inputs in the x_1 plane. This may be done by using a somewhat more complex hologram constructed in the same manner as shown in Figure 5 but with discrete inputs at both x_a and at x_b simultaneously. The electric field strength in the x_2 plane is given by the equation

$$E(x_2) = e^{-j\omega_x x_a} + e^{-j\omega_x x_b} + e^{-j\omega_x x_r} \tag{8}$$

x_1 x_a x_a x_b

$$H_{abr} \qquad\qquad H_{abr}$$

x_3

Left: 1 1   1 3 1   1 1

$-x_r$ $-x_r + (x_b - x_a)$ $-x_b$ $-x_a$ $-x_a + (x_b - x_a)$ $x_r - 2x_a$ $x_r - (x_b + x_a)$

Right: 1 2 1   1 4 4 1   1 2 1

$-x_r$ $-x_b$ $-x_a$ $x_r - (x_b + x_a)$
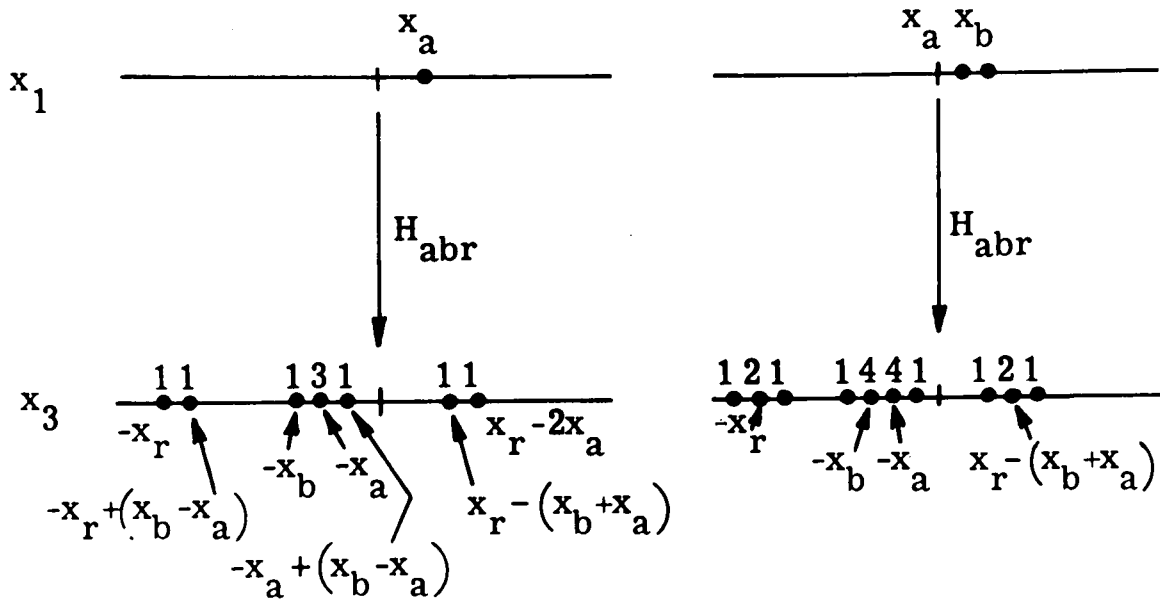
Figure 8. Abbreviated schematics showing the results of using the hologram H   in the Fourier plane with a single discrete input at x_a (left hand drawing) with two discrete inputs at the points x_a and x_b (right hand drawing).

and the hologram H_{abr} resulting from exposing an energy detector to this field is given by

$$H_{abr} = E(x_2)E^*(x_2)$$

$$= 3 + 2[\cos \omega_x(x_r - x_a) + \cos \omega_x(x_r - x_b) + \cos \omega_x(x_b - x_a)]$$

As can be seen there are three cosinusoidal terms. If we assume, as is usually the case, that the reference input at x_r is considerably removed from the optical axis, then two of the cosinusoidal terms represent high spatial frequencies while the other has a relatively low spatial frequency related to the difference in position between x_b and x_a).

When hologram H_{abr} is introduced in the x_2 plane and an input at x_a is present in the x_1 plane, the resultant output electric field distribution is shown in the left hand side of Figure 8. The reader should compare this result with that shown in the left hand side of Figure 7 which relates to the same input configuration when using hologram H_{ar}.

When using hologram H_{abr} a single input in the x_1 plane produces a holographic image of the input plane configuration for which H_{abr} is the hologram. Thus not only does an output delta function appear at $-x_r$ but there is another

INPUT (x_1)		OUTPUT (x_3)
x_a	x_b	$-x_r$
0°	0°	2
0°	180°	0
180°	0°	0
180°	180°	2

Figure 9. Electric field strength in the output plane at the point $-x_r$ produced using each of the four binary combinations of inputs at x_a and x_b.

delta function at a distance $(x_b - x_a)$ from it. Holographically speaking this is the "reconstruction" of the input configuration for which H_{abr} is the hologram (4).

The final and most important result is shown on the right hand side of Figure 8. Here the configuration of inputs in the x_1 plane is identical to that from which the hologram H_{abr} is made. When this is the case, the electric field strength at the point $-x_r$ in the output plane is the coherent summation of the electric fields at x_a and x_b in the input plane. Speaking from the point of view of matched filter theory, the electric field strength in the vicinity of $-x_r$ is the correlation function of the input configuration whereas that in the vicinity of the conjugate region at $[x_r - (x_b + x_a)]$ is the convolution function. Other inputs appear near the optical axis. These have the highest electric field and occur where the input configuration is imaged by the combined action of L_{12} and L_{23}.

In using holograms such as H_{abr} for performing digital holographic logic only the delta functions near $-x_r$ is of importance. Therefore in the discussion which follows only this region of the output plane is treated.

THE BINARY IDENTITY FUNCTION

In order to perform digital logic using H_{abr} it is necessary to elect a method for introducing the binary values of the input variables. The most straight-forward approach is to use zero phase for the binary 0 and the opposite phase (180°) for the binary 1. The resultant field strength in the output plane at the point $-x_r$ for this selection of the binary variables at x_a and x_b is tabulated in Figure 9. In all cases it is assumed that the electric field strengths at x_a and x_b are identical. As can be seen, when the phase of the electric field at x_a and

x_b are the same, the output field strength at $-x_r$ is finite. When the phases are opposite, the output at $-x_r$ is zero. Optically speaking, finite and zero outputs correspond to constructive and destructive interference, respectively. Logically speaking, the tabulation shown on Figure 9 may be considered to be a truth table for the identity function.

In order to completely appreciate the appearance of the output plane, refer to Figure 10 which shows in the two left hand columns the states of the input variables and in the three right hand columns the complete correlation function configuration in the vicinity of the point $-x_r$. Not only is the identity function (center column) shown but also the light distribution in its immediate vicinity for all four possible pairs of values of the input variables.

EXPERIMENTAL CONFIRMATION

An experiment was recently carried out in the laboratory where such a computation was performed using a hologram of the type given by H_{abr}. Specifically this hologram was created using two discrete inputs consisting of 50μm diameter pinholes with a 100μm separation. An input light modulator was then created by vapor deposition which is shown in Figure 11. This light modulator
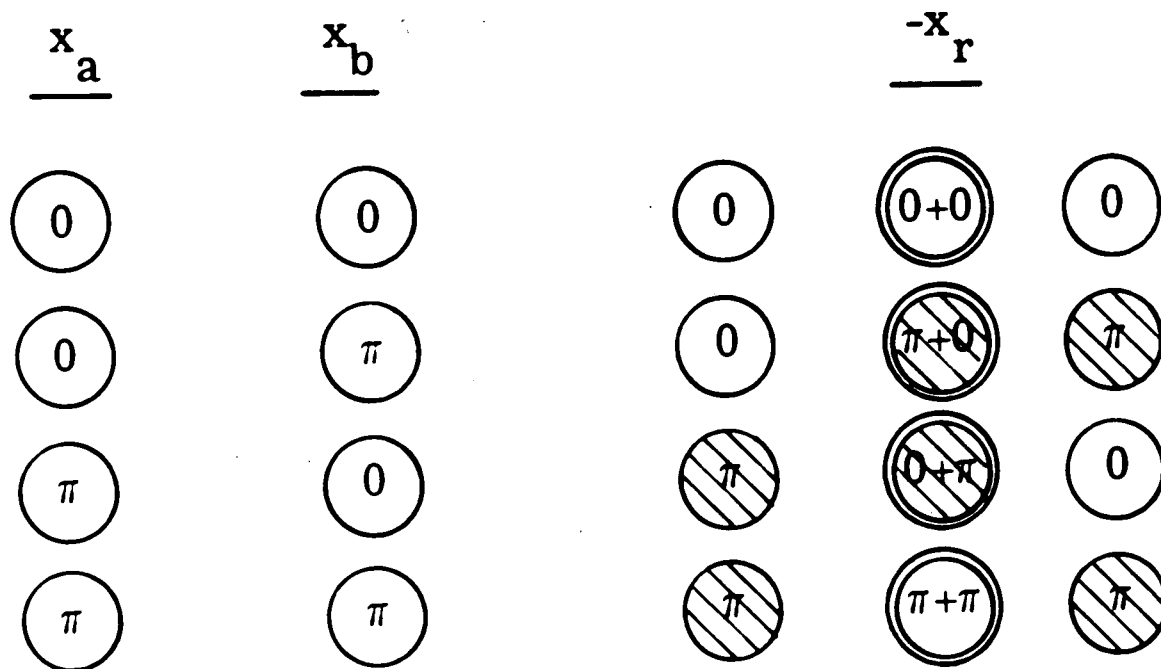

Figure 10. Diagram of the autocorrelation functions produced in the vicinity of the point $-x_r$ in the output plane for the four possible binary combinations of inputs at points x_a and x_b.
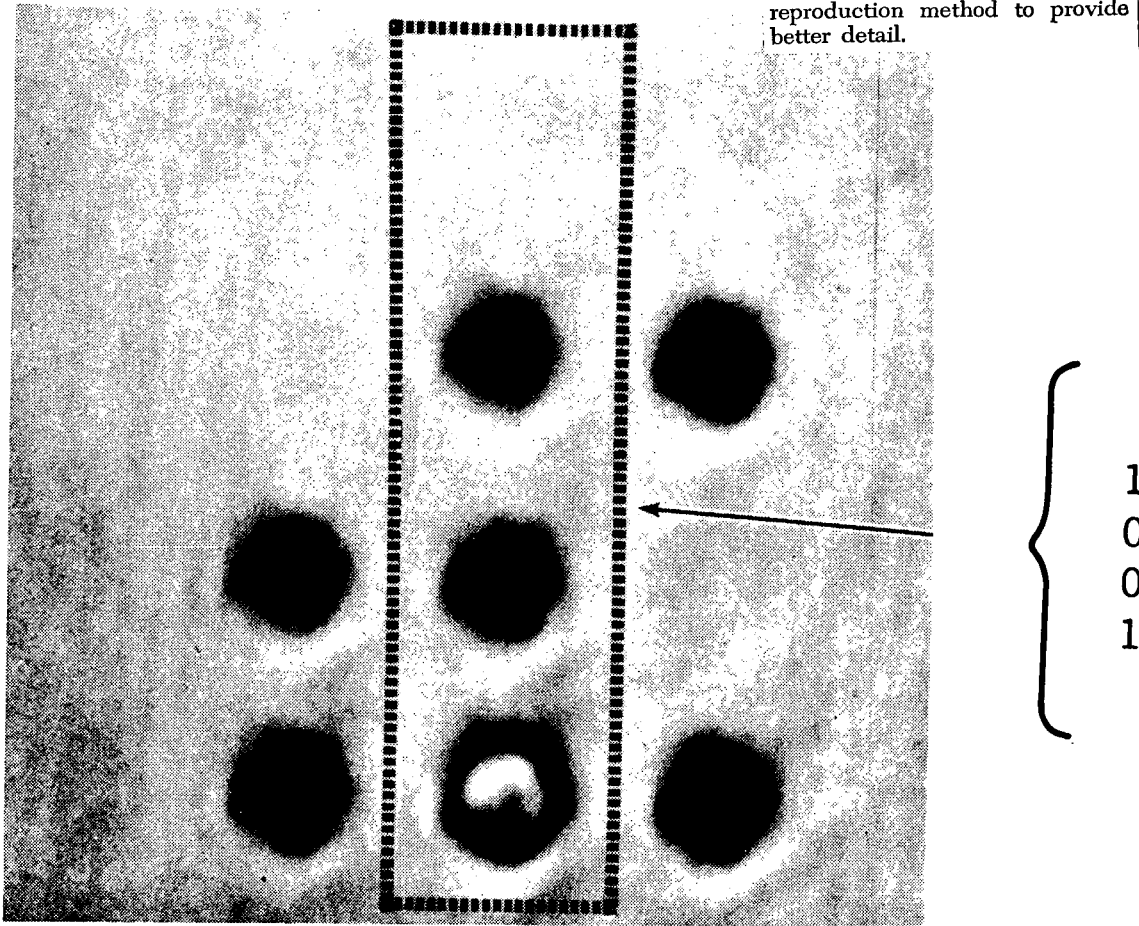
Figure 11. Photomicrograph of a two dimensional spatial light modulator having four phase modulating regions (encircled) whose action is to shift the phase of transmitted light by 180 degrees with respect to light passing through adjacent regions.

had its elements on a grid spacing of 100μm. Each element has 50μm in diameter. Four elements were created which shifted the phase of the transmitted light by 180° with respect to light passing through the background. These light modulating elements were arranged so that they would correspond to the input variable combinations given in Figure 10.

Figure 12 shows the resultant light intensity distribution in the output plane when the light modulator was placed in the input plane. There is a background of in-phase illumination. Regions 50μm in diameter showing both constructive and destructive interference may also be observed. In the central column the expected binary identification function is displayed. The "bright" output expected for the fourth value of the identity function is surrounded by a dark halo due to
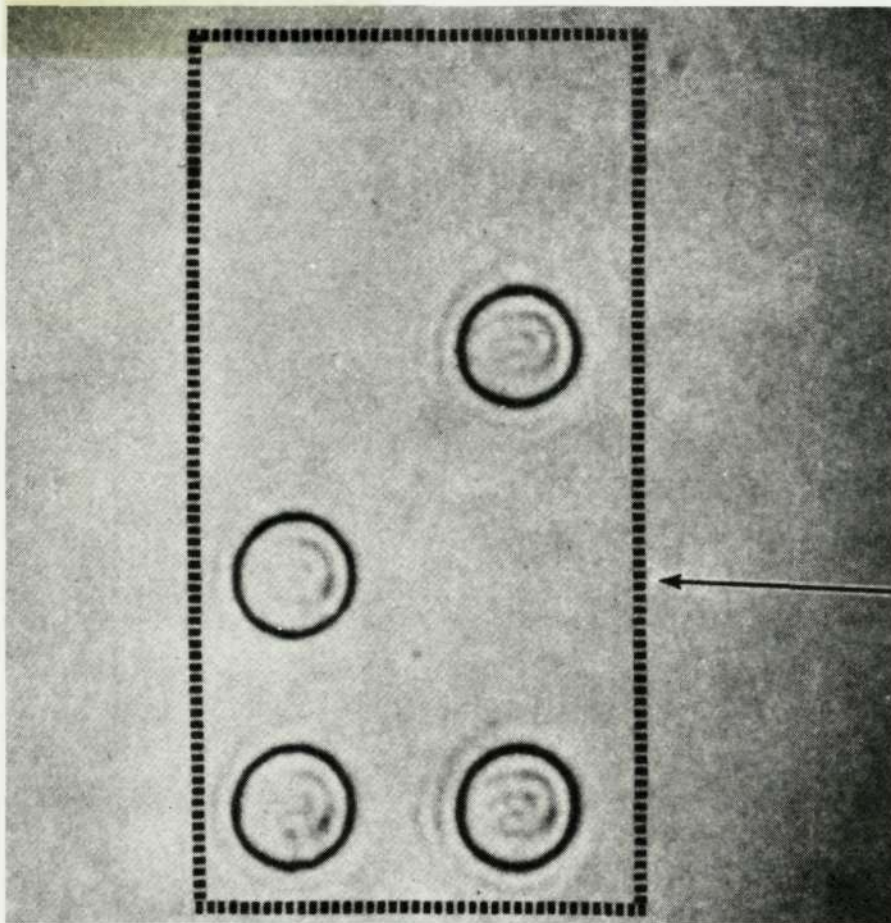
Figure 12. Photomicrograph of the output light intensity at a column of points (dashed lines) at $-x_r$ obtained when performing the binary identity function using digital holographic logic.

the fact that the high spatial frequencies corresponding to the border of the light modulating elements were not passed by the optical computer lens system. An improvement in performance was suggested and demonstrated by Dr. Ronald Grosso of Perkin-Elmer with the results shown in Figure 13. In this case the 1's complement of the binary identity function, namely, the Exclusive OR, was created. This was done by translating H_{abr} by one half cycle of the spatial frequency corresponding to the final term in equation (9). This has the effect of producing a relative phase shift of 180° between the output generated from the input at x_a with respect to that generated from the input at x_b. Thus all regions of constructive interference are replaced by regions of destructive interference and vice versa. The only regions of constructive interference exist where the values of the input variables are unequal in phase. As can be seen the signal to noise ratio is considerably enhanced. Thus is would appear that an inverting

183
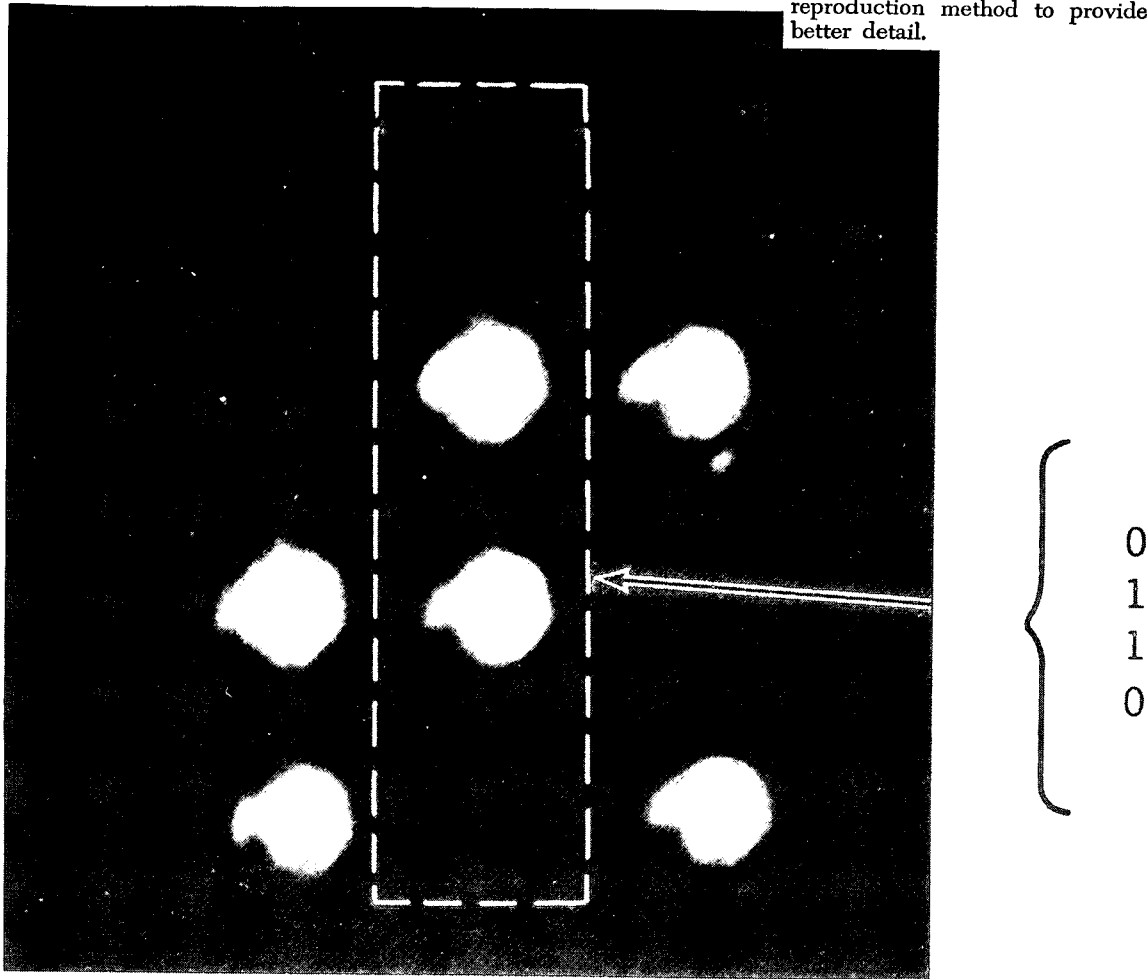
Figure 13. Photomicrograph of the light intensity in the output plane at point $-x_r$ (dashed lines) obtained when performing the Exclusive OR function using digital holographic logic.

logic corresponding to the 1's complement is more practical to use in optical computers performing digital holographic logic than the direct logic whose results are shown in Figure 12.

OPTICAL TO OPTICAL CONVERSION

In order to make coherent optical computers using digital holographic logic a practical reality it is necessary to obtain OTTO's for transducing the light intensity distribution in the output plane into appropriate input signals for the next block in the computer chain. One possible OTTO is shown schematically in Figure 14. This device is the PMLM (Photosensitive Membrane Light

REFLECTING
MEMBRANE

COLLECTING
ELECTRODE

60 V

N-TYPE
SILICON

N⁺ DIFFUSION

P⁺ DIFFUSION

RESISTIVE
LAYER
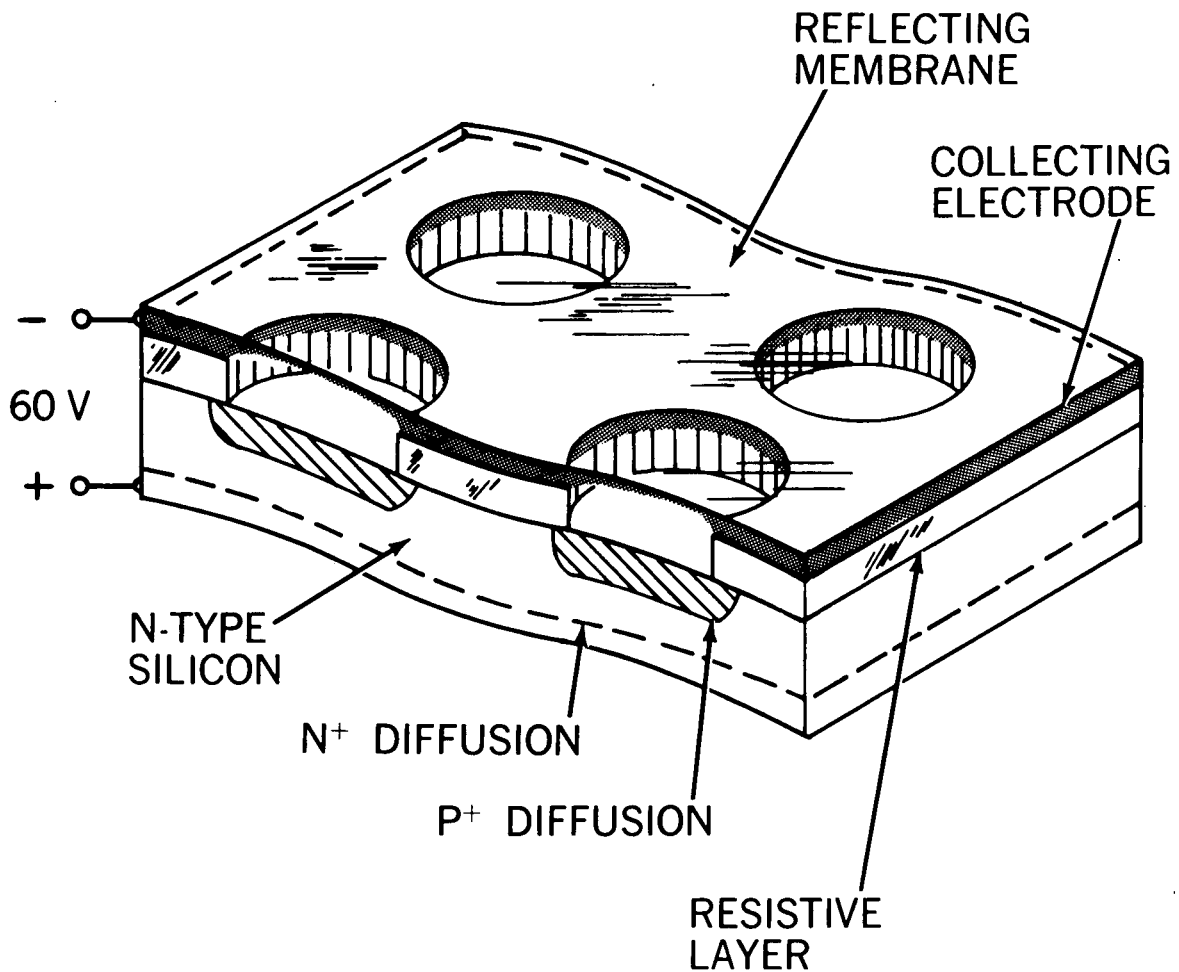
Figure 14. Isometric drawing showing the basic configuration of the photo
sensitive membrane light modulator (input surface below; output
surface above).

Modulator) originally described by Reizman (5). The PMLM is made from a
thin silicon substrate using integrated circuit technology. When n-type silicon
is used, a heavy n+ diffusion is made on the input surface to act as a transparent
electrode. On the opposite surface p+ diffusions are made having the size and
spacing of the required input array of phase modulating elements. These dif-
fusions form an array of pn junction diodes. Overlaying the diodes is a resistive
layer consisting of a semi-insulating material approximately 1 m thick. This
layer is interrupted with circular perforations registered with the p regions of
the diode array.

Three more layers complete the device. First there is a collecting elec-
trode on top of the semi-insulating layer (but not extending over the circular

perforations), next is a polymer membrane which is stretched tightly across the perforations, and finally, a layer of metalization which makes the polymer membrane reflective.

The PMLM is energized by a power supply poled so as to back bias all the diodes in the array. This places the positive terminal of the power supply on the transparent electrode and the negative terminal is common to both the collecting electrode and the membrane metalization. When the input surface of the PMLM is not illuminated, all diodes are back biased and, ideally, no current flows through the semi-insulating layer. This means that the entire potential of the power supply appears across the pn junctions leaving all p regions at the potential of the collecting electrode (and the membrane metalization). When light strikes locally in the vicinity of one diode, this diode conducts and the p region now becomes more positive. This introduces a potential difference between the p region and the membrane metalization. Due to electrostatic forces the membrane locally deflects. Phase modulation of reflected light results from this deflection.

The membrane surface of the PMLM is the output surface and it is coherently illuminated from an optical source. By adjusting the optical computer parameters properly, phase modulation due to deformations of the membrane elements may be made to correspond to the 0° and 180° points necessary for doing binary logic holographically. Interferograms showing the operation of two elements of an early PMLM are shown in Figure 15. Each interferogram is of the same portion of the PMLM. Two circular elements are shown which are approximately 40μm in diameter on approximately 100μm centers. From
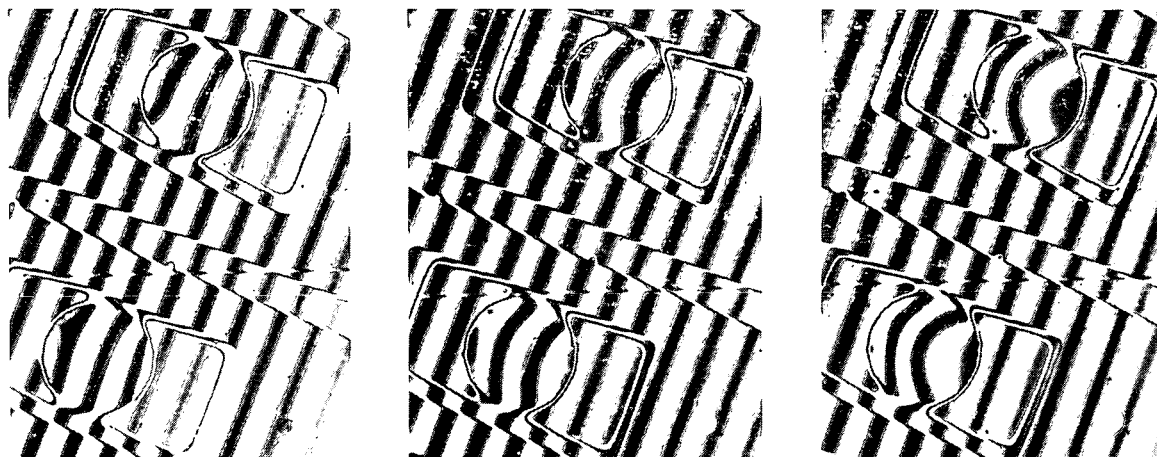

Figure 15. Interferomicrograms showing deflections of the output surface of a photo sensitive membrane light modulator (left to right): power off; power on, no illumination; power on and illuminated.

left to right in Figure 15 the first interferogram shows the membrane elements undeflected when no power is applied to the PMLM. With the power supply adjusted to 70 volts, both elements deflect due to spurious leakage current through the corresponding diodes. The deflection produces a phase modulation of the order of 180°. This phase level must therefore be utilized as the zero degree phase reference. When the input surface of the PMLM is illuminated, a further deflection takes place as is shown in the right hand interferogram. With proper design a further increase of 180° may be achieved. Thus the actual operating states of the membrane elements in question would be 180° to 360° rather than from 0° to 180°.

CONCLUSION

Although all propositional logic may not be carried out using the identity function or the exclusive OR, it is possible to expand the above techniques into a complete logical set by incorporating the logical OR function. To accomplish this one must use a three-state logic employing three input elements for each two-input function. One element is always at zero degrees of phase. The hologram used is made with three input elements at 0°, 120°, and 240°. The input/output truth table is as follows:

Input A	Input B	Output
0°	0°	Zero
0°	180°	Finite
180°	0°	Finite
180°	180°	Finite

The initial entry in the truth table causes the hologram to create a coherent summation in the output plane of three equal vectors of phase 0°, 120°, and 240°, respectively. This produces a null condition (destructive interference) and therefore a 0 output. In all other cases, where 180° is added to either or both of the inputs, the vector summation in the output plane is no longer null and a finite output occurs.

Using this simple modification of the original two-state logic described above, all propositional logic may be performed using the appropriate hologram.

REFERENCES

1. Preston, K., Jr., Coherent Optical Computers, Ch. 6, McGraw-Hill (1972).

2. Ibid., Ch. 4.

3. Vander Lugt, A., "Signal Detection by Complex Spatial Filtering," IEEE Trans. Inform. Theory IT-10, 139 (1964).

4. Leith, E. M., "Reconstructed Wavefronts and Communication Theory," J. Opt. Soc. Amer. 52 (10), 1123 (1962).

5. Reizman, F., "An Optical Spatial Phase Modulator Array Activated by Optical Signals," AGARD Conf. on Opto-El. Sig. Proc. Tech., Oslo, Norway (September 1969).

6. Golay, M. J. E., "Hexagonal Parallel Pattern Transformations," IEEE Trans. on Comp. C-18, 733 (1969).

7. Preston, K., Jr., "Use of the Golay Logic Processor in Pattern-Recognition Studies Using Hexagonal Neighborhood Logic," Computers and Automata, Polytechnic Press (1972).

WORKSHOP REPORTS

WORKSHOP NO. 1

Mr. Schaefer: Arnold, would you mind telling us, what are desirable image processing tasks to perform onboard Earth Observation Spacecraft and, in contrast, what are the desirable tasks that lend themselves to image processing on the ground ?

Mr. Shulman: Workshop No. 1 could not answer that question and many others that we raised.

In fact, I think we have gotten ourselves more problems than we have solved.

In talking with Mike, and just overhearing the discussion here, it seems that it is unanimous that we don't know what type problem we have, and what we are trying to solve.

As far as airborne processing goes, we don't know what answers we are looking for.

Right now, because of the user community requesting so many varied and different types of information, it only seems reasonable at this point in time to try to bring down as much of the information as possible, and process it with a hybrid parallel type processing on the ground to extract the specific types of information that the user community wants.

However, in regard to that, we strongly feel the need for some sort of standardization group to be formed to come up with a catalog, if you will, that presents the types of information that can be processed, or what the user community might expect, say, in five years, as a type of data processing that they should design their experiments around.

So that five years from now, the user community has been educated to feel, that from this catalog, — if I design my experiments this way or that, I will be able to get good data and it will limit the type of airborne computations that we may need to provide in the air.

We felt there might be a problem with present technology with regard to the bandwidth requirements for transmitting data to the ground. We could have addressed ourselves to bandwidth requirements with laser communications, which might be able to solve this type problem. If we do transmit all data to the

ground to be processed, it should be put in a format which would permit easy processing, which means some sort of memory device which doesn't ruin the information. Film right now is probably one of our better mediums for storing large amounts of data but is not the complete answer as it exists now, because there are considerable problems caused by the way it must be handled and the way it stores information. This is another area that may require looking into.

Once we have decided what type of information the user community wants, it then would become a relatively simple job to design airborne specialized computers to solve specific requirements, provided we could limit the requirements to these specific ones.

This gets back to the need for some sort of standardization committee to be formed to provide some guidance to the user community, as well as the designers, so that we know what to design for.

I believe that is as reasonably accurate results as I can give you from our workshop.

Mr. Schaefer: Can I sum it up? Do I read you right that—

Mr. Shulman: Mine was a summary.

Mr. Schaefer: —they came up forescore for a committee.

Mr. Shulman: Right.

Mr. Schaefer: Very good. It sounds like you had a very worthwhile time to me, even though you didn't answer the questions. I bet none of us did.

WORKSHOP NO. 2

Norman, how can image processing units aboard low altitude orbiters, those aboard synchronous orbiters, and those on the ground cooperatively interact?

Dr. MacLeod: Well, we viewed these questions as more or less potential users. We are talking about a future system in the 1980s, 1990s time frame, and I think we all agreed that it would be very nice to have a synchronous satellite that would beam every kind of desirable information into a farmer's TV. This was an ultimate system. Then we begin to back off from there. One has to consider the conflicting uses of many potential users.

We also considered that by that time people would know what they wanted
they would be, perhaps, used to acquiring and using remote sensing data.

Now, from that, there were some comments concerning the type of ground
station one might have. We felt that an experimental spacecraft system would
always be accompanying the operational spacecraft. We felt that simple sys-
tems like the APT, which is essentially a farmer's TV in the year 1990, might
be a useful kind of thing for operational needs where a map is coming down
directly, very much like a weather map. Such map producers would employ
onboard processing in either synchronous or low orbital spacecraft. We how-
ever felt that complex ground systems dealing with high data rates would be
involved with experimental spacecraft.

There was some discussion about whether or not it was useful to relay
very small amounts of information down, whether characterizers or classi-
fiers onboard the spacecraft could usefully send down simple indices of
various states of surface information or meteorological information. This
probably would be limited to users that had quite well known needs.

We also considered the frequency of observation. In some of these satel-
lites we can get a picture down every few minutes from synchronous altitudes,
but many of our users don't need this kind of frequent information. This has
an effect on the interaction or where you are going to process information.

One of the obvious places where the systems can interact, of course, is
between the spacecraft that would be, perhaps, in a polar orbit, and a geo-
stationary spacecraft essentially acting as a relay system.

We had a particularly difficult problem, I think, with knowing how much
we were going to know in the future, and also knowing what kind of sensors
and computational devices there would be available under such systems.

We had some discussion on these matters and I don't think we came to any
particular conclusion about this, except that we felt that the users probably
would know what questions they had in mind and that some of us, in fact, do
know already what questions we have in mind. It is a matter of knowing to
what stage of understanding of the application of that data that we would have
in the future which would affect the processing systems in the manners that I
have just spoken about.

The problem is to supply only the required information to the users, rather than having great masses of data coming down. In this sense the orbital space-craft, such as the ERTS spacecraft, is going to supply a great amount of information for some users that don't need great amounts of information, and not enough information for some users that need very frequent observations. And this situation, of course, would continue with the multistage kind of analysis that is going on, for instance, in forestry.

We returned several times to the question of multistage sampling and using these systems as direct interactive systems, where the altitudinal differences in spacecraft and aircraft would be utilized in a multistage sampling system.

But again the problem is, what are we going to know when the time comes to use these systems, and this will in effect assign us what we are going to be doing.

Mr. Schaefer: It sounds most fruitful, very interesting.

WORKSHOP NO. 3

Mr. Schaefer: Bill, did you answer your question? Let me read it.

Mr. Alford: I was going to read it, because that's half of my summary, reading the question.

What Earth Observation tasks are uniquely suited to coherent optical processing systems? To non-coherent systems? To parallel electronic systems?

No one dared admit that there was any one task that was uniquely suited. And that is the conclusion.

Now I will give you a little background.

We tried—just to give you a little of the frustration we went through—we tried to define what we were going to talk about and we decided that, first of all, let's look at the information objectives, you know, what are we really after? And I guess like everybody else, that quickly ground to a halt because no one could define that.

I guess primarily we have a lot of the technology people and not a lot of the end-users here, at least we didn't have a lot of end-users in our group to answer that question.

So we backed off and we said, well, let's look at techniques, and maybe we can define where those techniques fitted a little better in these three categories.

So we started looking at a lot of techniques, and I will just mention a couple.

We got off on correlation for picture rectification, radiometric corrections, multispectral classifications, enhancement, etc. You have heard a lot of them. And we started looking at some of these and no one recognized any of these as being uniquely suited to any of the three systems.

We think there are probably still some holes left like, in terms of application, like what can you do with coherent optics in terms of multispectral classification? We feel that maybe all we need are opinions or just comments from certain people on some of these questions.

We sort of concluded that in many cases the application probably has to be analyzed in terms of cost tradeoffs and throughput requirements. Again, nothing conclusive other than in many cases each situation has its own solution.

I wrote down what Arnold said, and I will say it again.

Once we decide what the information is that the user community wants, we can decide which techniques are going to be applicable.

Mr. Schaefer: I don't dare to summarize your summary.

WORKSHOP NO. 4

Mike, can you tell us, what are the image processing requirements for small easily available ground stations?

Mr. Michalak: Well, Dave, no, I don't think I can.

When we started talking about the APT station we very rapidly came to the conclusion that the data gathering end of such a ground station would probably be prohibitively expensive within the next two or three years, talking on the order of a quarter of a million dollars for an auto track antenna alone.

Now once we kind of did away with that, we started looking around as to how could we then reformat data, and how could we put it into such a form where an APT antenna might be more worthwhile?

193

We came around to the general idea of data management as starting out with a satellite which perhaps costs you hundreds of millions of dollars.

From the satellite, such as ERTS, we would beam down through a high data rate link to several global regions and in each global region would be a central menial task center, menial task being to reformat the data, put in all the latitude and longitude, do radiometric correction, that sort of thing. These things would run you about $25 million-or-so apiece, perhaps even a little bit more with inflation.

Then from the reformating stations, we go back to a geosynchronous orbiter and from the geosynch satellite we would beam down to district offices.

Now when we start talking about district offices, we started talking about the kind of market that earth resources and parallel image processing is going to have, and again we decided that we are going to have to develop our own market.

In other words, echoing what I have heard here today, we have to educate the user community as to what parallel processing can do, and more specifically, we have got to go out and demonstrate useful applications of this.

Now admittedly we don't know all of the possible applications, but things like flood control, area pollution monitoring, fault line detection, various things like this are probably good places to start to get a little handle on what is happening.

So I guess basically the problems that we ran into are

(1) the high data lines, and

(2) do we need parallel processing, if so, show me, show me what it is going to do for me.